Supporting Information for

Original article

Design, synthesis, and biological evaluation of quinazolin-4(3*H*)-one derivatives co-targeting poly(ADP-ribose) polymerase-1 and bromodomain containing protein 4 for breast cancer therapy

Xiaosa Chang[†], Dejuan Sun[†], Danfeng Shi[†], Guan Wang, Yanmei Chen, Kai Zhang, Huidan Tan, Jie Liu[*], Bo Liu[*], Liang Ouyang[*]

State Key Laboratory of Biotherapy and Cancer Center, West China Hospital, and Collaborative Innovation Center of Biotherapy, Sichuan University, Chengdu 610041, China

[†]These authors made equal contributions to this work.

Received 27 February 2020; received in revised form 8 May 2020; accepted 28 May 2020

[*]Corresponding authors. Tel./fax: +86 28 85503817 (Jie Liu), +86 28 85164063 (Bo Liu), +86 28 85503817 (Liang Ouyang).

E-mail addresses: liujie2011@scu.edu.cn (Jie Liu), liubo2400@163.com (Bo Liu), ouyangliang@scu.edu.cn (Liang Ouyang).

Table of contents **Page**

1. Supplementary results

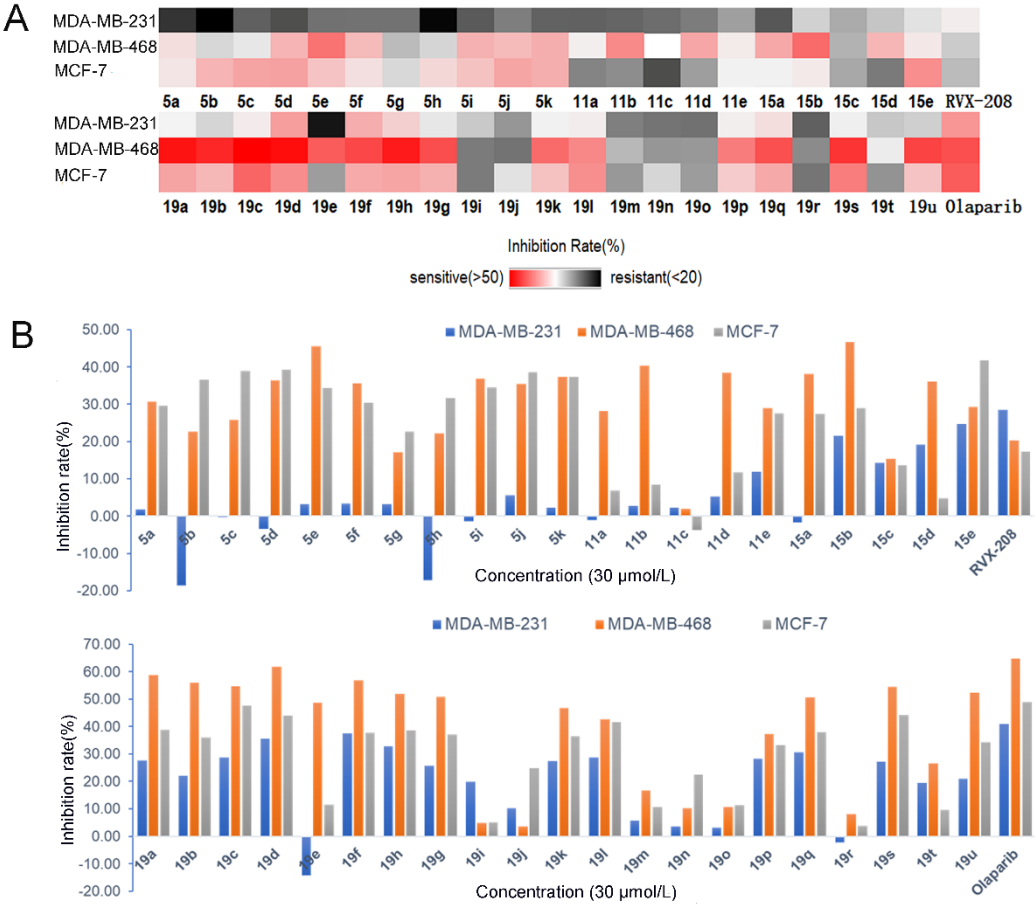

Figure S1 Cell viabilities were measured for top 42 candidate compounds by MTT assay. (A) Heat map of inhibition rate of anti-proliferative activity of compounds. (B) Histogram of inhibition rate of anti-proliferative activity of compounds. The cancer cell inhibitory activity of MDA-MB-231 cell, MDA-MB-468 cell and MCF-7 cell of top 42 candidate compounds were detected at 30 μmol/L.

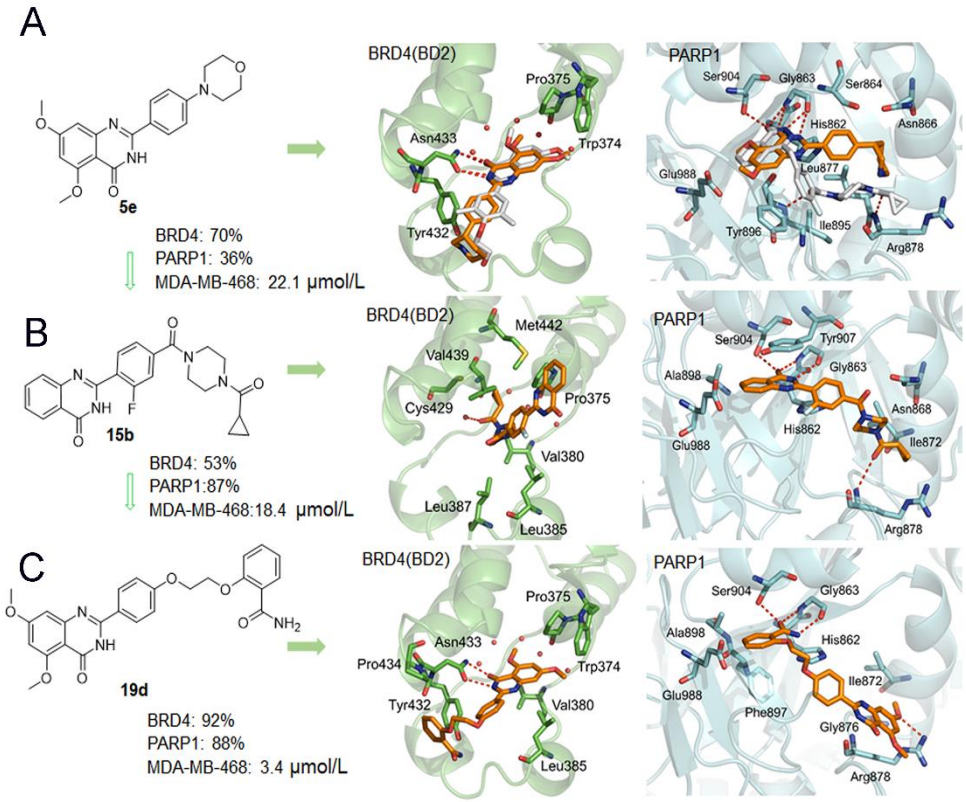

Figure S2 Target-binding series development from initial compound. Representative examples of target-binding compounds **5e** to **19d** guided by structural information. (A) Docking structures with the mode of binding of compound **5e** and Rvx-208 to BRD4(BD2) and PARP-1 in the pocket, respectively. (B) Docking structures with the mode of binding of compound **15b** and Rvx-208 to BRD4(BD2) and PARP1 in the pocket, respectively. (C) Binding mode of **19d** in the active site of BRD4(BD2) and PARP1, respectively. BRD4(BD2) (PDB code: 5UOO) was shown in green, PARP-1 (PDB code: 5DS3) was shown in grey.

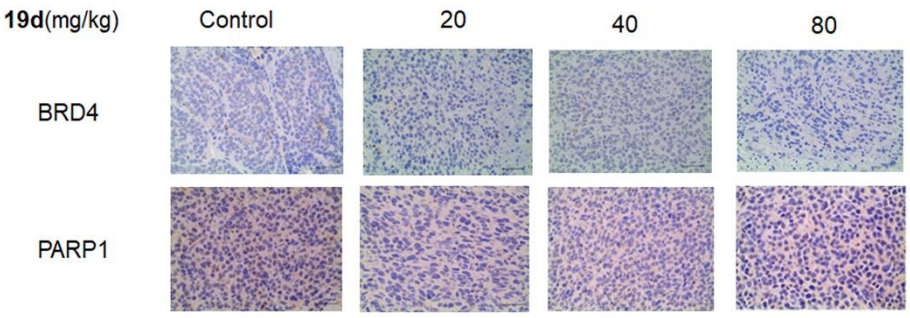

Figure S3 Immunohistochemical staining of PARP1 and BRD4 in the MCF-7 tumor tissues from **19d**-treated mice and vehicle groups (200×).

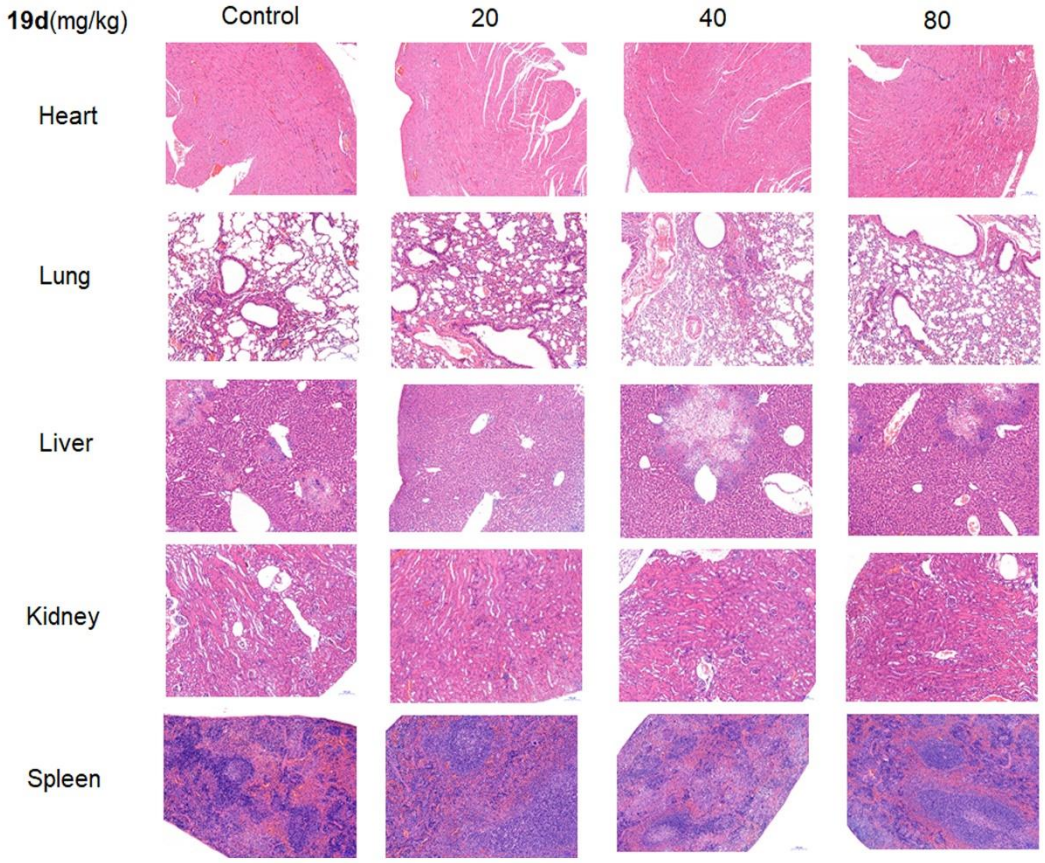

Figure S4 Various mouse organs from treated and control groups were stained with hematoxylin and eosin (H&E) to evaluate the toxicity of compound **19d** in the MDA-MB-468 tumor xenograft model. Photographs were obtained under magnification, ×100.

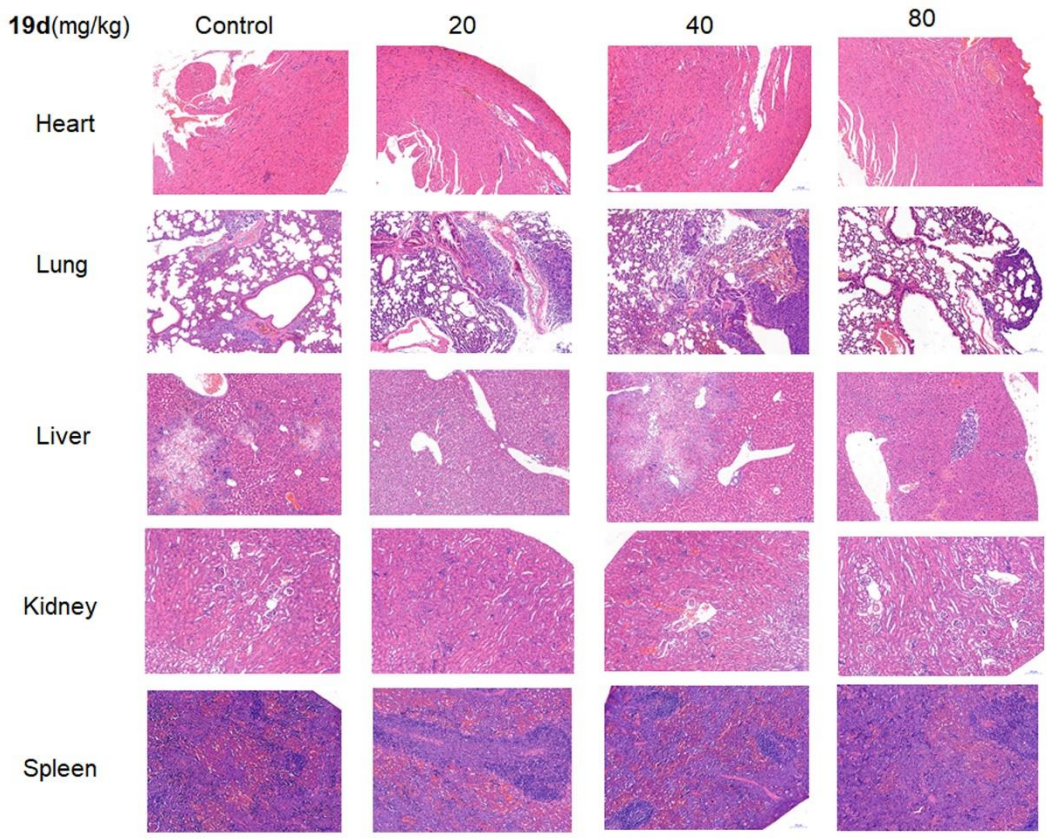

Figure S5 Various mouse organs from treated and control groups were stained with hematoxylin and eosin (H&E) to evaluate the toxicity of compound **19d** in the MCF-7 tumor xenograft model. Photographs were obtained under magnification, ×100.

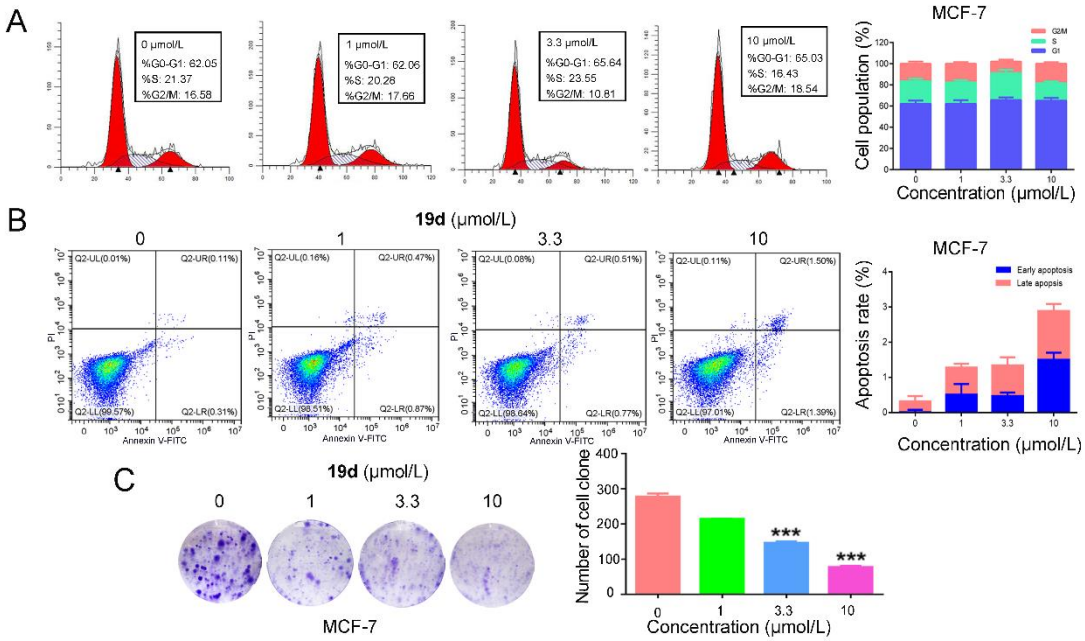

Figure S6 Effect of **19d** on MCF-7 cells cell cycle progression. (A) Cell cycle distribution was measured by flow cytometry using PI stain with 0, 1, 3.3 and 10 μmol/L of **19d** separately treated MCF-7 cells. (B) Apoptosis rates were detected by Annexin V-FITC/PI staining after treatment with **19d**. (C) Clonogenic survival assay of MCF-7 cells was measured by after treatment with Compound **19d**. The statistics of clonogenic survival assay. $^{***}P < 0.001$ compared with control group. Data are present as means ± SDs, $n = 3$.

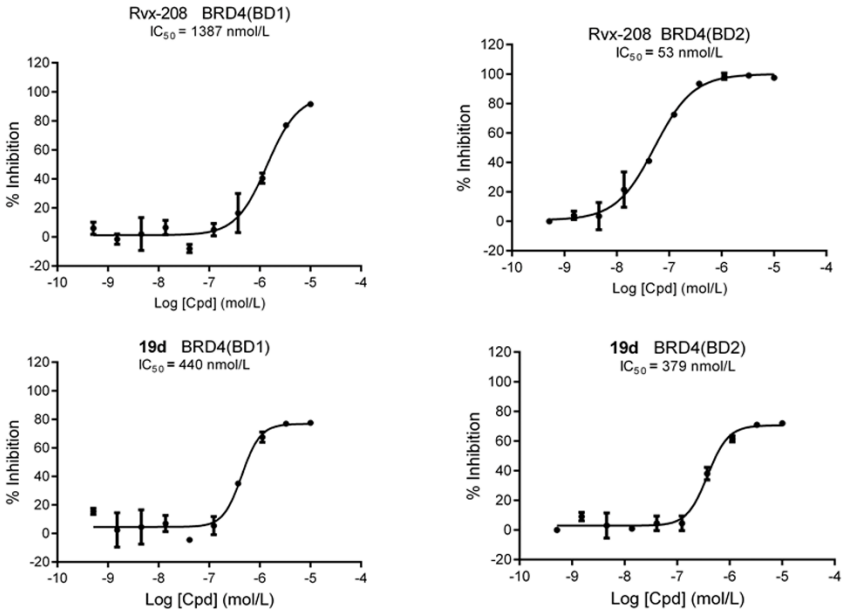

Figure S7 The IC_{50} values of Rvx-208 and compound **19d** against BRD4(BD1) and BRD4(BD2), respectively.

Figure S8 The 2D interactive modes of **19d**, RVX-208 and Olaparib. (A) and (B) Interactive modes of **19d** and RVX-208 in the BD1 domain of BRD4. (C) and (D) Interactive modes of **19d** and RVX-208 in the BD2 domain of BRD4. (E) and (F) Interactive modes of **19d** and Olaparib in the active site of PARP1.

Table S1 22 PARP1 inhibitors.

No.	Structure/Name	Core	Fragments	IC_{50} & Target	Ref.
Type 1: benzoamide-based					
1	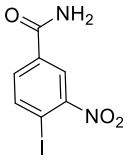 Iniparib	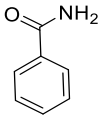	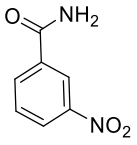	Used in the research of TNBC	1,2
2	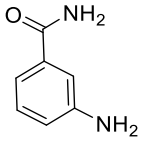	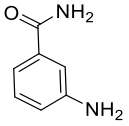	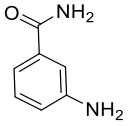	CHO cells: IC_{50} = 50 nmol/L	3
3	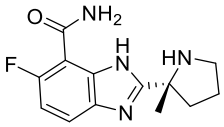 Veliparib	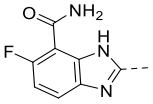	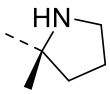	PARP1: IC_{50} = 5.2 nmol/L PARP2: IC_{50} = 2.9 nmol/L	4
4	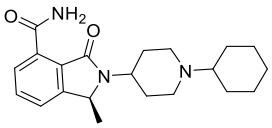 NMS-P515	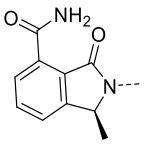	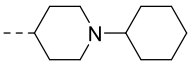	PARP-1: 27 nmol/L (IC_{50}, in HeLa cells)	5
5	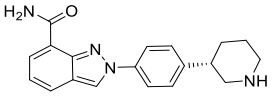 Niraparib	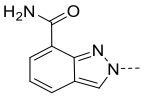	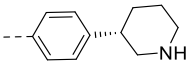	PARP1: IC_{50} = 3.8 nmol/L PARP2: IC_{50} = 2.1 nmol/L	6
6	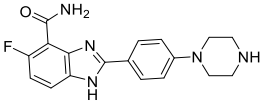	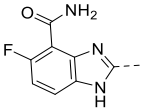	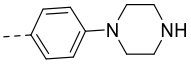	PARP1: IC_{50} = 43.7 nmol/L HCT116 cell: IC_{50} = 7.4 μmol/L	7
7	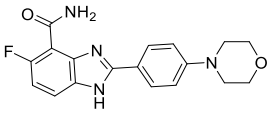	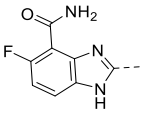	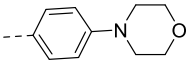	PARP-1: IC_{50} = 21.8 nmol	7
Type 2: tricyclic indole carboxamide-based					
8	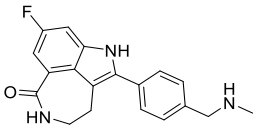 Rucaparib	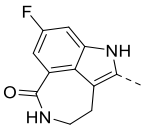	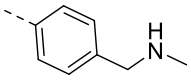	PARP1: *K*i = 1.4 nmol/L	8

9	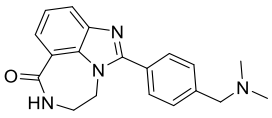 AG14361	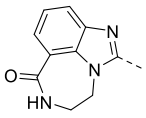	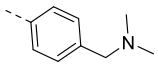	PARP1: *Ki* < 5 nmol/L PARP1: IC_{50} = 29 nmol/L	9
Type 3: tricyclic indole carboxamide-based					
10	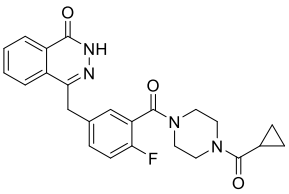 Olaparib	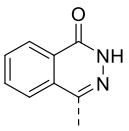	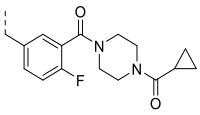	PARP1: IC_{50} = 5 nmol/L PARP2: IC_{50} = 1 nmol/L	10
11	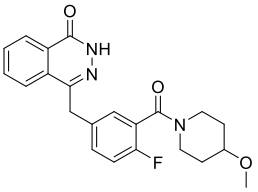 AZD-2461	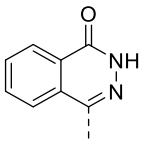	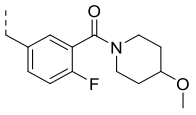	PARP1: IC_{50} = 5 nmol/L PARP2: IC_{50} = 2 nmol/L PARP3: IC_{50} = 200 nmol/L	11
12	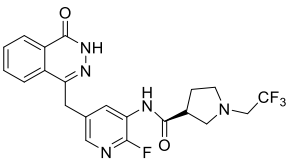 PARP-2-IN-1	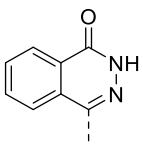	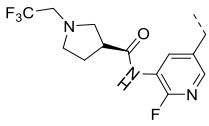	PARP2: IC_{50} = 11.5nmol/L	12
Type 4: phthalazine ketones					
13	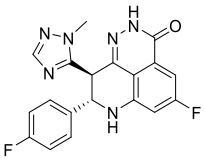	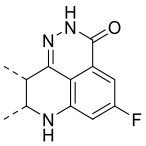		PARP1: IC_{50} = 0.57 nmol/L	13
14	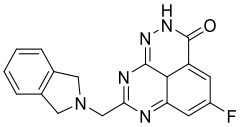 E7449	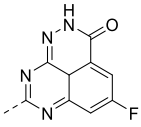	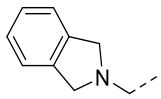	PARP1: IC_{50} = 2 nmol/L PARP2: IC_{50} = 1 nmol/L	14
15	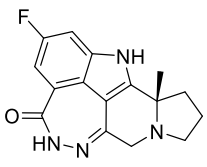 Pamiparib	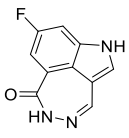	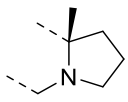	PARP1: IC_{50} = 0.9 nmol/L PARP2: IC_{50} = 0.5 nmol/L	15
Type 5: isoindolinone-based					

16	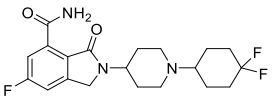 NMS-P118	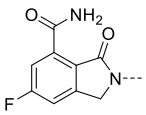	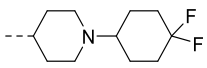	HeLa cell: PARP1: IC_{50} = 0.04 μmol/L	16
Type 6: benzofuran-based					
17	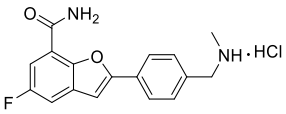	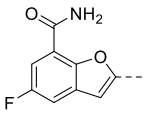	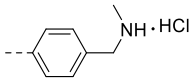	PARP1: IC_{50} = 3.2 nmol/L	17
Type 7: nicotinamide oximes					
18	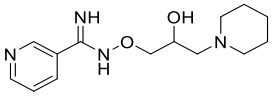 BGP-15	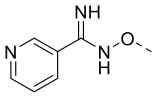	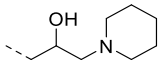	IC_{50} = 120 μmol/L, *K*i = 57 μmol/L	18
Others					
19	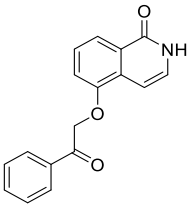 UPF 1069	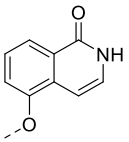	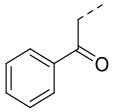	PARP1: IC_{50} = 8 μmol/L PARP2: IC_{50} = 0.3 μmol/L	19
20	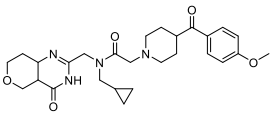	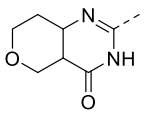	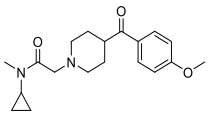	PARP2: IC_{50} = 32 μmol/L	20
21	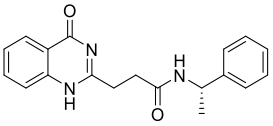 ME0328	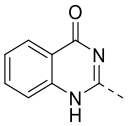	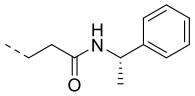	ARTD1/PARP1: IC_{50} = 6.3 μmol/L ARTD2/PARP2: IC_{50} = 10.8 μmol/L ARTD3/PARP3: IC_{50} = 0.89 μmol/L	21
22	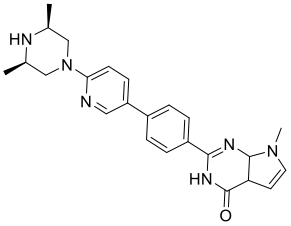 AZ6102	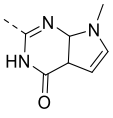	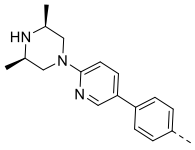	PARP1: IC_{50} = 2 μmol/L PARP2: IC_{50} = 0.5 μmol/L	22

Referrence

1. Ma W, Halweg CJ, Menendez D, Resnick MA. Differential effects of poly(ADP-ribose) polymerase inhibition on DNA break repair in human cells are revealed with Epstein-Barr virus. *Proc Natl Acad Sci U S A* 2012;**109**:6590–5.
2. Yin S, Cheryan VT, Xu L, Rishi AK, Reddy KB. Myc mediates cancer stem-like cells and EMT changes in triple negative breast cancers cells. *PLoS One* 2017;**12**:e0183578.
3. Radovits T, Lin LN, Zotkina J, Gero D, Szabó C, Karck M, et al. Poly(ADP-ribose) polymerase inhibition improves endothelial dysfunction induced by reactive oxidant hydrogen peroxide *in vitro*. *Eur J Pharmacol* 2007;**564**:158–66.
4. Donawho CK, Luo Y, Penning TD, Bauch JL, Bouska JJ, Bontcheva-Diaz VD, et al. ABT-888, an orally active poly(ADP-ribose) polymerase inhibitor that potentiates DNA-damaging agents in preclinical tumor models. *Clin Cancer Res* 2007;**13**:2728–37.
5. Papeo G, Orsini P, Avanzi NR, Borghi D, Casale E, Ciomei M, et al. Discovery of stereospecific PARP-1 inhibitor isoindolinone NMS-P515. *ACS Med Chem Lett* 2019;**10**:534–8.
6. Jones P, Ferrigno F, Fonsi M, Giomini C, Lamartina S, Monteagudo E, et al. Discovery of 2-{4-[(3*S*)-piperidin-3-yl]phenyl}-2*H*-indazole-7-carboxamide (MK-4827): a novel oral poly(ADP-ribose)polymerase (PARP) inhibitor efficacious in BRCA-1 and -2 mutant tumors. *J Med Chem* 2009;**52**:7170–85.
7. Wang J, Wang X, LI H, Ji D, Li Y, Xu Y, et al. Design. synthesis and biological evaluation of novel 5-fluoro-1*H*-benzimidazole-4-carboxamide derivatives as potent PARP-1 inhibitors. *ACS Med Chem Lett* 2016;**26**:4127–32.
8. Thomas HD, Calabrese CR, Batey MA, Canan S, Hostomsky Z, Kyle S, et al. Preclinical selection of a novel poly(ADP-ribose) polymerase inhibitor for clinical trial. *Mol Cancer Ther* 2007;**6**:945–56.
9. Calabrese CR, Almassy R, Barton S, Batey MA, Calvert AH, Canan-Koch S, et al. Anticancer chemosensitization and radiosensitization by the novel poly(ADP-ribose) polymerase-1 inhibitor AG14361. *J Natl Cancer Inst* 2004;**96**:56–67.
10. Menear KA, Adcock C, Boulter R, Cockcroft XL, Copsey L, Cranston A, et al. 4-[3-(4-Cyclopropanecarbonylpiperazine-1-carbonyl)-4-fluorobenzyl]-2*H*-phthalazi

n-1-one: a novel bioavailable inhibitor of poly(ADP-ribose) polymerase-1. *J Med Chem* 2008;**51**:6581–91.

11. Jaspers JE, Kersbergen A, Boon U, Sol W, van Deemter L, Zander SA, et al. Loss of 53BP1 causes PARP inhibitor resistance in Brca1-mutated mouse mammary tumors. *Cancer Discov* 2013;**3**:68–81.
12. Zhao H, Ji M, Cui G, Zhou J, Lai F, Chen X, et al. Discovery of novel quinazoline-2,4(1*H*,3*H*)-dione derivatives as potent PARP-2 selective inhibitors. *Bioorg Med Chem* 2017;**25**:4045–54.
13. Shen Y, Rehman FL, Feng Y, Boshuizen J, Bajrami I, Elliott R, et al. BMN 673, a novel and highly potent PARP1/2 inhibitor for the treatment of human cancers with DNA repair deficiency. *Clin Cancer Res* 2013;**19**:5003–15.
14. McGonigle S, Chen Z, Wu J, Chang P, Kolber-Simonds D, Ackermann K, et al. E7449: A dual inhibitor of PARP1/2 and tankyrase1/2 inhibits growth of DNA repair deficient tumors and antagonizes Wnt signaling. *Oncotarget* 2015;**6**:41307–23.
15. Changyou Z. Fused tetra or penta-cyclic dihydrodiazepinocarbazolones as parp inhibitors. WO 2013097225 A1. 2013 Sep 9.
16. Papeo G, Borghi D, Busel AA, Caprera F, Casale E, Ciomei M, et al. Discovery of 2-[1-(4,4-difluorocyclohexyl)piperidin-4-yl]-6-fluoro-3-oxo-2,3-dihydro-1*H*-isoindole-4-carboxamide (NMS-P118): a potent, orally available, and highly selective PARP-1 inhibitor for cancer therapy. *J Med Chem* 2015;**58**:6875–98.
17. He JX, Wang M, Huan XJ. Novel PARP1/2 inhibitor mefuparib hydrochloride elicits potent *in vitro* and *in vivo* anticancer activity, characteristic of high tissue distribution. *Oncotarget* 2017;**8**:4156–68.
18. Sarszegi Z, Bognar E, Gaszner B, Kónyi A, Gallyas F Jr, Sumegi B, et al. BGP-15, a PARP-inhibitor, prevents imatinib-induced cardiotoxicity by activating Akt and suppressing JNK and p38 MAP kinases. *Mol Cell Biochem*2012;**365**:129–37.
19. Pellicciari R, Camaioni E, Costantino G, Formentini L, Sabbatini P, Venturoni F, et al. On the way to selective PARP-2 inhibitors. Design, synthesis, and preliminary evaluation of a series of isoquinolinone derivatives. *ChemMedChem* 2008;**3**:914–23.

20. Shultz MD, Cheung AK, Kirby CA, Firestone B, Fan J, Chen CH, et al. Identification of NVP-TNKS656: the use of structure−efficiency relationships to generate a highly potent, selective, and orally active tankyrase inhibitor. *J Med Chem* 2013;**56**:6495–511.
21. Lindgren AE, Karlberg T, Thorsell AG, Hesse M, Spjut S, Ekblad T, et al. PARP inhibitor with selectivity toward ADP-ribosyltransferase ARTD3/PARP3. *ACS Chem Biol* 2013;**8**:1698–703.
22. Johannes JW, Almeida L, Barlaam B, Boriack-Sjodin PA, Casella R, Croft RA, et al. Pyrimidinone nicotinamide mimetics as selective tankyrase and wnt pathway inhibitors suitable for *in vivo* pharmacology. *ACS Med Chem Lett* 2015;**6**:254–9.

Table S2 71 BRD4 inhibitors.

No.	structure	Core	Fragment	IC_{50} & Target	Ref.
Type 1: triazoloazepine					
1	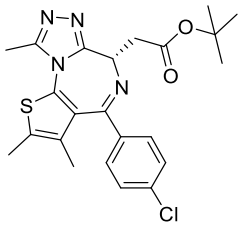	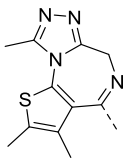	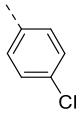	BRD4(1): IC_{50} = 77 nmol/L; BRD4(2): IC_{50} = 33 nmol/L	1
	(+)-JQ1				
2	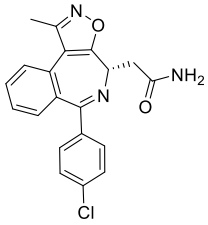	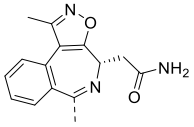	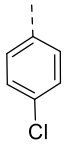	BRD4-BD1: IC_{50} = 39 nmol/L	2
	CPI-0610				
3	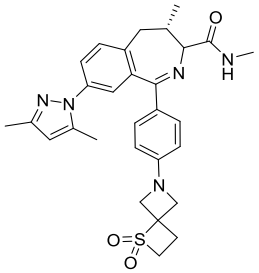	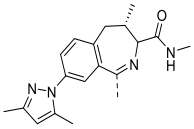	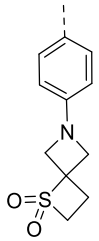	BRD4(1): IC_{50} = 10 nmol/L; MV4-11 cell: IC_{50} = 80 nmol/L	3
4	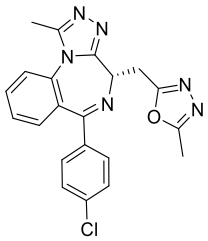	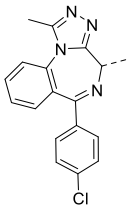	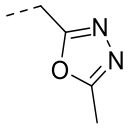	BRD4(1): IC_{50} = 20 nmol/L	4
5	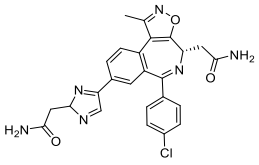	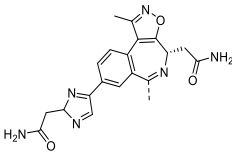	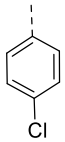	BRD4(1): IC_{50} = 20 nmol/L; MYC: IC_{50} = 32 nmol/L	5
6	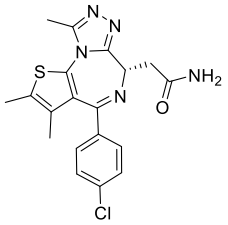	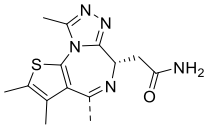	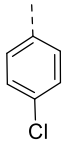	BRD4(1): IC_{50} = 77 nmol/L; BRD4(2): IC_{50} = 33 nmol/L	6
Type 2: triazoloazepines-based					

7	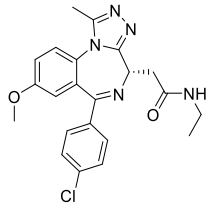 I-BET-762	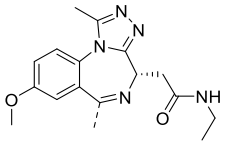	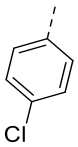	BRD4: IC_{50} = 35 nmol/L	7,8
8	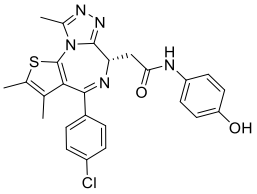 OTX015	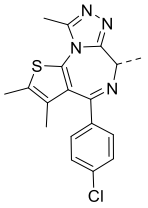	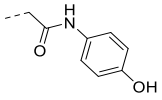	BRD2, BRD3, BRD4: EC_{50} = 10−19 nmol/L	9
9	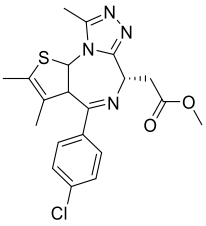 MS417	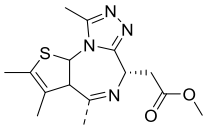	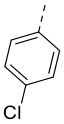	BRD4-BD1: IC_{50} = 30 nmol/L; BRD4-BD2: IC_{50} = 46 nmol/L; BRD4-BD1: K_d = 36.1 nmol/L; BRD4-BD2: K_d =25.4 nmol/L	10
11	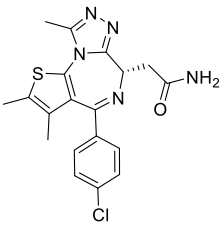 CPI-203	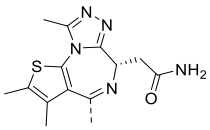	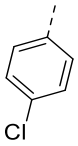	BRD4: IC_{50}=37 nmol/L	11
Type 3: isoxazole-based					
12	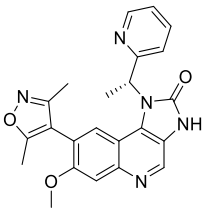 I-BET-151	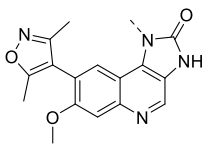	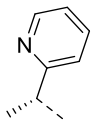	BRD2: IC_{50} = 0.5 μmol/L; BRD3: IC_{50} = 0.25 μmol/L; BRD4: IC_{50} = 0.79 μmol/L	12,13
13	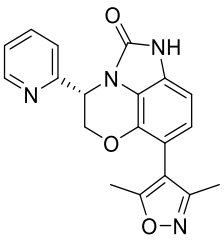	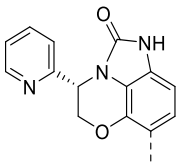	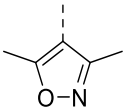	Lymphoma cell 4: IC_{50} < 0.2 μmol/L	14

14	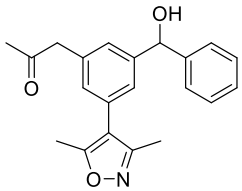	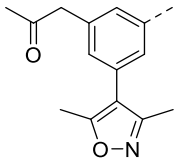	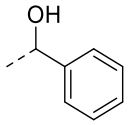	BRD4(1): IC_{50} = 0.371 μmol/L	15
15	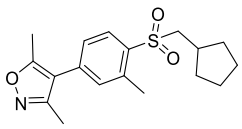	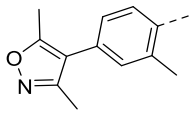	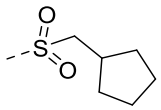	BRD4-BD1: IC_{50} = 0.5 μmol/L; BRD4-BD2: IC_{50} = 0.5 μmol/L	16
16	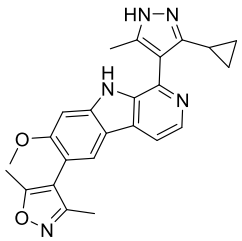	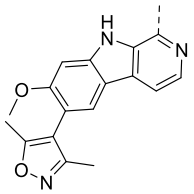	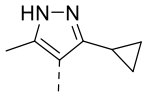	BRD4-BD2: K_i = 3.2−24.7 nmol/L, K_d = 670 nmol/L	17
17	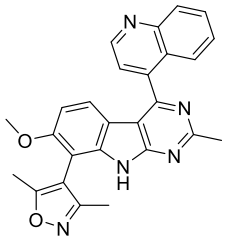	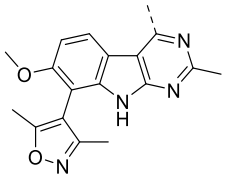	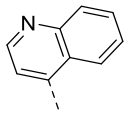	BRD4(1): K_i = 8.2 nmol/L; BRD4(2): K_i = 1.4 nmol/L	18
CD161					
18	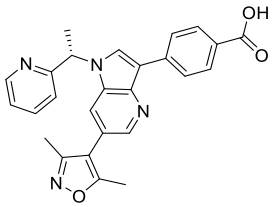	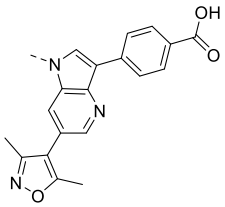	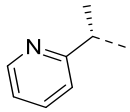	BRD4(1): K_d = 1.7 nmol/L; BRD4(2): K_d = 6.1 nmol/L	19
PLX51107					
19	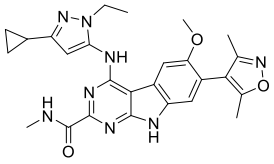	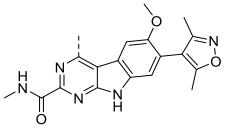	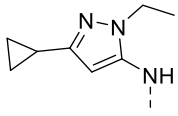	BRD4-BD1: K_i= 0.5 ± 0.2 nmol/L; BRD4-BD2: K_i=1.0 ± 0.1 nmol/L	20
20	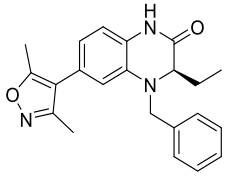	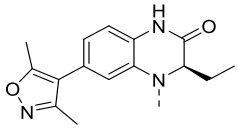	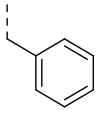	BRD4-BD1: IC_{50} = 70 nmol/L	21

21	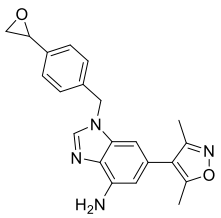 ZEN-3411	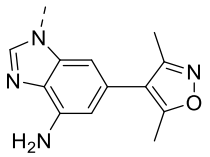	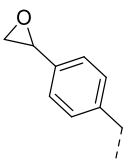	BRD4(BD1): IC_{50}=0.03 μmol/L; BRD4(BD2): IC_{50}=0.05 μmol/L; BRD4: IC_{50}= 0.06 μmol/L	21
22	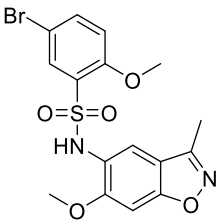	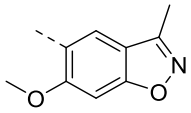	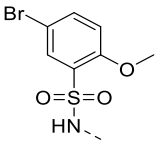	BRD4-BD1: IC_{50}=82 nmol/L; C4-2B cell: IC_{50}=0.84 μmol/L	22
23	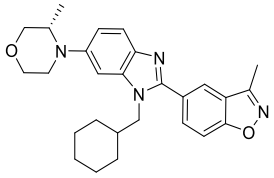 Y06137	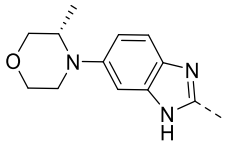	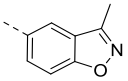	BRD4(1): K_d = 81 nmol/L	22
24	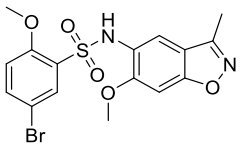 Y06036	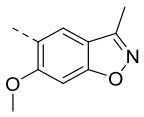	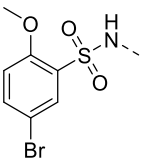	BRD4(BD1): K_d = 82 nmol/L	22
25	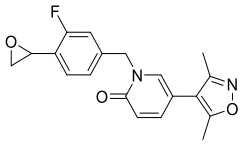 ZEN-3862	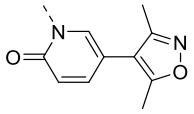	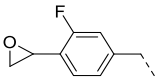	BRD4-BD1: IC_{50}=0.16 μmol/L BRD4-BD2: IC_{50}=0.13 μmol/L	23
26	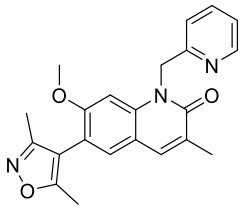 BET-IN-4	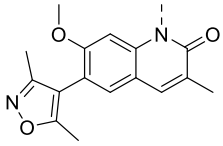	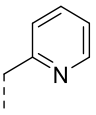	BRD4: IC_{50} < 1 μmol/L	24
27	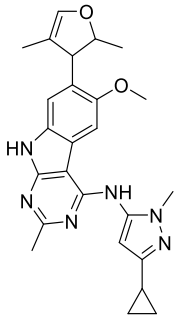 CF53	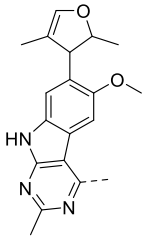	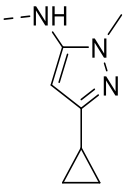	BRD4(BD1): K_i < 1 nmol/L; BRD4(BD1): IC_{50} = 2 nmol/L; BRD4(BD1): K_d = 2.2 nmol/L; BRD4(BD2): K_d = 0.8 nmol/L	25

Type 4: pyridines-based

28	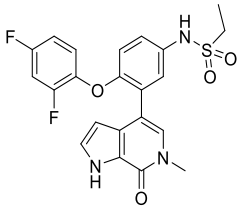	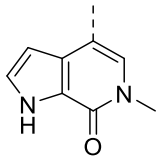	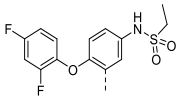	BRD2/4/T: K_i = 1−2.2 nmol/L; BRD3: K_i = 12.2 nmol/L	26
39	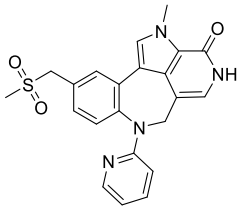	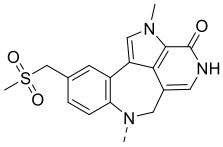		BRD4(BD1): K_i = 1.1 nmol/L; BRD4(BD2): K_i = 2.1 nmol/L; EC_{50} = 16 nmol/L	27
30	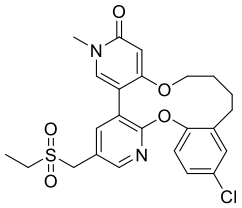	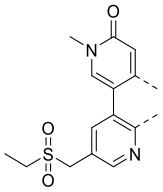	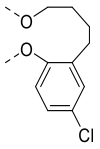	BRD4: K_i = 8.9 nmol/L; MX-1: EC_{50} = 33 nmol/L	28
31	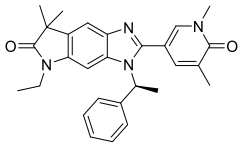	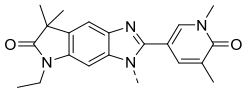	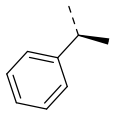	BRD4(1): IC_{50} = 12 nmol/L	29
32	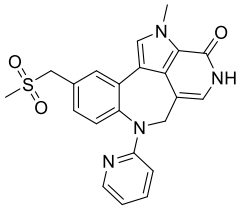	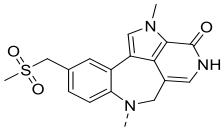		BRD4: K_i = 13 nmol/L; MX-1: EC_{50} = 47 nmol/L	30
33	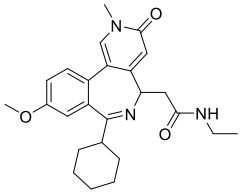	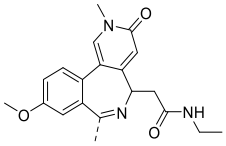		BRD4(1): IC_{50} = 2.0 nmol/L; MV4-11: EC_{50} = 8.0 nmol/L	31
34	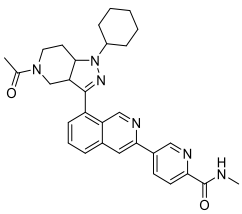 GNE-207	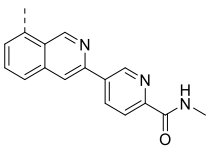	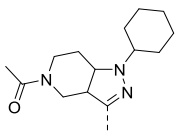	CBP: IC_{50} = 1 nmol/L; BRD4(1): IC_{50} = 3.1 μmol/L	32
35	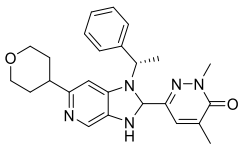 BRD4 Inhibitor-10	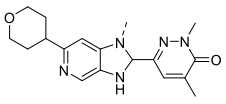	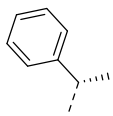	BRD4(BD1): IC_{50} = 8 nmol/L	33

36	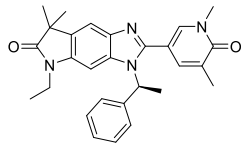	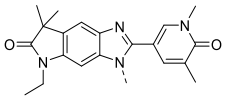	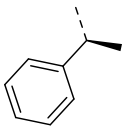	BRD4(1): IC_{50} = 1.3 nmol/L	33
37	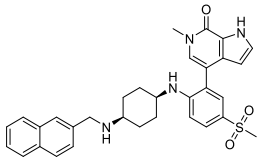	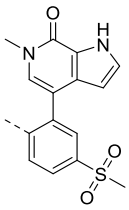	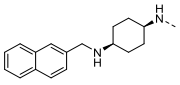	BRD4(1): K_i = 1.1 nmol/L; BRD4(2): K_i = 2.2 nmol/L; MX-1: EC_{50} = 10 nmol/L	34
Type 5: quinolines-based					
38	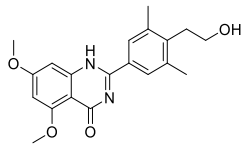 Rvx-208	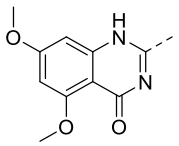	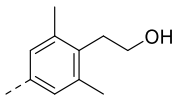	BRD4(BD1): IC_{50} = 87 μmol/L BRD4(BD2): IC_{50}=0.51 μmol/L	35
39	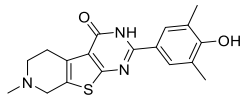 FL-411	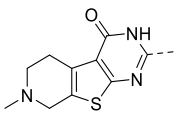	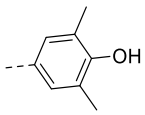	BRD4(1): IC_{50} = 0.43 μmol/L	36
40	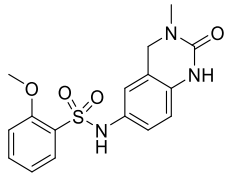	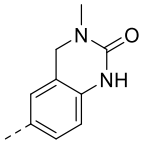	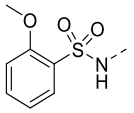	BRD4: IC_{50} = 0.22 μmol/L	37
41	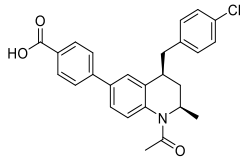 I-BET726	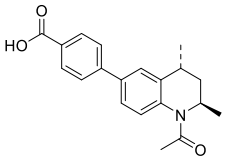	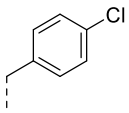	BRD4: IC_{50} = 22 nmol/L; BRD3: IC_{50} = 31 nmol/L; BRD2: IC_{50} = 41 nmol/L	38
42	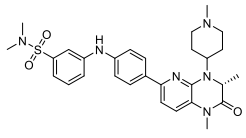	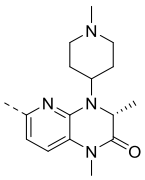	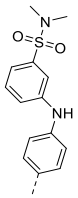	BRD4(1): IC_{50} < 100 nmol/L; BRD4(2): IC_{50} < 50 nmol/L	39
43	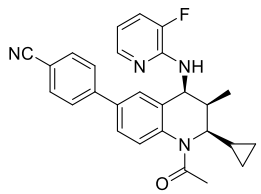	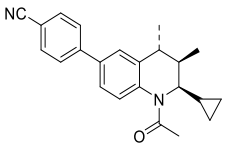	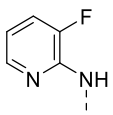	BRD4(2): IC_{50} < 100 nmol/L	39

44	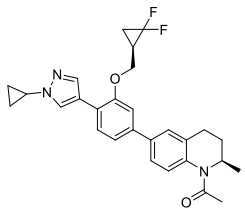	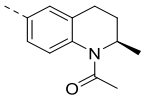	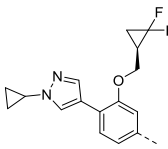	BRD4(1): IC_{50} = 20 nmol/L; BRD4(2): IC_{50} = 45 nmol/L	40
45	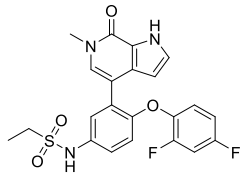 ABBV-075	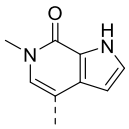	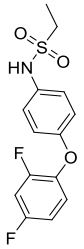	BET: IC_{50} = 1.5 nmol/L	41
46	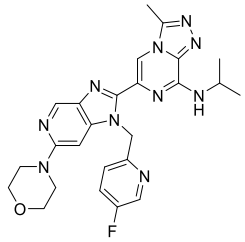	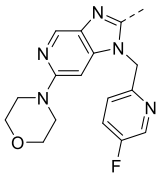	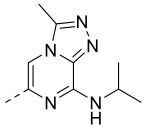	BRD4(BD1): IC_{50} = 1 nmol/L	42
47	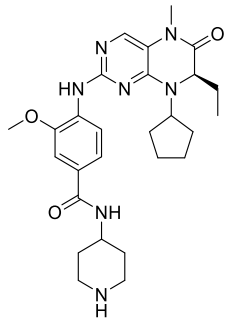 Bi-2536	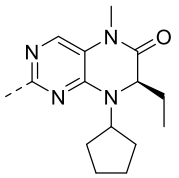	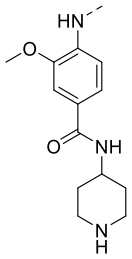	PLK1: IC_{50} = 0.83 nmol/L; BRD4: IC_{50} = 25 nmol/L	43
48	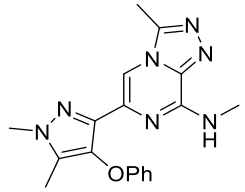	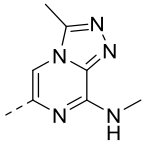	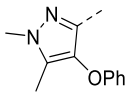	BRD4(BD1): IC_{50} = 1 nmol/L	44
49	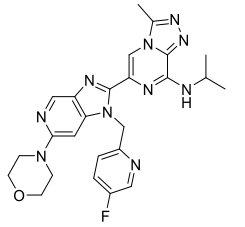	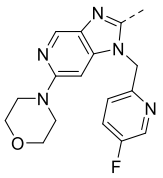	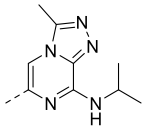	BRD4(BD1): IC_{50} = 3 nmol/L	45

Type 6: triazolopyridine-based

50	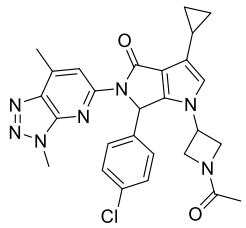	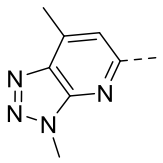	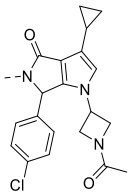	BRD4: IC_{50} < 11 nmol/L; MV4-11: GI_{50} = 0.1 nmol/L	46
51	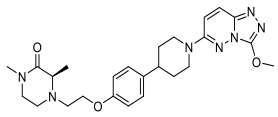	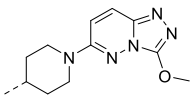	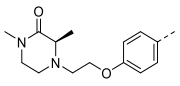	BRD4: IC_{50} =1.7 nmol/L	47
52	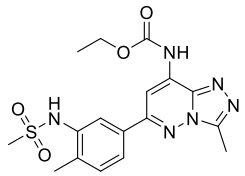 Bromosporine	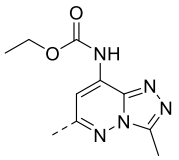	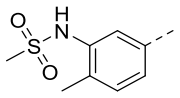	BRD2: IC_{50} = 410 nmol/L; BRD4: IC_{50} = 290 nmol/L	48
53	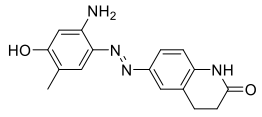 diazene	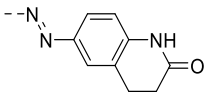	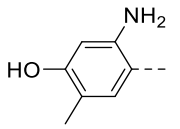	BRD4(BD1): IC_{50} = 27 nmol/L BRD4(BD2): IC_{50} = 32 nmol/L	49
54	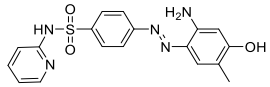 MS436	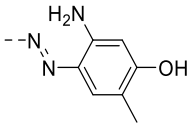	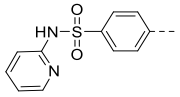	BRD4: K_i = 30–50 nmol/L	50
55	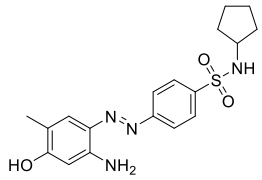 ZL0454	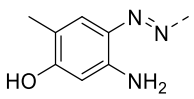	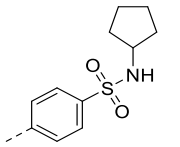	BRD4(BD1): IC_{50} = 49 nmol/L BRD4(BD2): IC_{50} = 32 nmol/L	51
Type 7: 4-acyl pyrrole-based					
56	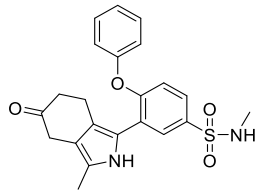	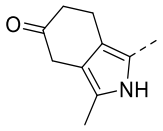	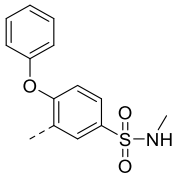	BRD4(BD1): IC_{50} = 15 nmol/L BRD4(BD2): IC_{50} = 43 nmol/L	52
57	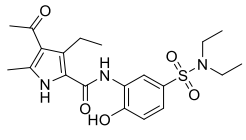	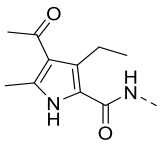	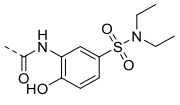	BRD4(1): K_d = 237 nmol/L	53

58	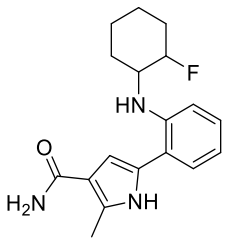	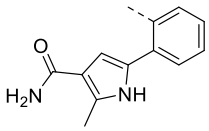	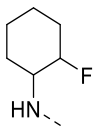	BRD4(1): K_i = 38 nmol/L; BRD4(2): K_i = 225 nmol/L; MX-1: EC_{50} = 433 nmol/L	54
Type 8: 2-thiazolidinone-based					
59	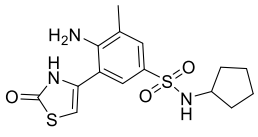	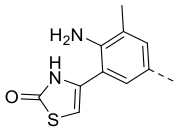	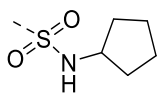	BRD4(BD1): IC_{50} = 0.79 μmol/L	55
60	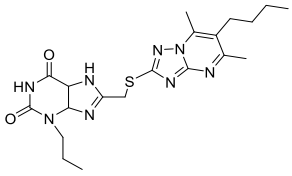	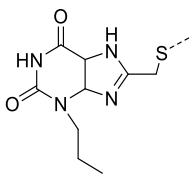	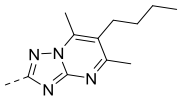	BRD4(1): IC_{50} = 2.33 μmol/L	56
Others					
61	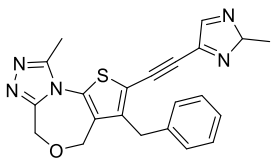	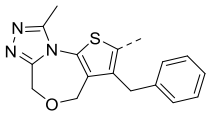	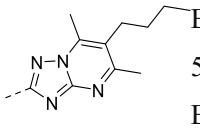	BRD4(1): IC_{50} = 5.0 μmol/L; BRD2/3: IC_{50} > 50 μmol/L Jurkat T cell: EC_{50} =27 μmol/L	56
62	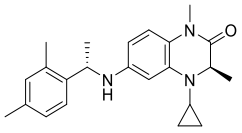	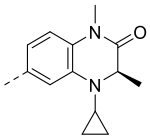	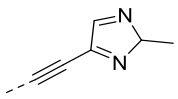	BRD4(1): IC_{50} = 10nmol/L; K_i = 2.3 nmol/L	57
63	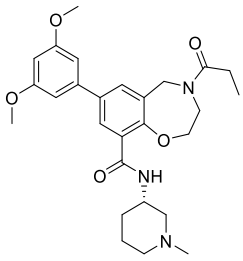	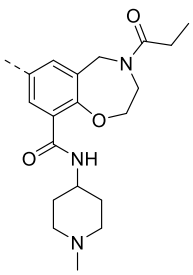	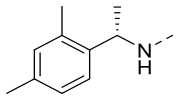	BRD4(BD1): IC_{50} = 52 nmol/L	58
TPOP146					
64	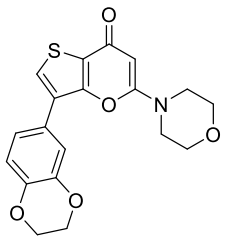	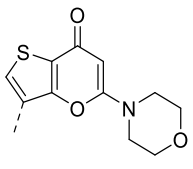	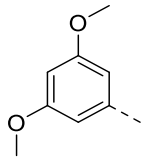	BRD4: IC_{50} = 5.02 μmol/L; CBP: IC_{50} = 134 nmol/L	59
SF2523					

65	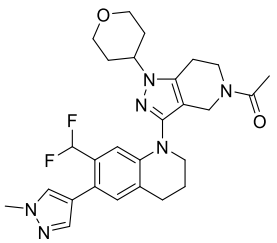 GNE-049	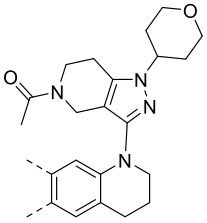	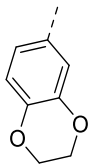	PI3Kα: IC_{50} = 34 nmol/L; PI3Kγ: IC_{50} = 158 nmol/L; BRD4(BD1): IC_{50} =241 nmol/L; mTOR: IC_{50} = 280 nmol/L	60
66	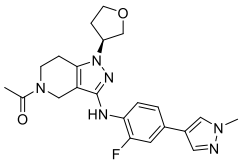	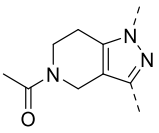	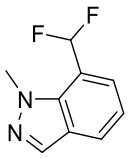	BRD4(BD1): IC_{50} = 4.2 μmol/L; BRET: IC_{50} = 12 nmol/L	61
67	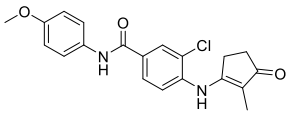	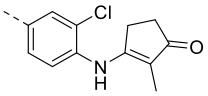	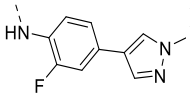	BRD4: IC_{50} = 13 μmol/L; EP300: IC_{50}=0.03 μmol/L	62
68	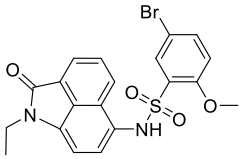	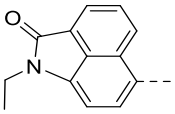	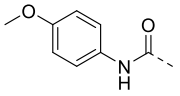	BRD4(BD1): *K*i = 77 nmol/L; BRD4(BD2): *K*i = 718 nmol/L	63
69	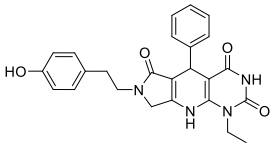	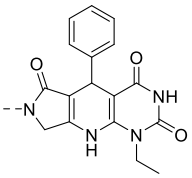	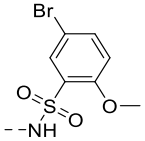	BRD4(1): IC_{50} = 410 nmol/L; BRD4(1): K_d = 130 nmol/L	64
70	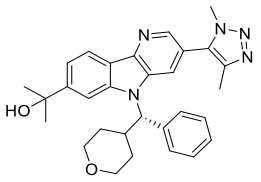 BMS-986158	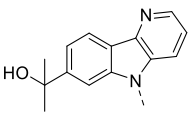	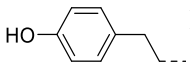	BRD4(1): K_i = 110 nmol/L; BRDT(1): K_i = 200 nmol/L	65
71	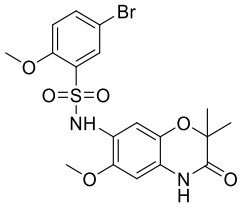	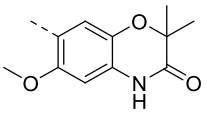	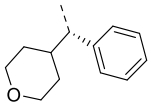	BRD4(1): K_i = 155 nmol/L	66

References

1. Filippakopoulos P, Qi J, Picaud S, Shen Y, Smith WB, Fedorov O, et al. Selective inhibition of BET bromodomains. *Nature* 2010;**468**:1067-73.
2. Albrecht BK, Gehling VS, Hewitt MC, Vaswani RG, Côté A, Leblanc Y, et al. Identification of a benzoisoxazoloazepine inhibitor (CPI-0610) of the bromodomain and extra-terminal (BET) family as a candidate for human clinical trials. *J Med Chem* 2016;**59**:1330–9.
3. Siegel SSB, Cleve A, Haendler B, Fernandez AM. Montalvan U, Krause S, et al. Bicyclo 2,3-benzodiazepines and spirocyclically substituted 2,3-benzodiazepines. WO2014128067 A1, 2014 Aug 28.
4. Schmees NK, Haendler J, Neuhaus B, Lejeune R, Fernandez-Montalvan M, Künzer AE, et al. BET protein-inhibiting 5-aryl triazole azepines. WO2014048945 A1, 2014 Apr 3.
5. Hewitt MC, Leblanc Y, Gehling VS, Vaswani RG, Cote A, Nasveschuk CG, et al. Development of methyl isoxazoleazepines as inhibitors of BET. *Bioorg Med Chem Lett* 2015;**25**:1842–8.
6. Mahe M, Dufour F, Neyret-Kahn H, Moreno-Vega A, Beraud C, Shi M, et al. An FGFR3/MYC positive feedback loop provides new opportunities for targeted therapies in bladder cancers. *EMBO Mol Med* 2018;**10**:4.
7. Nicodeme E, Jeffrey KL, Schaefer U, Beinke S, Dewell S, Chung CW, et al. Suppression of inflammation by a synthetic histone mimic. *Nature* 2010;**468**:1119–23.
8. Asangani IA, Kraut N. Therapeutic targeting of BET bromodomain proteins in castration-resistant prostate cancer. *Nature* 2014;**510**:278–82.
9. Vázquez R, Riveiro ME, Astorgues-Xerri L, Odore E, Rezai K, Erba E, et al. The bromodomain inhibitor OTX015 (MK-8628) exerts anti-tumor activity in triple-negative breast cancer models as single agent and in combination with everolimus. *Oncotarget* 2017;**8**:7598–613.
10. Zhang G, Liu R, Zhong Y, Plotnikov AN, Zhang W, Zeng L, et al. Down-regulation of NF-*κ*B transcriptional activity in HIV-associated kidney disease by BRD4 inhibition. *J Biol Chem* 2012;**287**:28840–51.
11. Devaiah BN, Lewis BA, Cherman N, Hewitt MC, Albrecht BK, Robey PG, et al. BRD4 is an atypical kinase that phosphorylates serine2 of the RNA polymerase II carboxy-terminal domain. *Proc Natl Acad Sci U S A* 2012, **109**:6927–32.

12. Seal J, Lamotte Y, Donche F, Bouillot A, Mirguet O, Gellibert F, et al. Identification of a novel series of BET family bromodomain inhibitors: Binding mode and profile of I-BET151 (GSK1210151A). *Bioorg Med Chem Lett* 2012;**22**:2968–72.
13. Chaidos A, Caputo V, Gouvedenou K, Liu B, Marigo I, Chaudhry MS, et al. Potent antimyeloma activity of the novel bromodomain inhibitors I-BET151 and I-BET762. *Blood* 2014;**123**:697–705.
14. Ali I, Lee J, Go A, Choi G, Lee K. Discovery of novel [1,2,4]triazolo[4,3-*a*]quinoxaline aminophenyl derivatives as BET inhibitors for cancer treatment. *Bioorg Med Chem Lett* 2017;**27**:4606–13.
15. Hewings DS, Fedorov O, Filippakopoulos P, Martin S, Picaud S, Tumber A, et al. Optimization of 3,5-dimethylisoxazole derivatives as potent bromodomain ligands. *J Med Chem* 2013;**56**:3217–27.
16. Bamborough P, Diallo H, Goodacre JD, Gordon L, Lewis A, Seal JT, et al. Fragment-based discovery of bromodomain inhibitors part 2: optimization of phenylisoxazole sulfonamides. *J Med Chem* 2012;**55**:587–96.
17. Ran X, Zhao Y, Liu L, Bai L, Yang CY, Zhou B, et al. Structure-based design of γ-carboline analogues as potent and specific BET bromodomain inhibitors. *J Med Chem* 2015, **58**;4927–39.
18. Wang L, Wu X, Wang R, Yang C, Li Z, Wang C, et al. BRD4 inhibition suppresses cell growth, migration and invasion of salivary adenoid cystic carcinoma. *Biol Res* 2017;**50**:19.
19. Ozer HG, El-Gamal D, Powell B, Hing ZA, Blachly JS, Harrington B, et al. BRD4 profiling identifies critical chronic lymphocytic leukemia oncogenic circuits and reveals sensitivity to PLX51107, a novel structurally distinct BET inhibitor. *Cancer Discov* 2018;**8**:458–77.
20. Zhou B, Hu J, Xu F, Chen Z, Bai L, Fernandez-Salas E, et al. Discovery of a small-molecule degrader of bromodomain and extra-terminal (BET) proteins with picomolar cellular potencies and capable of achieving tumor regression. *J Med Chem* 2018;**61**:462–81.
21. Yang Y, Zhao L, Xu B, Yang L, Zhang J, Zhang H, et al. Design, synthesis and biological evaluation of dihydroquinoxalinone derivatives as BRD4 inhibitors. *Bioorg Chem* 2016;**68**:236–44.

22. Zhang M, Zhang Y, Song M, Xue X, Wang J, Wang C, et al. Structure-based discovery and optimization of benzo[*d*]isoxazole derivatives as potent and selective BET inhibitors for potential treatment of castration-resistant prostate cancer (CRPC). *J Med Chem* 2018;**61**:3037–58.
23. Kharenko OA, Patel RG, Brown SD, Calosing C, White A, Lakshminarasimhan D, et al. Design and characterization of novel covalent bromodomain and extra-terminal domain (BET) inhibitors targeting a methionine. *J Med Chem* 2018;**61**:8202–11.
24. Xue X, Zhang Y, Wang C, Zhang M, Xiang Q, Wang J, et al. Benzoxazinone-containing 3,5-dimethylisoxazole derivatives as BET bromodomain inhibitors for treatment of castration-resistant prostate cancer. *Eur J Med Chem* 2018;**152**:542–59.
25. Zhao Y, Zhou B, Bai L, Liu L, Yang CY, Meagher JL, et al. Structure-based discovery of CF53 as a potent and orally bioavailable bromodomain and extra-terminal (BET) bromodomain inhibitor. *J Med Chem* 2018;**61**:6110–20.
26. Bui MH, Lin X, Albert DH, Li L, Lam LT, Faivre EJ, et al. Preclinical characterization of BET family bromodomain inhibitor ABBV-075 suggests combination therapeutic strategies. *Cancer Res* 2017;**77**: 2976–89.
27. Liu D, Pratt J, Wang L, Hasvold LA, Bogdan A. Bromodomain inhibitors. US20140256710, 2014 Feb 9.
28. Wang L, Pratt JK, Soltwedel T, Sheppard GS, Fidanze SD, Liu D, et al. Fragment-based, structure-enabled discovery of novel pyridones and pyridone macrocycles as potent bromodomain and extra-terminal domain (BET) family bromodomain inhibitors. *J Med Chem* 2017;**60**:3828–50.
29. Engelhardt HM, Smethurst L, Pyridinones C. WO2015022332 Al, 2015 Feb 19.
30. Vadivelu S, Rajagopal S.; Chinnapattu M, Gondrala PK, Sivanandhan D, Mulakala, C. Tricyclic fused derivatives of 1-(cyclo) alkyl pyridin-2-one useful for the treatment of cancer. WO2016157221 Al, 2016 Oct 6.
31. Liu DP, Wang J, Hasvold L, Bogdan ALA. Bromodomain inhibitors. US20140256710, 2014 Feb 8.
32. Lai KW, Romero FA, Tsui V, Beresini MH, de Leon Boenig G, Bronner SM, et al. Design and synthesis of a biaryl series as inhibitors for the bromodomains of CBP/P300. *Med Chem Lett* 2018;**28**:15–23.

33. Duan Y, Guan Y, Qin W, Zhai X, Yu B, Liu H. Targeting Brd4 for cancer therapy: inhibitors and degraders. *Medchemcomm* 2018;**9**:1779–802.
34. Engelhardt H. Benzimidazole derivatives. WO2015169962 A1, 2015 Nov 12.
35. Picaud S, Wells C, Felletar I, Brotherton D, Martin S, Savitsky P, et al. RVX-208, an inhibitor of BET transcriptional regulators with selectivity for the second bromodomain. *Proc Natl Acad Sci U S A* 2013;**110**:19754–9.
36. Ouyang L, Zhang L, Liu J, Fu L, Yao D, Zhao Y, et al. Discovery of a small-molecule bromodomain-containing protein 4 (BRD4) inhibitor that induces AMP-activated protein kinase-modulated autophagy-associated cell death in breast cancer. *J Med Chem* 2017;**60**:9990–10012.
37. Fish PV, Filippakopoulos P, Bish G, Brennan PE, Bunnage ME, Cook AS, et al. Identification of a chemical probe for bromo and extra C-terminal bromodomain inhibition through optimization of a fragment-derived hit. *J Med Chem* 2012;**55**:9831–7.
38. Gosmini R, Nguyen VL, Toum J, Simon C, Brusq JM, Krysa G, et al. The discovery of I-BET726 (GSK1324726A), a potent tetrahydroquinoline ApoA1 up-regulator and selective BET bromodomain inhibitor. *J Med Chem* 2014;**57**:8111–31.
39. Bair KWH, Kauffman T, Kayser-Bricker GS, Luke KJ, Martin GP, Millan MW, et al. Tetrahydroquinoline composition as BET bromodomain inhibitors. WO2015074064 A1, 2015 Jul 9.
40. Schmees NH, Stockigt B, Gallenkamp D, Bissell D, Bouglas RA. Modified BET-protein-inhibiting dihydroquinolones and dihydropyridopyrazinones. WO2015004075 Al, 2015 Jan 15.
41. Faivre EJ, Wilcox D, Lin X, Hessler P, Torrent M, He W, et al. Exploitation of castration-resistant prostate cancer transcription factor dependencies by the novel BET inhibitor ABBV-075. *Mol Cancer Res* 2017;**15**:35–44.
42. Engelhardt HG, Smethurst, DC. Substituted [1,2,4]triazolo[4,3-*a*]pyrazines as BRD4 inhibitors. US20160129001, 2016 May 12.
43. Chen L, Yap JL, Yoshioka M, Lanning ME, Fountain RN, Raje M, et al. BRD4 structure−activity relationships of dual PLK1 kinase/BRD4 bromodomain inhibitor BI-2536. *ACS Med Chem Lett* 2015;**6**:764–9.
44. Duan Y, Guan Y, Qin W, Zhai X, Yu B, Liu H. Targeting Brd4 for cancer therapy: inhibitors and degraders. *Medchemcomm.* 2018;**9**:1779–802.

45. Engelhardt H, Gianni D, Smethurst C. Substituted [1,2,4]triazolo[4,3-*a*]pyrazines as BRD4 inhibitors. US20160129001 Al, 2016 Jul 7.

46. Blank J, Bold G, Bordas V, Cotesta S, Guagnano V, Rueger H, et al. Pyrrolopyrrolone derivatives and their use as BET inhibitors. WO2015075665 Al, 2015 May 28.

47. Rhyasen GW, Hattersley MM, Yao Y, Dulak A, Wang W, Petteruti P, et al. AZD5153: a novel bivalent BET bromodomain inhibitor highly active against hematologic malignancies. *Mol Cancer Ther* 2016;**15**:2563–74.

48. Pan H, Lu P, Shen Y, Wang Y, Jiang Z, Yang X, et al. The bromodomain and extraterminal domain inhibitor bromosporine synergistically reactivates latent HIV-1 in latently infected cells. *Oncotarget* 2017;**8**:94104–16.

49. Liu Z, Tian B, Chen H, Wang P, Brasier AR, Zhou J. Discovery of potent and selective BRD4 inhibitors capable of blocking TLR3-induced acute airway inflammation. *Eur J Med Chem* 2018;**151**:450–61.

50. Zhang G, Plotnikov AN, Rusinova E, Shen T, Morohashi K, Joshua J, et al. Structure-guided design of potent diazobenzene inhibitors for the BET bromodomains. *J Med Chem* 2013;**56**:9251–64.

51. Hasvold LAL, Park D, Pratt CH, Sheppard JK, GS Wang, L. Isoindolinone derivative. WO2013158952 A1, 2013 Oct 24.

52. Hugle M, Lucas X, Weitzel G, Ostrovskyi D, Breit B, Gerhardt S, et al. 4-Acyl pyrrole derivatives yield novel vectors for designing inhibitors of the acetyl-lysine recognition site of BRD4(1). *J Med Chem* 2016;**59**:1518−30.

53. Hasvold LA, Pratt JK, Mcdaniel KF, Sheppard GS, Liu D, Elmore SW, et al. *Pyrrole amide inhibitors.* US20140275079 Al, 2014 Feb 15.

54. Zhao L, Cao D, Chen T, Wang Y, Miao Z, Xu Y, et al. Fragment-based drug discovery of 2-thiazolidinones as inhibitors of the histone reader BRD4 bromodomain. *J Med Chem* 2013;**56**:3833−51.

55. Raux B, Voitovich Y, Derviaux C, Lugari A, Rebuffet E, Milhas S, et al. Exploring selective inhibition of the first bromodomain of the human bromodomain and extra-terminal domain (BET) proteins. *J Med Chem* 2016;**59**:1634–41.

56. Liu J, Duan Z, Guo W, Zeng L, Wu Y, Chen Y, et al. Targeting the BRD4/FOXO3a/CDK6 axis sensitizes AKT inhibition in luminal breast cancer. *Nat Commun* 2018;**9**:5200.

57. Hu J, Wang Y, Li Y, Xu L, Cao D, Song S, et al. Discovery of a series of dihydroquinoxalin-2(1*H*)-ones as selective BET inhibitors from a dual PLK1-BRD4 inhibitor. *Eur J Med Chem*. 2017;**137**:176–95.

58. Popp TA, Tallant C, Rogers C, Fedorov O, Brennan PE, Müller S, et al. Development of selective CBP/P300 benzoxazepine bromodomain inhibitors. *J Med Chem* 2016;**59**:88.

59. Andrews FH, Singh AR, Joshi S, Smith CA, Morales GA, Garlich JR, et al. Dual-activity PI3K-BRD4 inhibitor for the orthogonal inhibition of MYC to block tumor growth and metastasis. *Proc Natl Acad Sci U S A* 2017;**114**: E1072–80.

60. Romero FA, Murray J, Lai KW, Tsui V, Albrecht BK, An L, et al. GNE-781, A highly advanced potent and selective bromodomain inhibitor of cyclic adenosine monophosphate response element binding protein, binding protein (CBP). *J Med Chem* 2017;**60**:9162–83.

61. Crawford TD, Romero FA, Lai KW, Tsui V, Taylor AM, de Leon Boenig G, et al. Discovery of a potent and selective *in vivo* probe (GNE-272) for the bromodomains of CBP/EP300. *J Med Chem* 2016;**59**:10549–63.

62. Cheung K, Lu G, Sharma R, Vincek A, Zhang R, Plotnikov AN, et al. BET N-terminal bromodomain inhibition selectively blocks Th17 cell differentiation and ameliorates colitis in mice. *Proc Natl Acad Sci U S A* 2017;**114**:2952–7.

63. Xue X, Zhang Y, Liu Z, Song M, Xing Y, Xiang Q, et al. Discovery of Benzo[*cd*]indol-2(1*H*)-ones as potent and specific BET bromodomain inhibitors: structure-based virtual screening, optimization, and biological evaluation. *J Med Chem* 2016;**59**:1565–79.

64. Ayoub AM, Hawk LML, Herzig RJ, Jiang J, Wisniewski AJ, Gee CT, et al. BET bromodomain inhibitors with one-step synthesis discovered from virtual screen. *J Med Chem* 2017;**60**:4805–17.

65. von Schaper E. Roche bets on bromodomains. *Nat Biotechnol* 2016;**34**:361−2.

66. Xiang Q, Zhang Y, Li J, Xue X, Wang C, Song M, et al. Y08060: A Selective BET inhibitor for treatment of prostate cancer. *ACS Med Chem Lett* 2018;**9**: 262–7.

2. NMR spectra

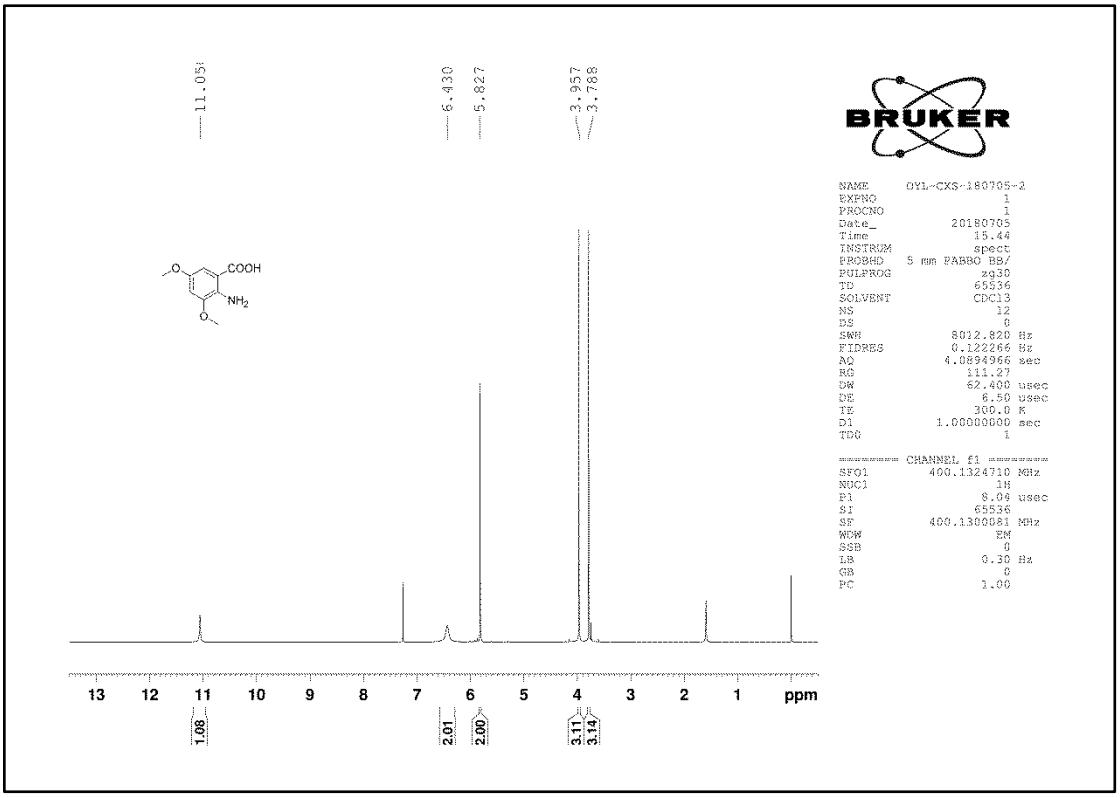

^{1}H NMR Spectrum of Compound **3a**

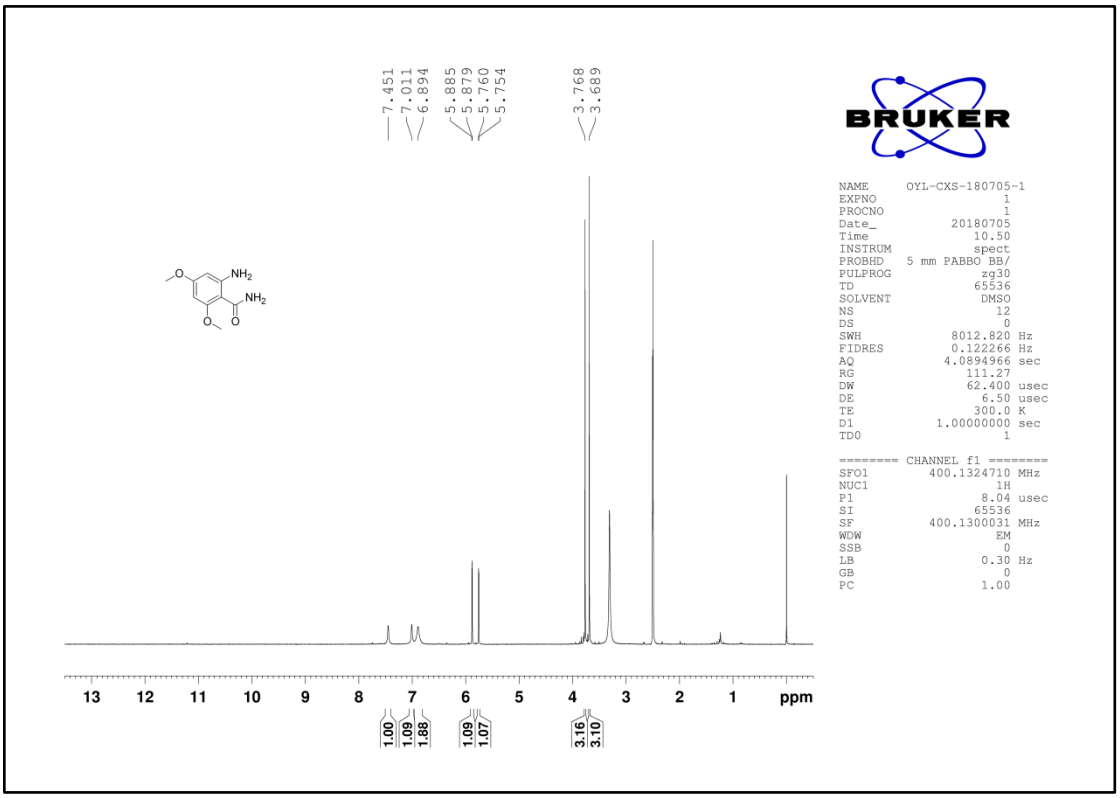

^{1}H NMR Spectrum of Compound **4a**

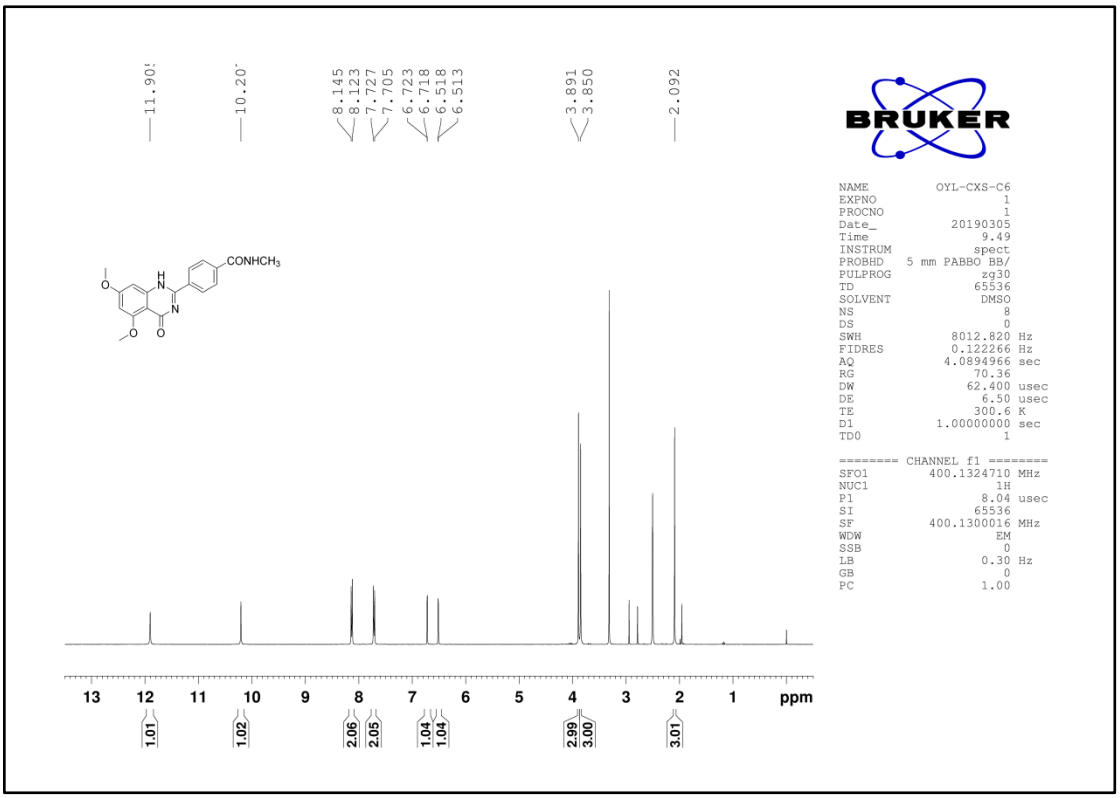

^{1}H NMR Spectrum of Compound **5a**

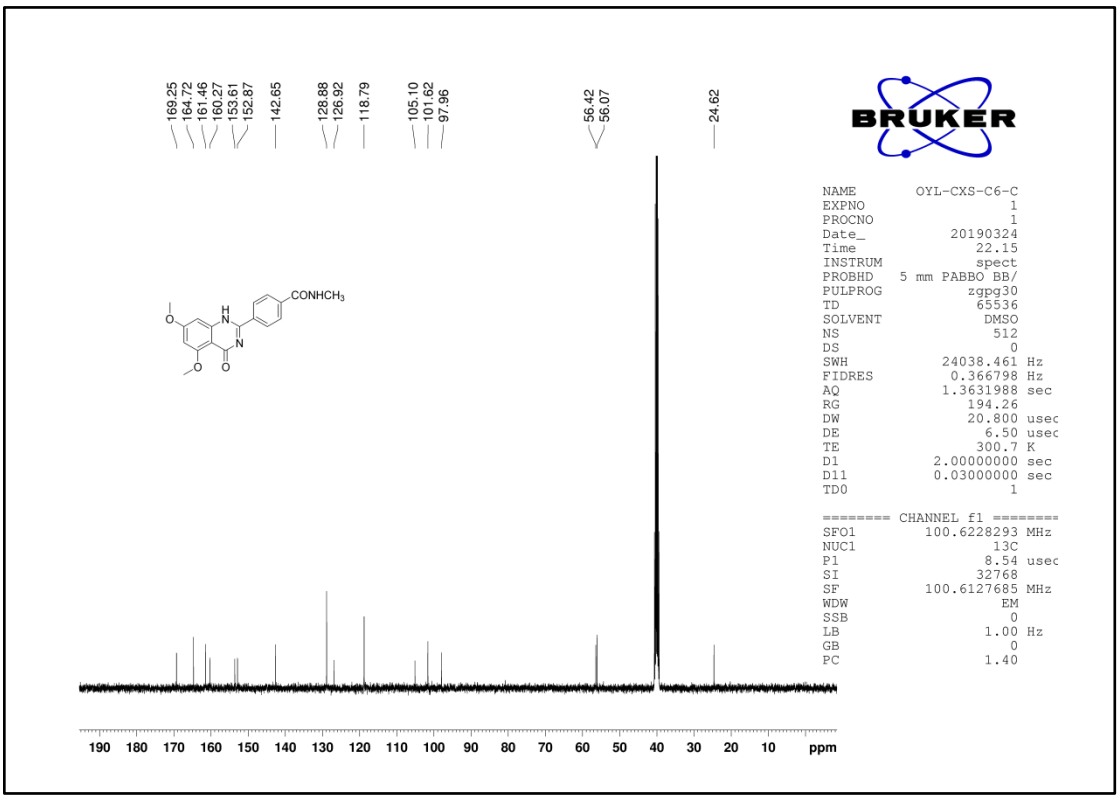

^{13}C NMR Spectrum of Compound **5a**

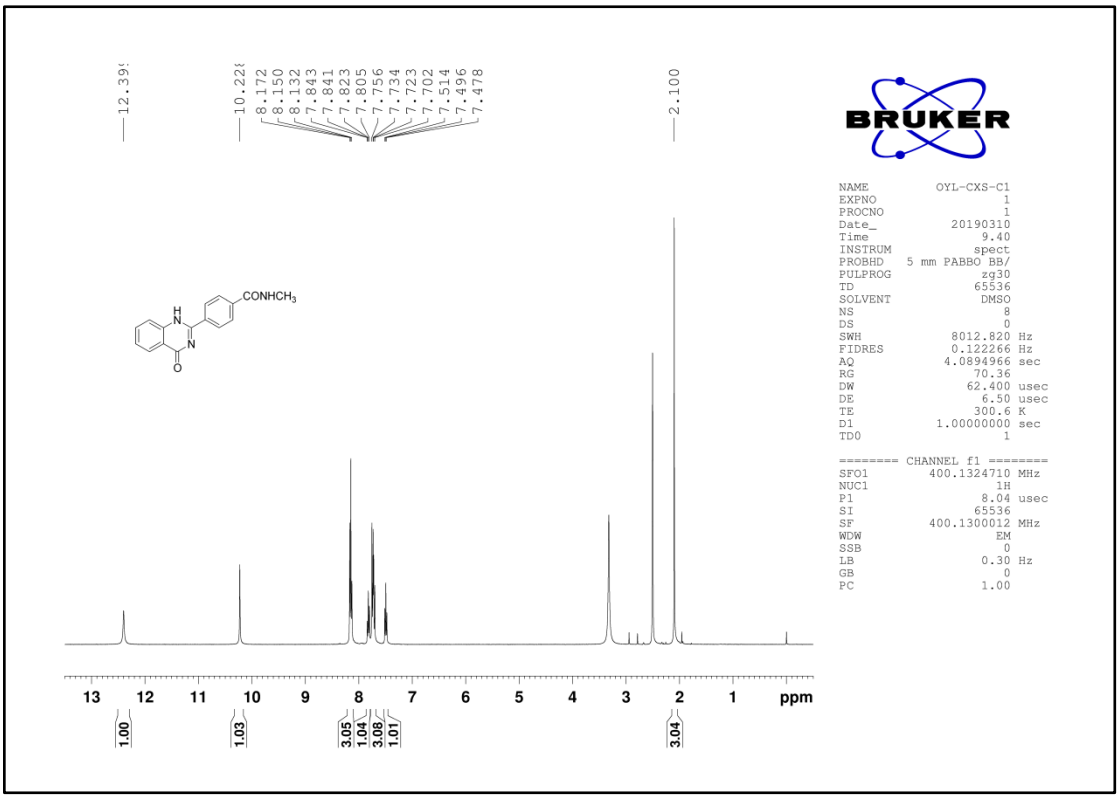

^{1}H NMR Spectrum of Compound **5b**

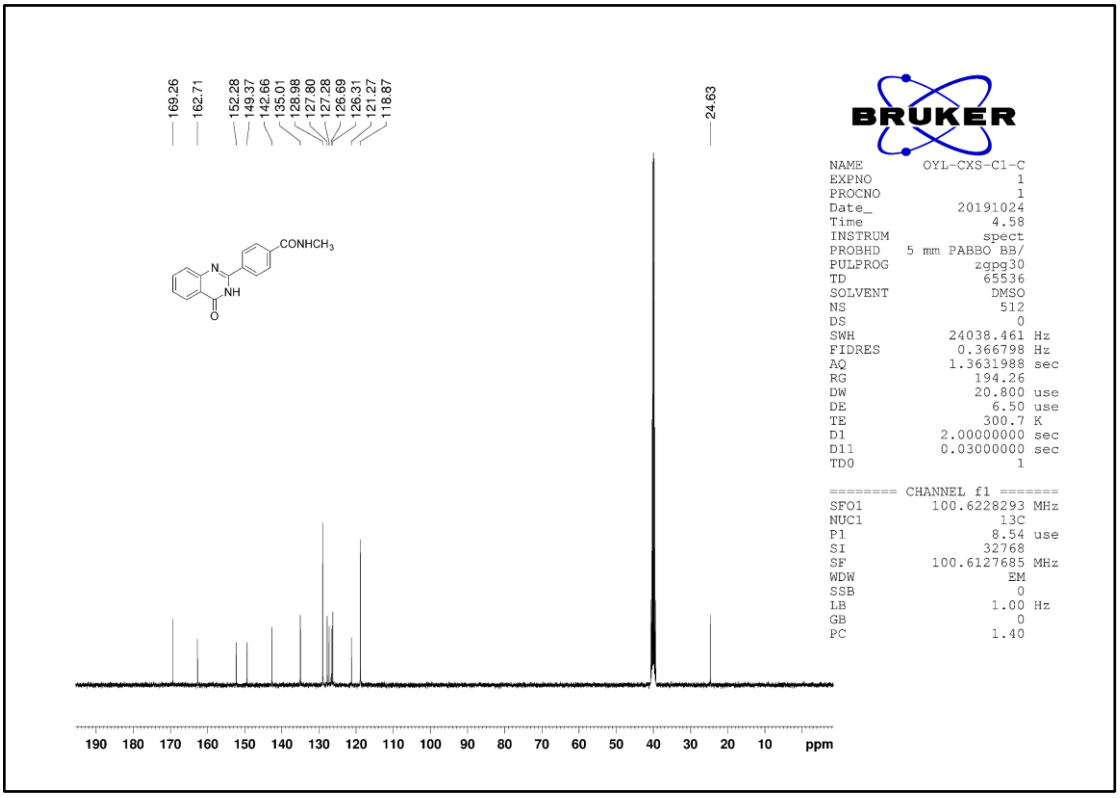

^{13}C NMR Spectrum of Compound **5b**

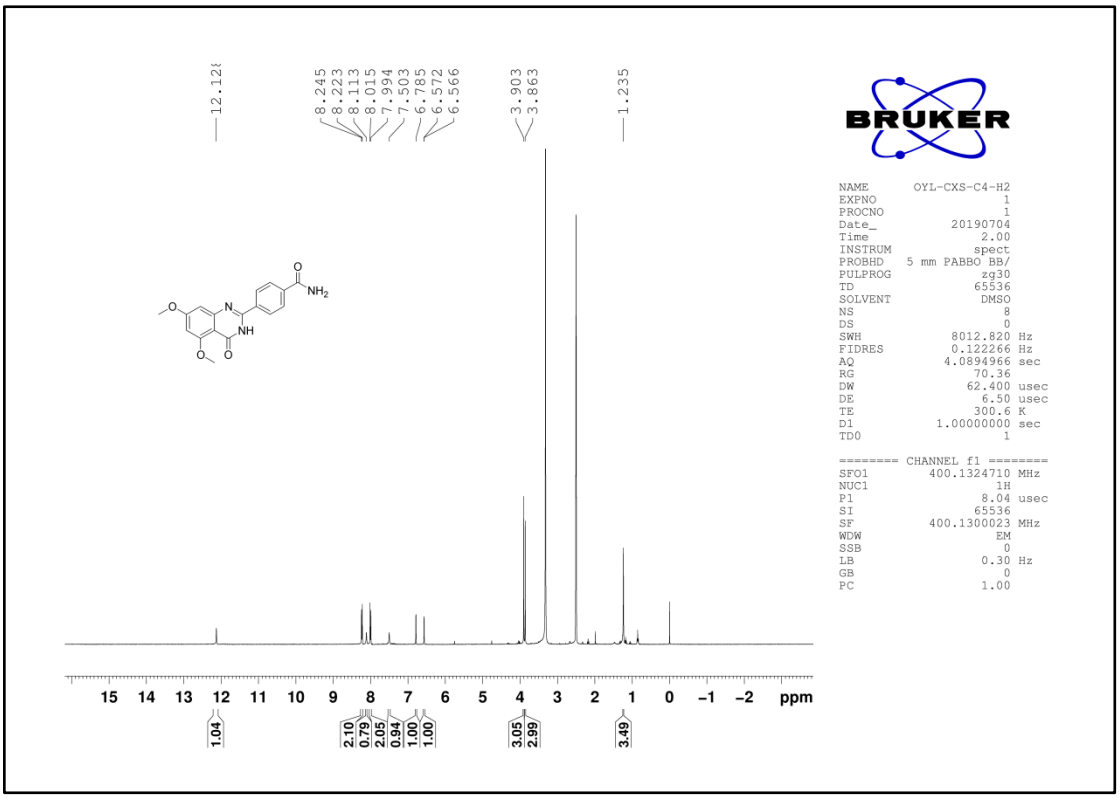

^{1}H NMR Spectrum of Compound **5c**

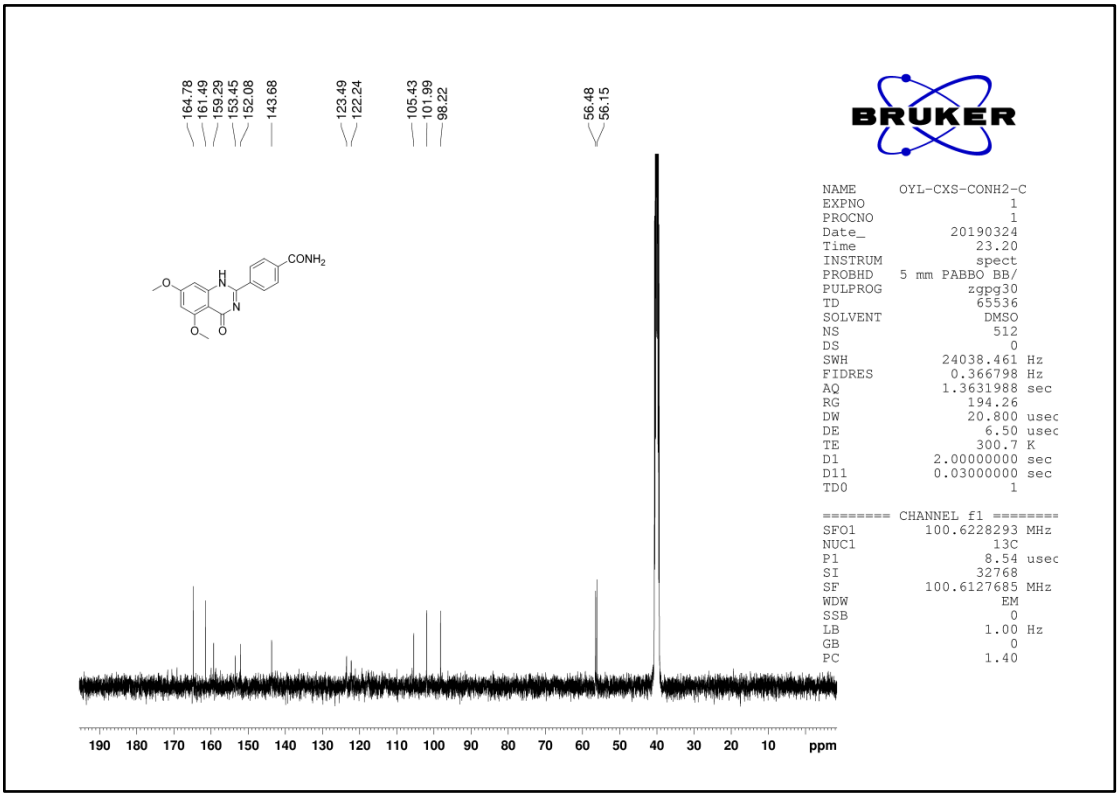

^{13}C NMR Spectrum of Compound **5c**

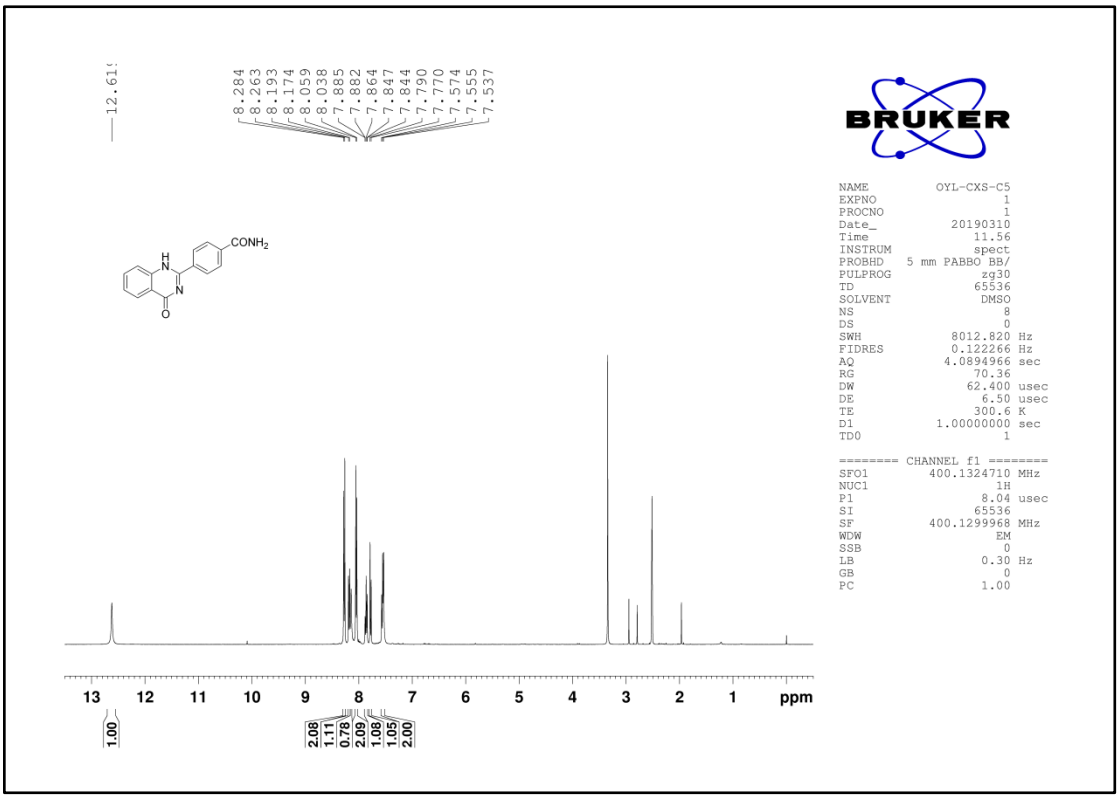

^{1}H NMR Spectrum of Compound **5d**

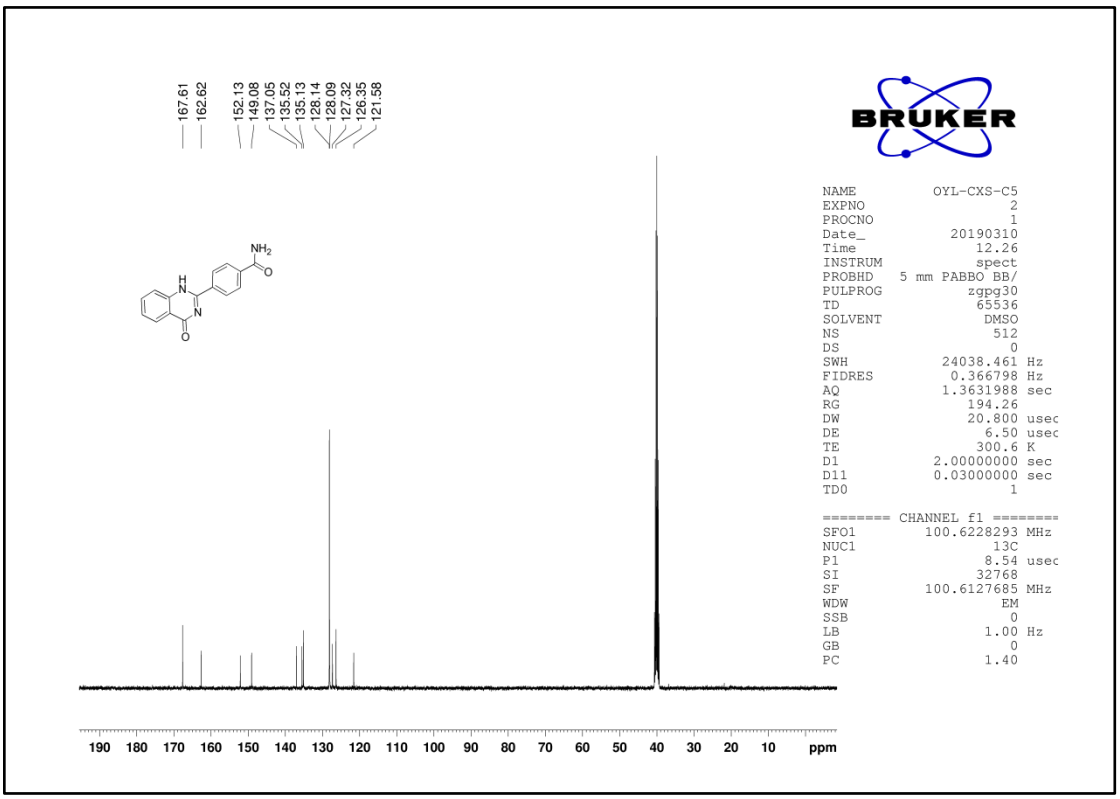

^{13}C NMR Spectrum of Compound **5d**

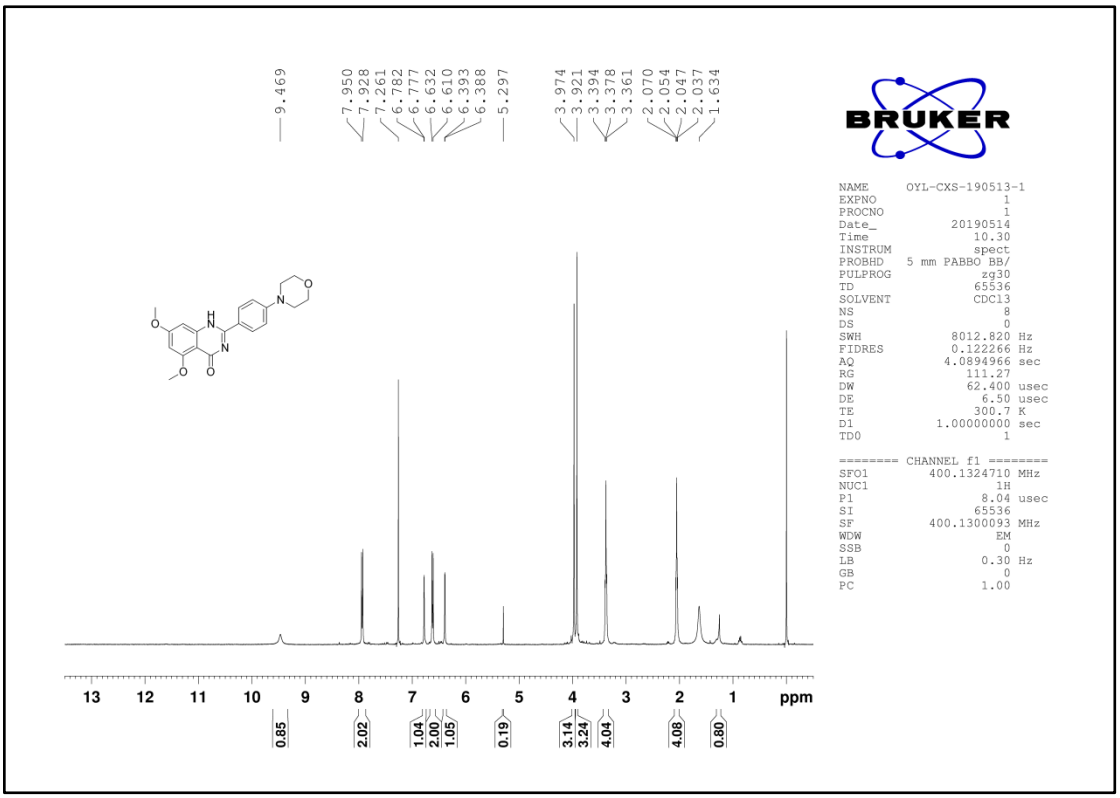

^{1}H NMR Spectrum of Compound **5e**

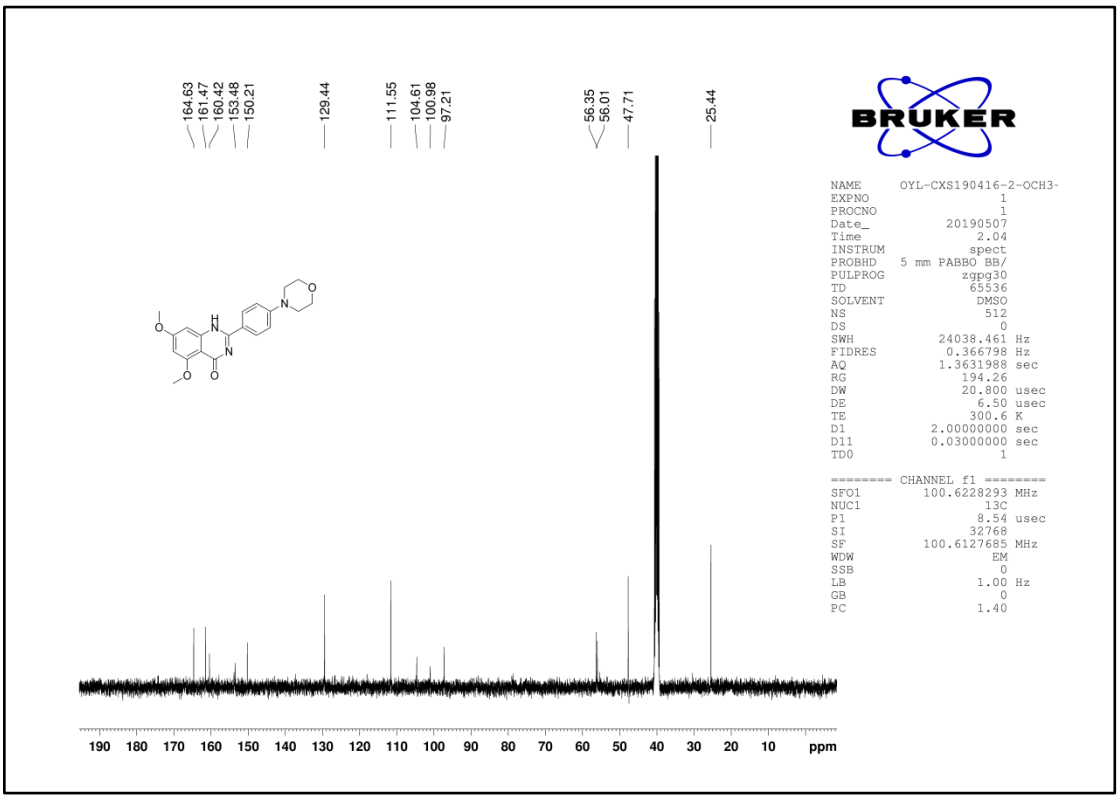

^{13}C NMR Spectrum of Compound **5e**

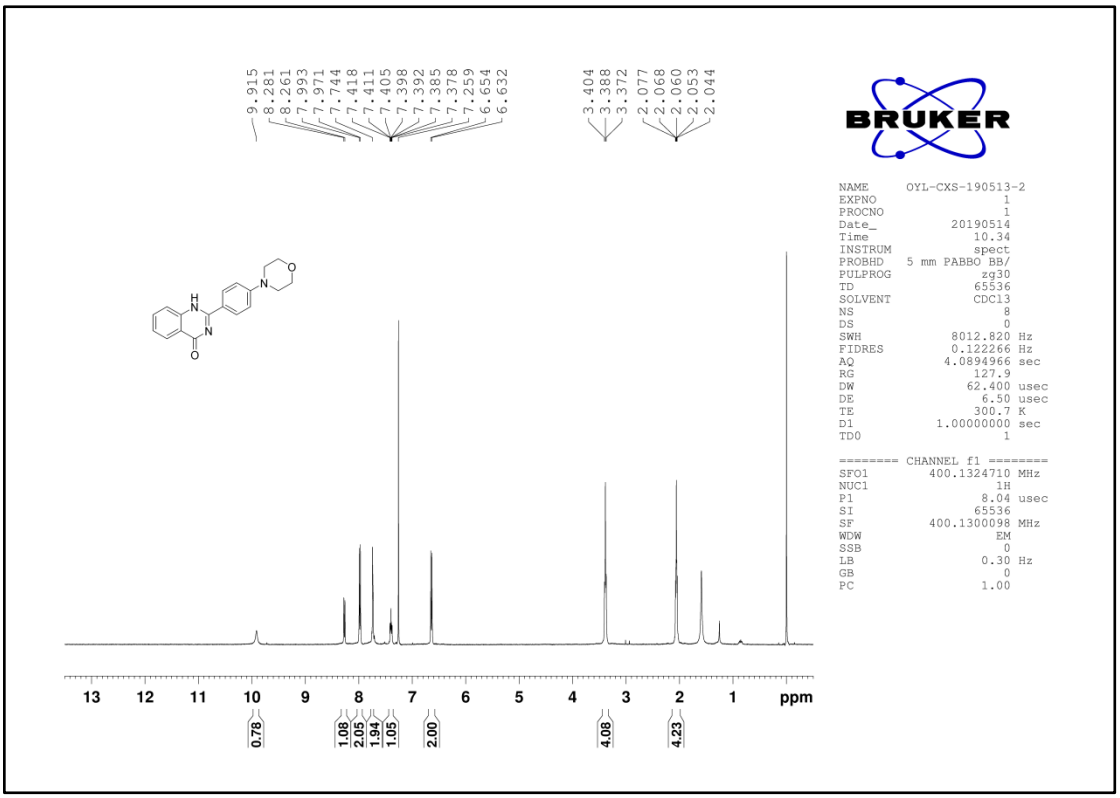

^{1}H NMR Spectrum of Compound **5f**

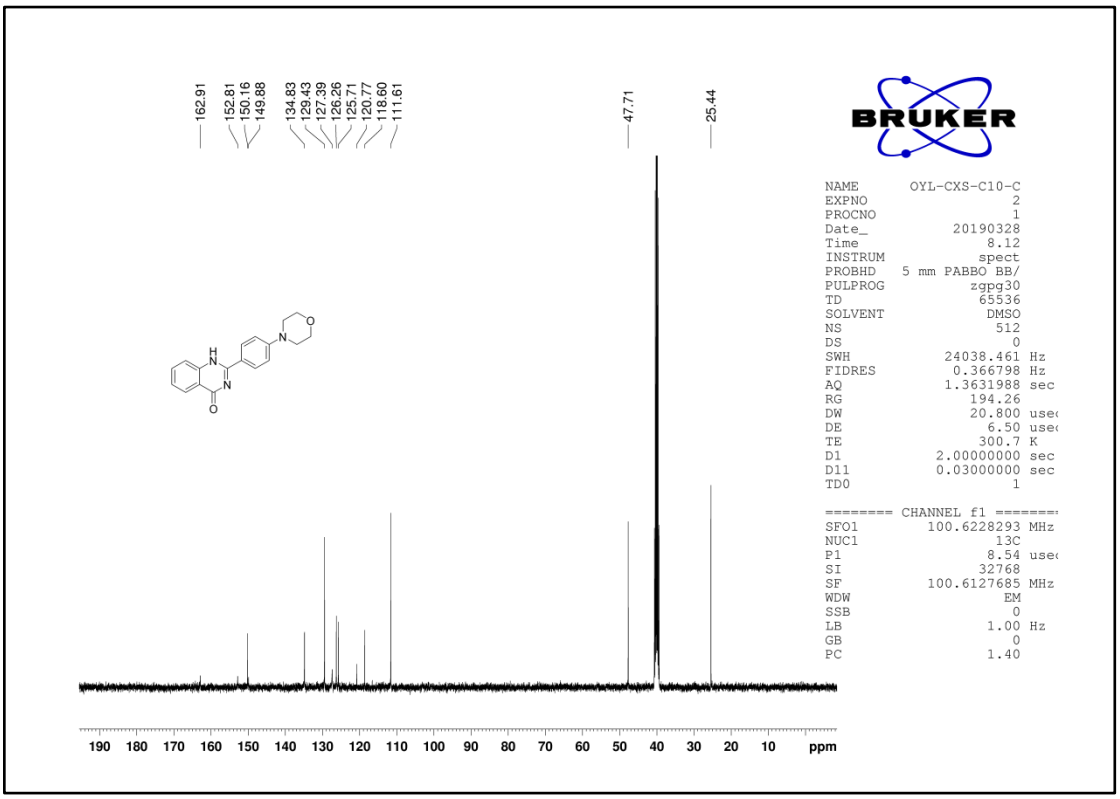

^{13}C NMR Spectrum of Compound **5f**

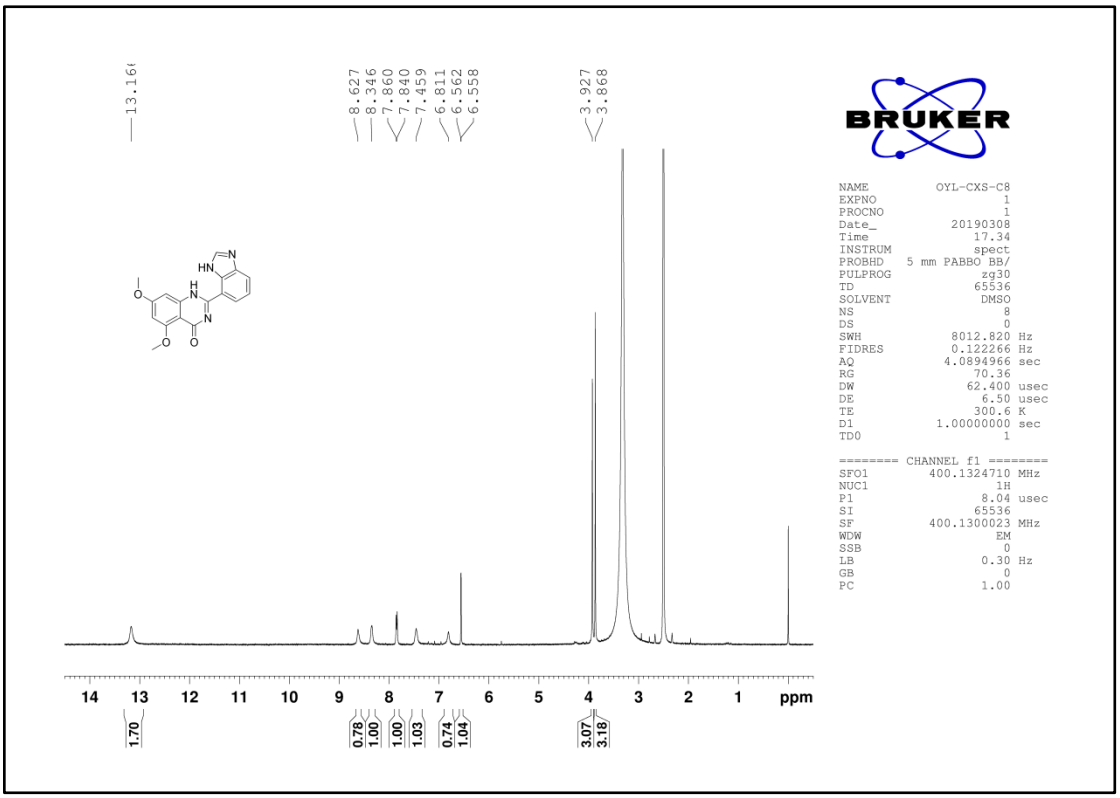

^{1}H NMR Spectrum of Compound **5g**

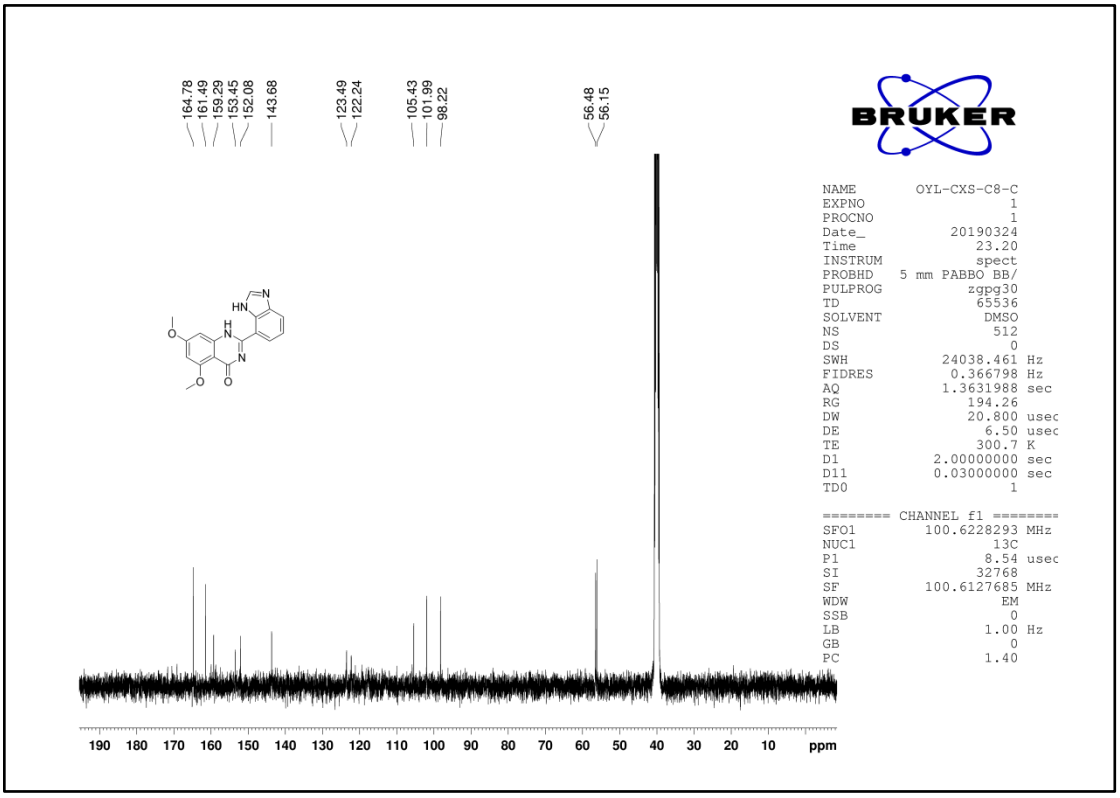

^{13}C NMR Spectrum of Compound **5g**

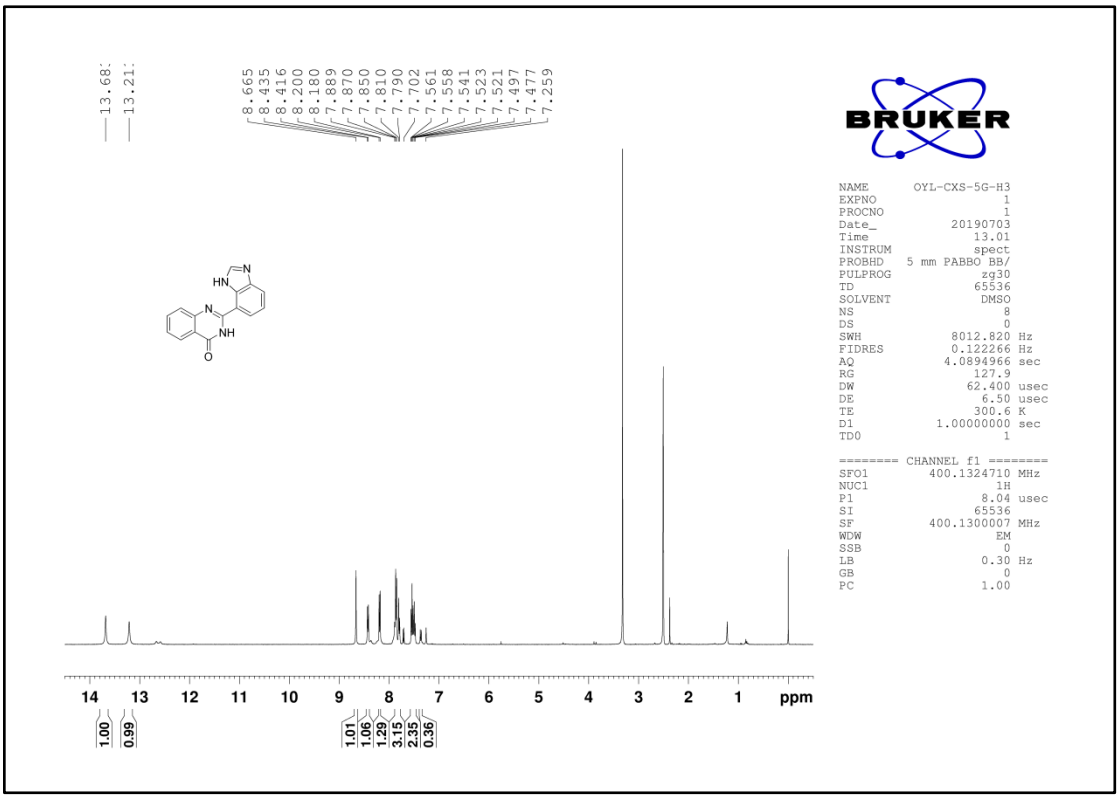

^{1}H NMR Spectrum of Compound **5h**

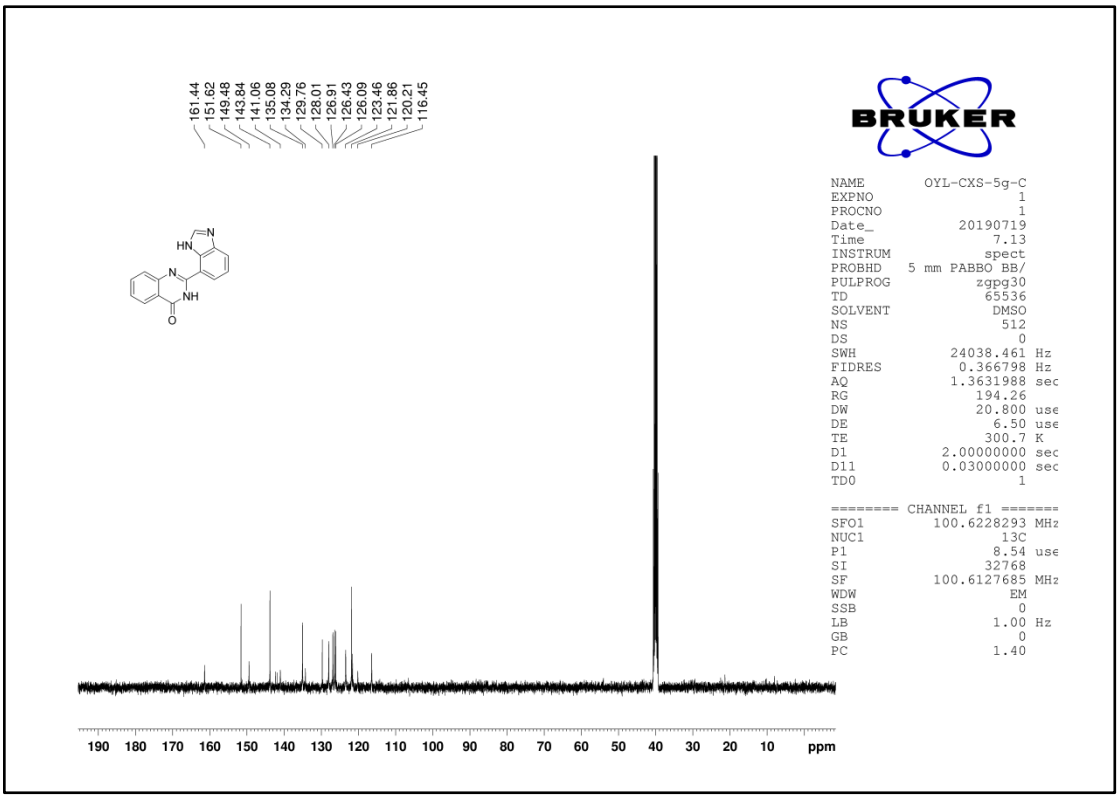

^{13}C NMR Spectrum of Compound **5h**

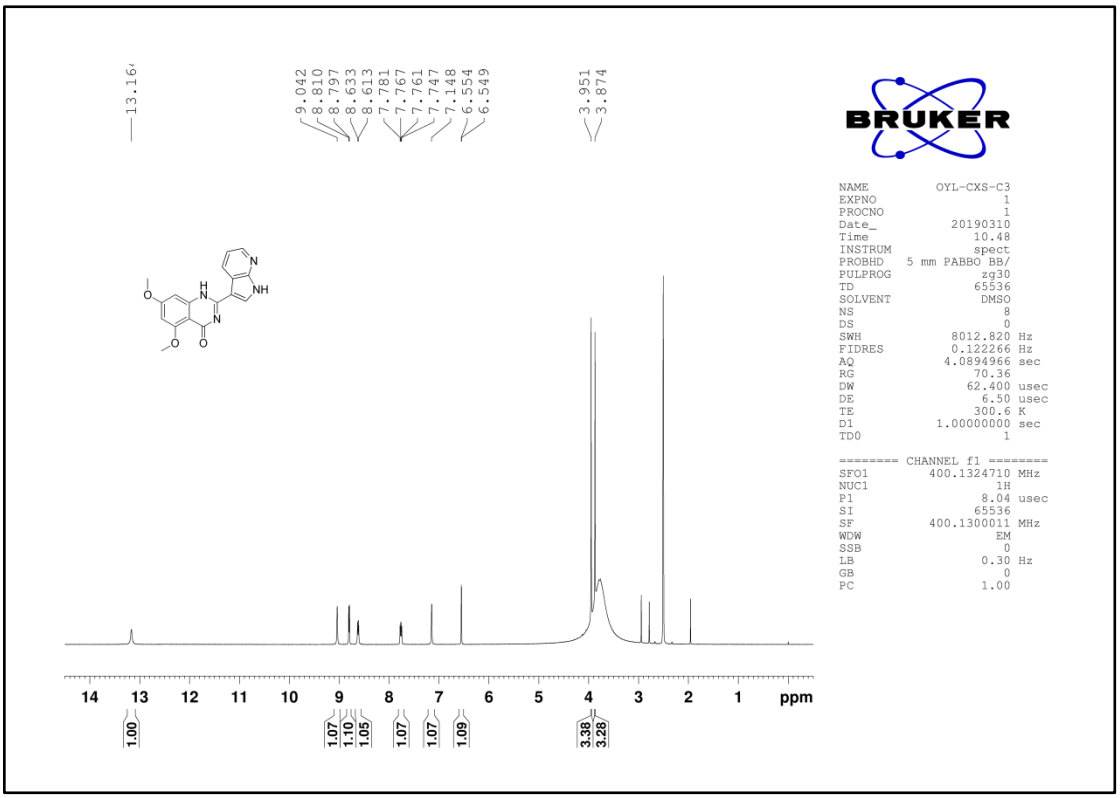

^{1}H NMR Spectrum of Compound **5i**

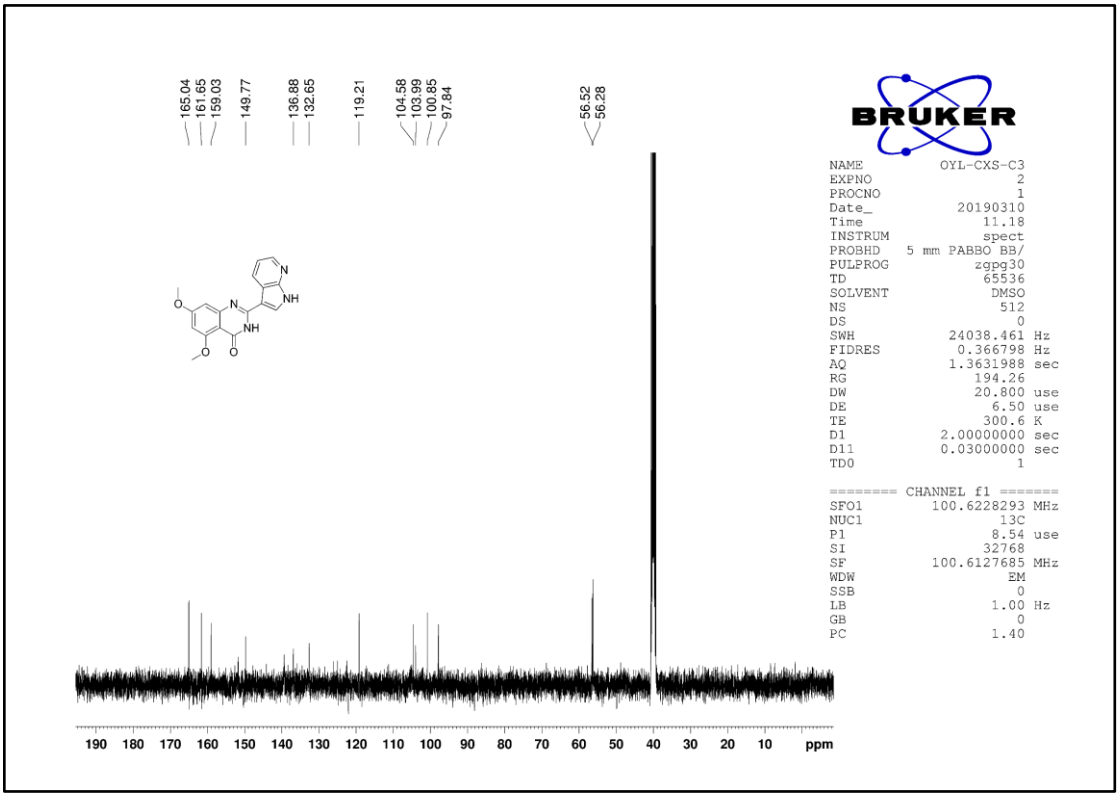

^{13}C NMR Spectrum of Compound **5i**

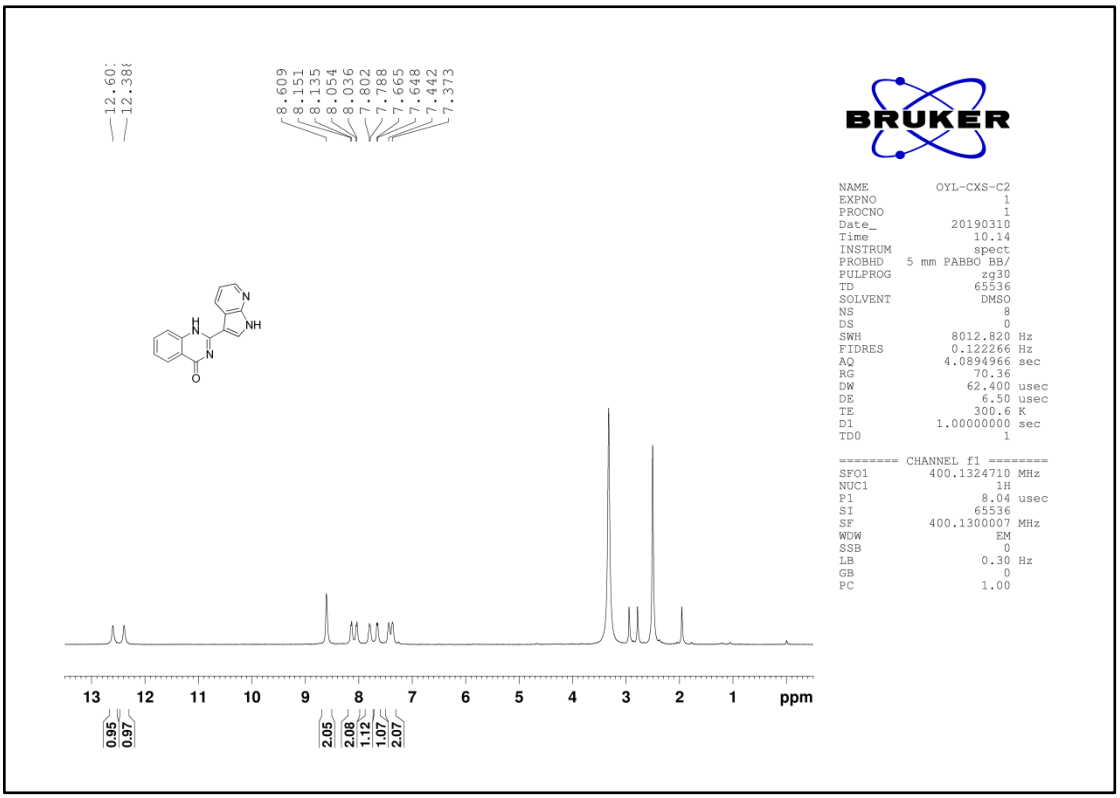

^{1}H NMR Spectrum of Compound **5j**

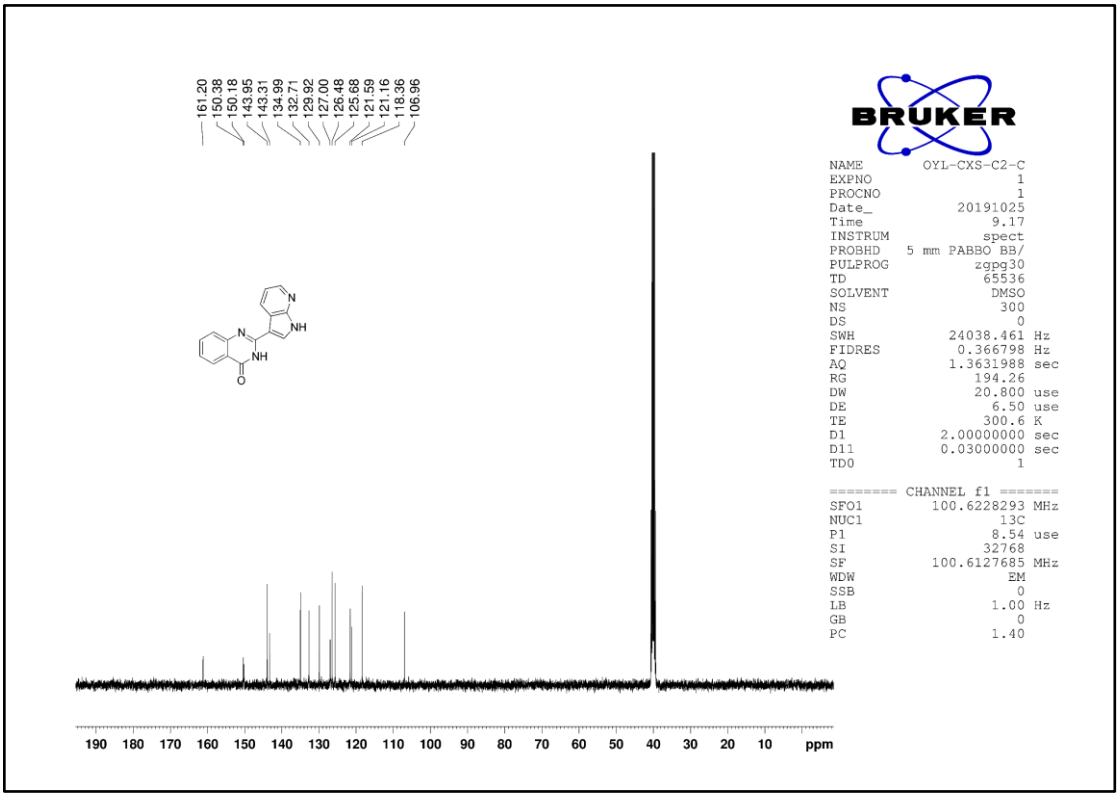

^{13}C NMR Spectrum of Compound **5j**

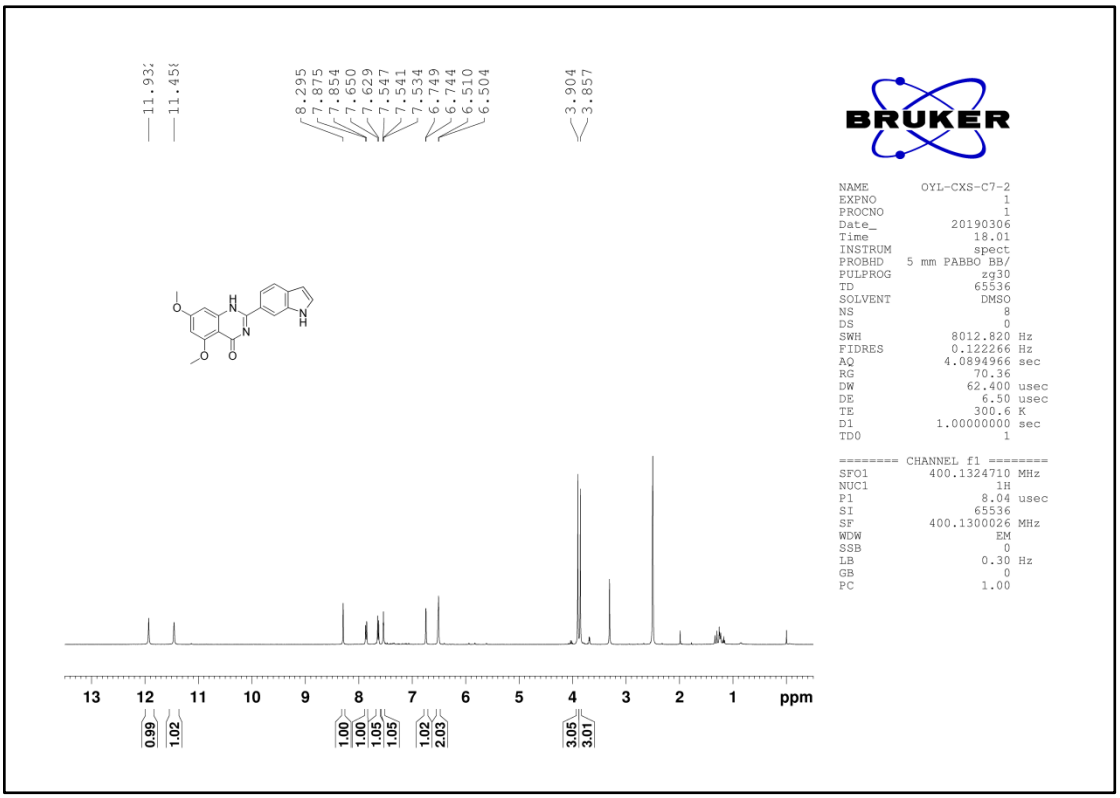

^{1}H NMR Spectrum of Compound **5k**

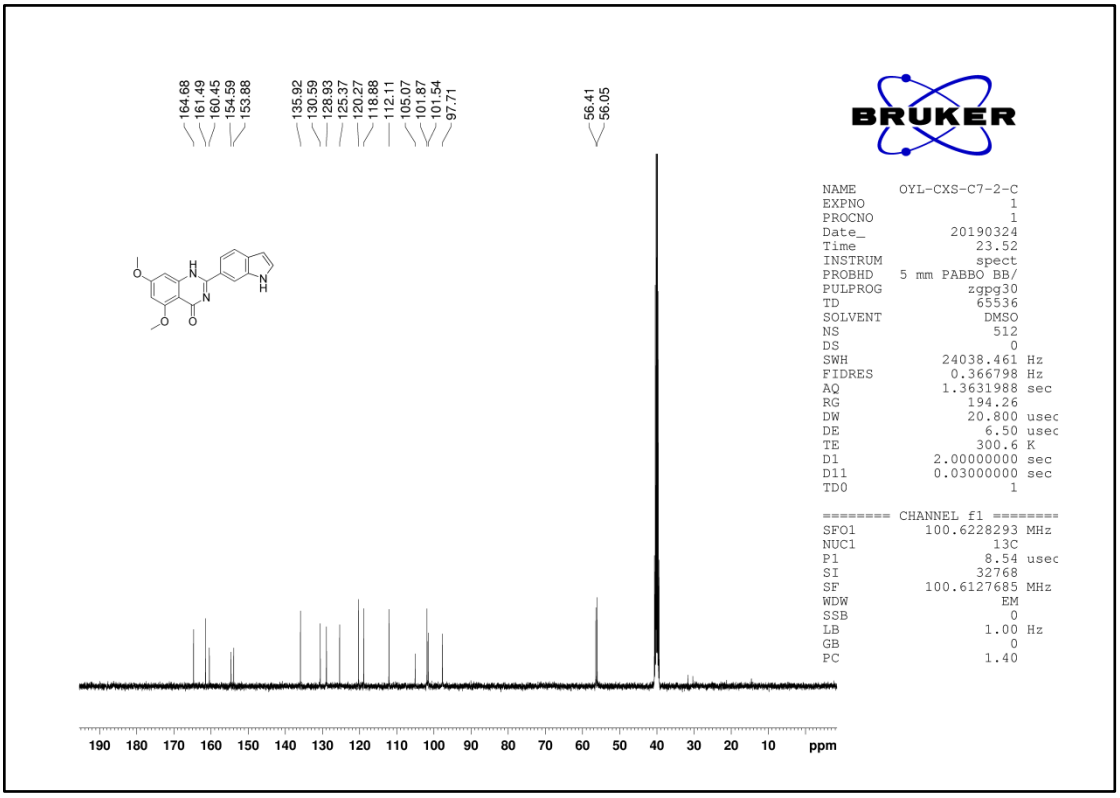

^{13}C NMR Spectrum of Compound **5k**

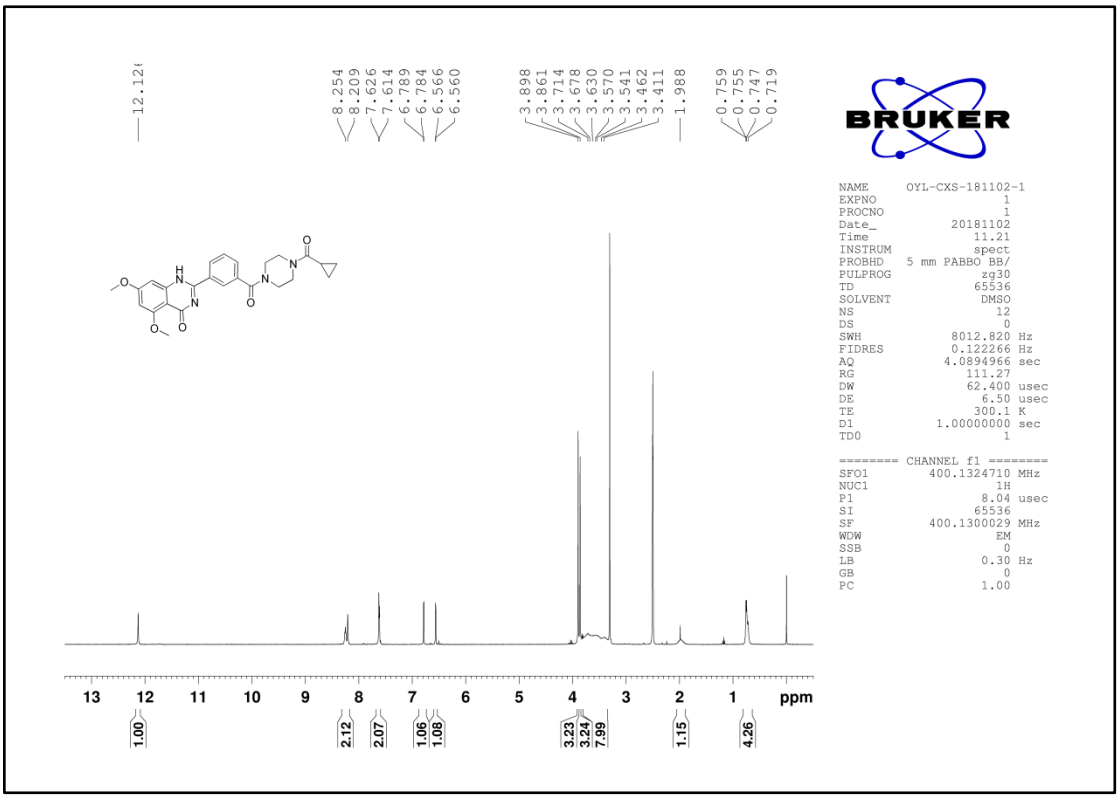

^{1}H NMR Spectrum of Compound **11a**

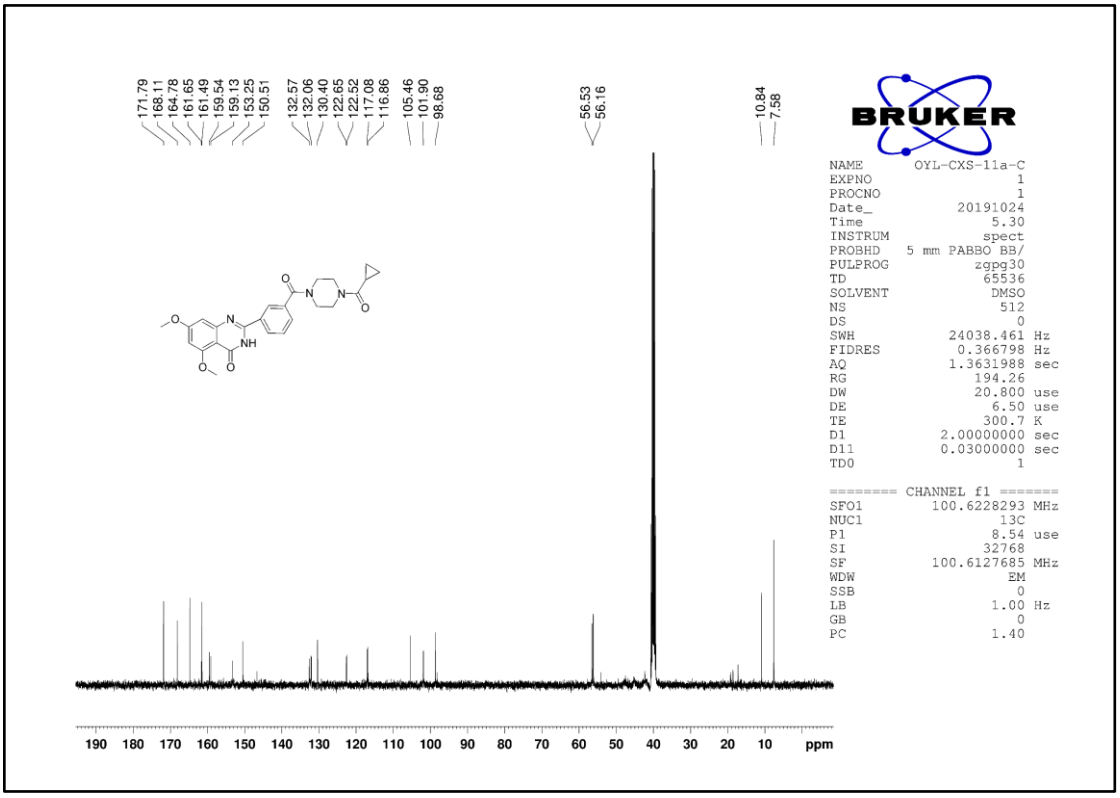

^{13}C NMR Spectrum of Compound **11a**

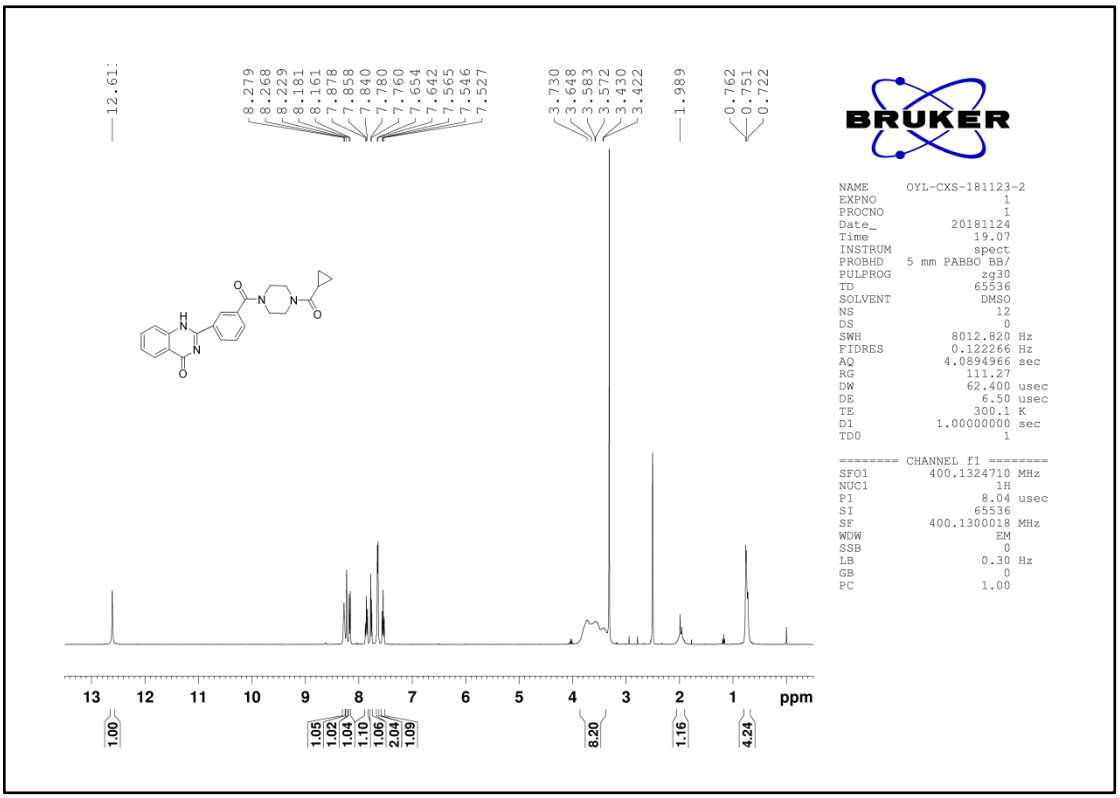

^{1}H NMR Spectrum of Compound **11b**

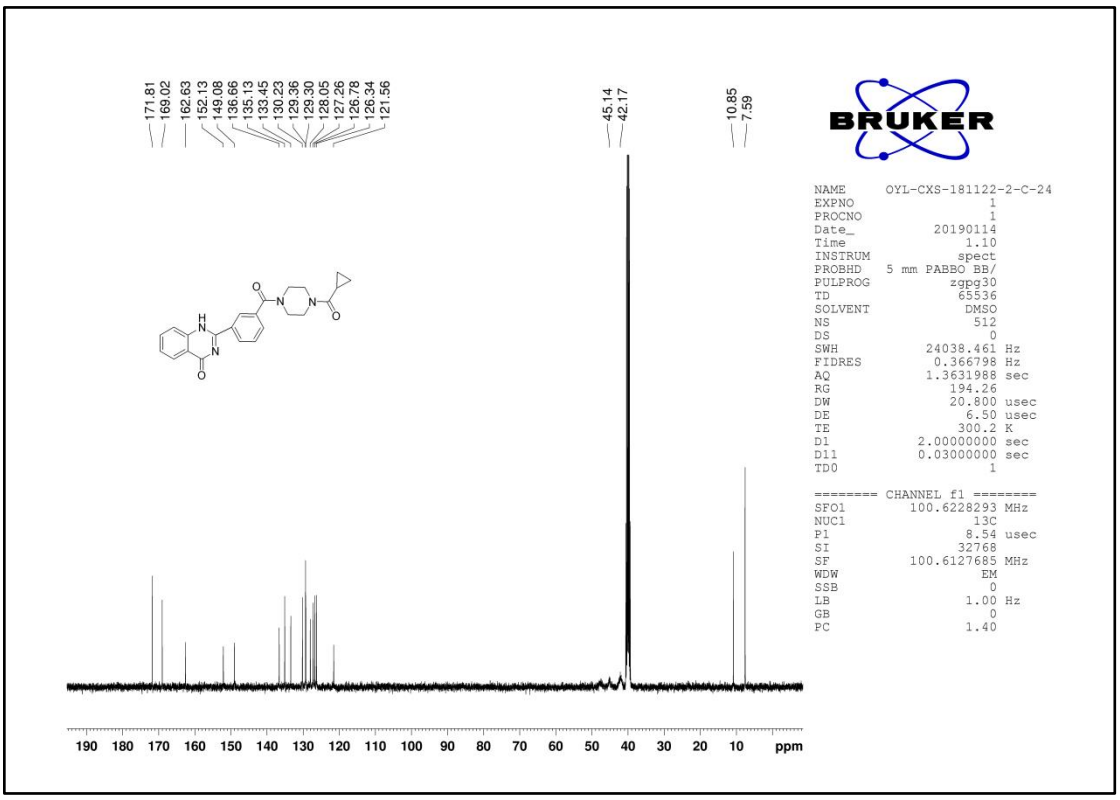

^{13}C NMR Spectrum of Compound **11b**

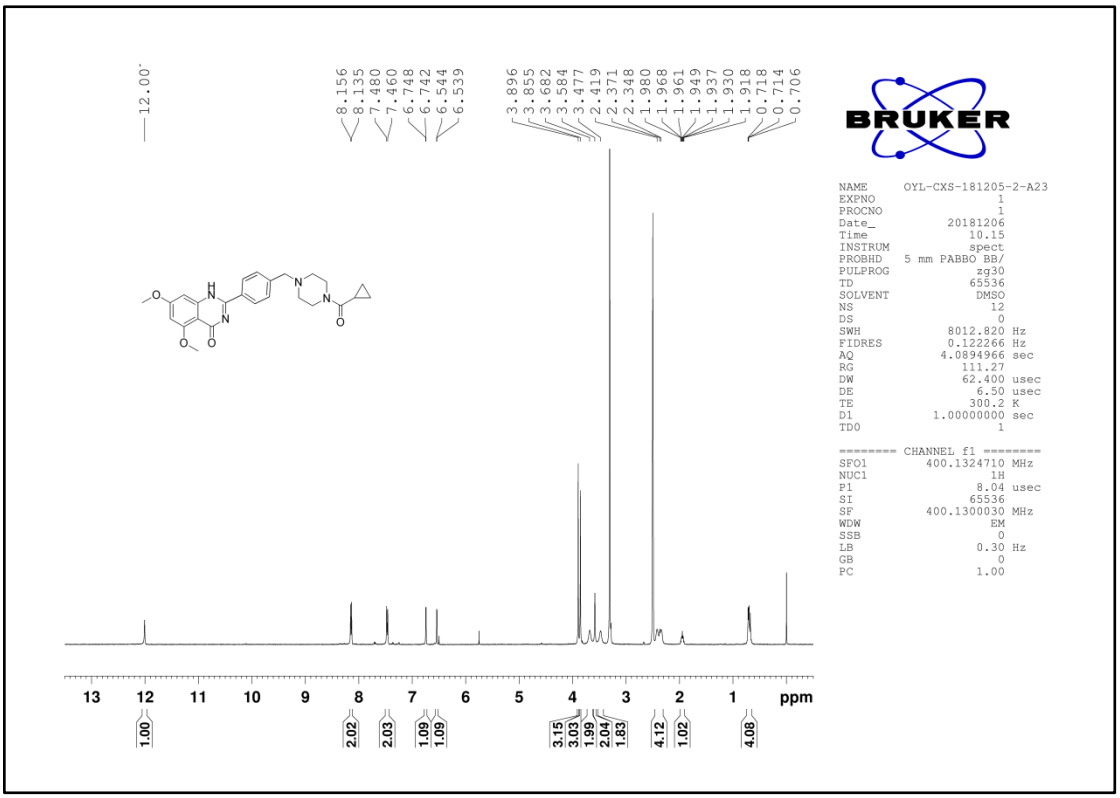

^{1}H NMR Spectrum of Compound **11c**

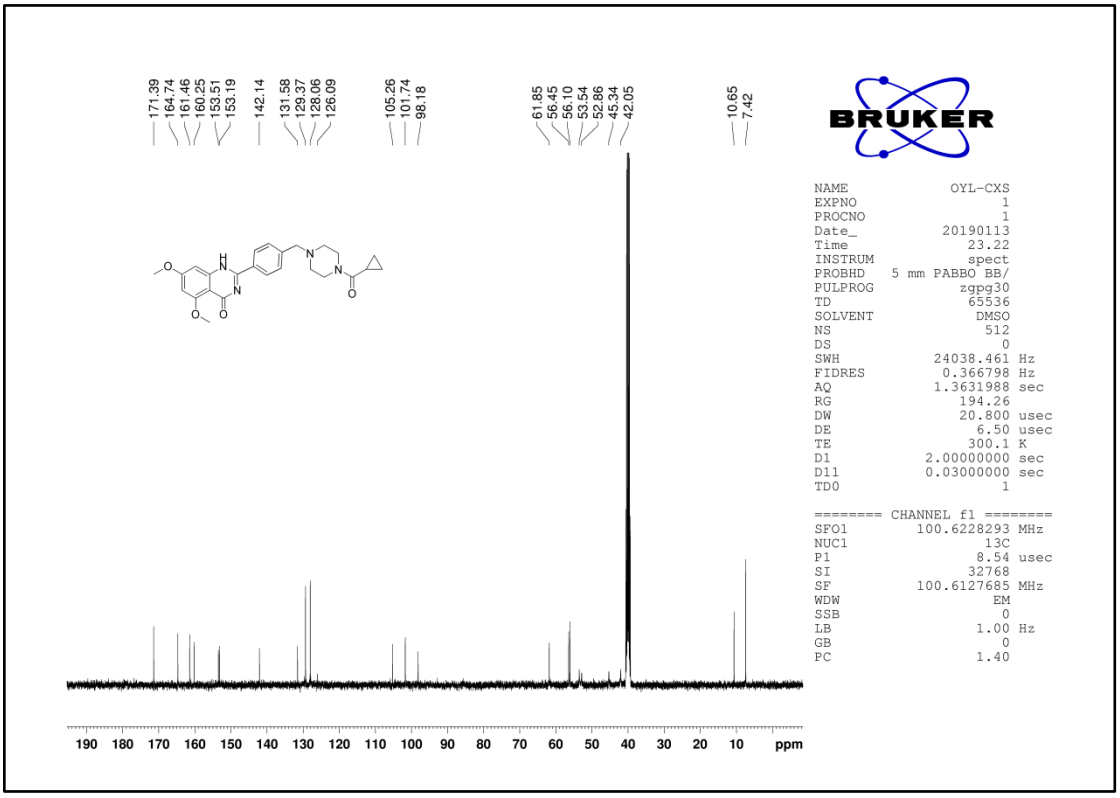

^{13}C NMR Spectrum of Compound **11c**

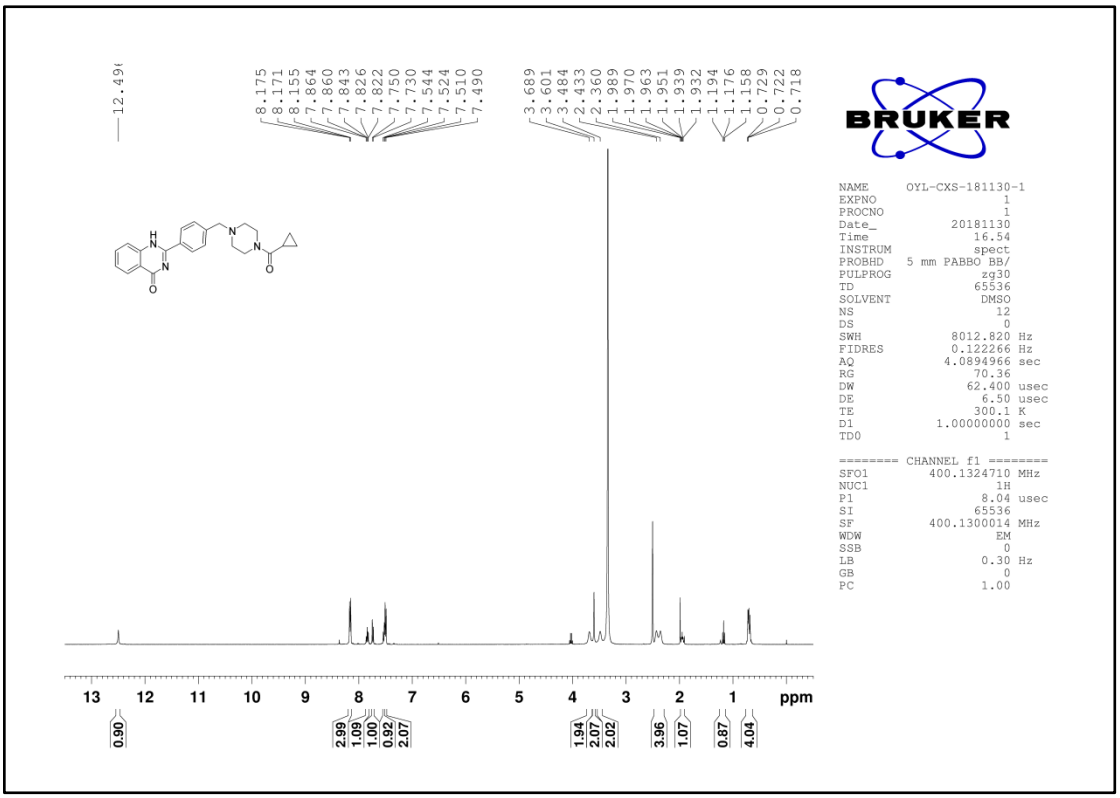

^{1}H NMR Spectrum of Compound **11d**

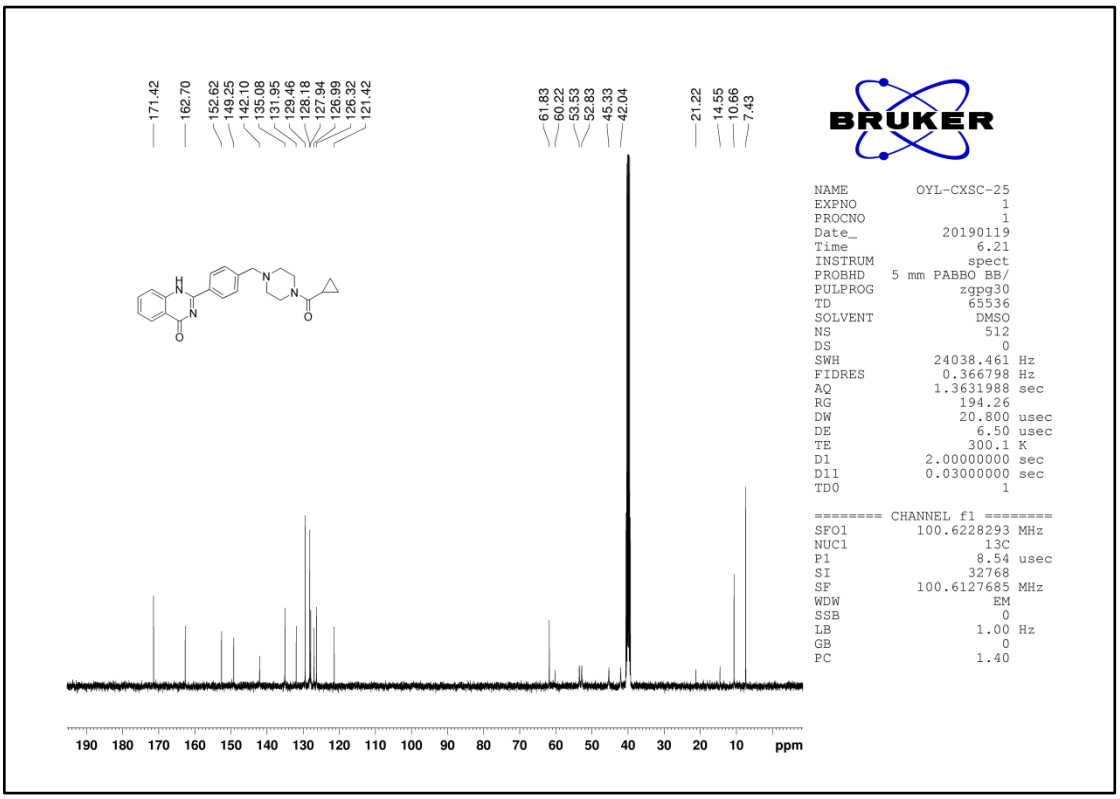

^{13}C NMR Spectrum of Compound **11d**

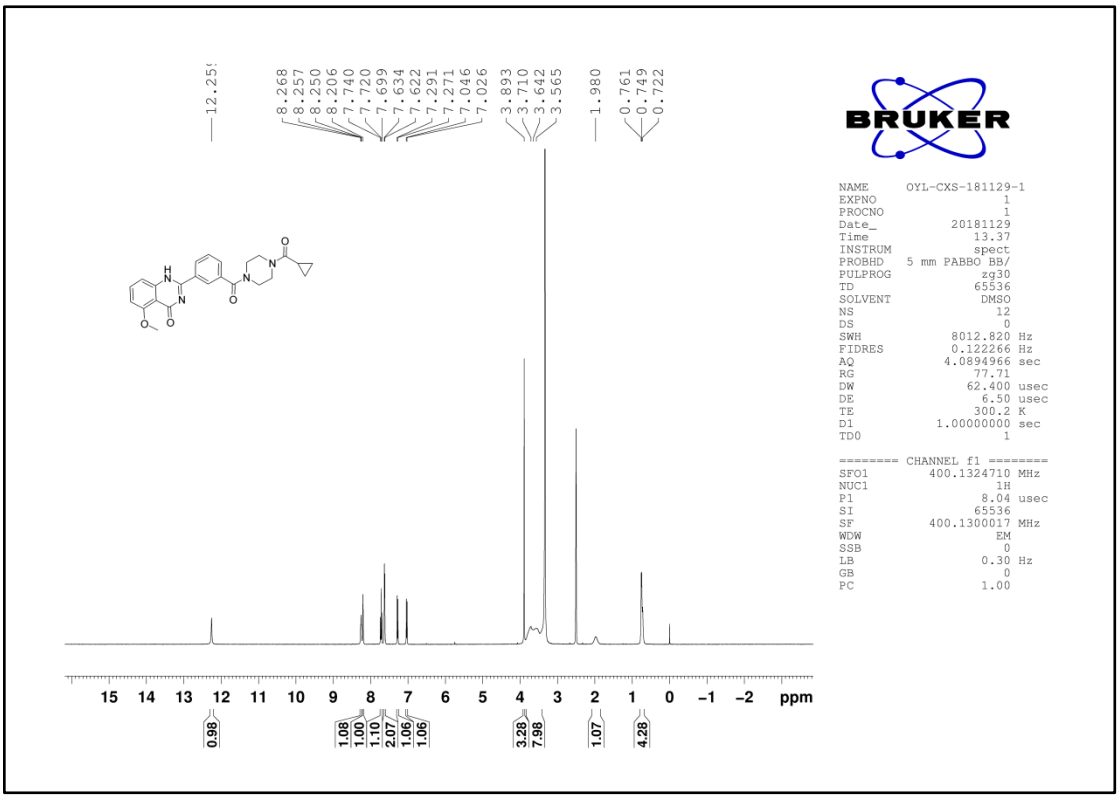

^{1}H NMR Spectrum of Compound **11e**

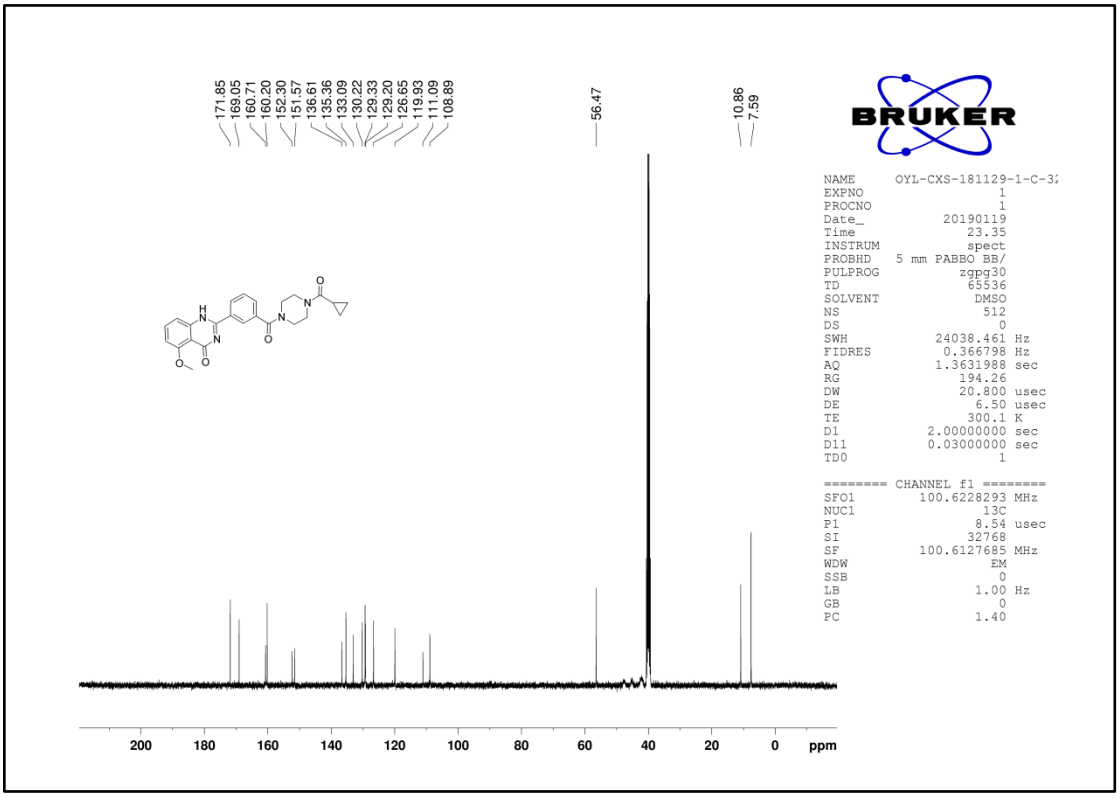

^{13}C NMR Spectrum of Compound **11e**

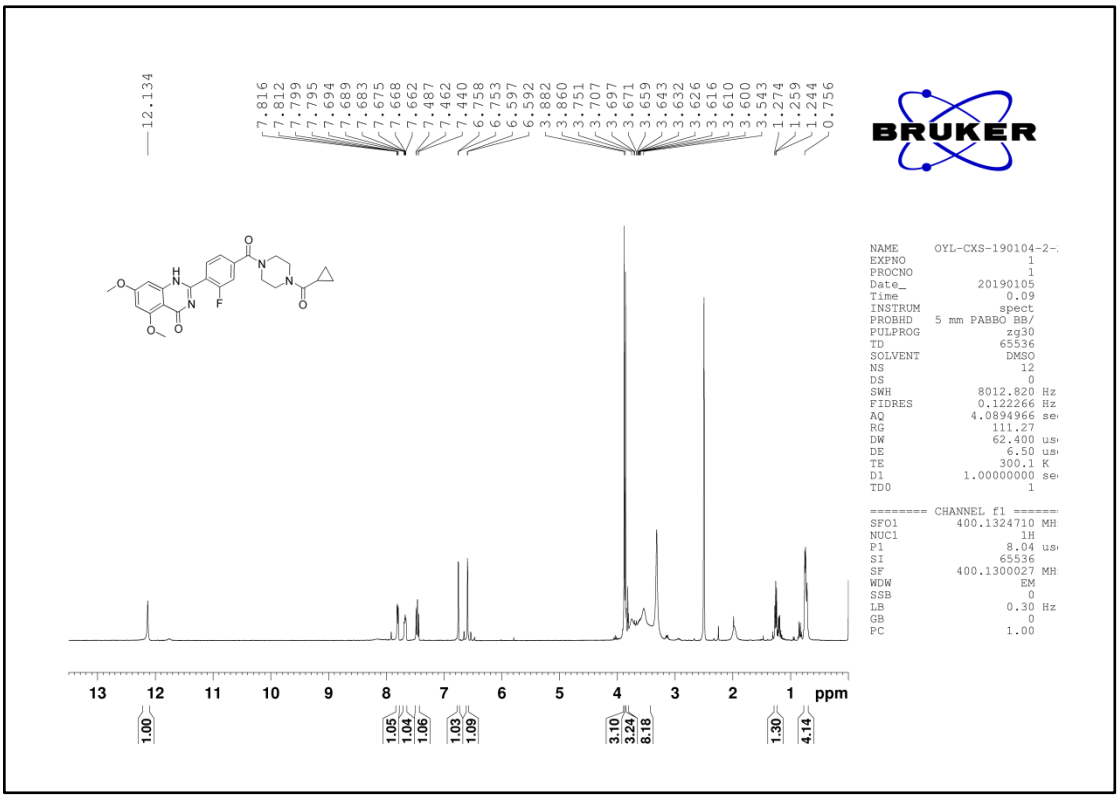

^{1}H NMR Spectrum of Compound **15a**

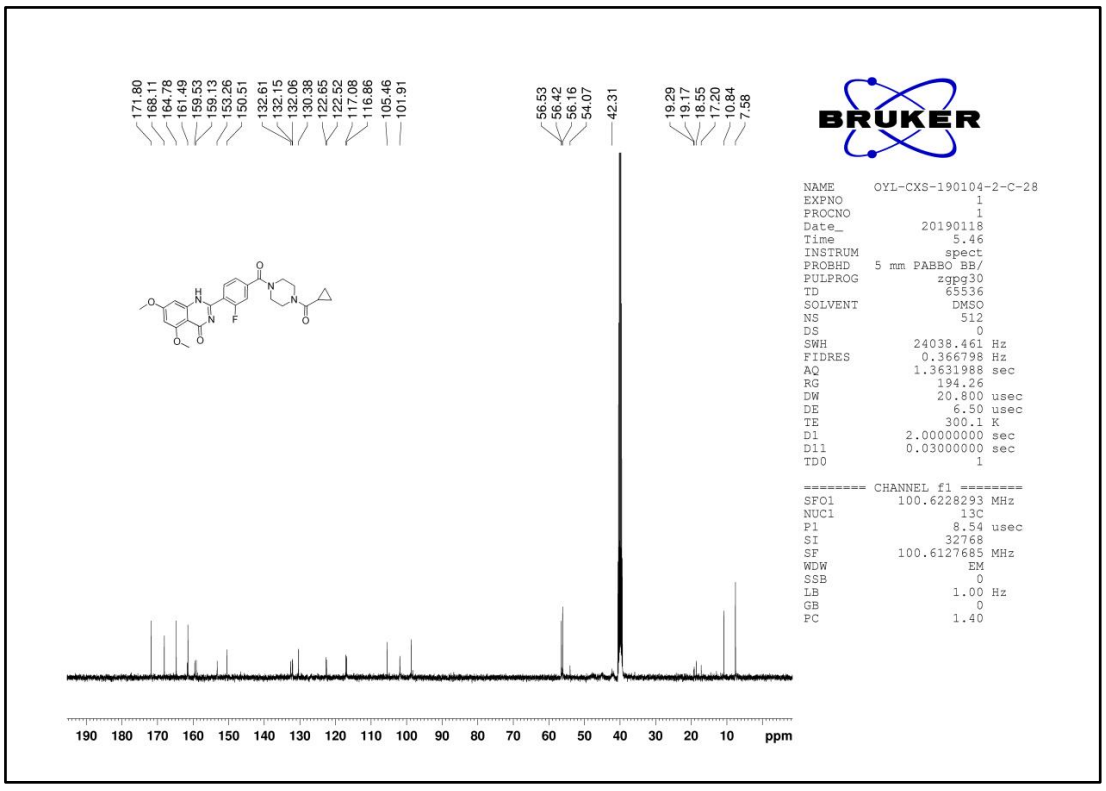

^{13}C NMR Spectrum of Compound **15a**

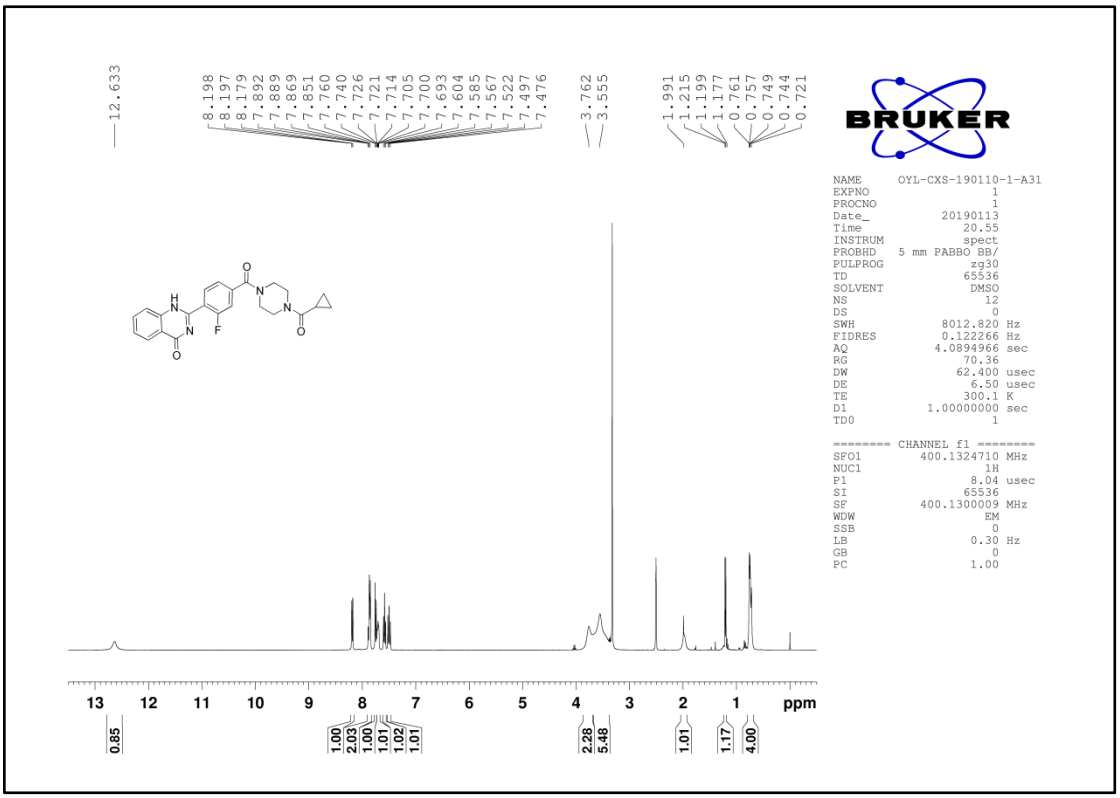

^{1}H NMR Spectrum of Compound **15b**

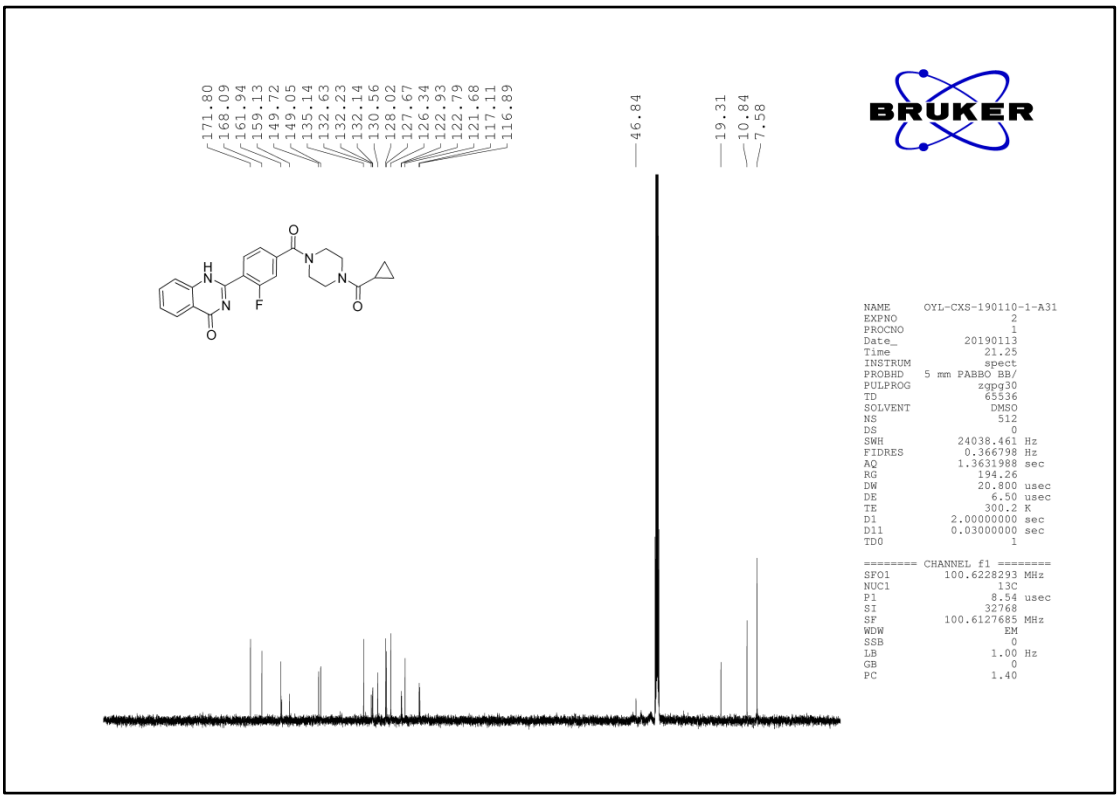

^{13}C NMR Spectrum of Compound **15b**

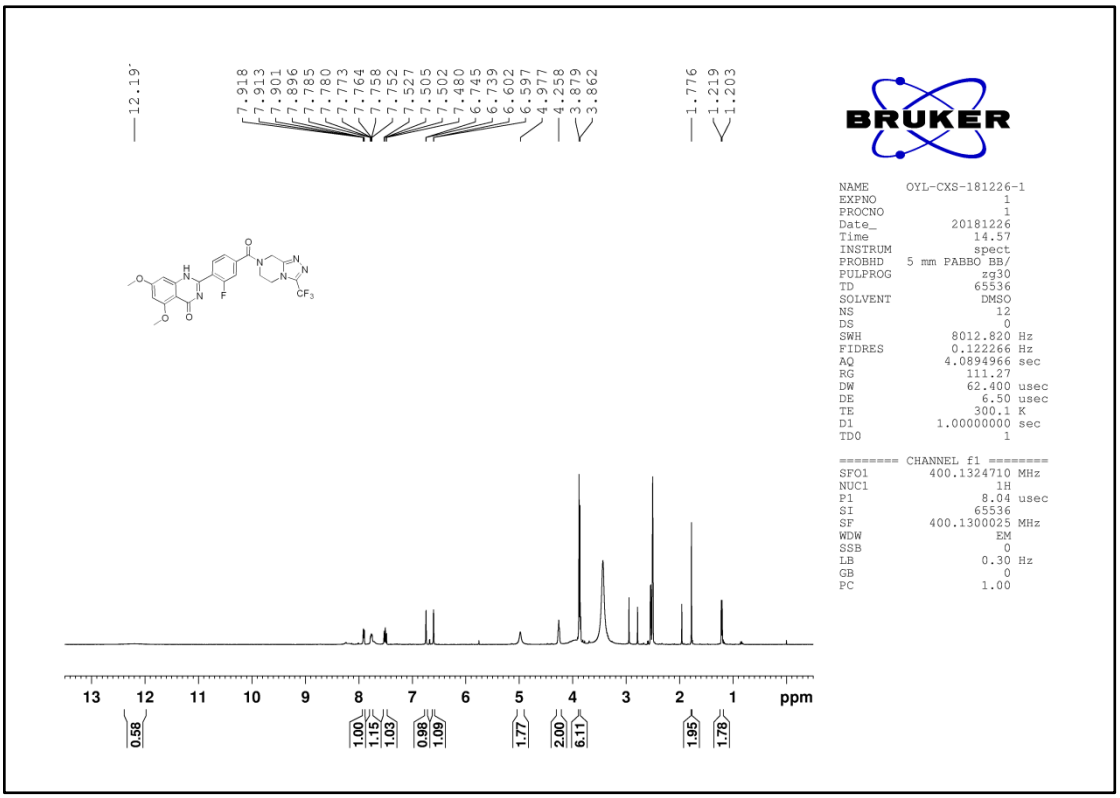

^{1}H NMR Spectrum of Compound **15c**

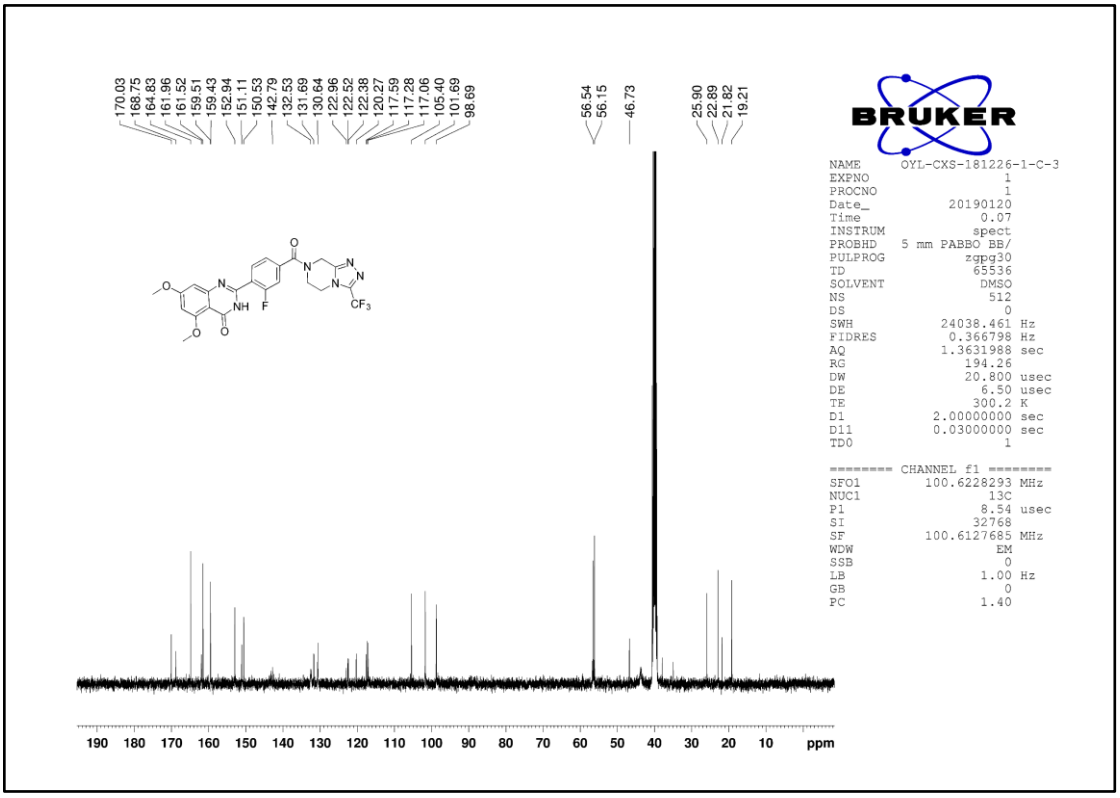

^{13}C NMR Spectrum of Compound **15c**

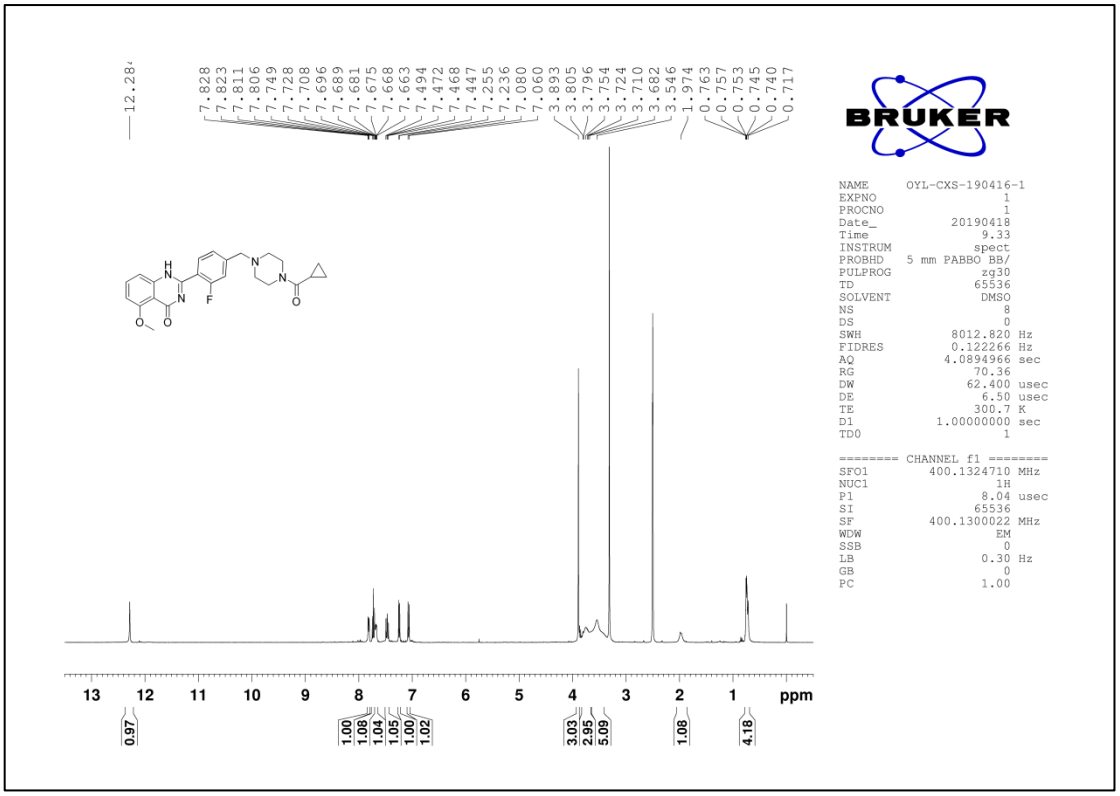

^{1}H NMR Spectrum of Compound **15d**

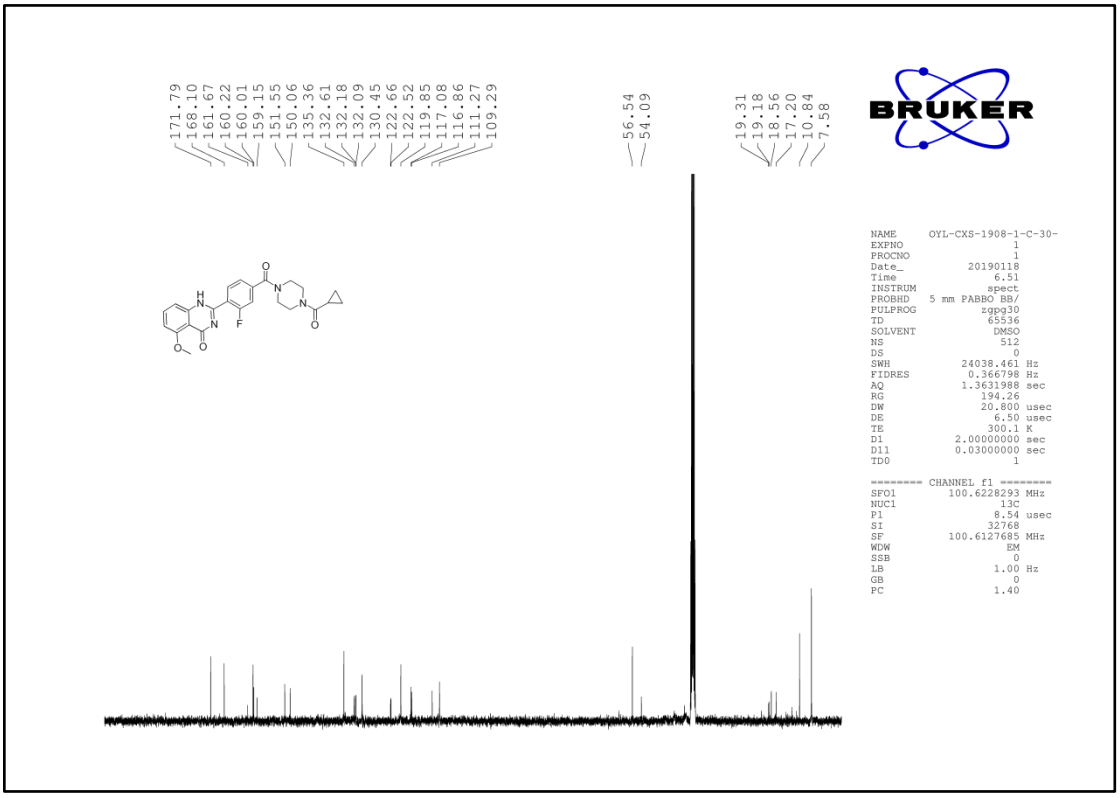

^{13}C NMR Spectrum of Compound **15d**

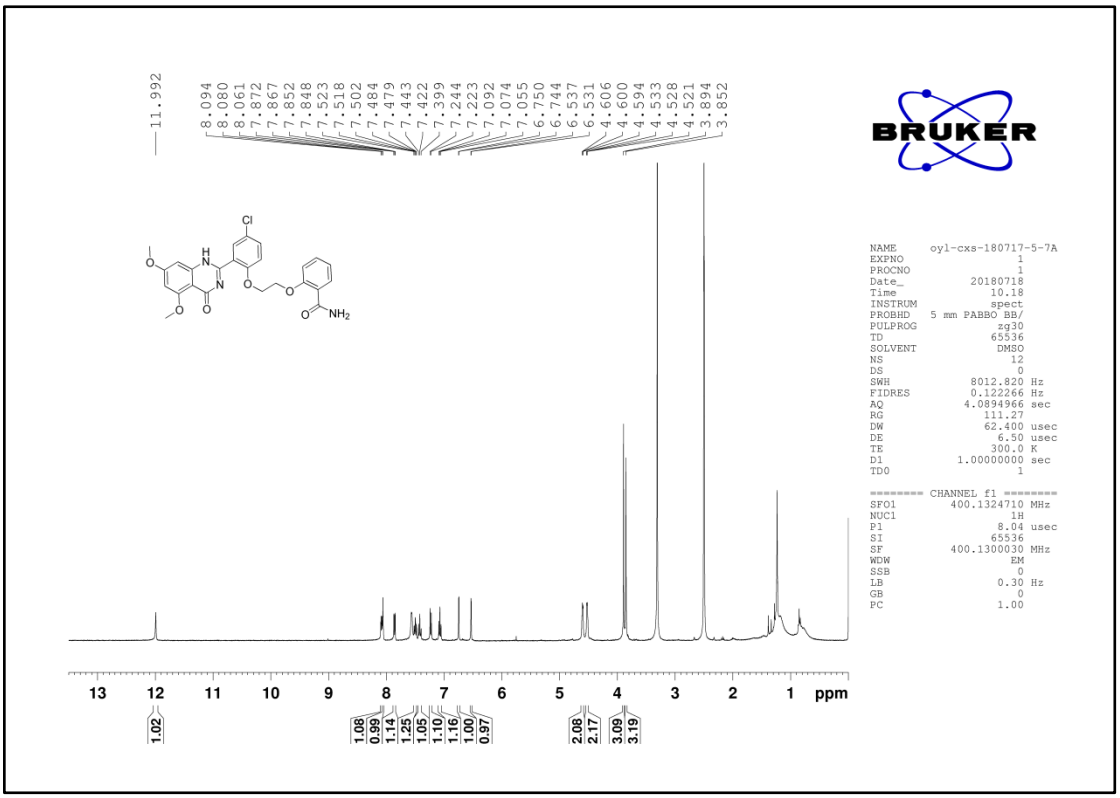

^{1}H NMR Spectrum of Compound **19a**

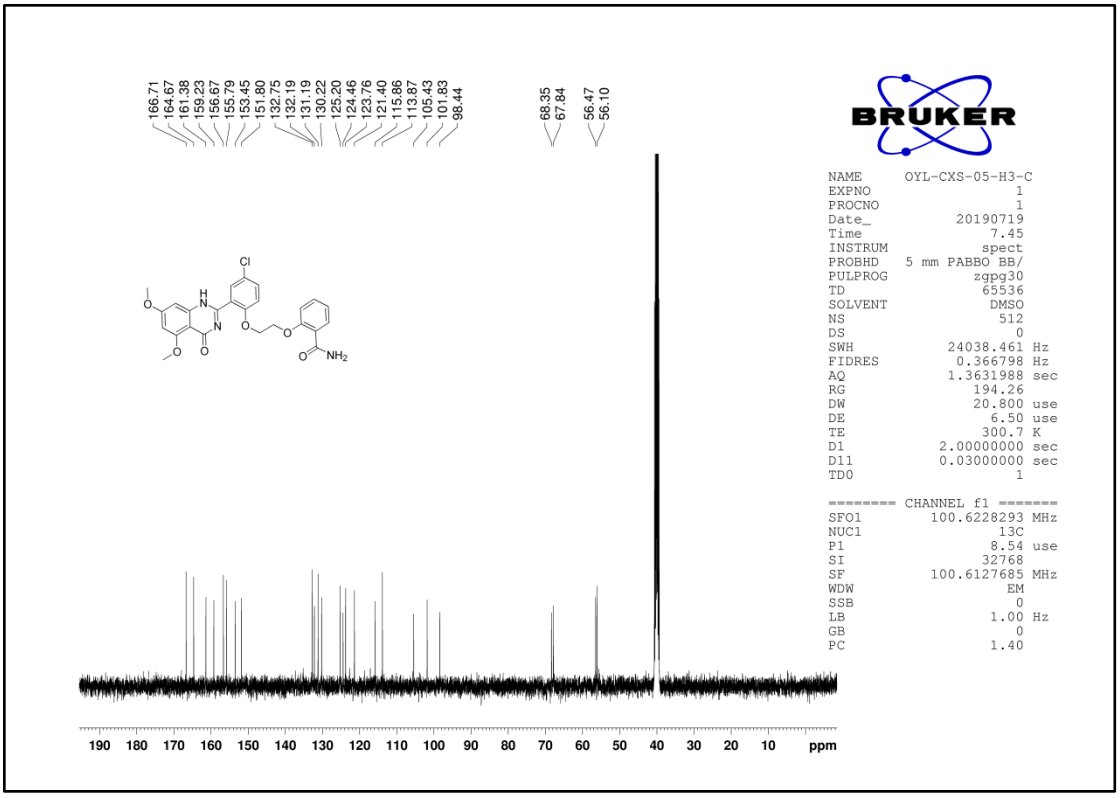

^{13}C NMR Spectrum of Compound **19a**

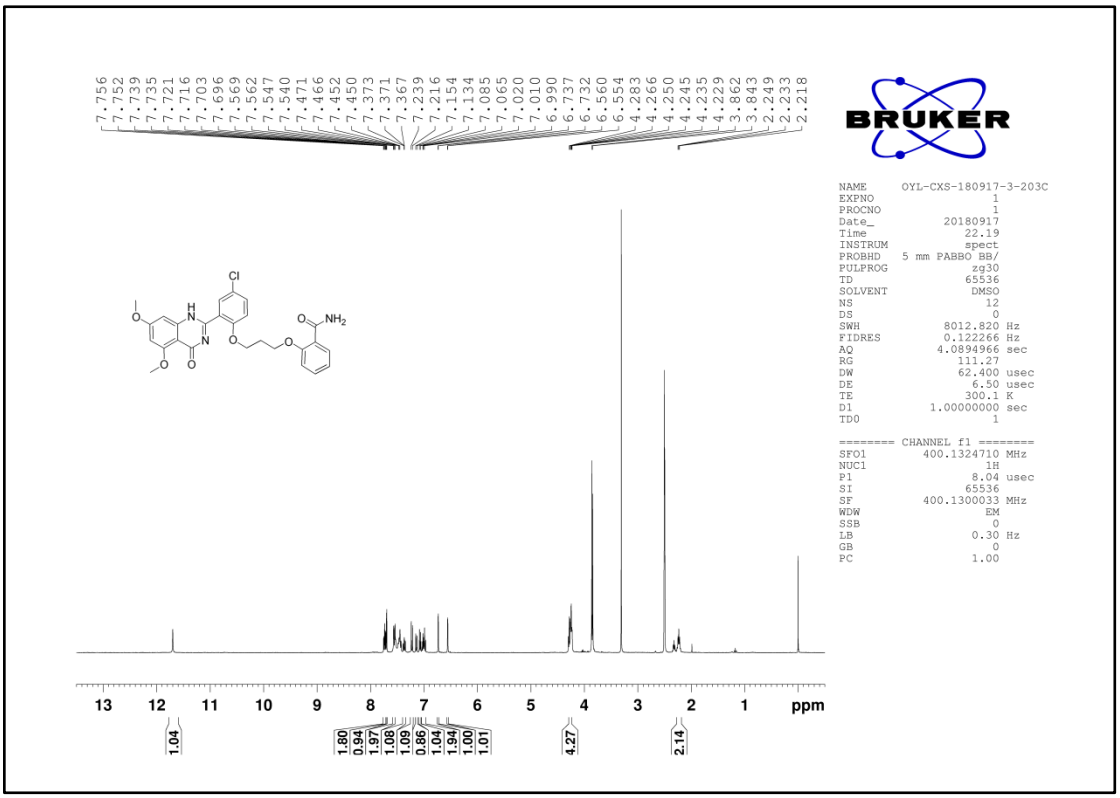

^{1}H NMR Spectrum of Compound **19b**

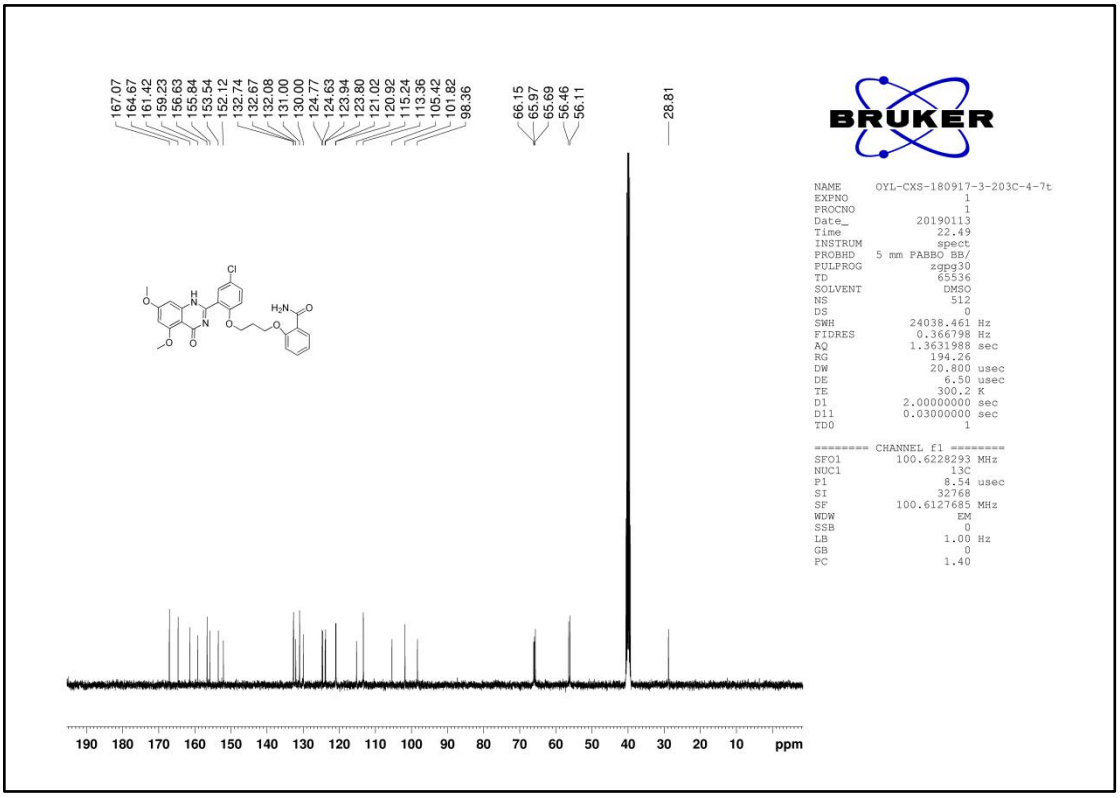

^{13}C NMR Spectrum of Compound **19b**

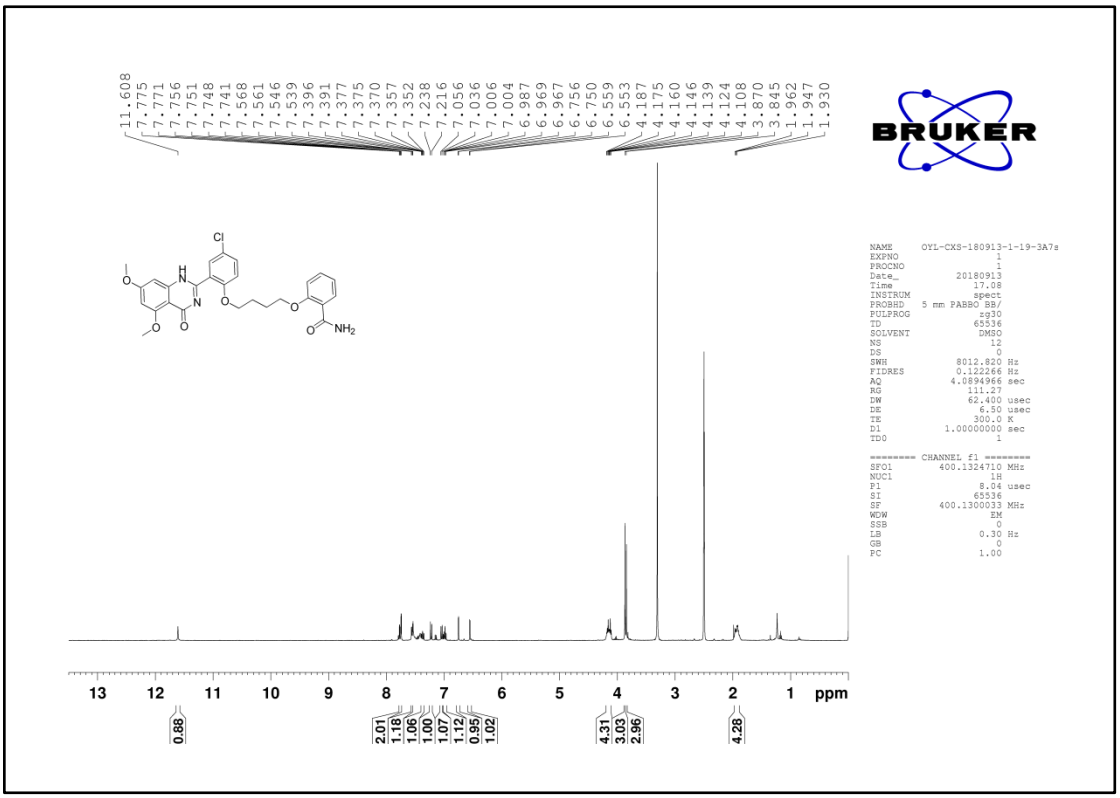

^{1}H NMR Spectrum of Compound **19c**

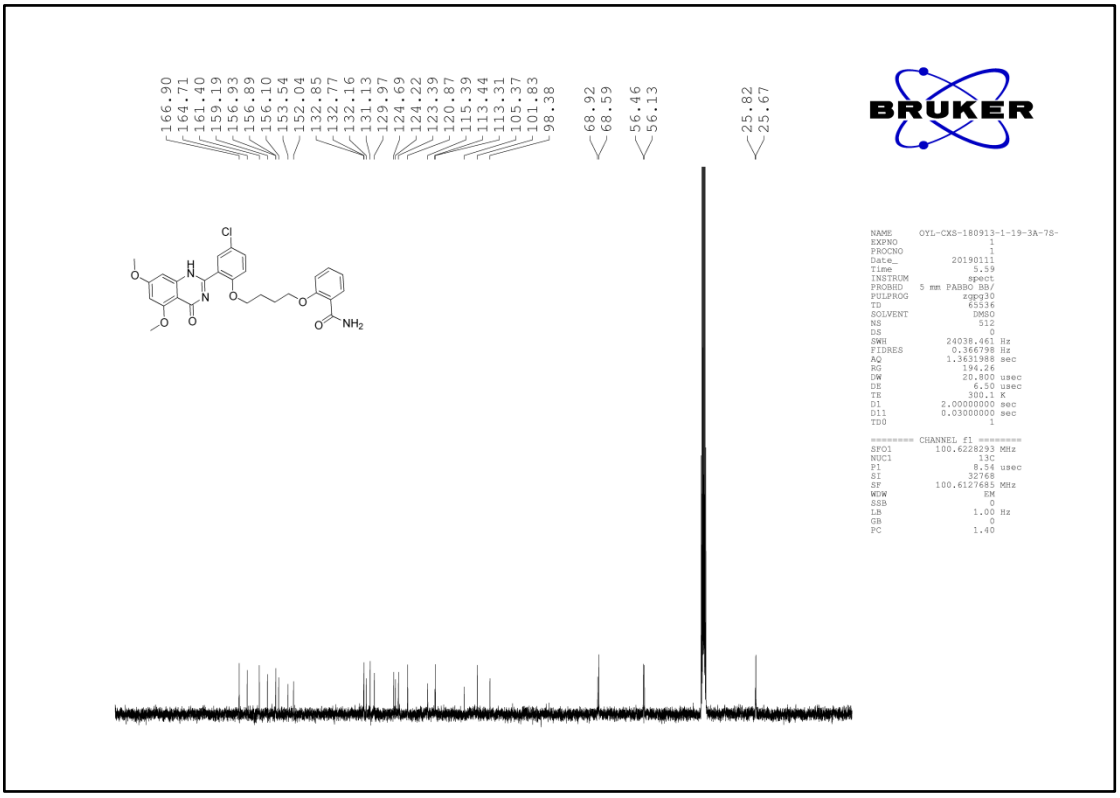

^{13}C NMR Spectrum of Compound **19c**

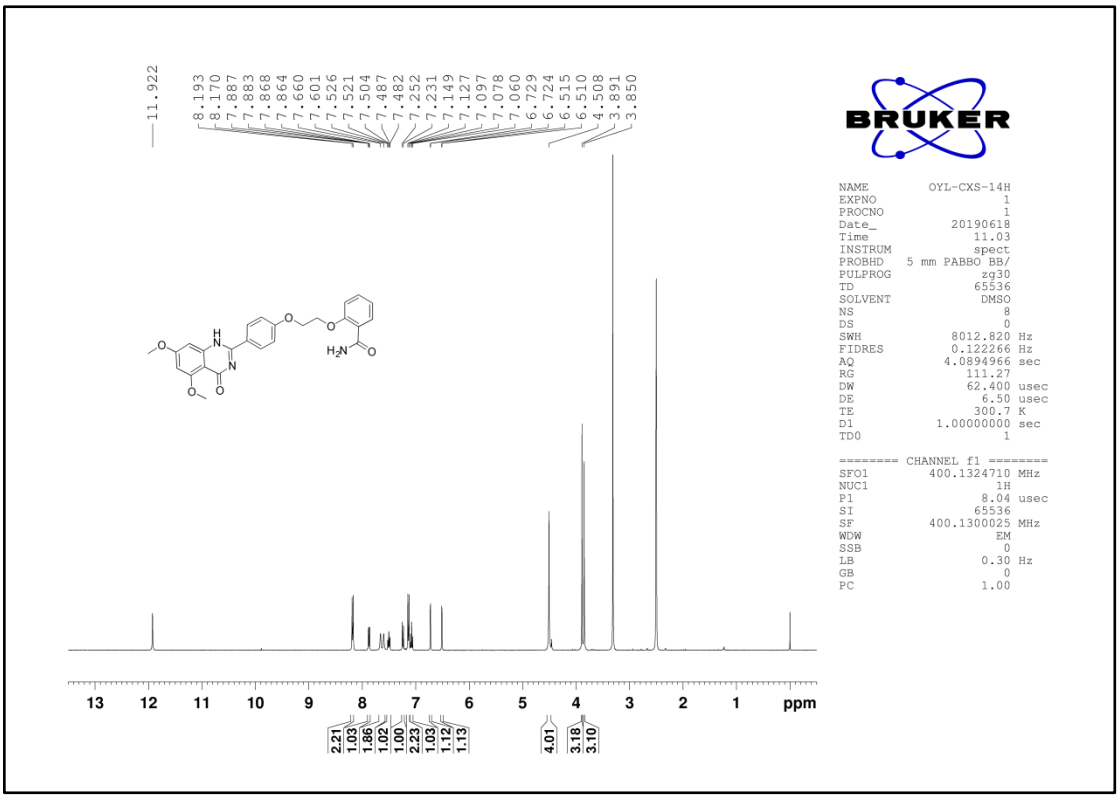

^{1}H NMR Spectrum of Compound **19d**

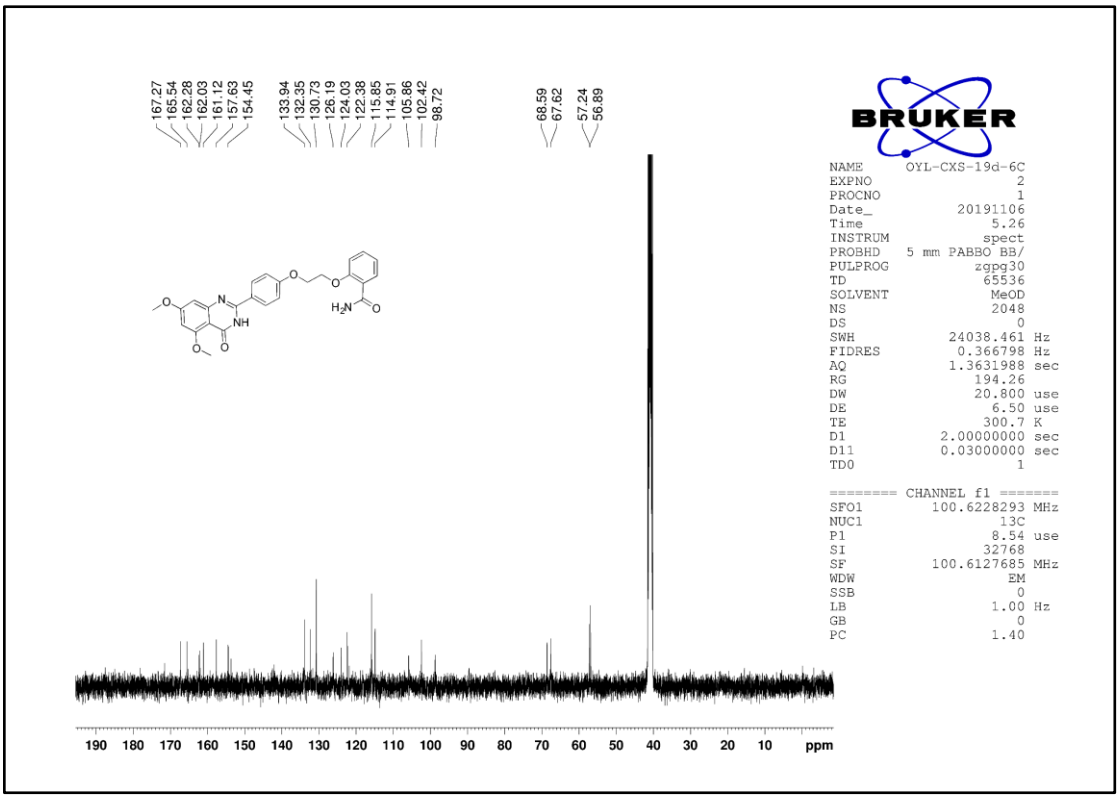

^{13}C NMR Spectrum of Compound **19d**

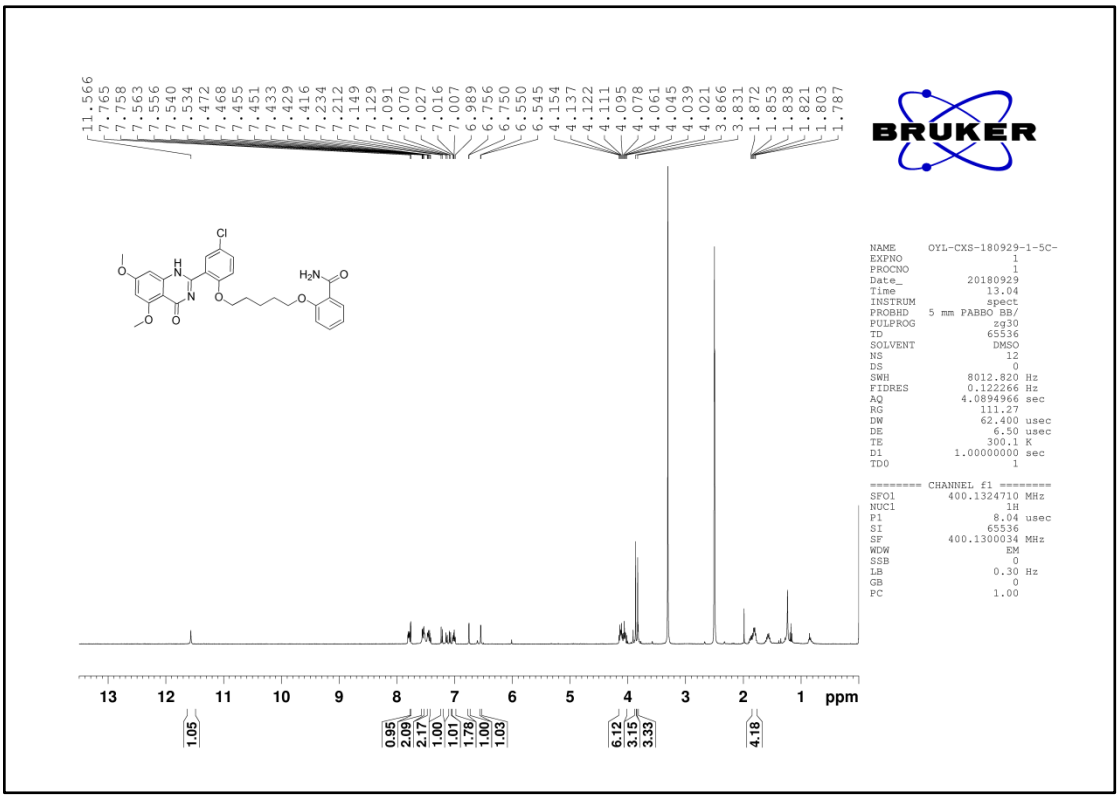

^{1}H NMR Spectrum of Compound **19e**

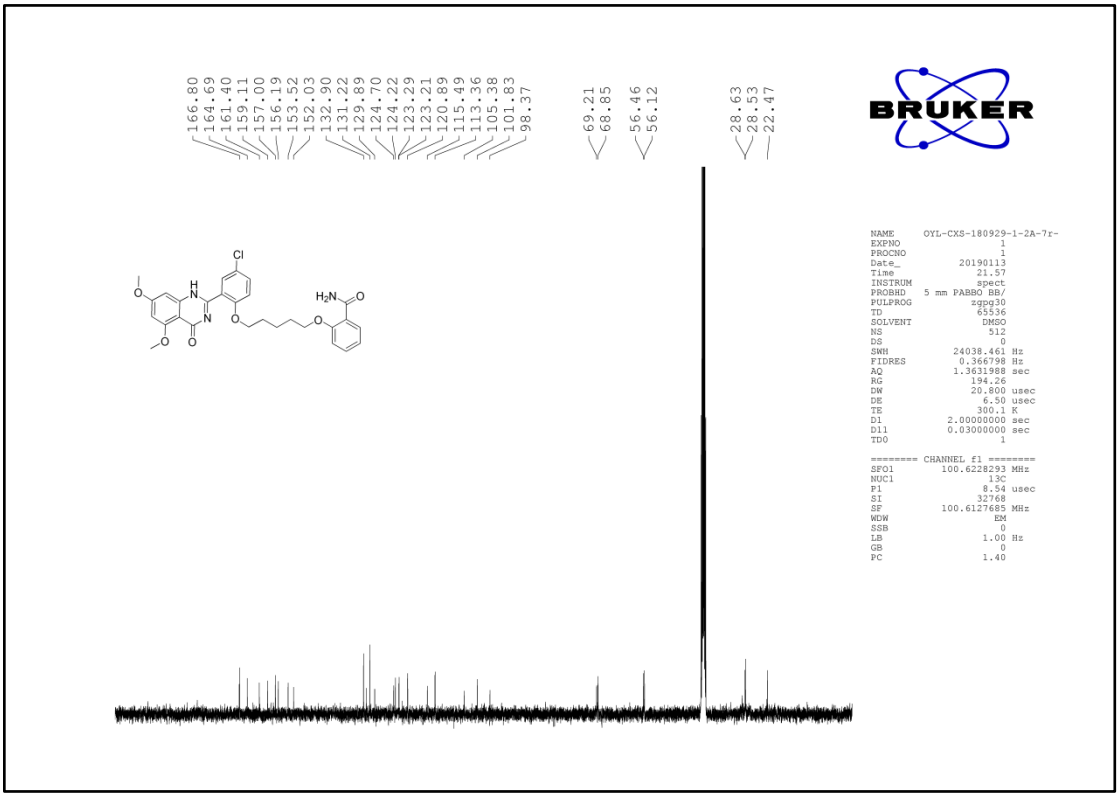

^{13}C NMR Spectrum of Compound **19e**

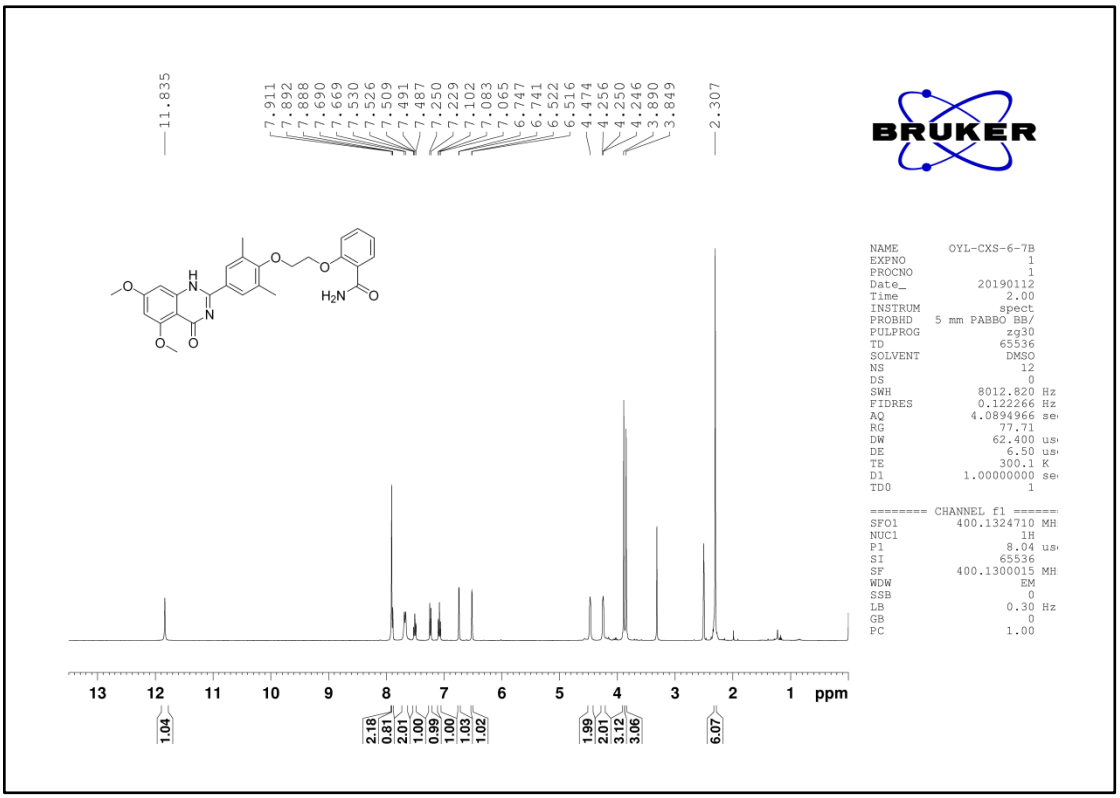

^{1}H NMR Spectrum of Compound **19f**

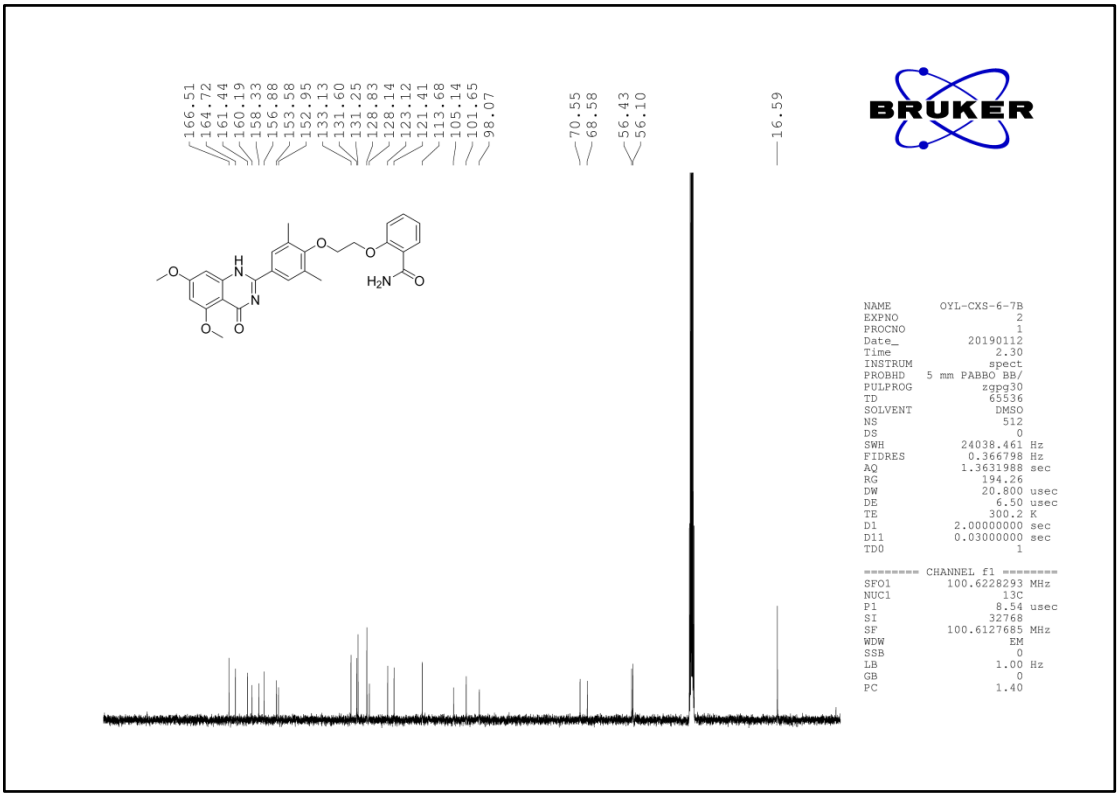

^{13}C NMR Spectrum of Compound **19f**

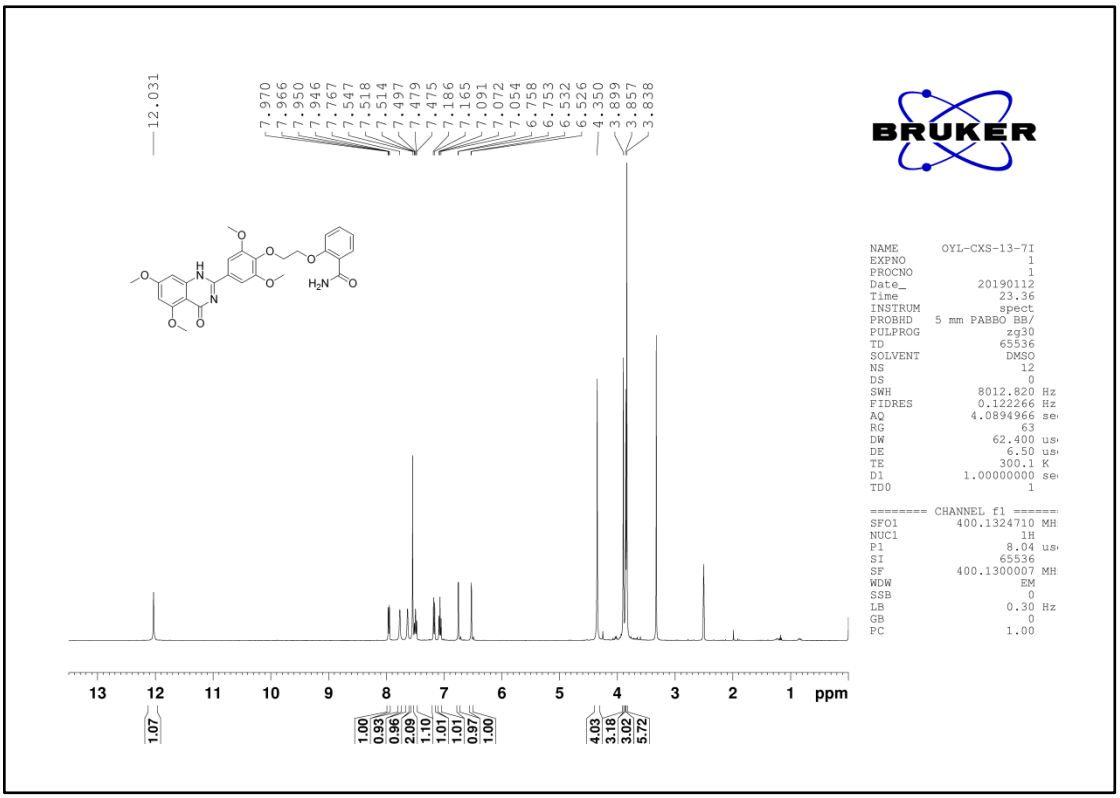

^{1}H NMR Spectrum of Compound **19g**

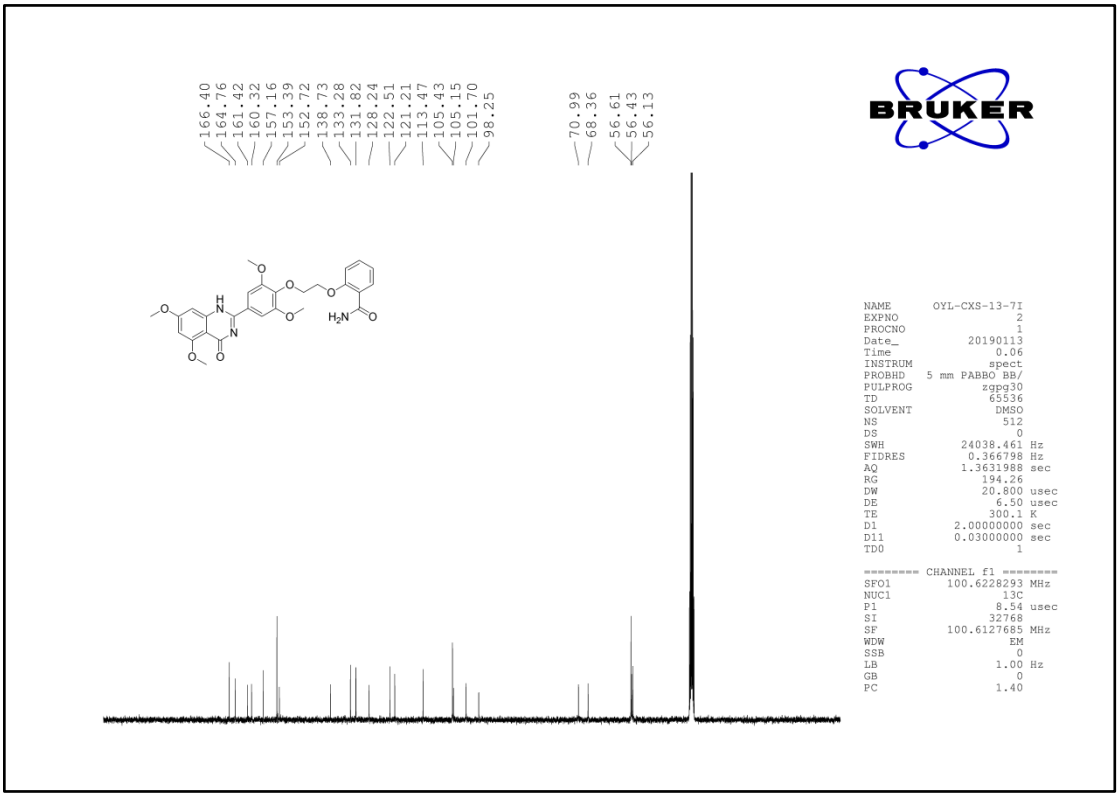

^{13}C NMR Spectrum of Compound **19g**

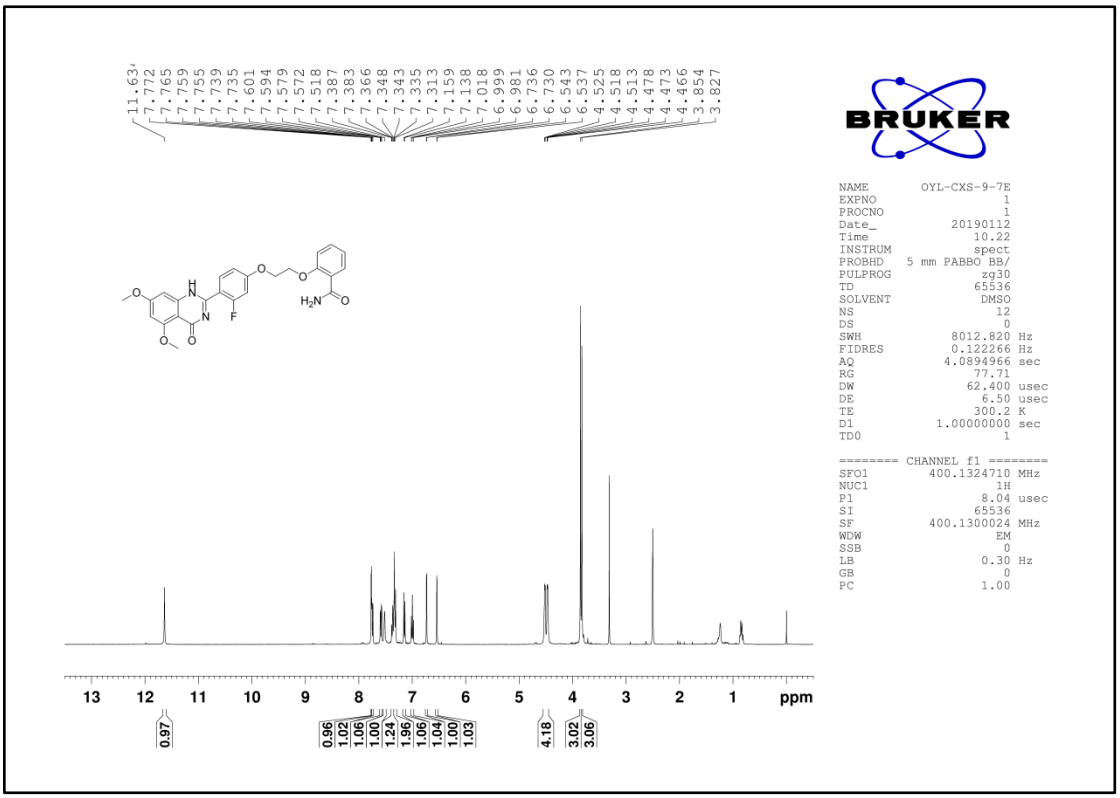

^{1}H NMR Spectrum of Compound **19h**

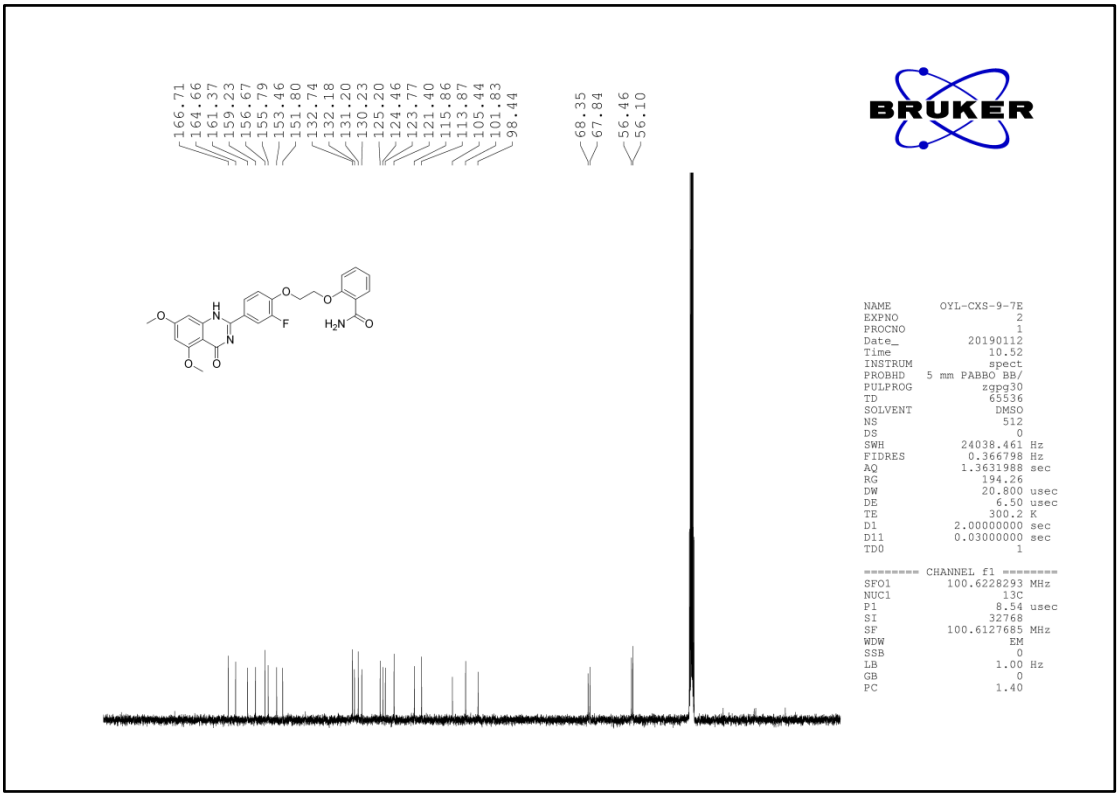

^{13}C NMR Spectrum of Compound **19h**

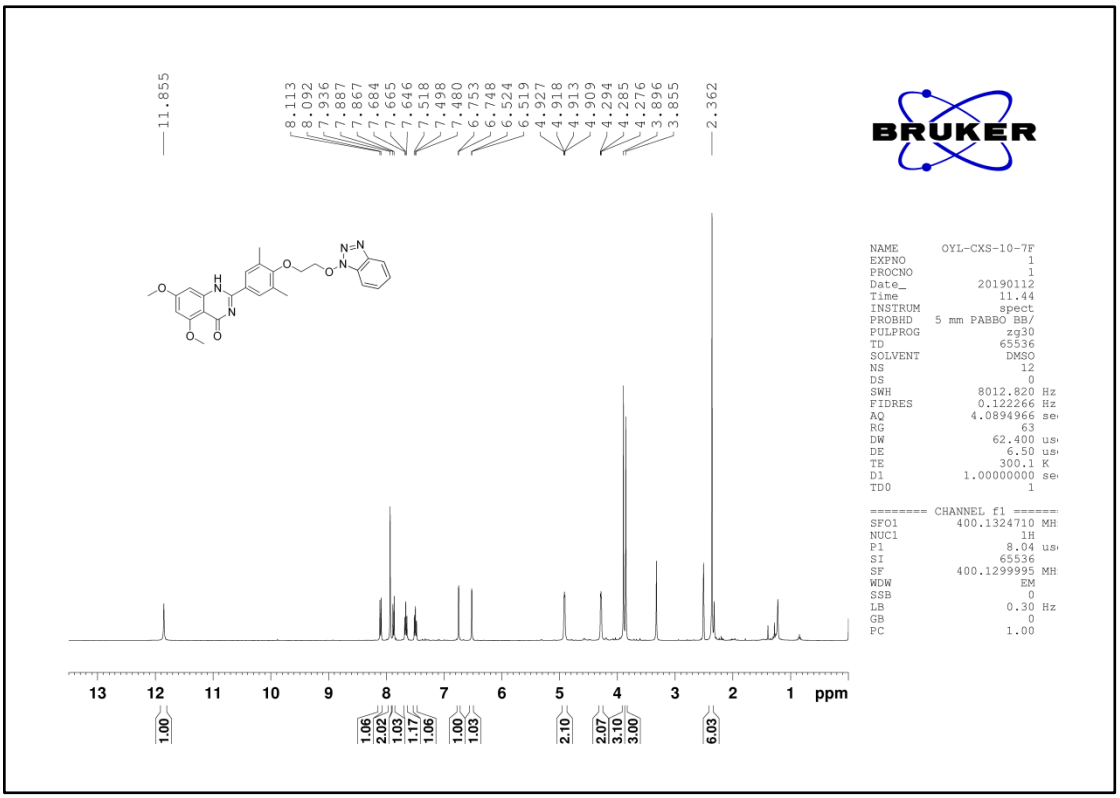

^{1}H NMR Spectrum of Compound **19i**

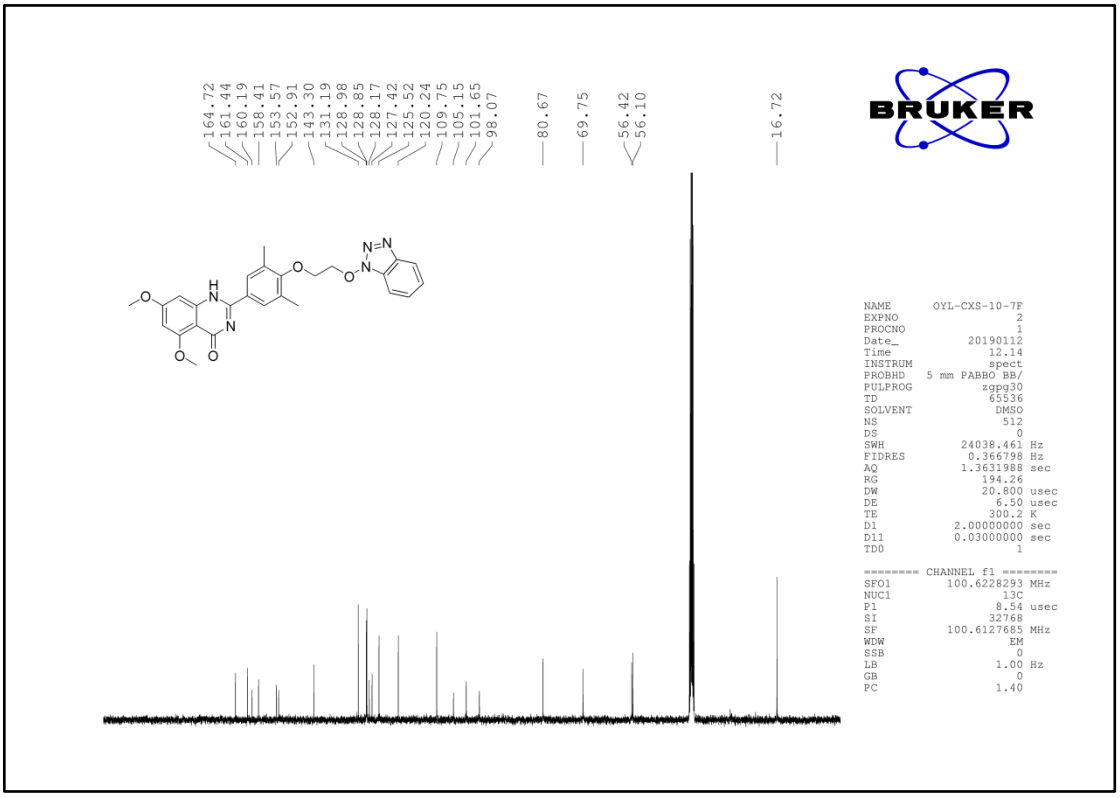

^{13}C NMR Spectrum of Compound **19i**

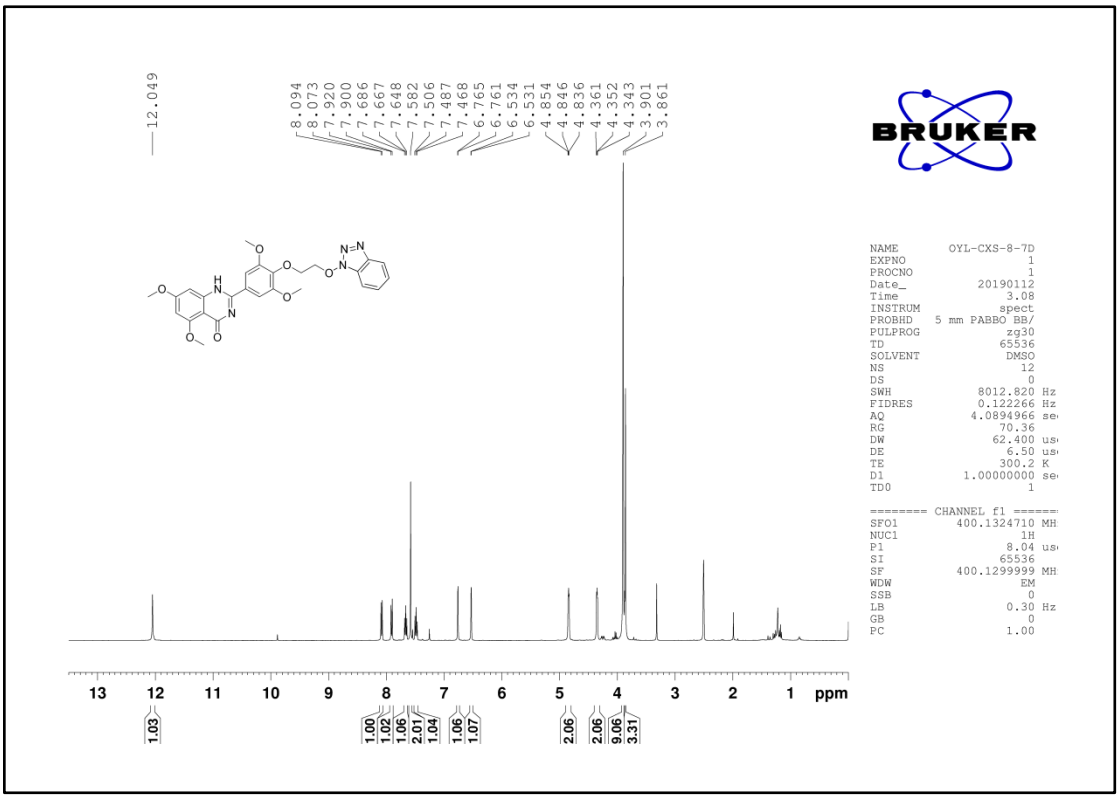

^{1}H NMR Spectrum of Compound **19j**

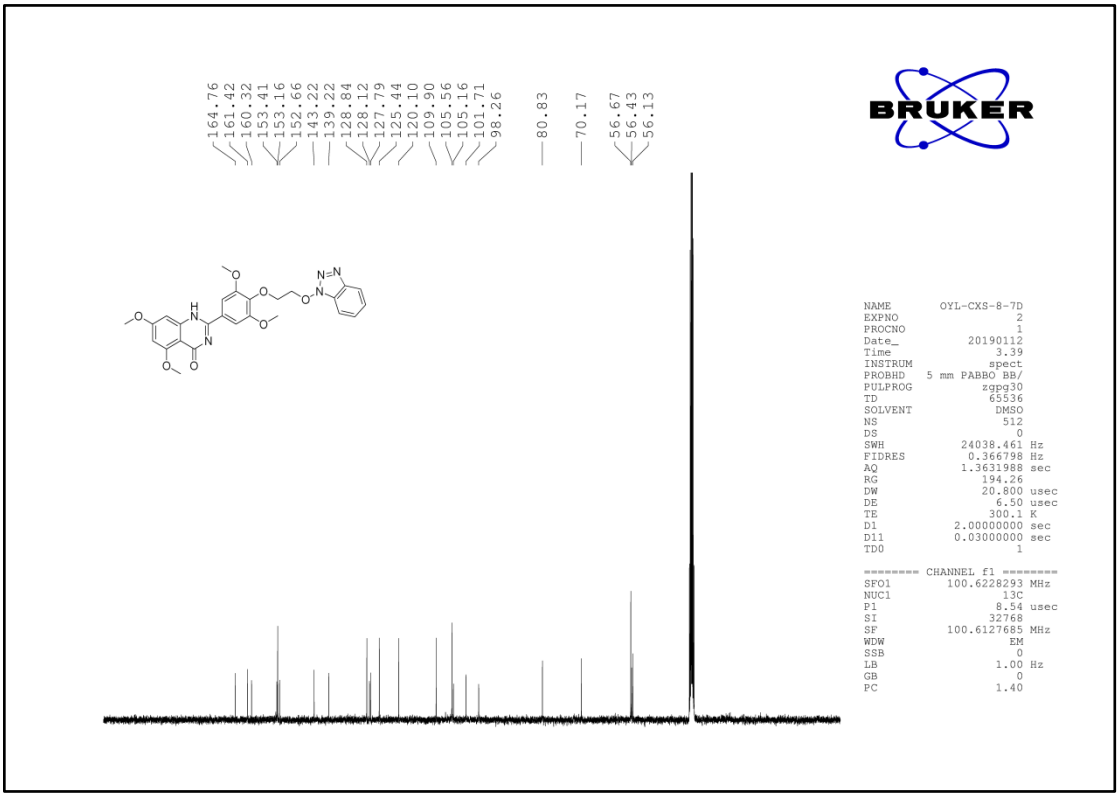

^{13}C NMR Spectrum of Compound **19j**

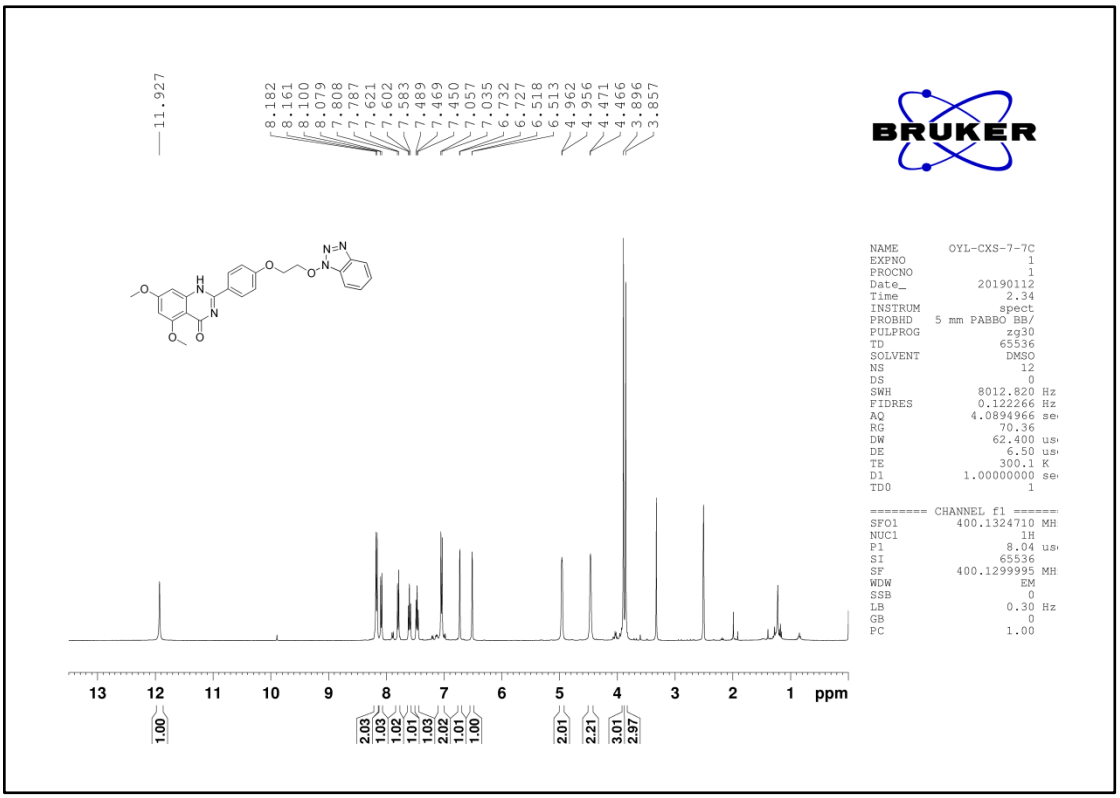

^{1}H NMR Spectrum of Compound **19k**

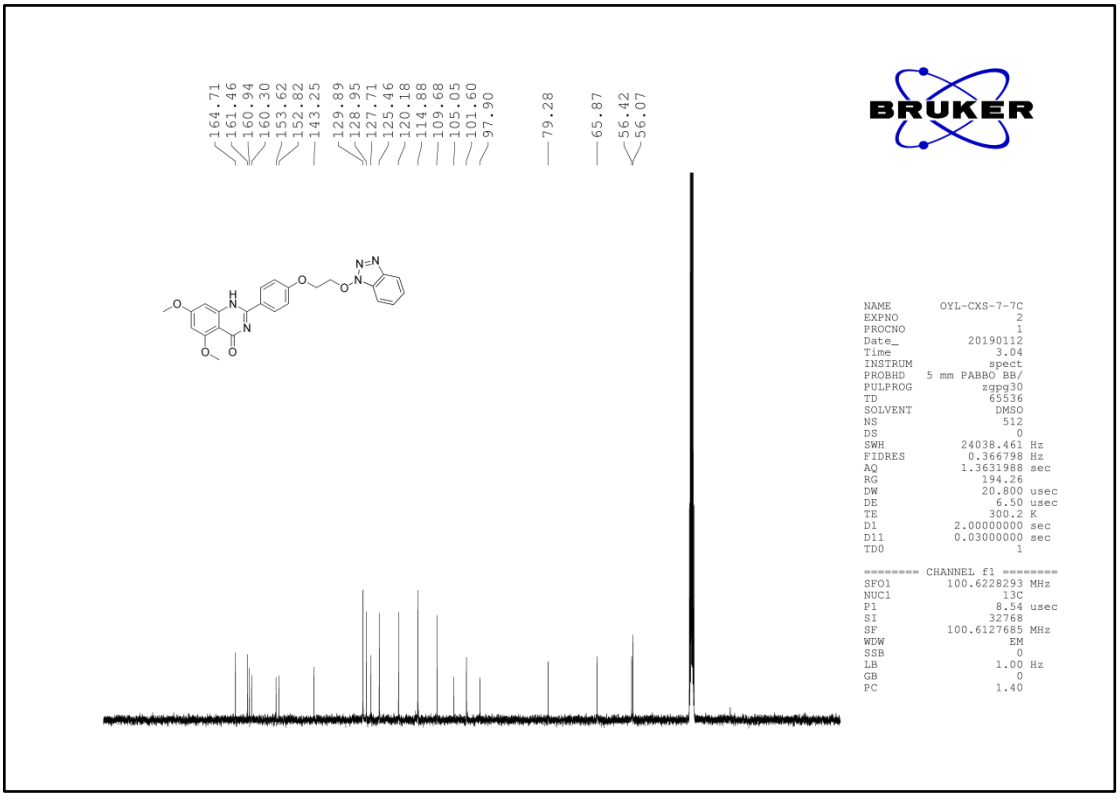

^{13}C NMR Spectrum of Compound **19k**

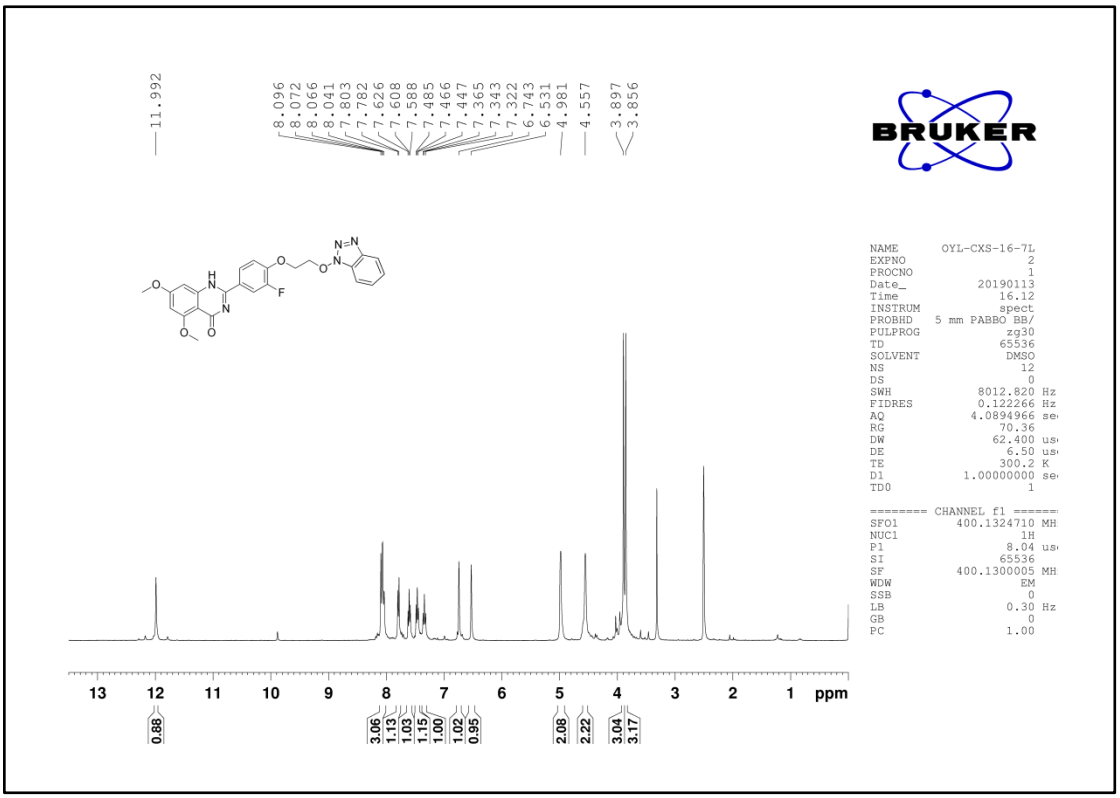

^{1}H NMR Spectrum of Compound **19l**

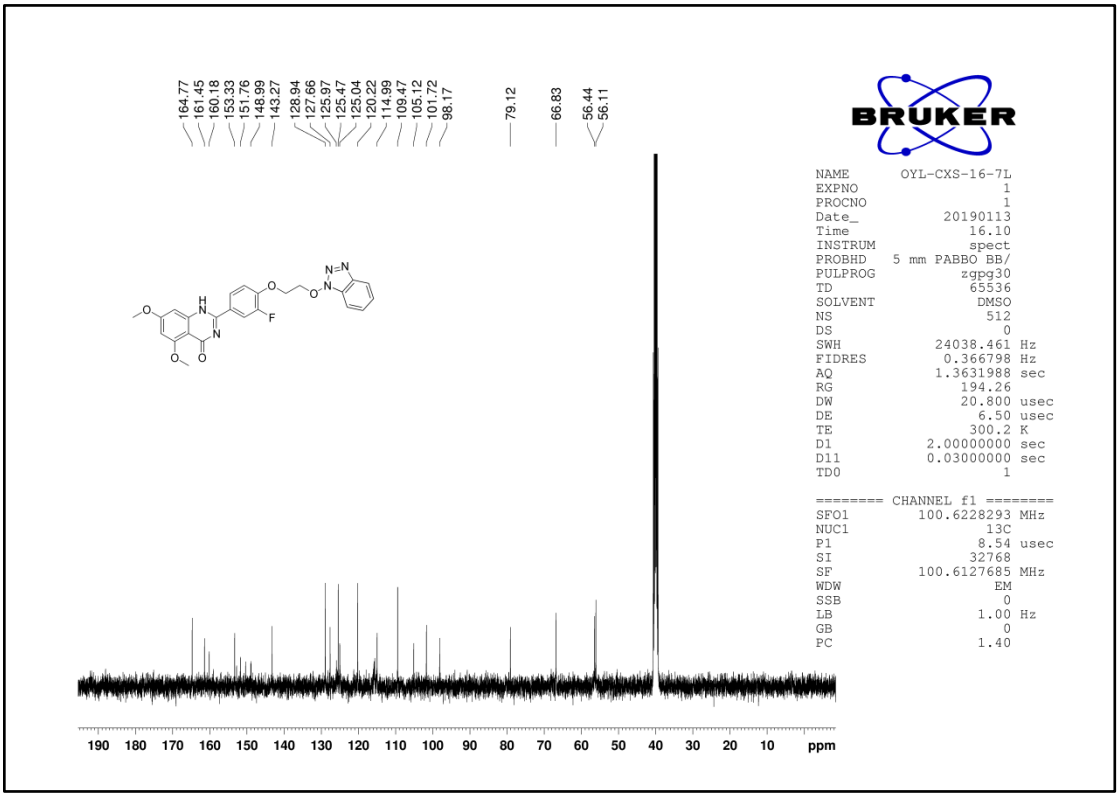

^{13}C NMR Spectrum of Compound **19l**

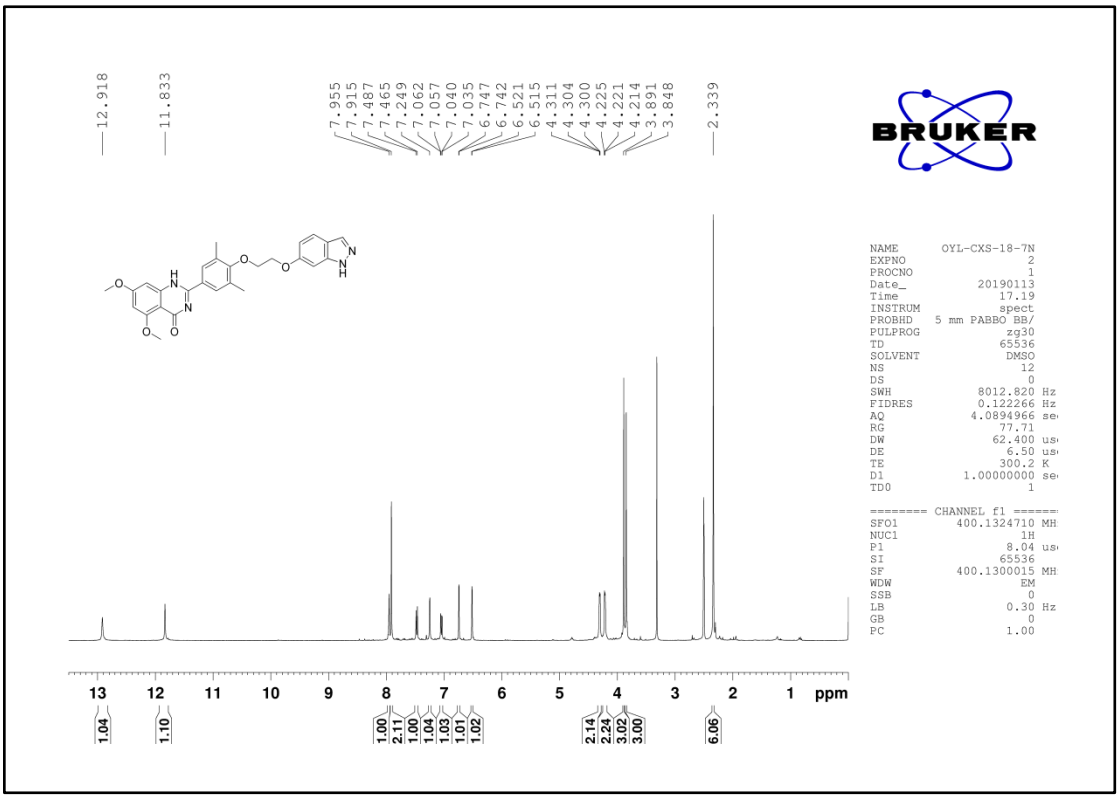

^{1}H NMR Spectrum of Compound **19m**

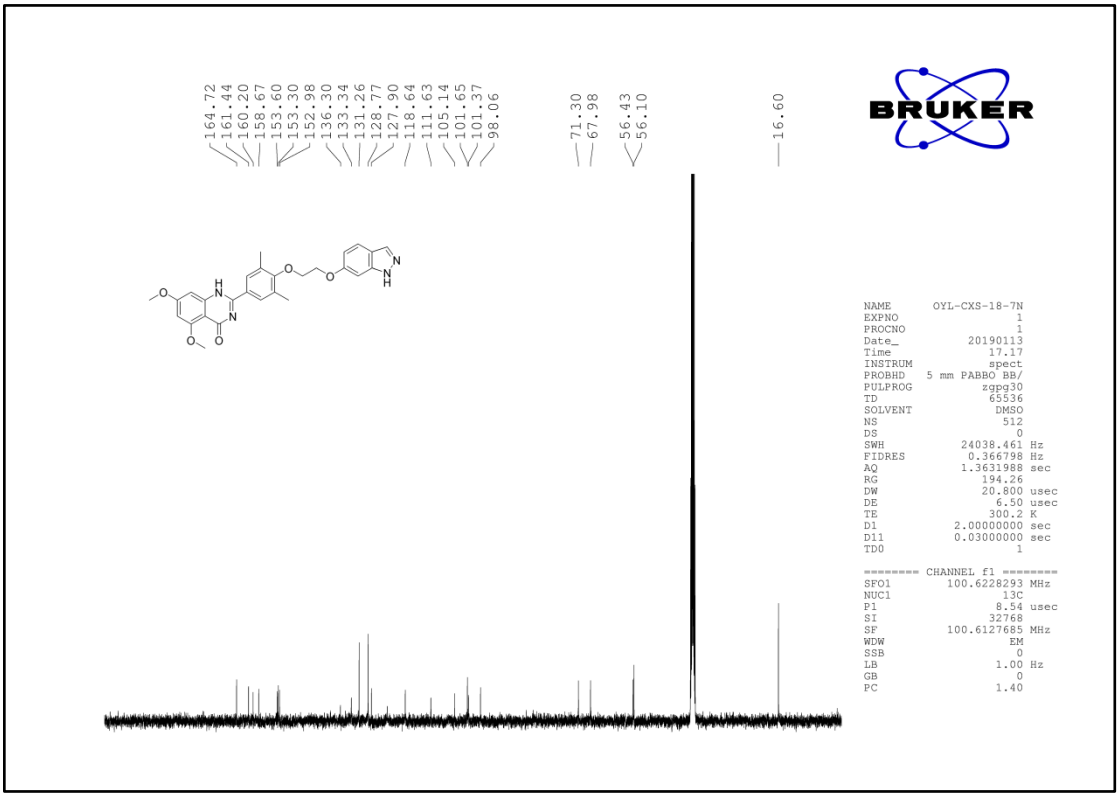

^{13}C NMR Spectrum of Compound **19m**

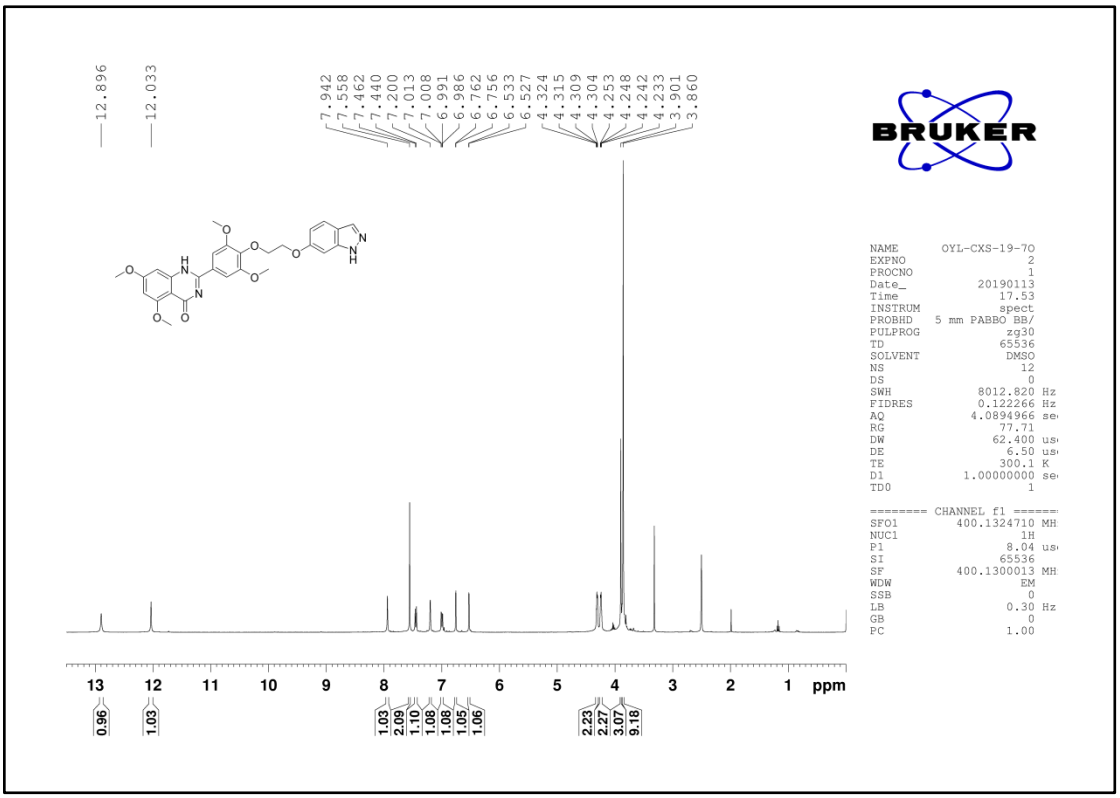

^{1}H NMR Spectrum of Compound **19n**

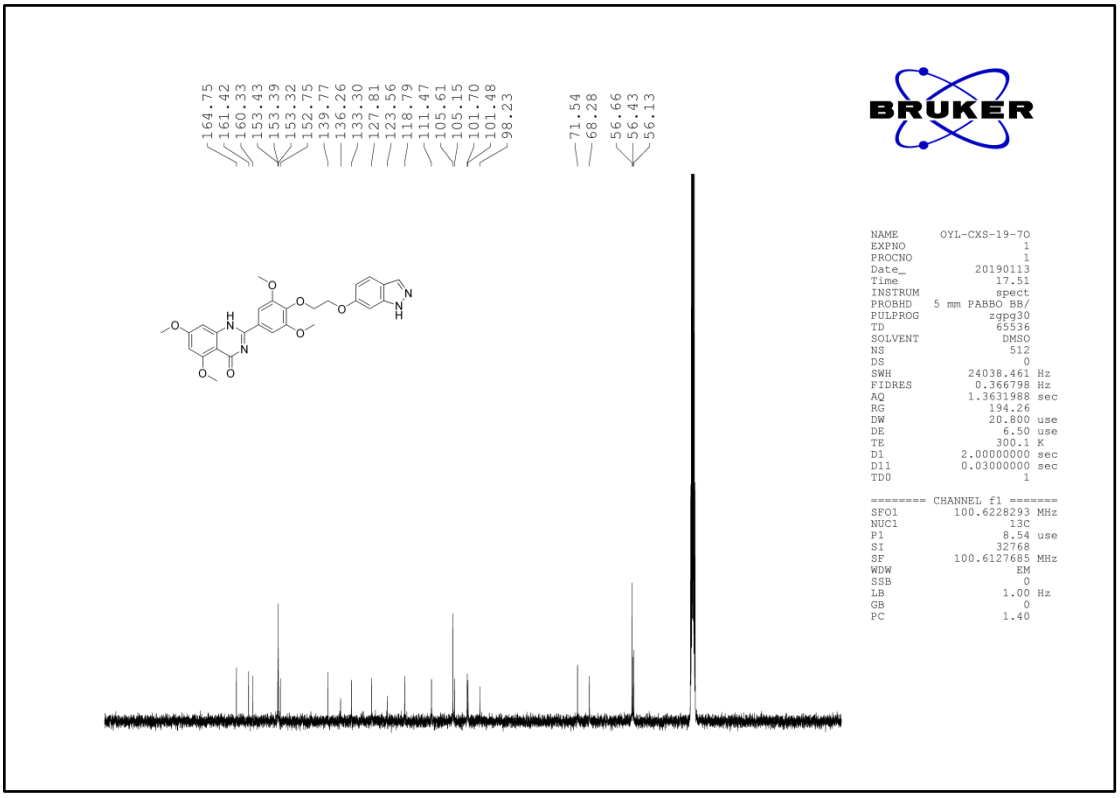

^{13}C NMR Spectrum of Compound **19n**

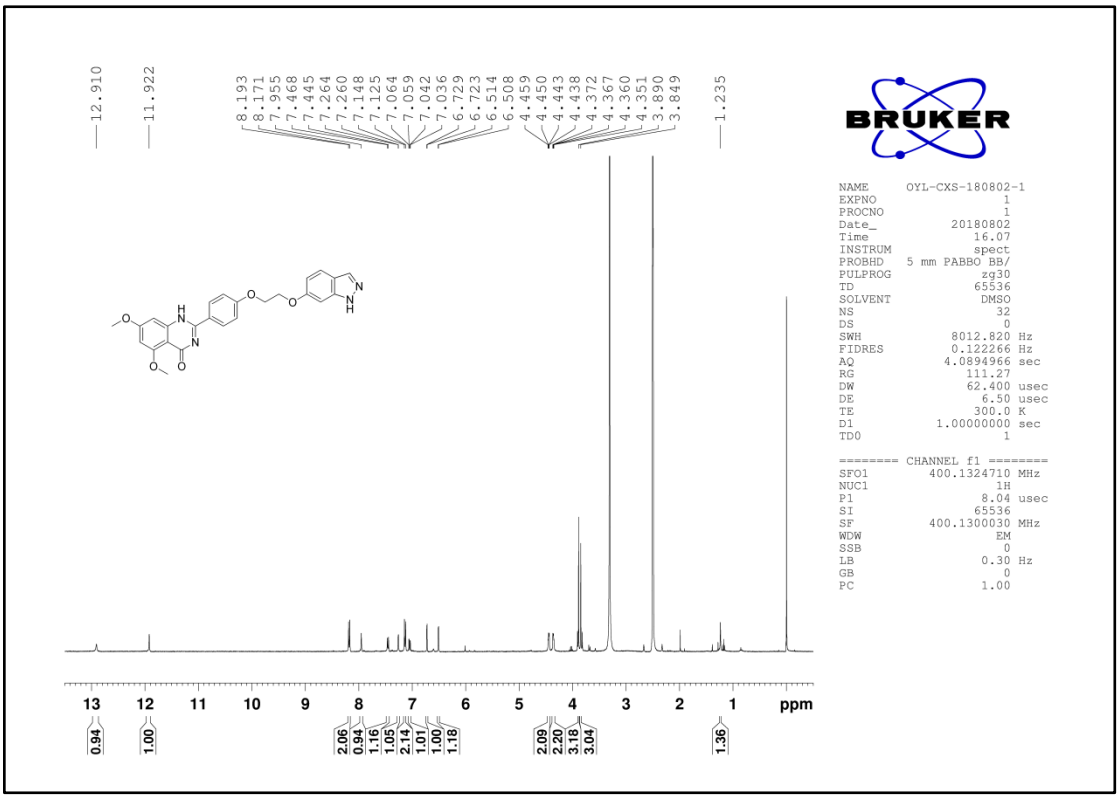


```
NAME      OYL-CXS-180802-1
EXPNO               1
PROCNO              1
Date_        20180802
Time            16.07
INSTRUM         spect
PROBHD   5 mm PABBO BB/
PULPROG          zg30
TD              65536
SOLVENT          DMSO
NS                 32
DS                  0
SWH          8012.820 Hz
FIDRES       0.122266 Hz
AQ           4.0894966 sec
RG              111.27
DW               62.400 usec
DE                6.50 usec
TE               300.0 K
D1          1.00000000 sec
TD0                 1

======== CHANNEL f1 ========
SFO1       400.1324710 MHz
NUC1              1H
P1              8.04 usec
SI             65536
SF         400.1300030 MHz
WDW               EM
SSB                0
LB              0.30 Hz
GB                 0
PC              1.00
```

^{1}H NMR Spectrum of Compound **19o**

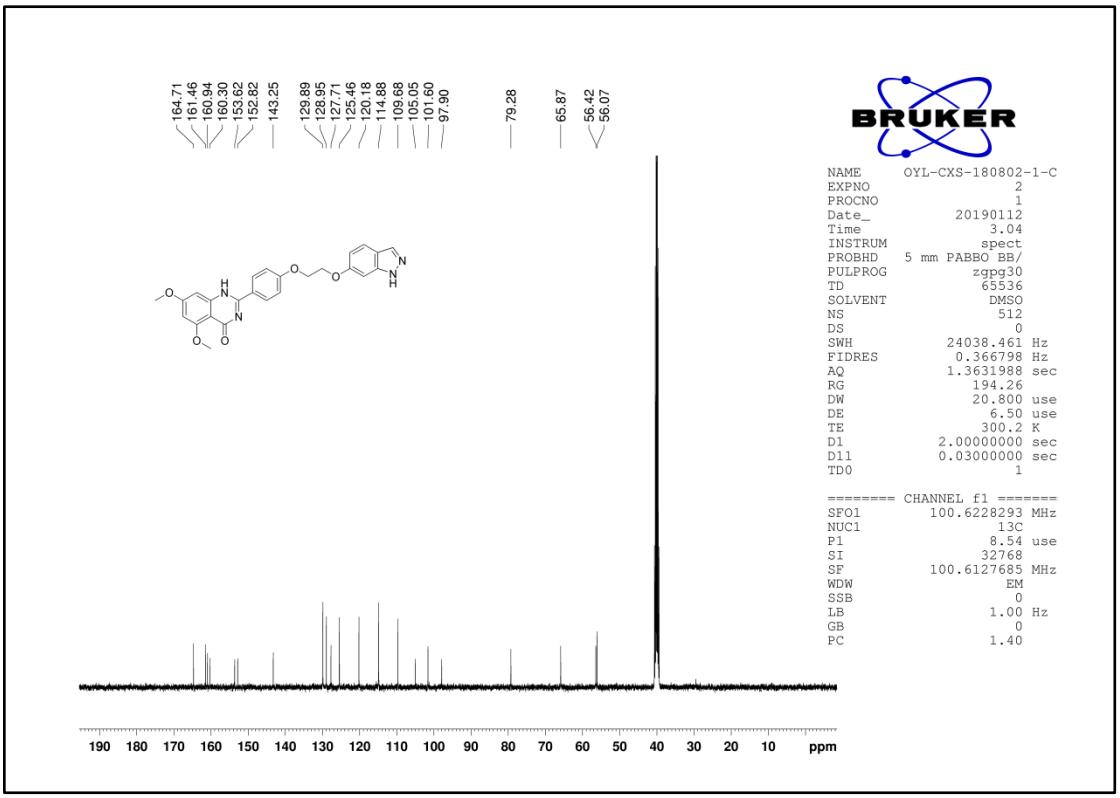


```
NAME      OYL-CXS-180802-1-C
EXPNO               2
PROCNO              1
Date_        20190112
Time            3.04
INSTRUM         spect
PROBHD   5 mm PABBO BB/
PULPROG         zgpg30
TD              65536
SOLVENT          DMSO
NS                512
DS                  0
SWH         24038.461 Hz
FIDRES       0.366798 Hz
AQ           1.3631988 sec
RG              194.26
DW               20.800 use
DE                6.50 use
TE               300.2 K
D1          2.00000000 sec
D11         0.03000000 sec
TD0                 1

======== CHANNEL f1 =======
SFO1       100.6228293 MHz
NUC1              13C
P1              8.54 use
SI             32768
SF         100.6127685 MHz
WDW               EM
SSB                0
LB              1.00 Hz
GB                 0
PC              1.40
```

^{13}C NMR Spectrum of Compound **19o**

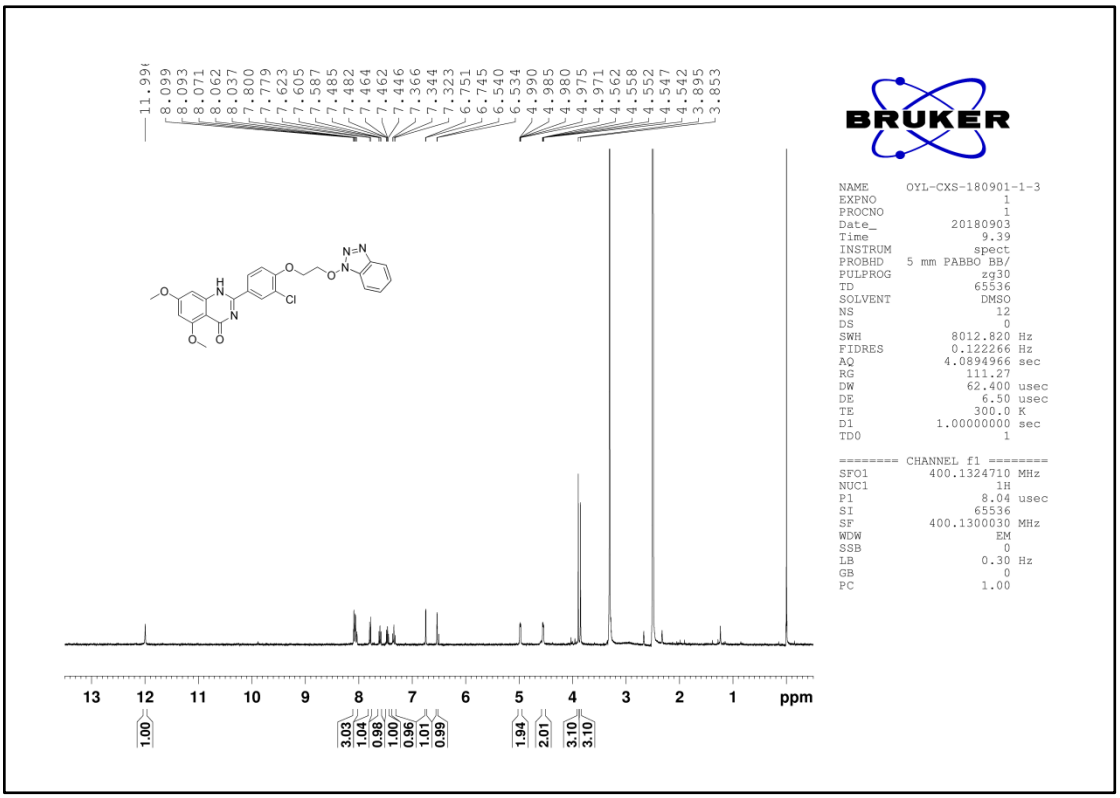

^{1}H NMR Spectrum of Compound **19p**

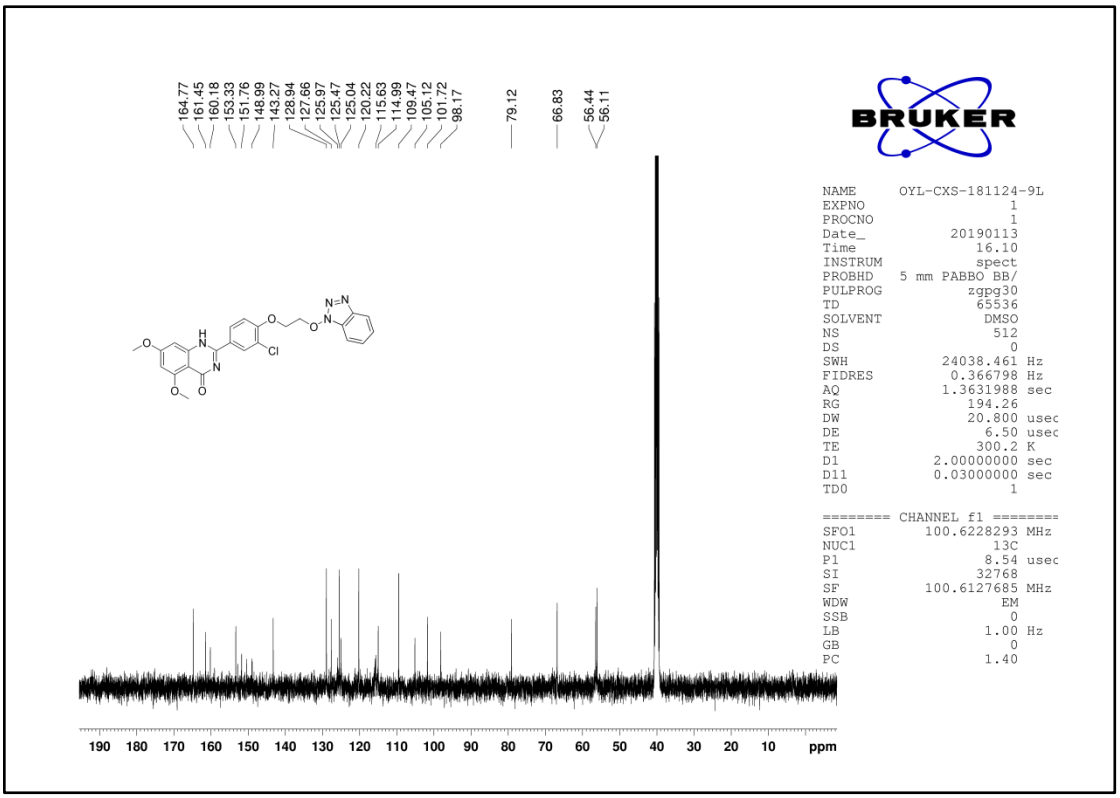

^{13}C NMR Spectrum of Compound **19p**

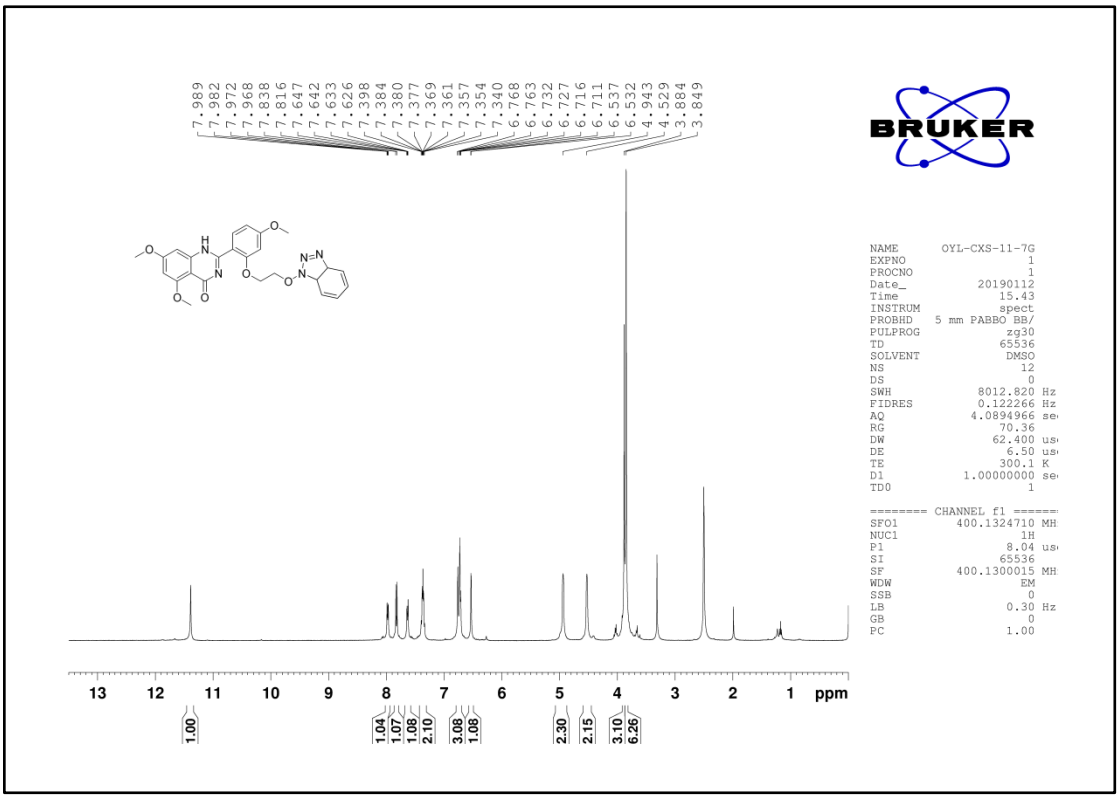

^{1}H NMR Spectrum of Compound **19q**

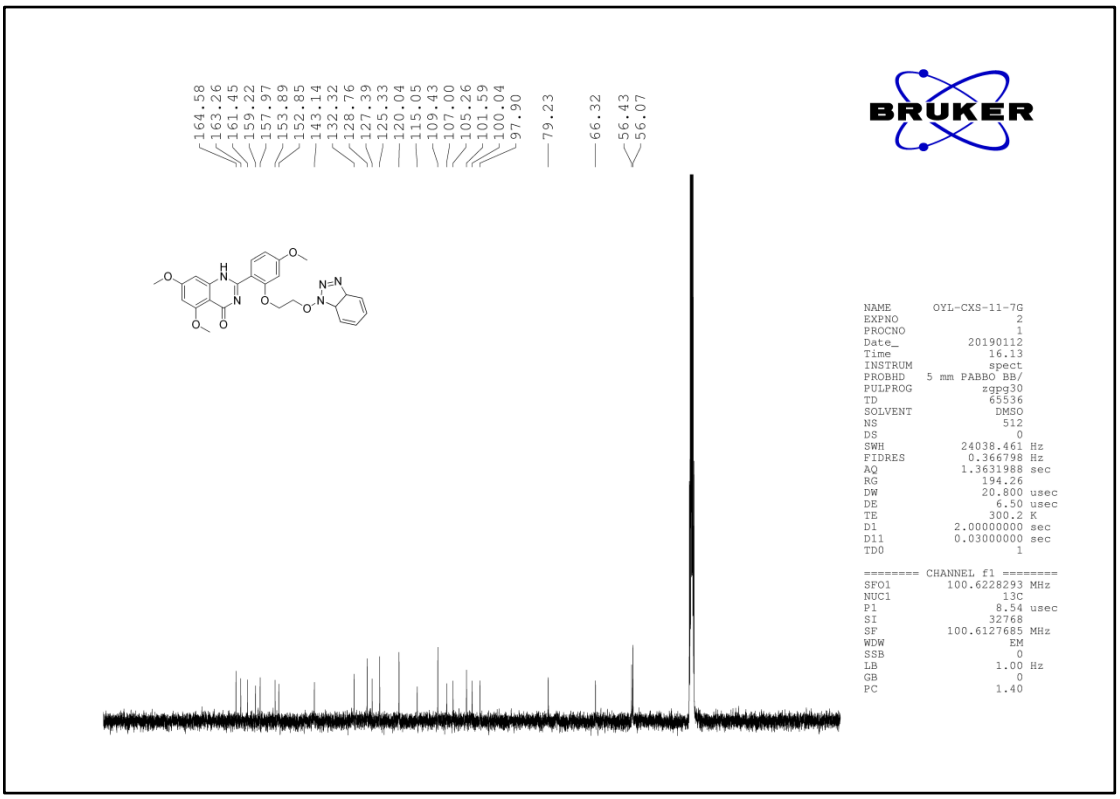

^{13}C NMR Spectrum of Compound **19q**

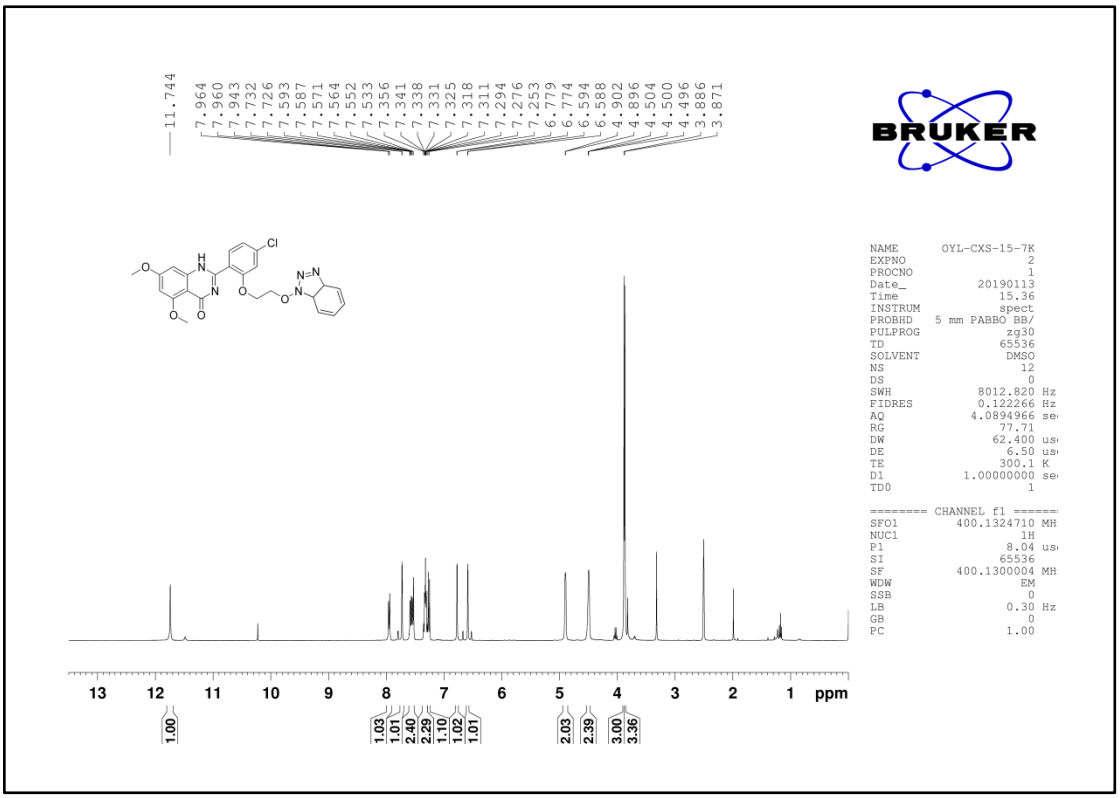

^{1}H NMR Spectrum of Compound **19r**

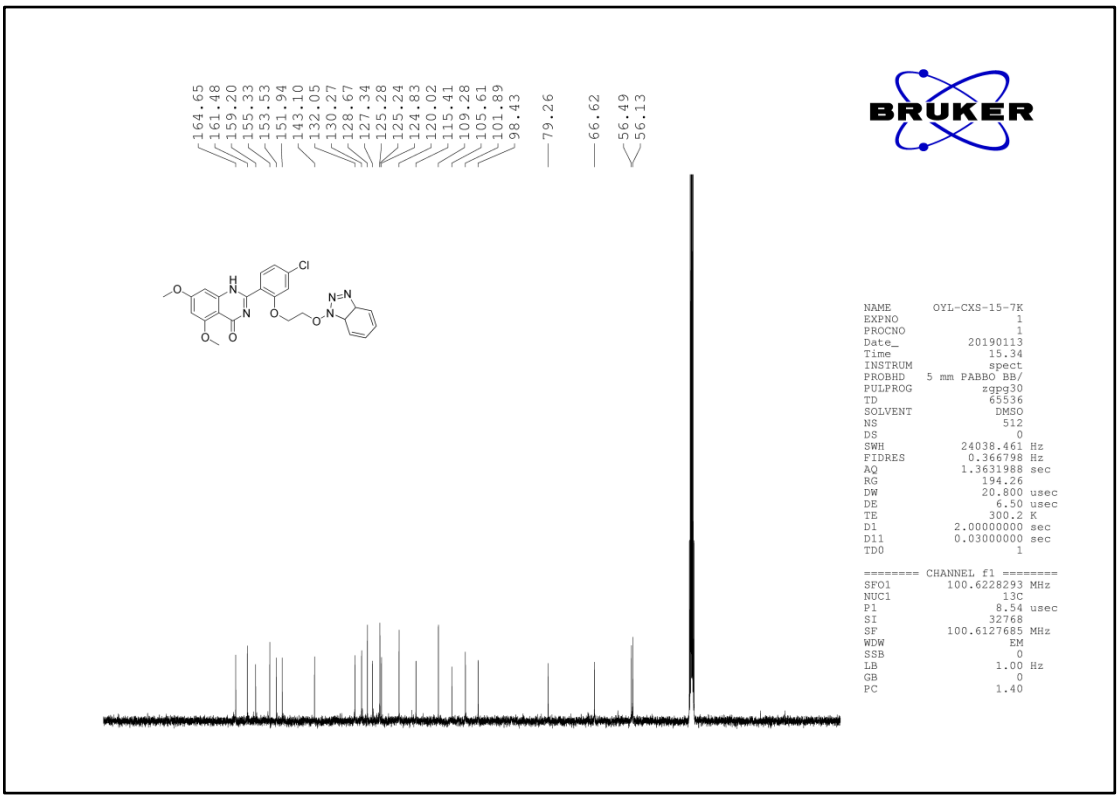

^{13}C NMR Spectrum of Compound **19r**

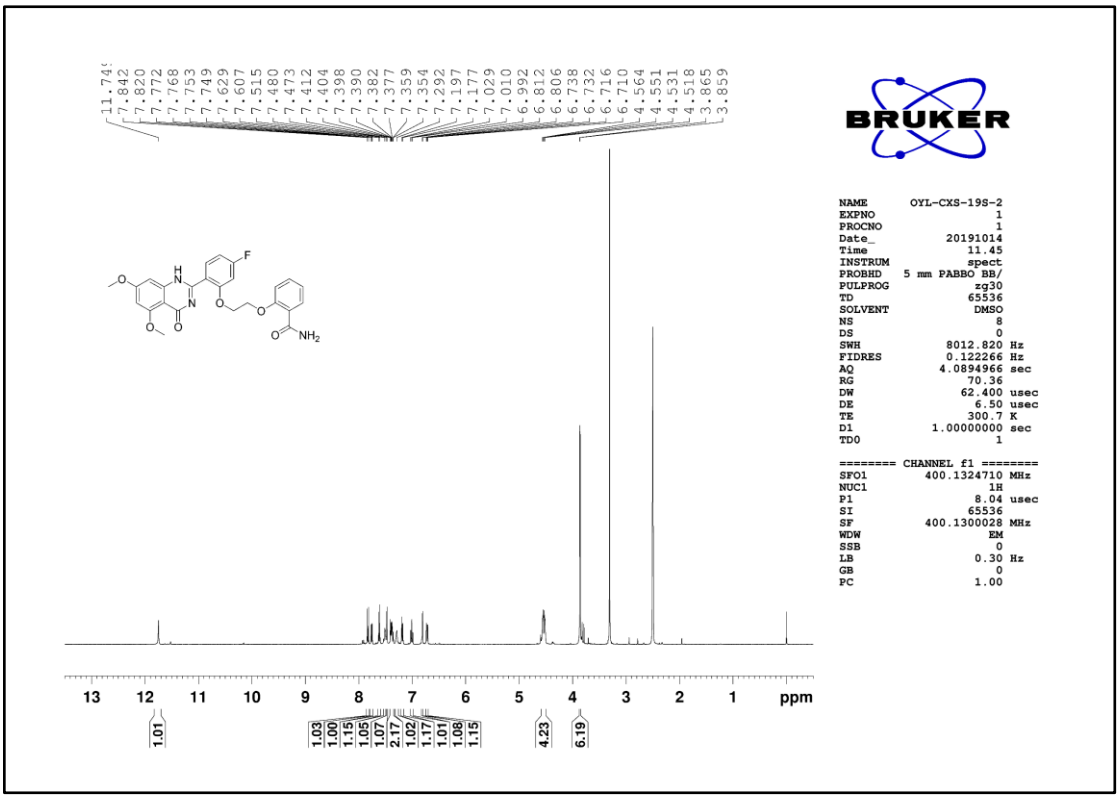

^{1}H NMR Spectrum of Compound **19s**

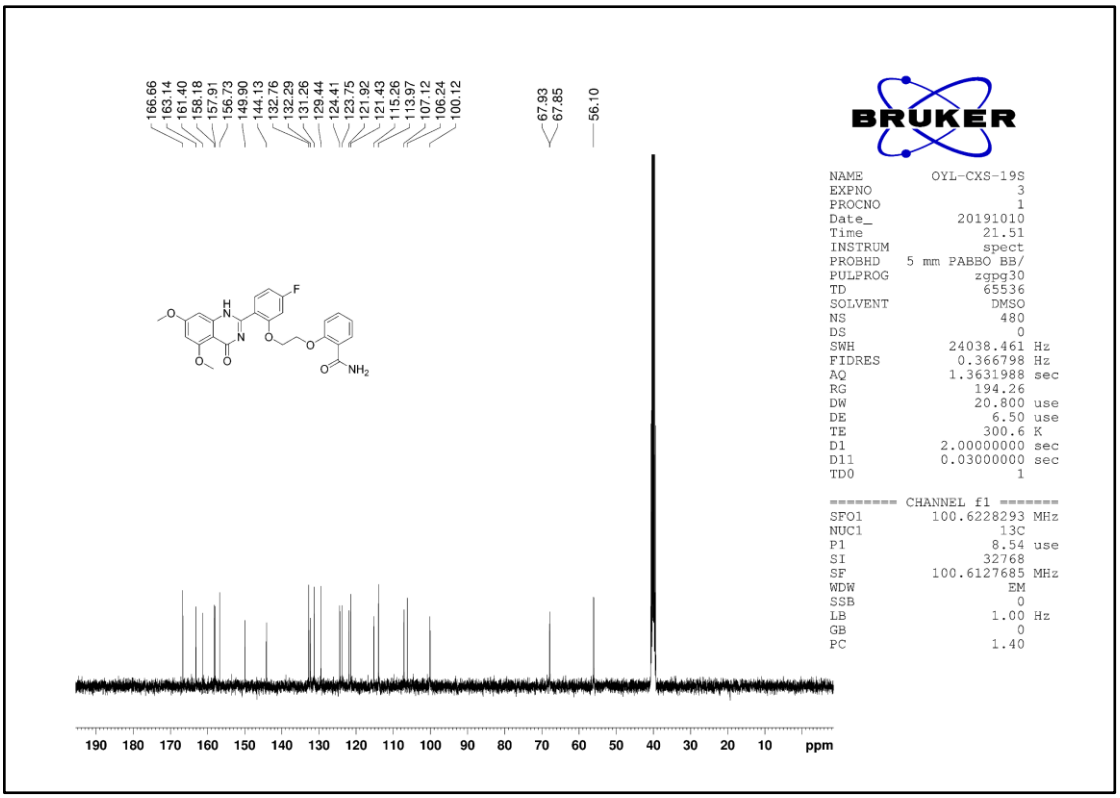

^{13}C NMR Spectrum of Compound 19**s**

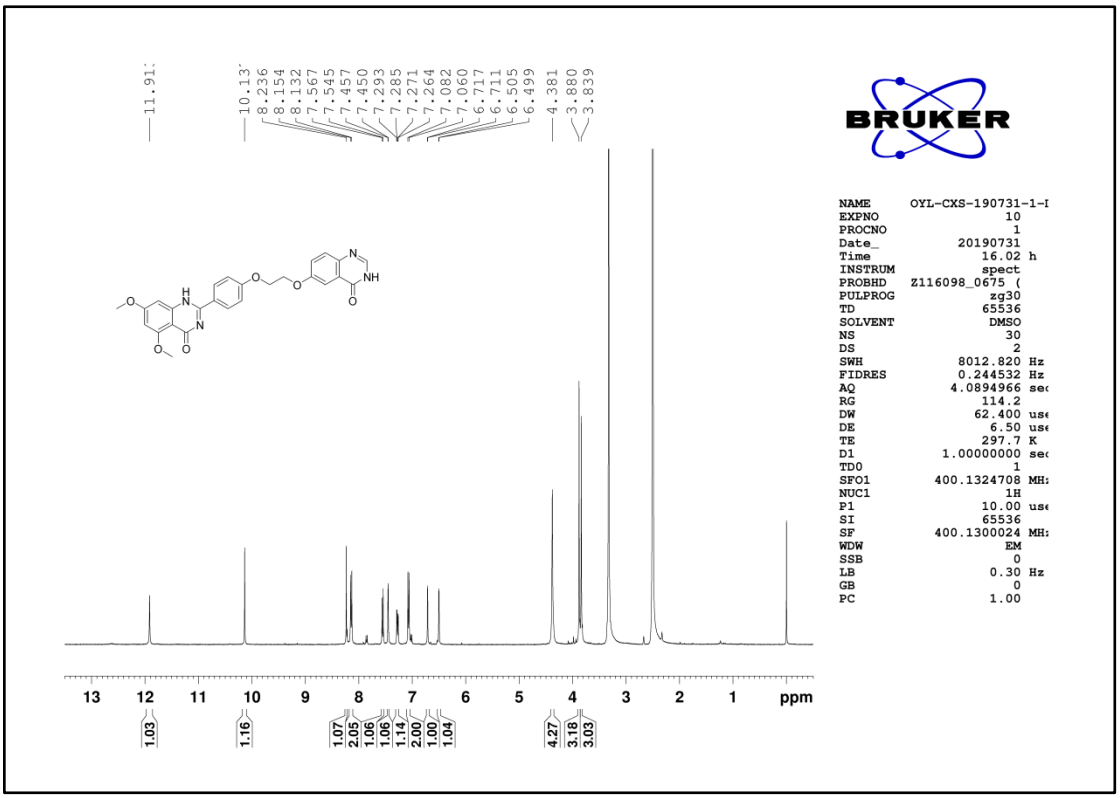

^{1}H NMR Spectrum of Compound **19t**

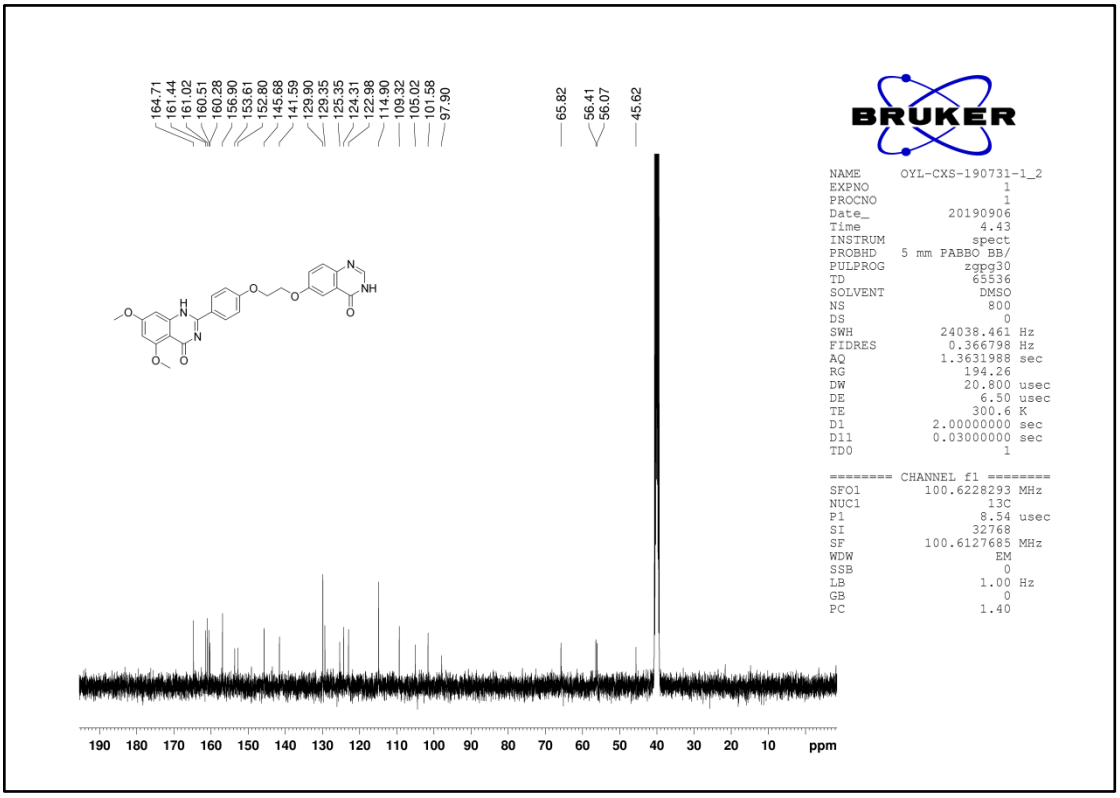

^{13}C NMR Spectrum of Compound **19t**

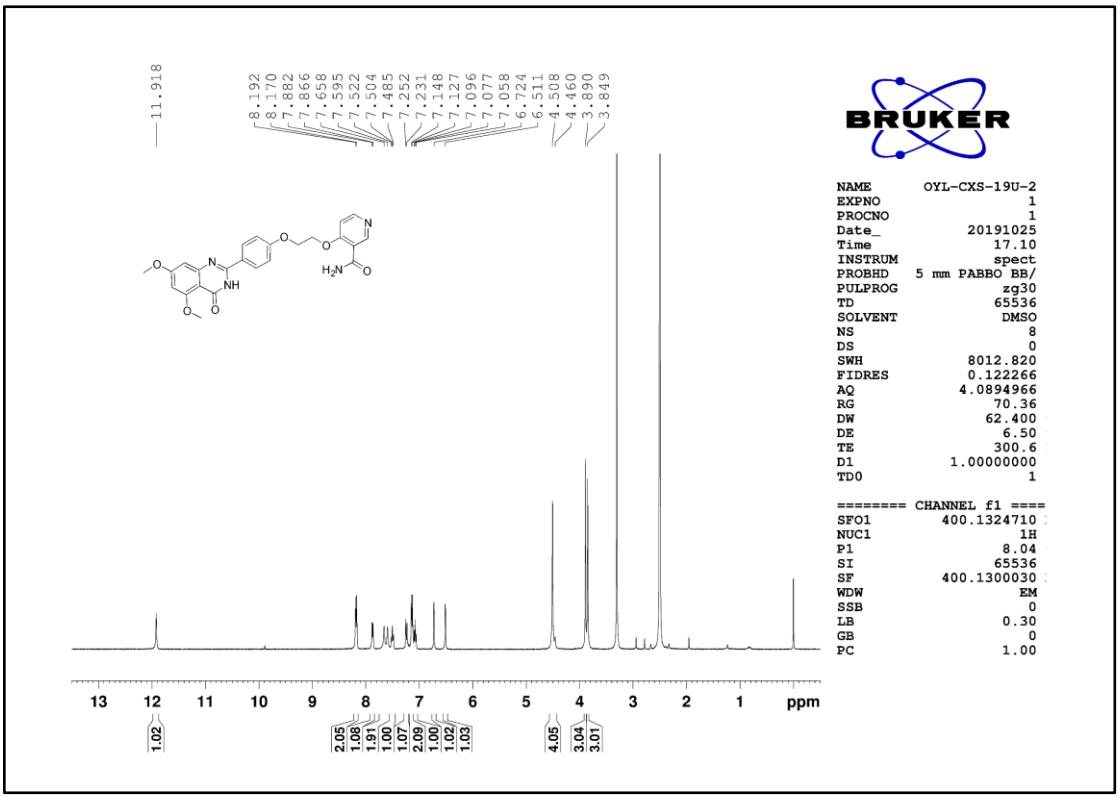

^{1}H NMR Spectrum of Compound **19u**

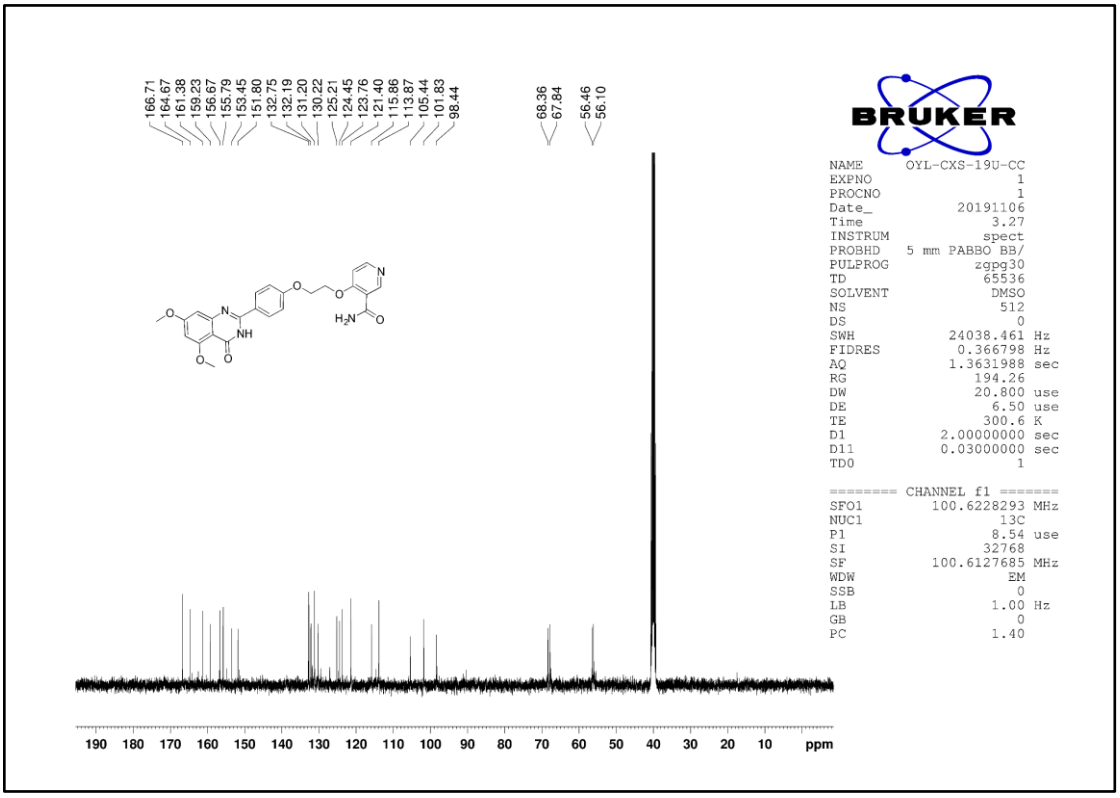

^{13}C NMR Spectrum of Compound **19u**

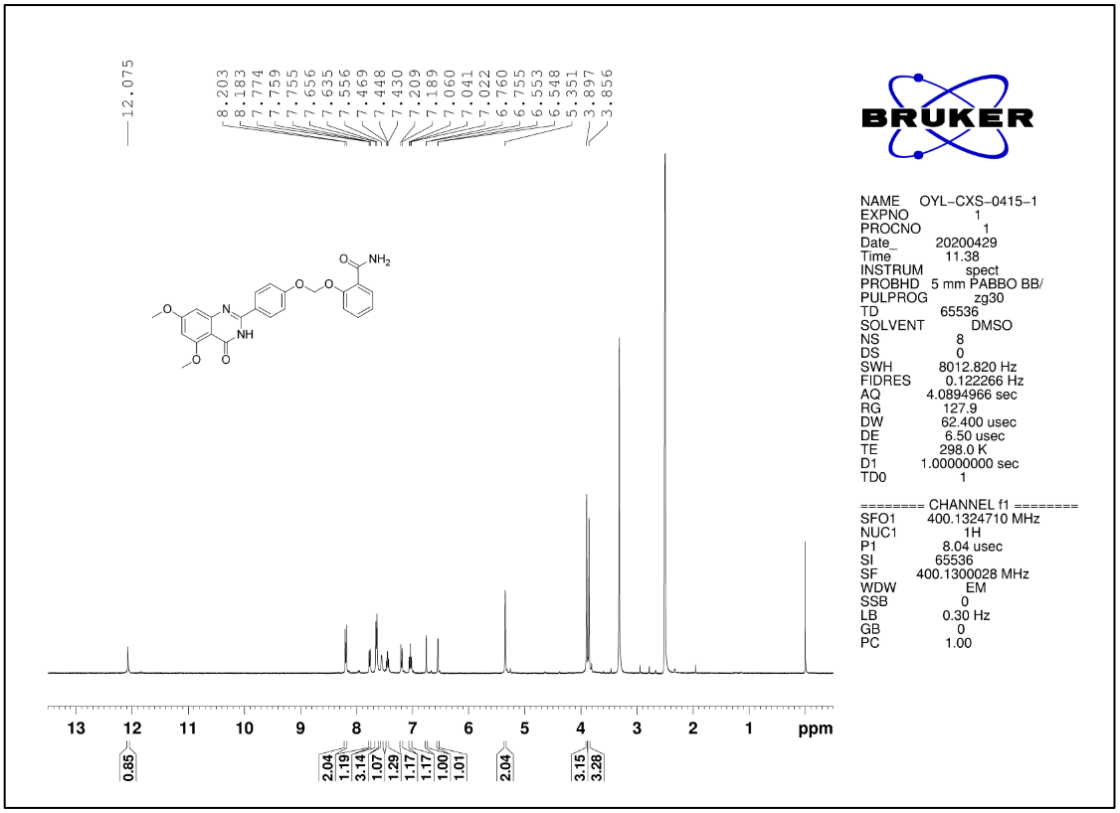

^{1}H NMR Spectrum of Compound **19v**

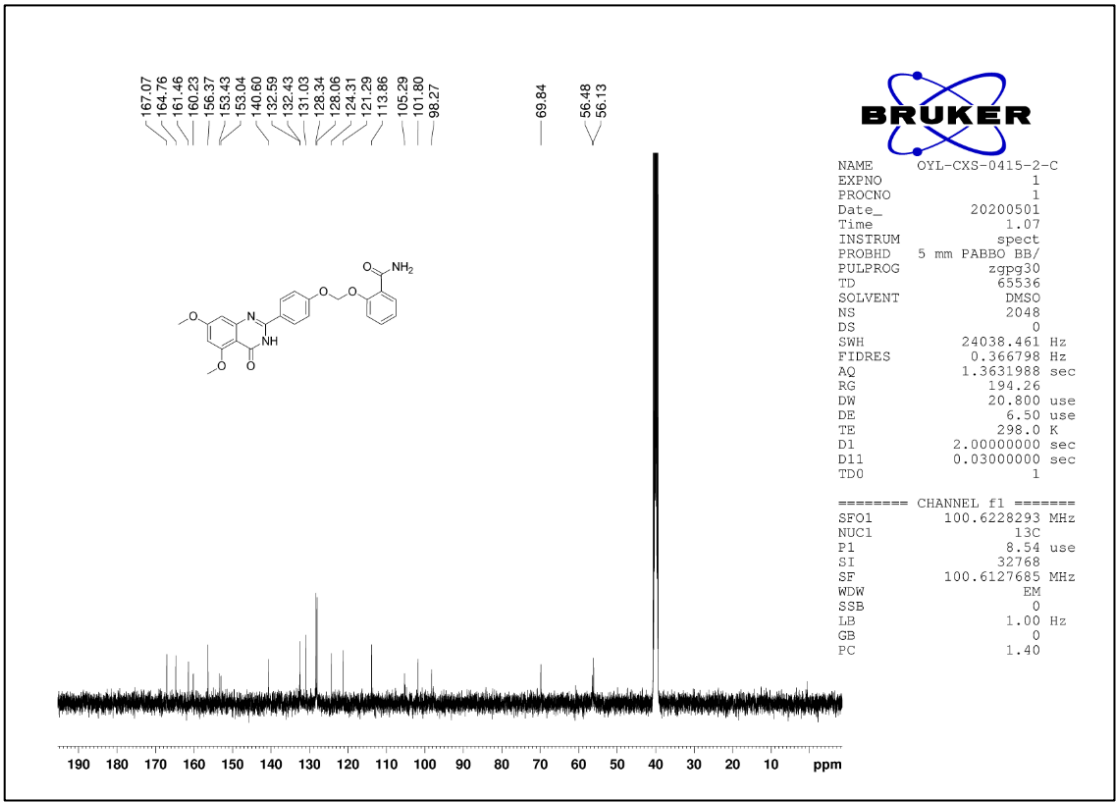

^{13}C NMR Spectrum of Compound **19v**

3. Representative HPLC traces of biologically tested compounds

compound **5a**

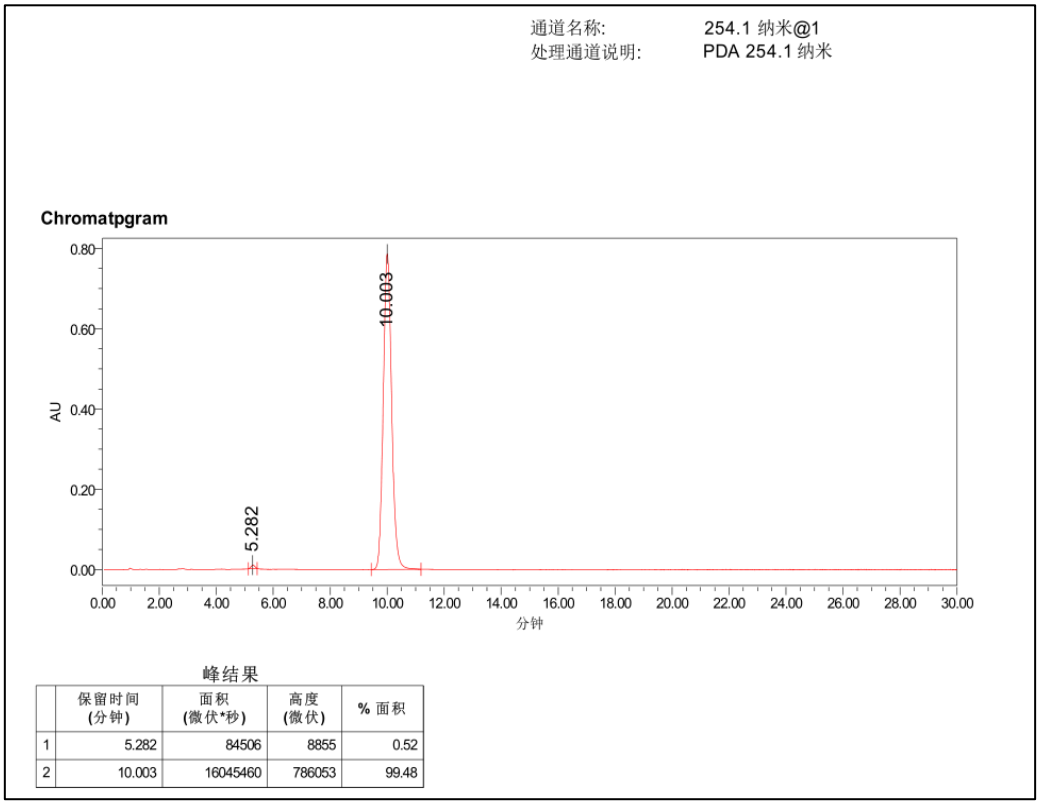

峰结果

	保留时间 (分钟)	面积 (微伏*秒)	高度 (微伏)	% 面积
1	5.282	84506	8855	0.52
2	10.003	16045460	786053	99.48

compound **5b**

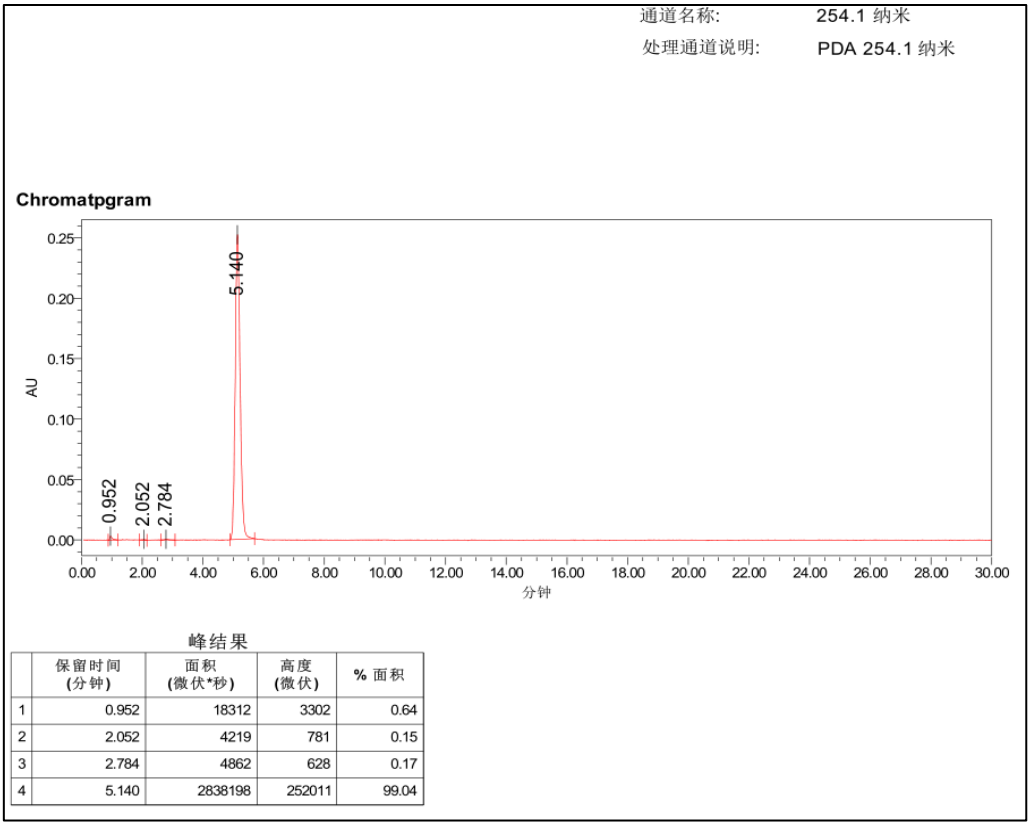

峰结果

	保留时间 (分钟)	面积 (微伏*秒)	高度 (微伏)	% 面积
1	0.952	18312	3302	0.64
2	2.052	4219	781	0.15
3	2.784	4862	628	0.17
4	5.140	2838198	252011	99.04

compound **5c**

通道名称: 254.1 纳米
处理通道说明: PDA 254.1 纳米

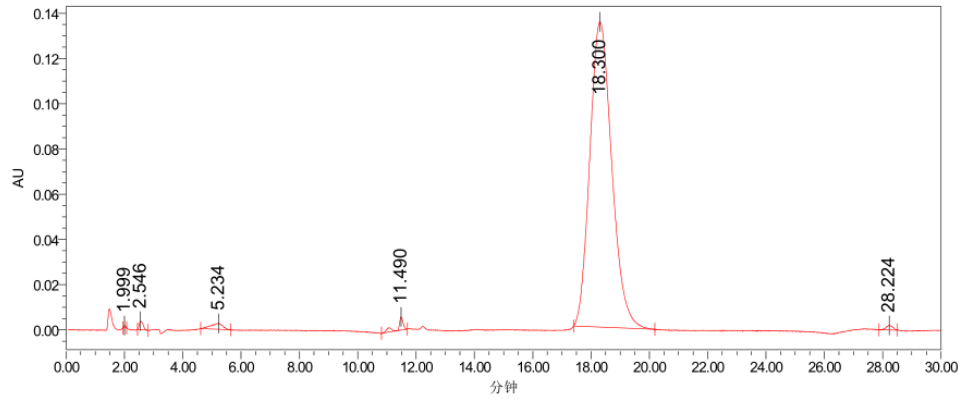

峰结果

	保留时间 (分钟)	面积 (微伏*秒)	高度 (微伏)	% 面积
1	1.999	4427	1024	0.06
2	2.546	35075	3721	0.48
3	5.234	73533	2628	1.01
4	11.490	69182	5849	0.95
5	18.300	7079899	135006	97.07
6	28.224	31828	1980	0.44

compound **5e**

通道名称: 254.1 纳米
处理通道说明: PDA 254.1 纳米

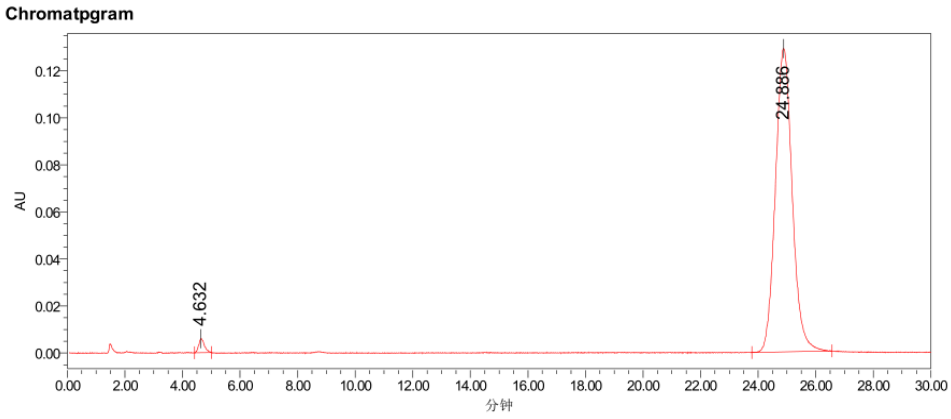

峰结果

	保留时间 (分钟)	面积 (微伏*秒)	高度 (微伏)	% 面积
1	4.632	83615	5963	1.57
2	24.886	5243918	129015	98.43

compound **5k**

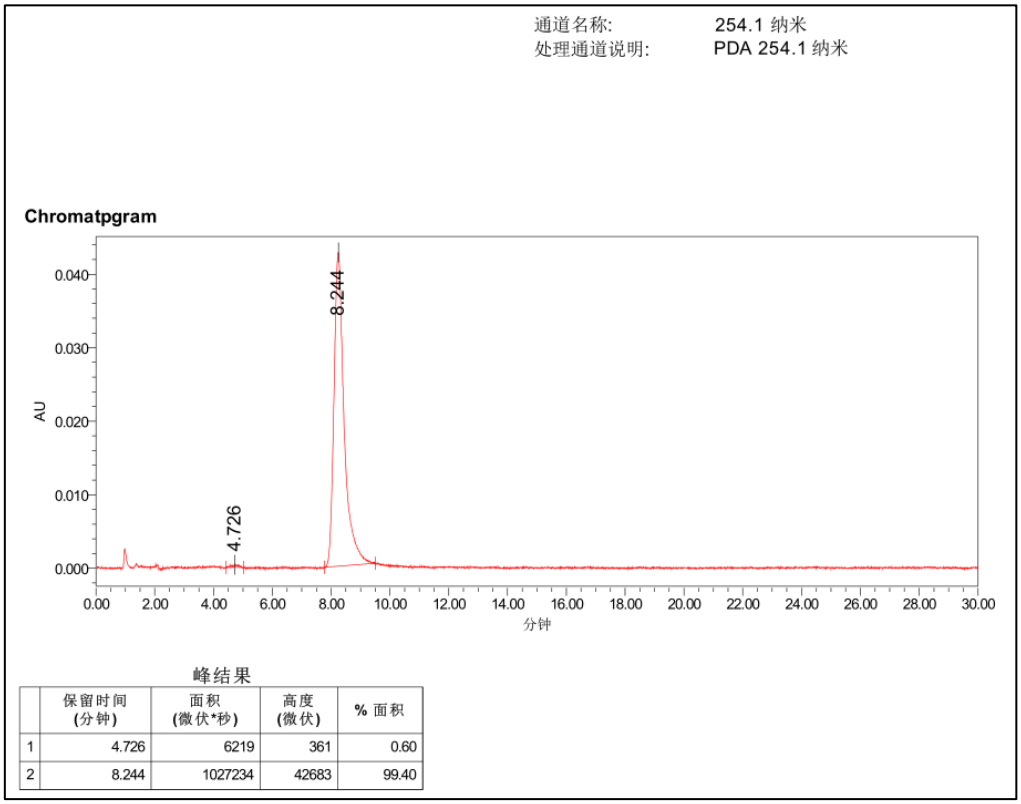

峰结果

	保留时间 (分钟)	面积 (微伏*秒)	高度 (微伏)	% 面积
1	4.726	6219	361	0.60
2	8.244	1027234	42683	99.40

compound **5i**

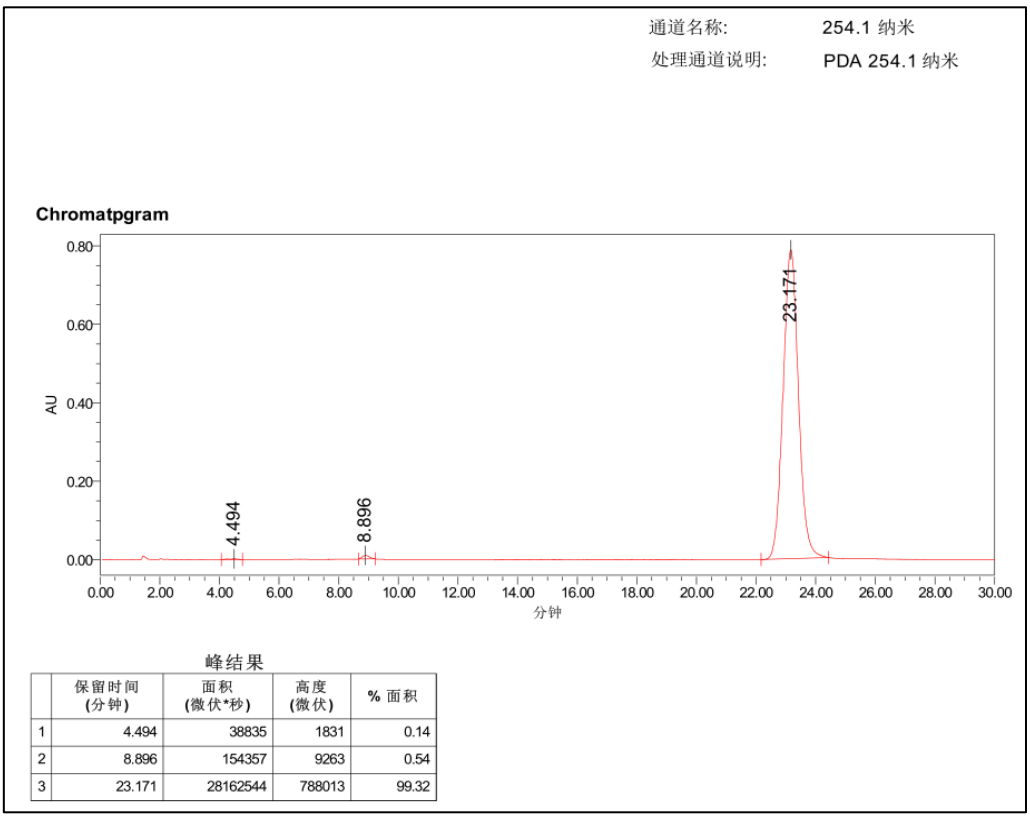

峰结果

	保留时间 (分钟)	面积 (微伏*秒)	高度 (微伏)	% 面积
1	4.494	38835	1831	0.14
2	8.896	154357	9263	0.54
3	23.171	28162544	788013	99.32

compound **5g**

通道名称: 254.1 纳米
处理通道说明: PDA 254.1 纳米

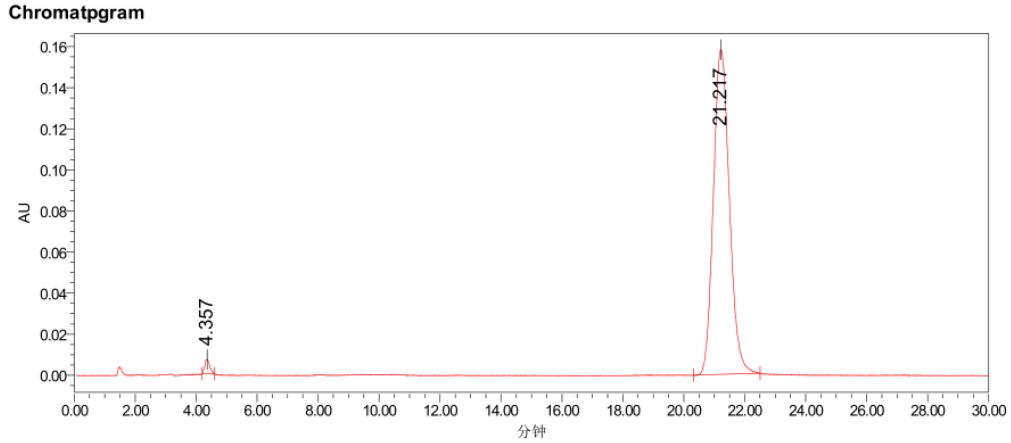

峰结果

	保留时间 (分钟)	面积 (微伏*秒)	高度 (微伏)	% 面积
1	4.357	79300	7040	1.36
2	21.217	5745685	158074	98.64

compound **11b**

通道名称: 254.1 纳米
处理通道说明: PDA 254.1 纳米

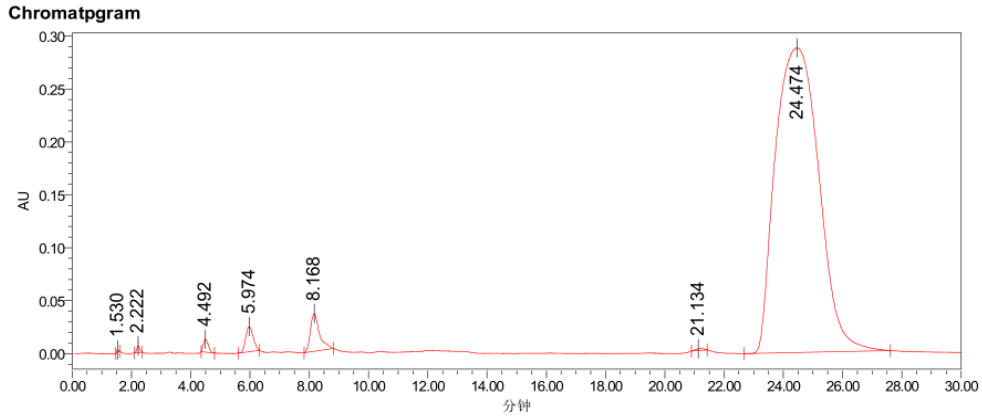

峰结果

	保留时间 (分钟)	面积 (微伏*秒)	高度 (微伏)	% 面积
1	1.530	11203	2421	0.04
2	2.222	41696	6292	0.14
3	4.492	143047	12261	0.46
4	5.974	423789	23791	1.38
5	8.168	745578	35485	2.42
6	21.134	34545	1823	0.11
7	24.474	29395251	287736	95.45

compound **11d**

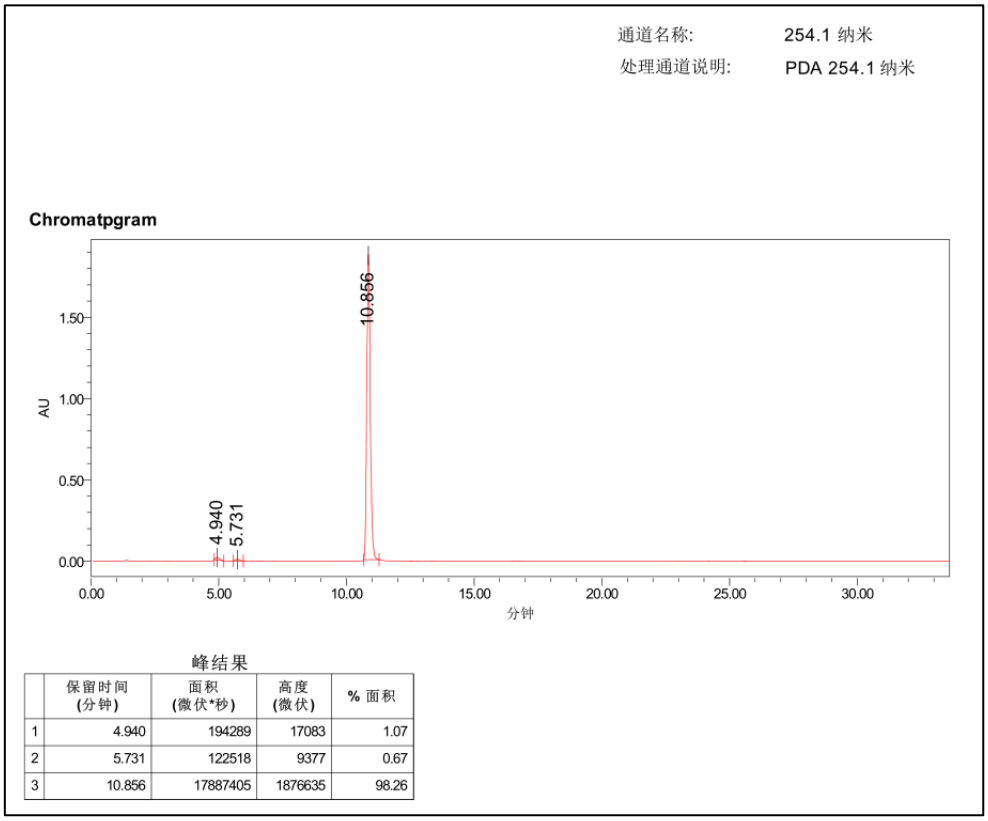

峰结果

	保留时间 (分钟)	面积 (微伏*秒)	高度 (微伏)	% 面积
1	4.940	194289	17083	1.07
2	5.731	122518	9377	0.67
3	10.856	17887405	1876635	98.26

compound **11e**

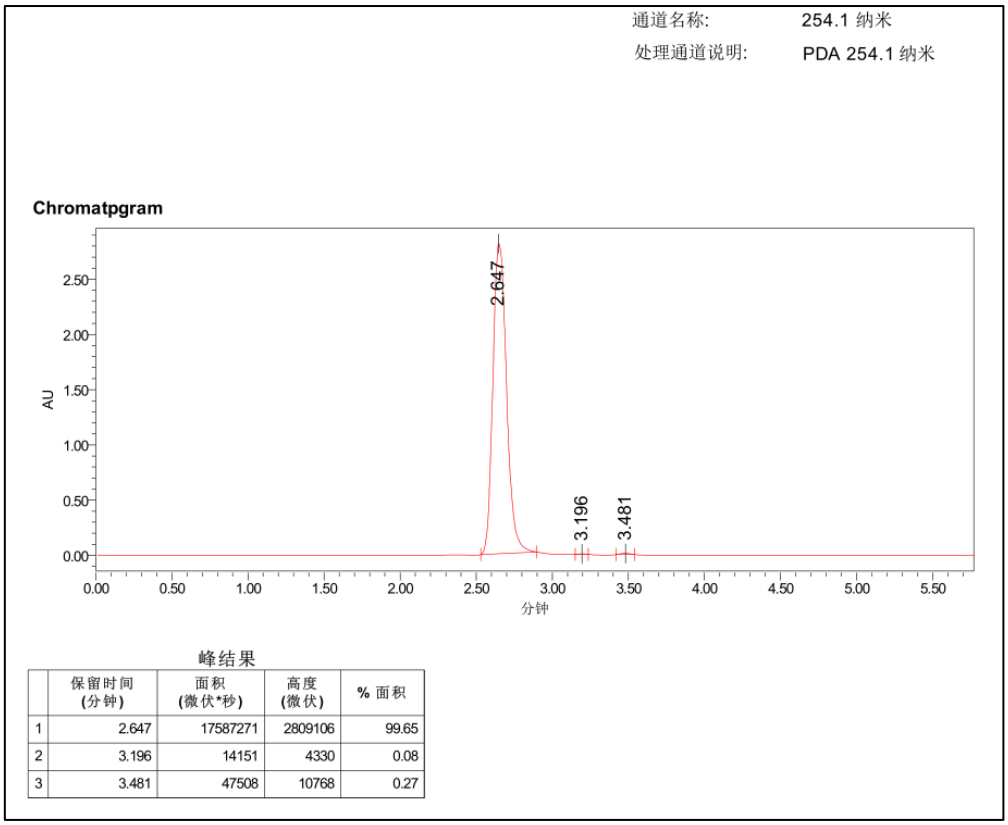

峰结果

	保留时间 (分钟)	面积 (微伏*秒)	高度 (微伏)	% 面积
1	2.647	17587271	2809106	99.65
2	3.196	14151	4330	0.08
3	3.481	47508	10768	0.27

compound **15a**

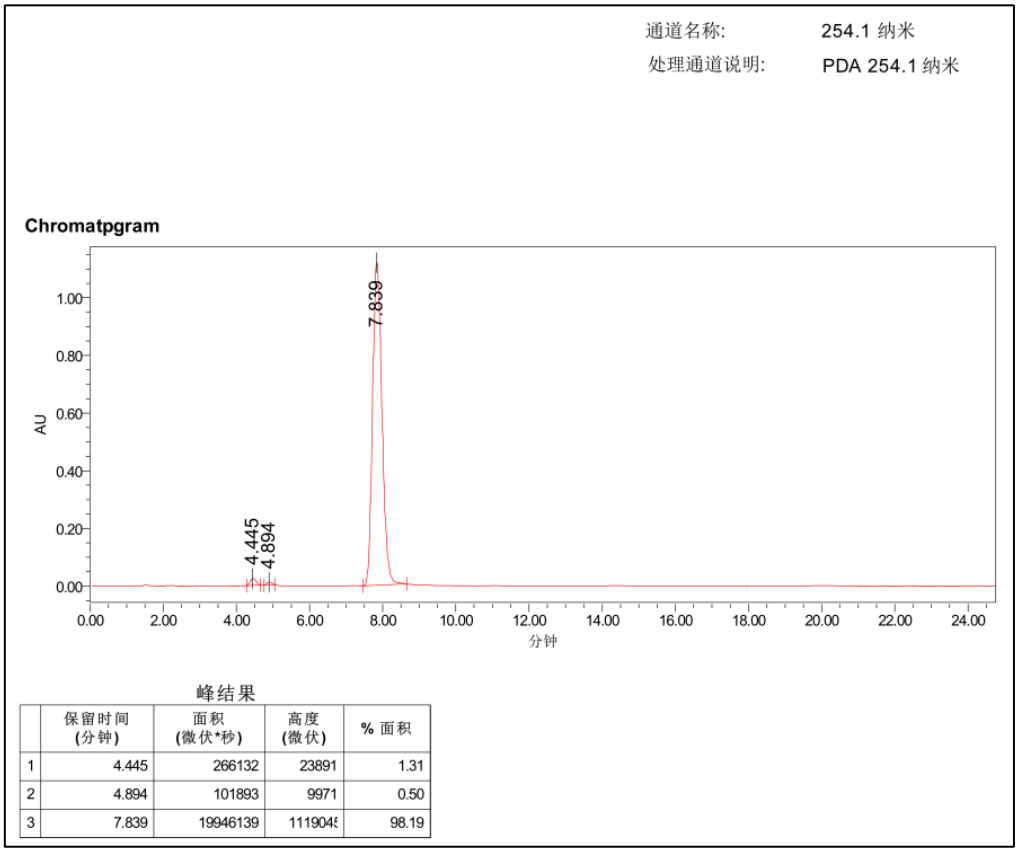

峰结果

	保留时间 (分钟)	面积 (微伏*秒)	高度 (微伏)	% 面积
1	4.445	266132	23891	1.31
2	4.894	101893	9971	0.50
3	7.839	19946139	111904	98.19

compound **15b**

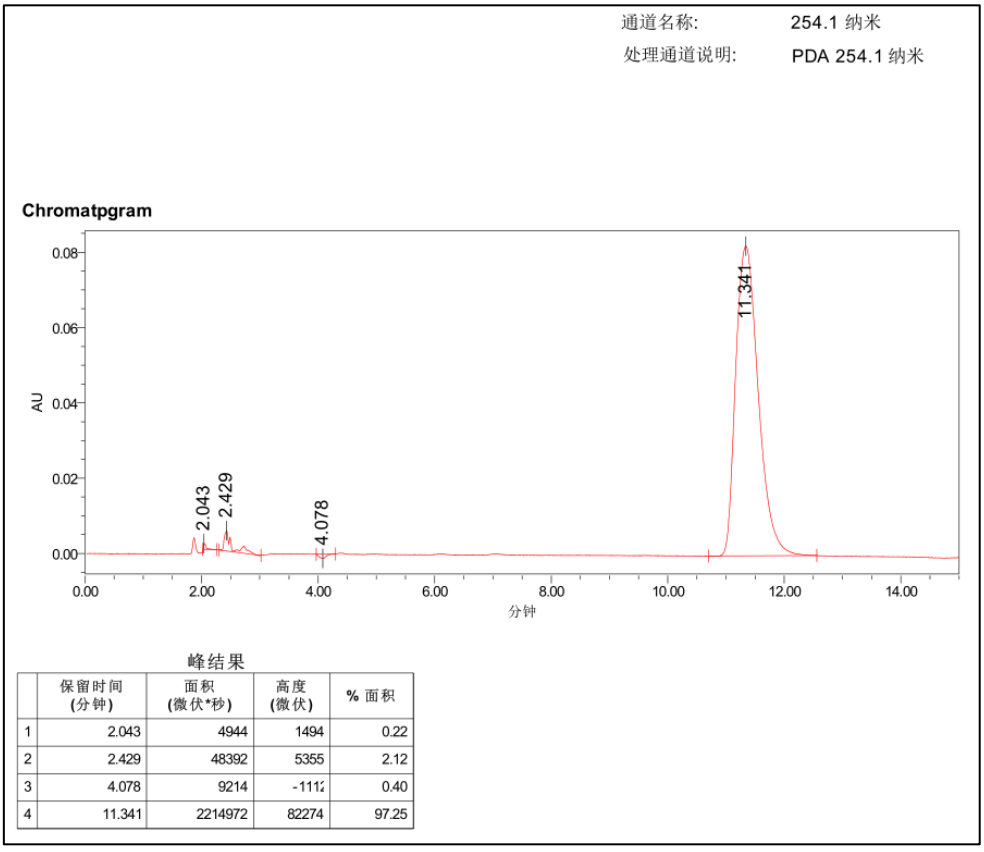

峰结果

	保留时间 (分钟)	面积 (微伏*秒)	高度 (微伏)	% 面积
1	2.043	4944	1494	0.22
2	2.429	48392	5355	2.12
3	4.078	9214	-111	0.40
4	11.341	2214972	82274	97.25

compound **19a**

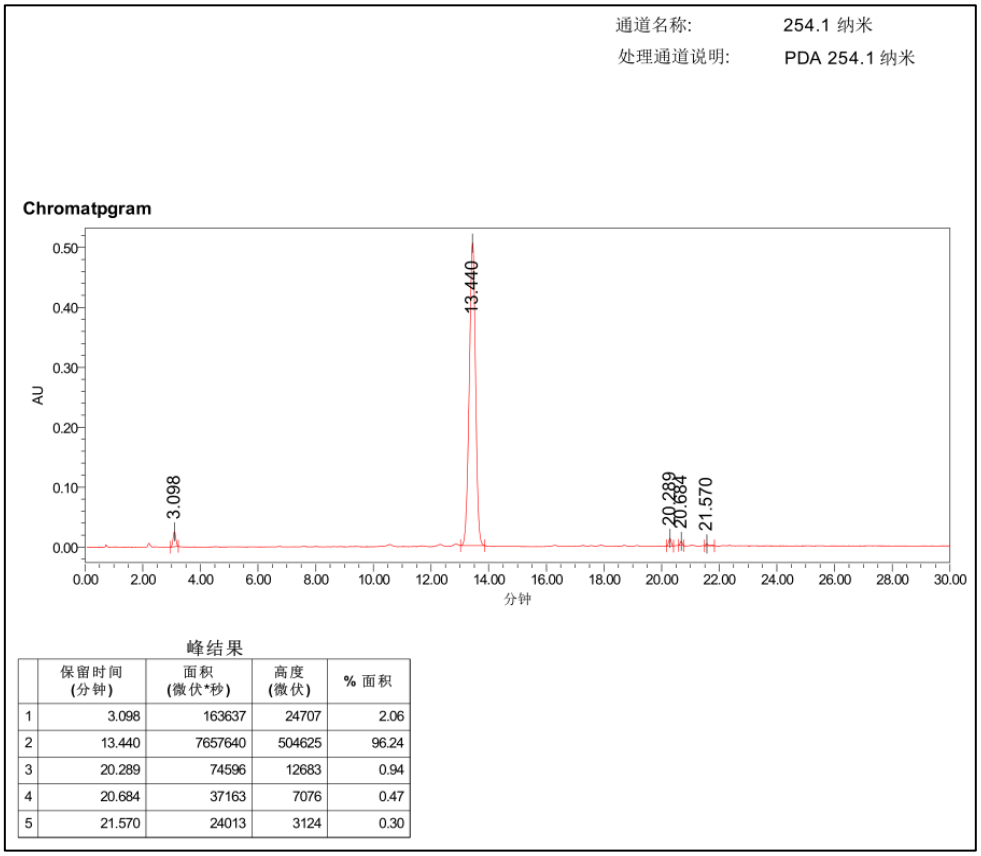

峰结果

	保留时间 (分钟)	面积 (微伏*秒)	高度 (微伏)	% 面积
1	3.098	163637	24707	2.06
2	13.440	7657640	504625	96.24
3	20.289	74596	12683	0.94
4	20.684	37163	7076	0.47
5	21.570	24013	3124	0.30

compound **19d**

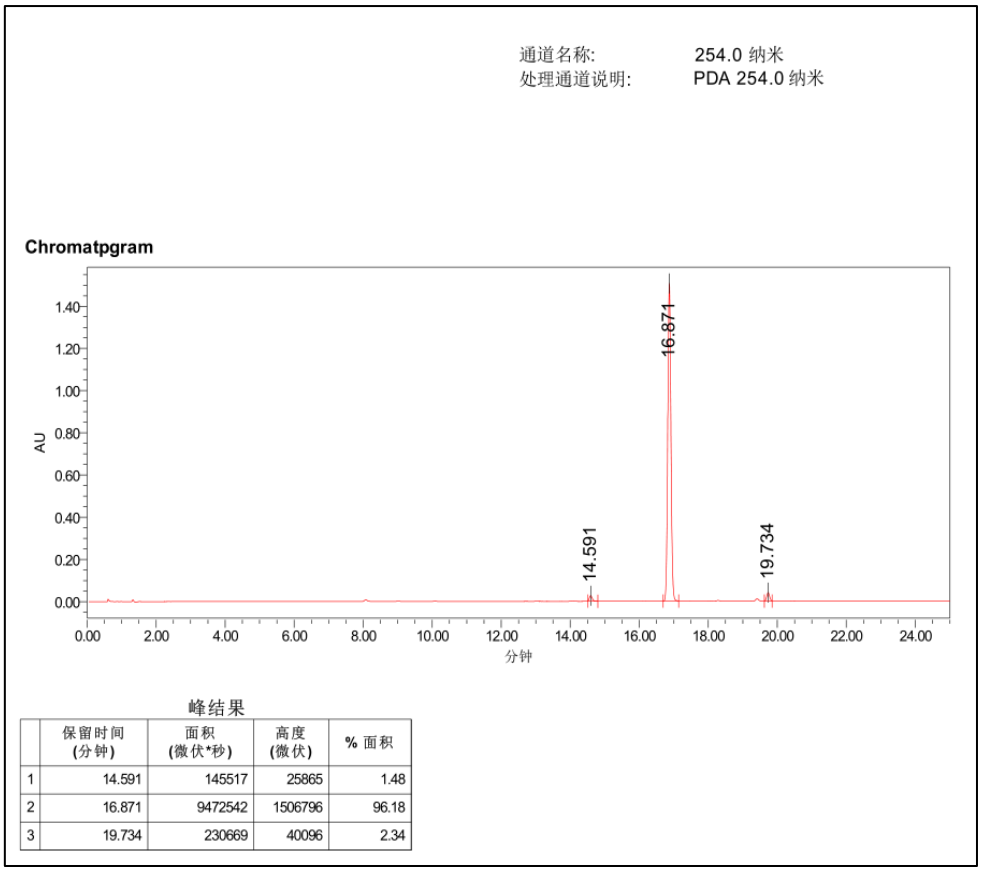

峰结果

	保留时间 (分钟)	面积 (微伏*秒)	高度 (微伏)	% 面积
1	14.591	145517	25865	1.48
2	16.871	9472542	1506796	96.18
3	19.734	230669	40096	2.34

compound **19f**

通道名称: 254.1 纳米
处理通道说明: PDA 254.1 纳米

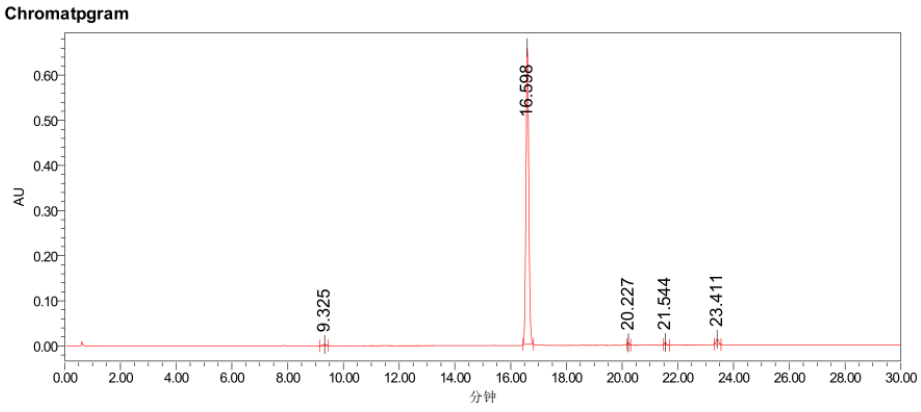

峰结果

	保留时间 (分钟)	面积 (微伏*秒)	高度 (微伏)	% 面积
1	9.325	22257	2744	0.47
2	16.598	4594246	657798	96.92
3	20.227	18948	4330	0.40
4	21.544	20753	4709	0.44
5	23.411	84107	11579	1.77

compound **19i**

通道名称: 254.1 纳米
处理通道说明: PDA 254.1 纳米

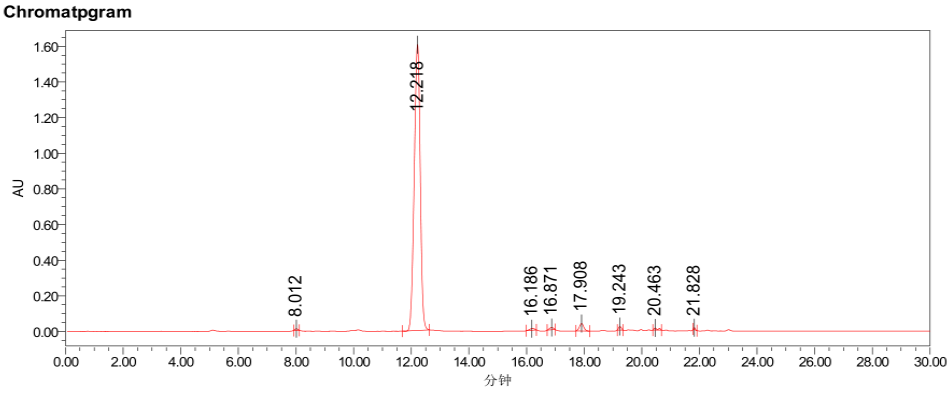

峰结果

	保留时间 (分钟)	面积 (微伏*秒)	高度 (微伏)	% 面积
1	8.012	63966	9005	0.27
2	12.218	23001623	1603306	95.69
3	16.186	116394	9773	0.48
4	16.871	134476	13335	0.56
5	17.908	440428	41468	1.83
6	19.243	129760	19451	0.54
7	20.463	111546	12202	0.46
8	21.828	39431	10300	0.16

compound **19g**

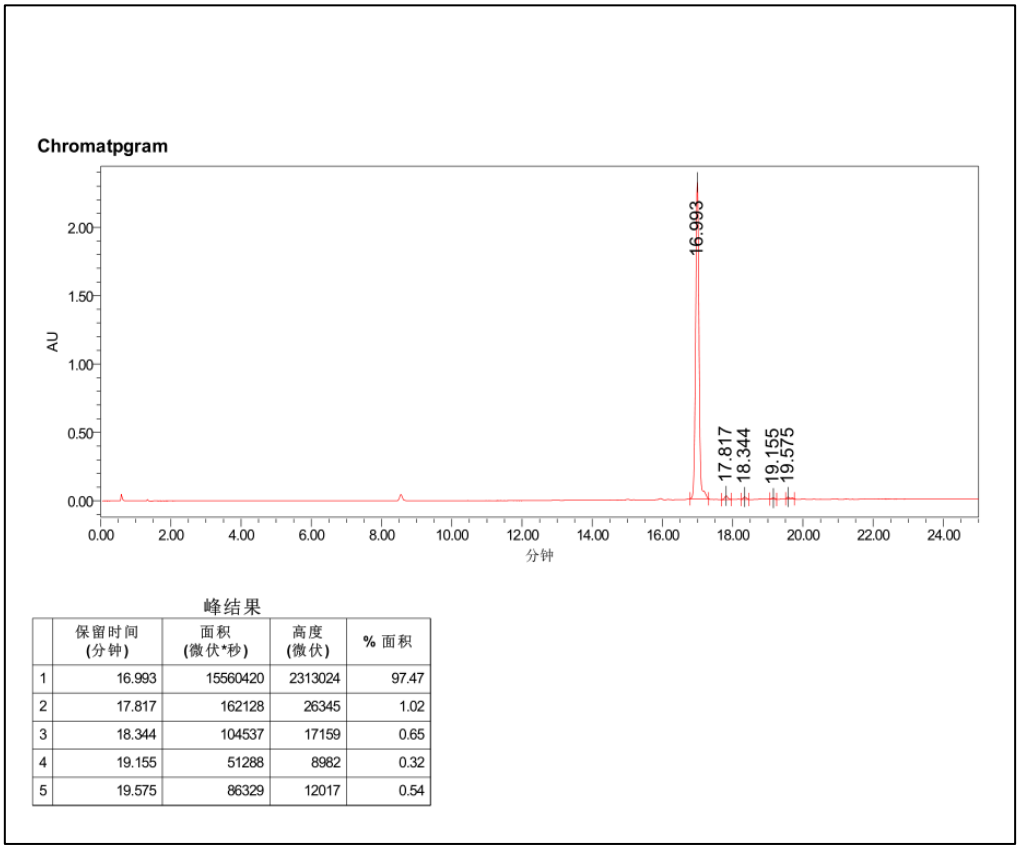

峰结果

	保留时间 (分钟)	面积 (微伏*秒)	高度 (微伏)	% 面积
1	16.993	15560420	2313024	97.47
2	17.817	162128	26345	1.02
3	18.344	104537	17159	0.65
4	19.155	51288	8982	0.32
5	19.575	86329	12017	0.54

compound **19h**

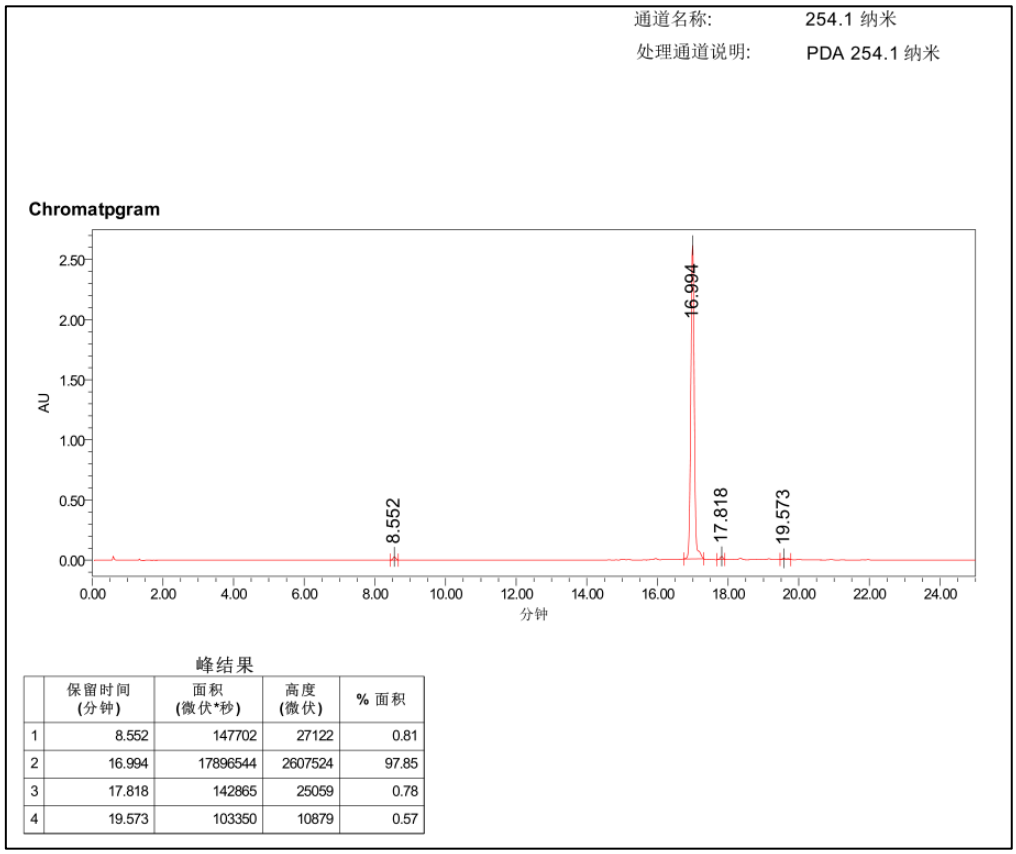

峰结果

	保留时间 (分钟)	面积 (微伏*秒)	高度 (微伏)	% 面积
1	8.552	147702	27122	0.81
2	16.994	17896544	2607524	97.85
3	17.818	142865	25059	0.78
4	19.573	103350	10879	0.57

compound **19k**

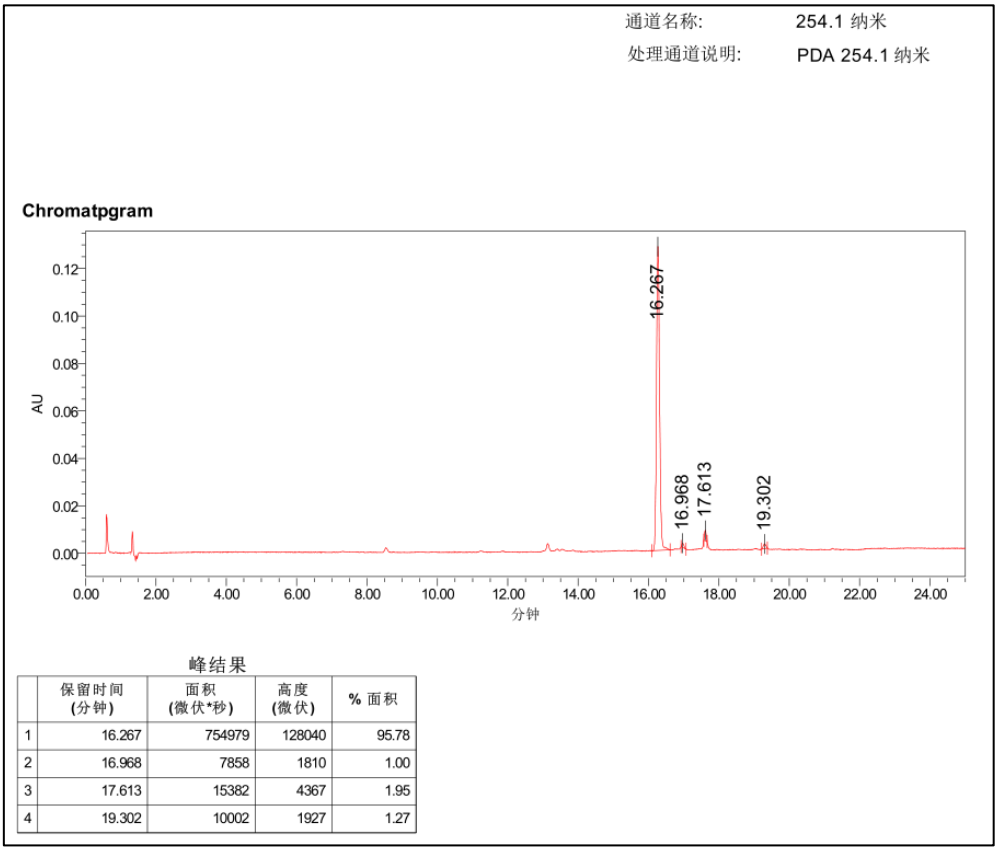

峰结果

	保留时间 (分钟)	面积 (微伏*秒)	高度 (微伏)	% 面积
1	16.267	754979	128040	95.78
2	16.968	7858	1810	1.00
3	17.613	15382	4367	1.95
4	19.302	10002	1927	1.27

compound **19o**

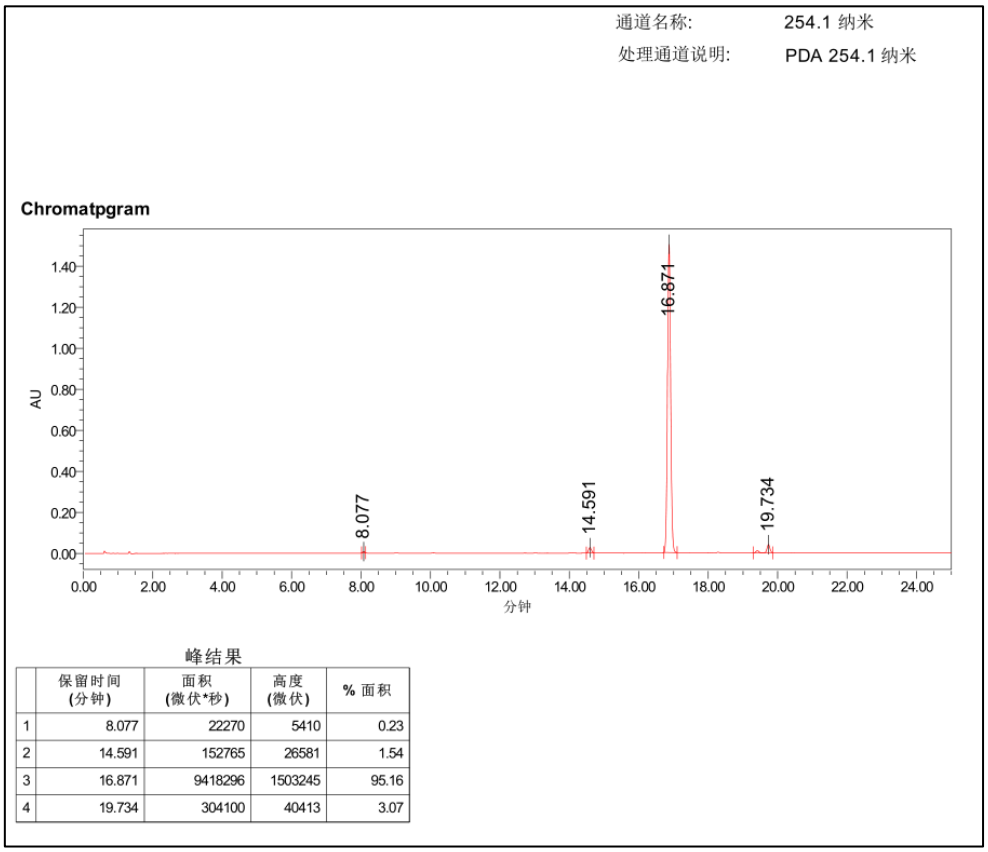

峰结果

	保留时间 (分钟)	面积 (微伏*秒)	高度 (微伏)	% 面积
1	8.077	22270	5410	0.23
2	14.591	152765	26581	1.54
3	16.871	9418296	1503245	95.16
4	19.734	304100	40413	3.07

compound **19q**

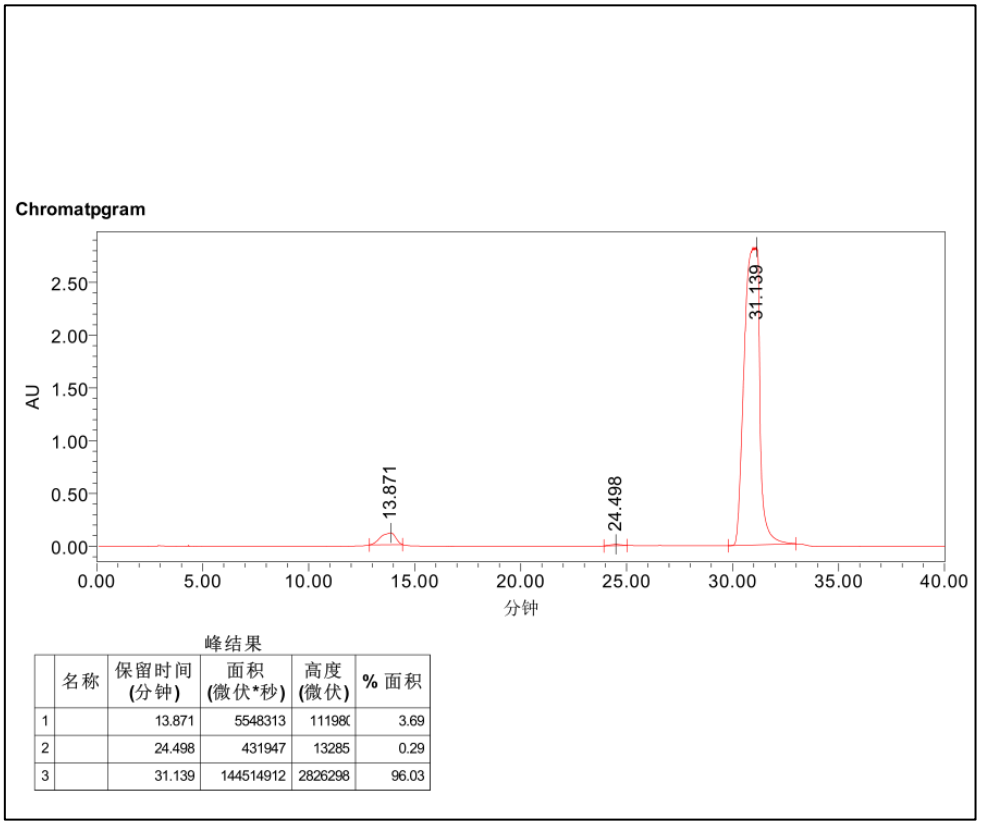

峰结果

	名称	保留时间 (分钟)	面积 (微伏*秒)	高度 (微伏)	% 面积
1		13.871	5548313	11198(	3.69
2		24.498	431947	13285	0.29
3		31.139	144514912	2826298	96.03

compound **19t**

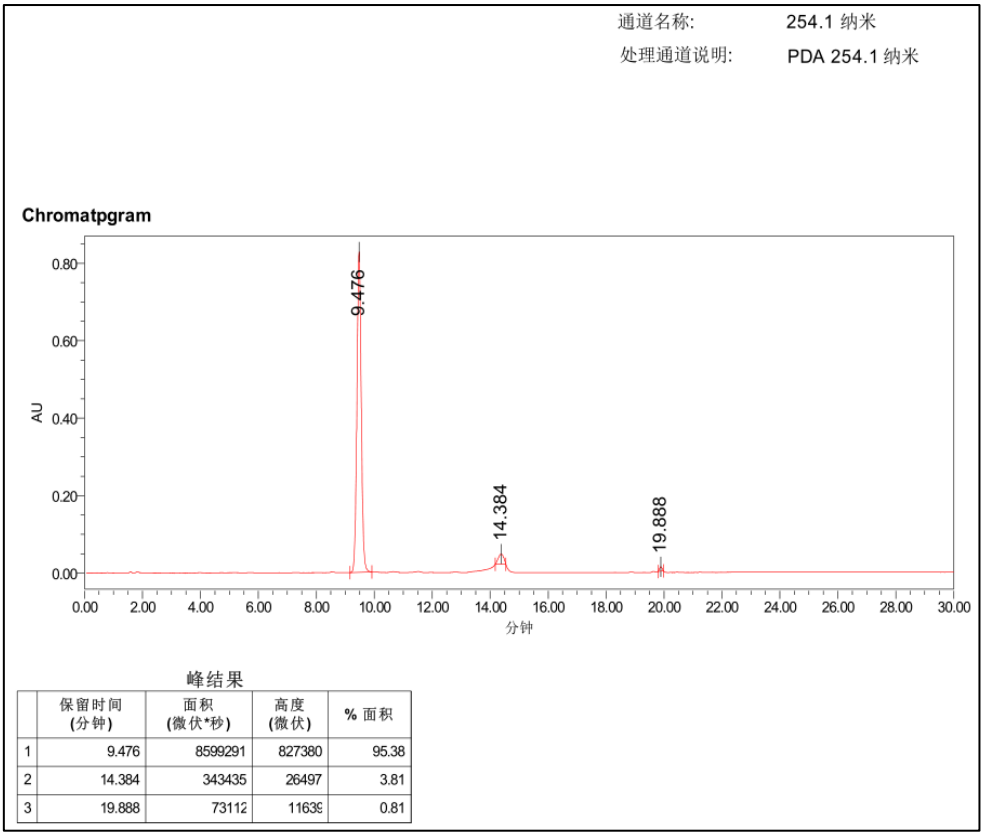

峰结果

	保留时间 (分钟)	面积 (微伏*秒)	高度 (微伏)	% 面积
1	9.476	8599291	827380	95.38
2	14.384	343435	26497	3.81
3	19.888	73112	11639	0.81

compound **19s**

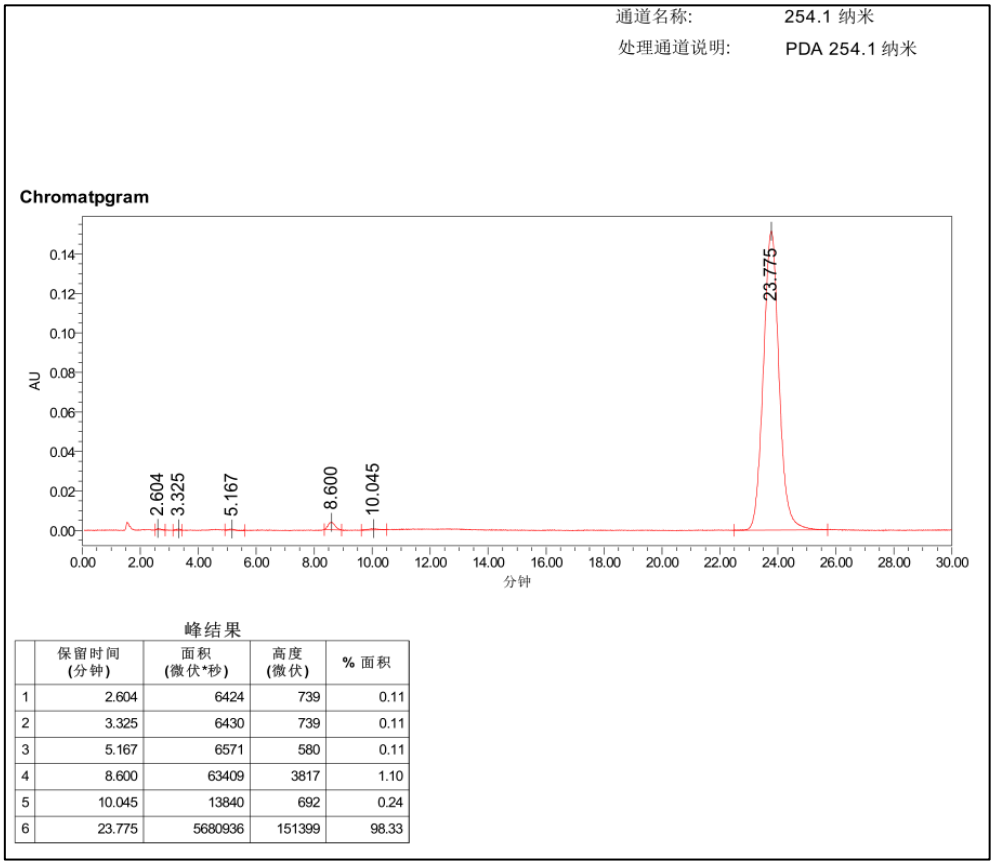

峰结果

	保留时间 (分钟)	面积 (微伏*秒)	高度 (微伏)	% 面积
1	2.604	6424	739	0.11
2	3.325	6430	739	0.11
3	5.167	6571	580	0.11
4	8.600	63409	3817	1.10
5	10.045	13840	692	0.24
6	23.775	5680936	151399	98.33

compound **19u**

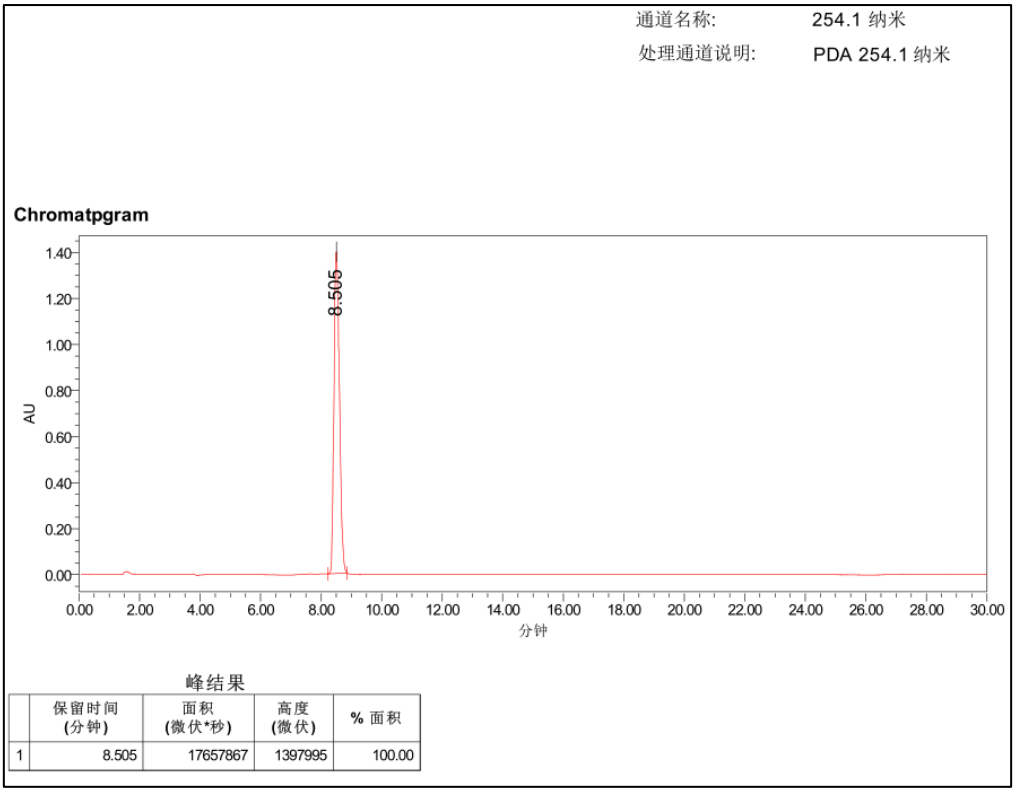

峰结果

	保留时间 (分钟)	面积 (微伏*秒)	高度 (微伏)	% 面积
1	8.505	17657867	1397995	100.00

4. HRMS spectra

compound **5a**

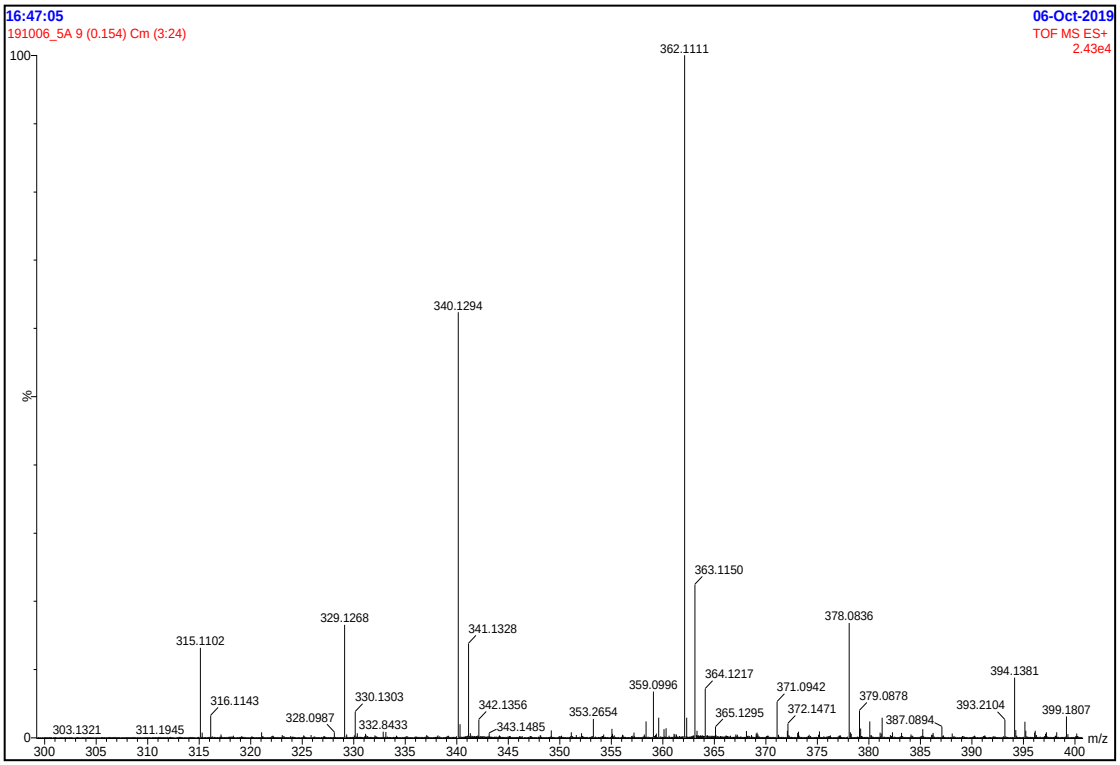

compound **5b**

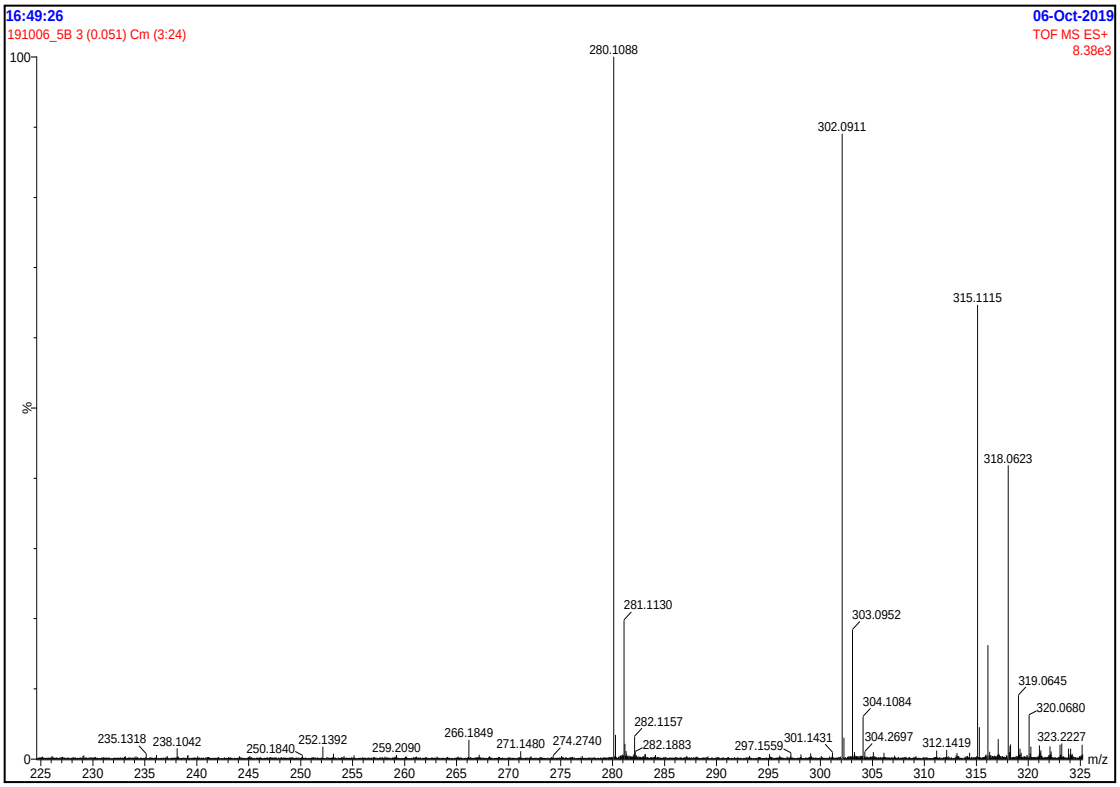

compound **5c**

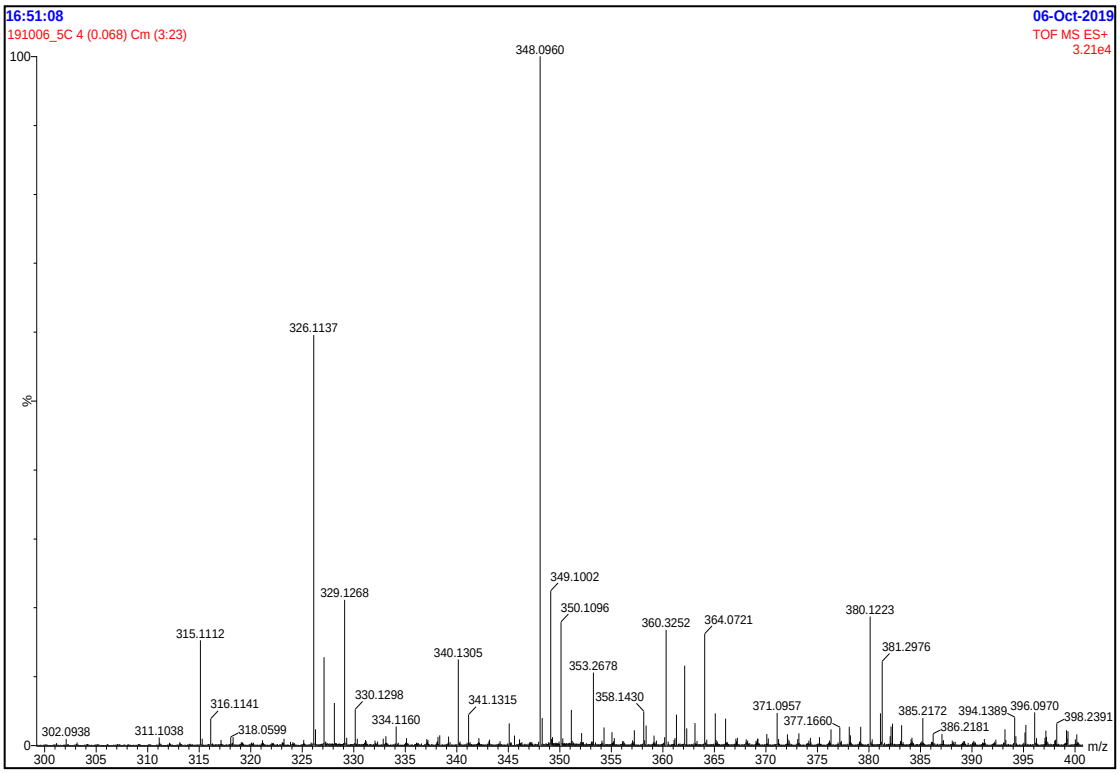

compound **5d**

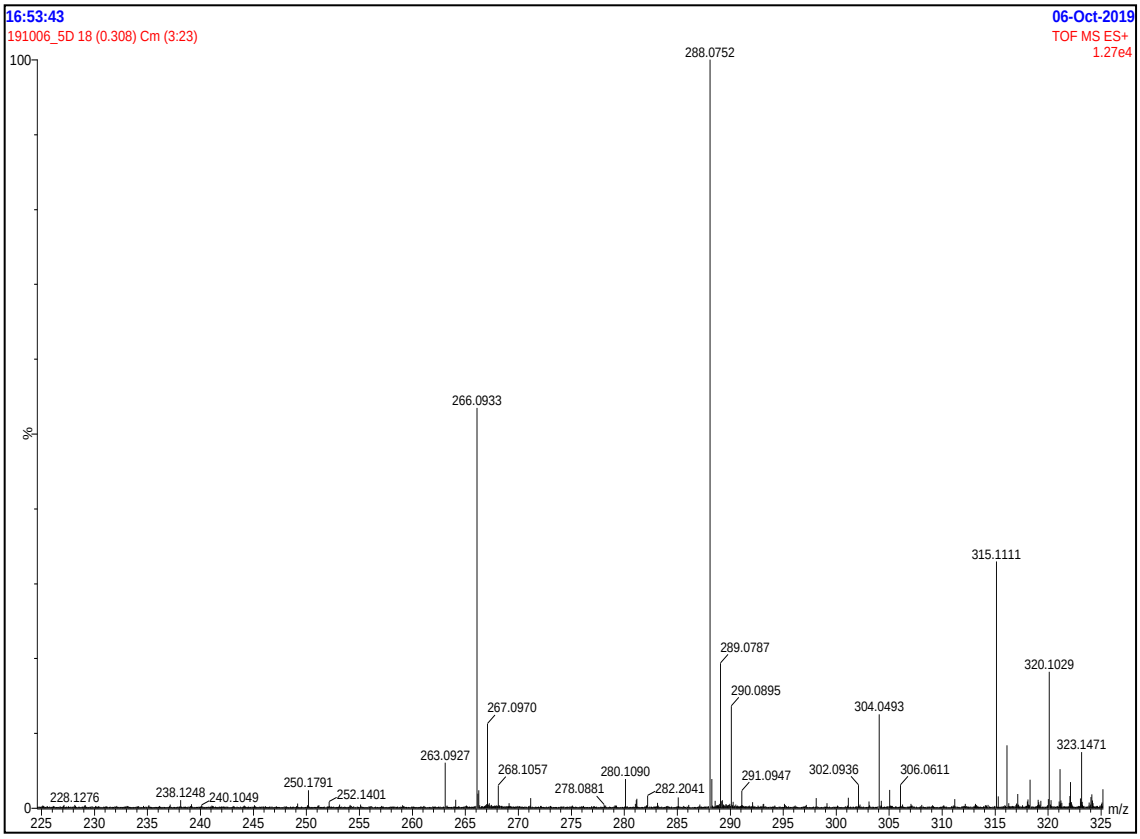

compound **5g**

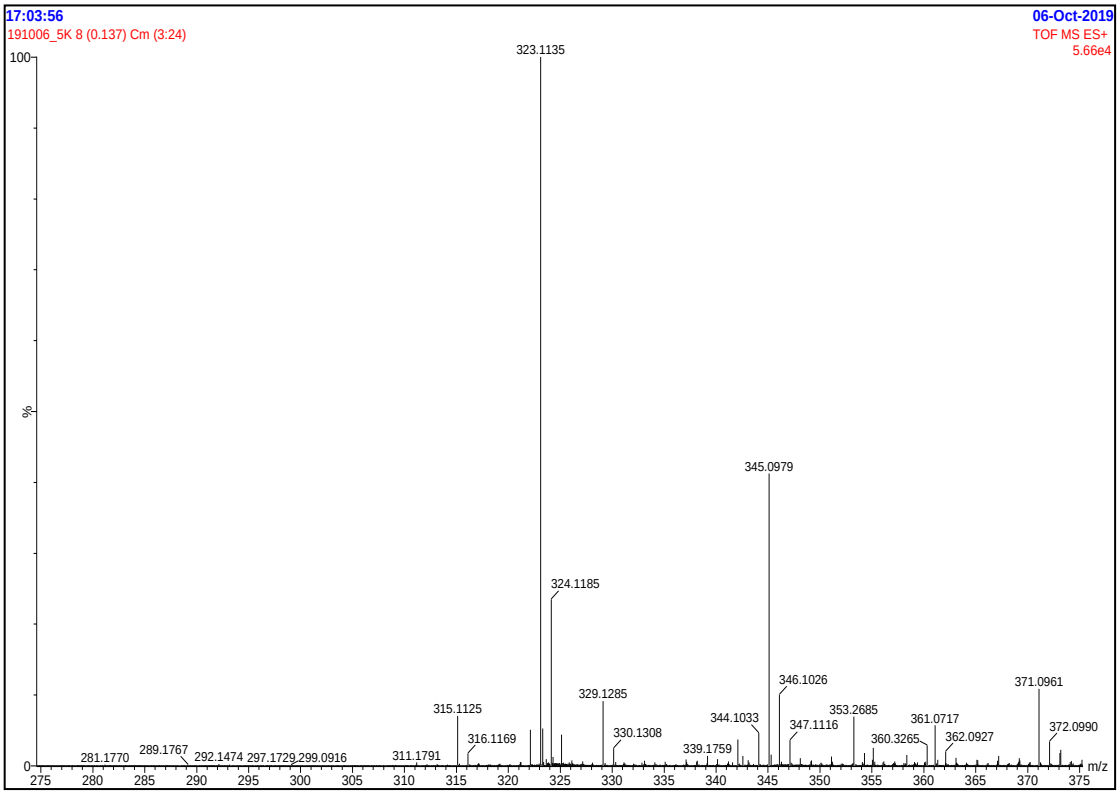

compound **5h**

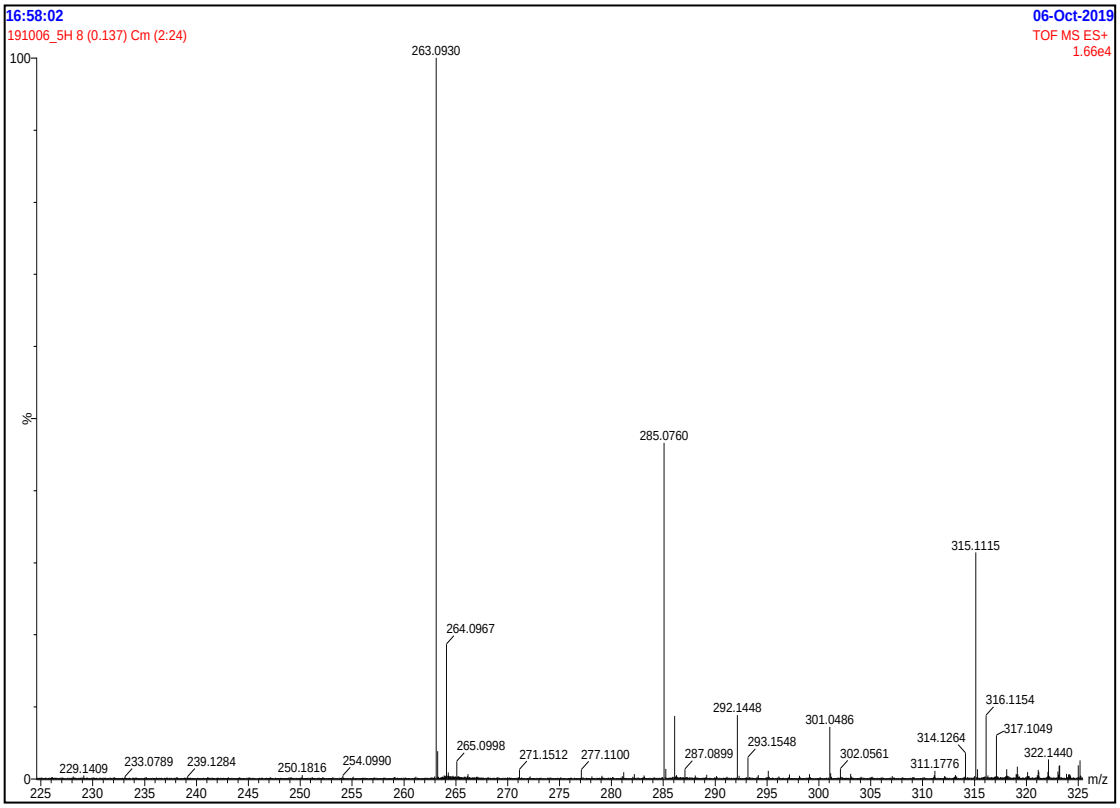

compound **5i**

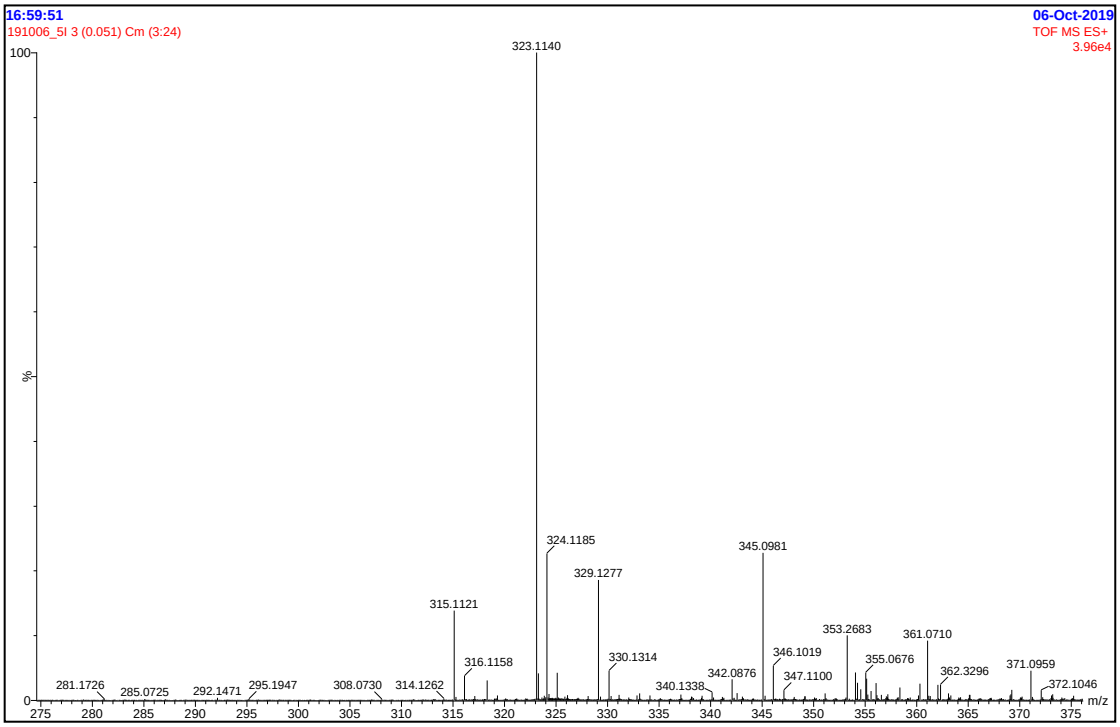

compound **5j**

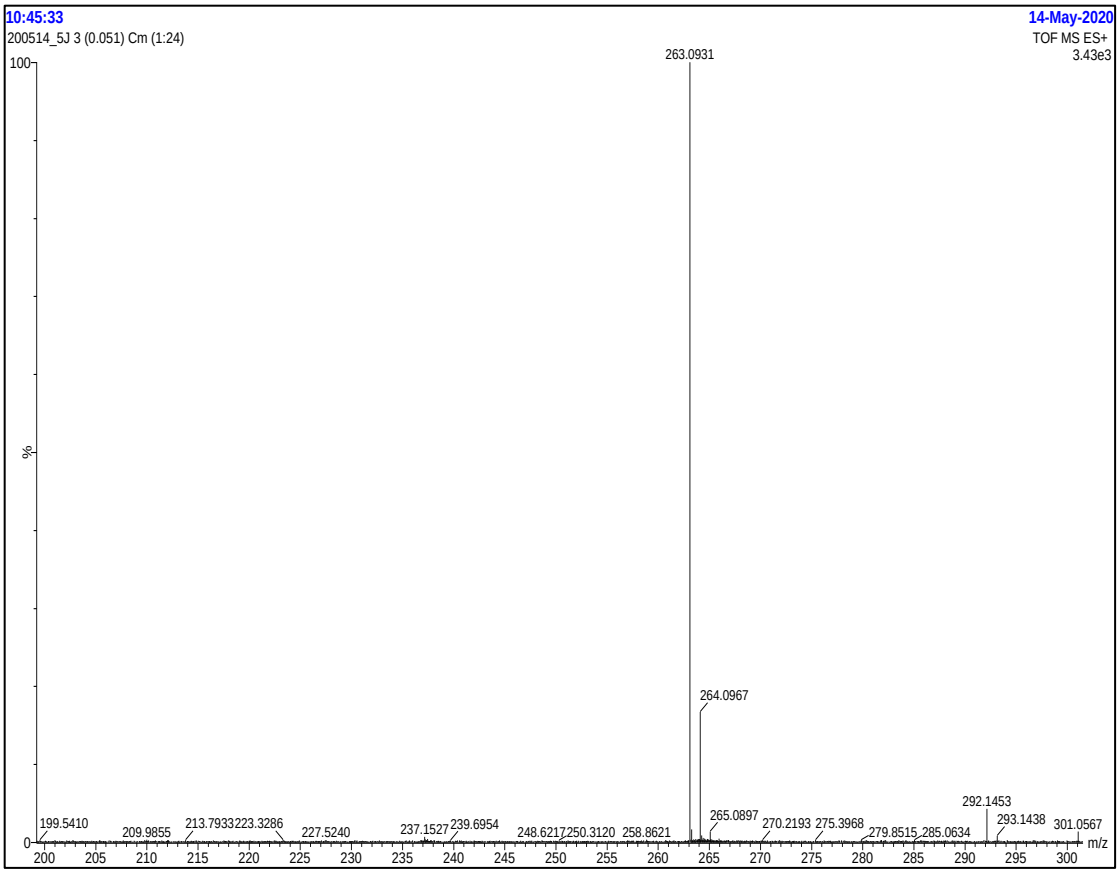

compound **5k**

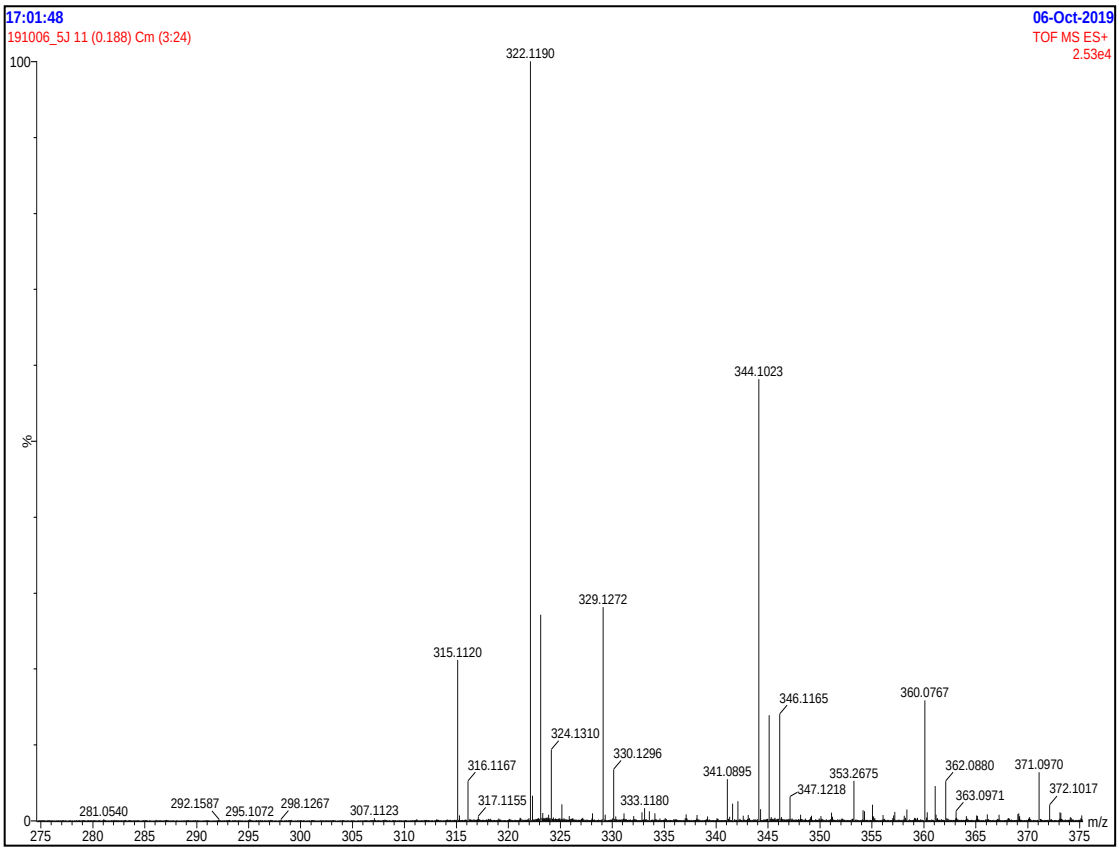

compound **11a**

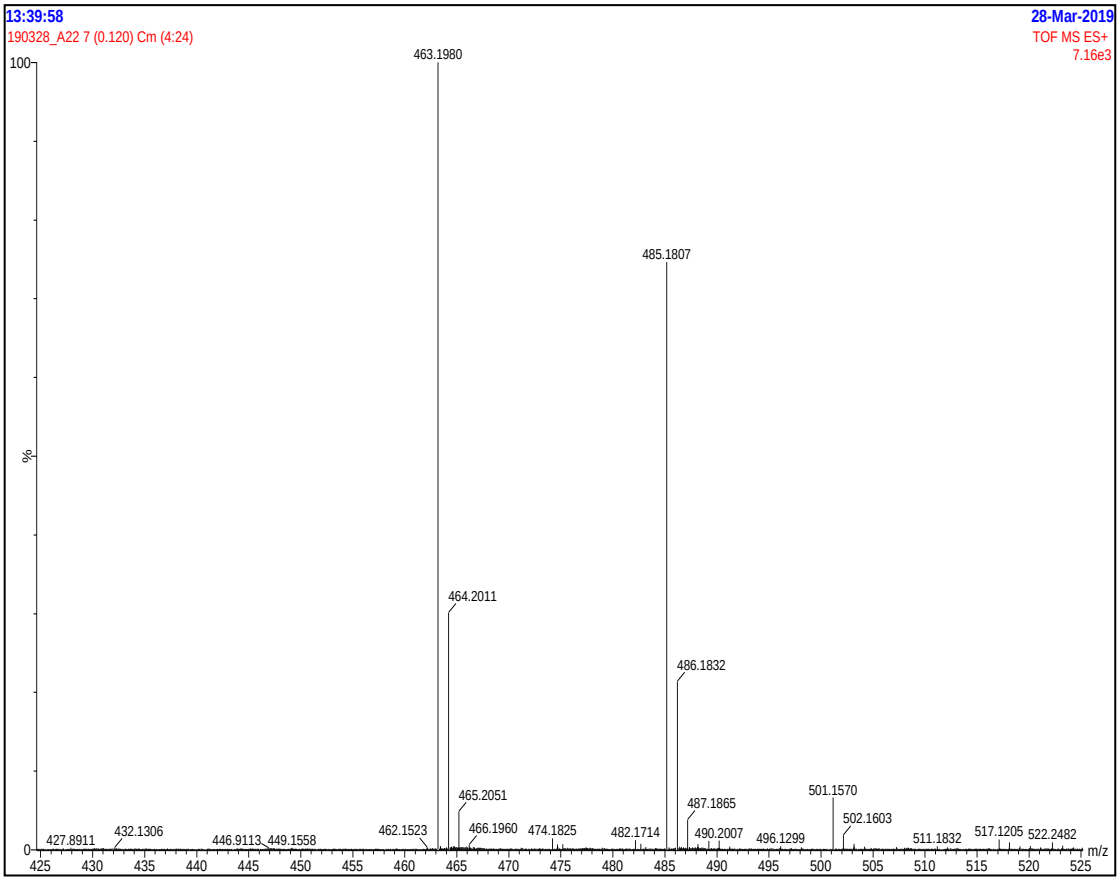

compound **11b**

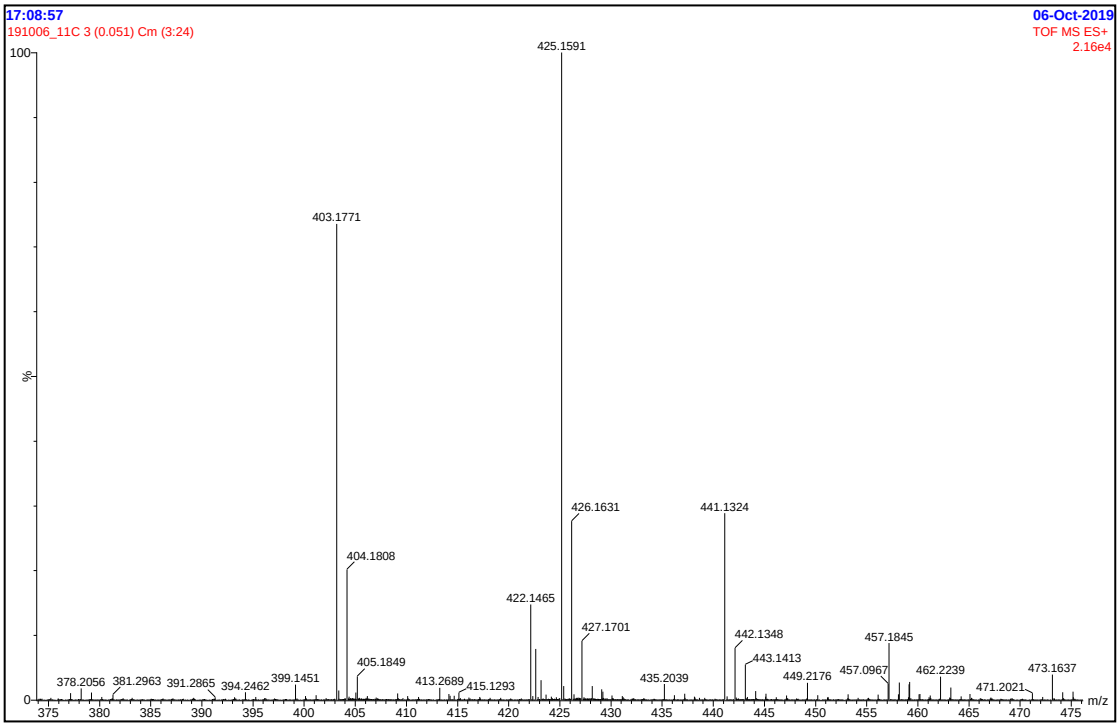

compound **11c**

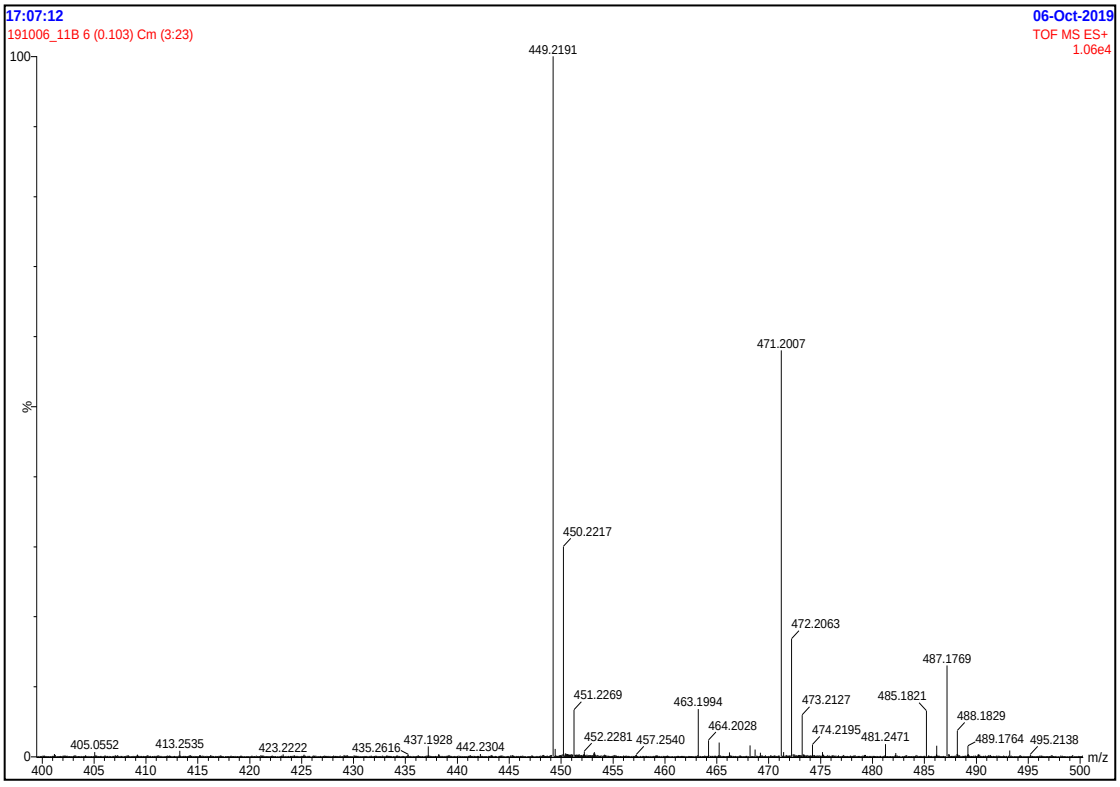

compound **11e**

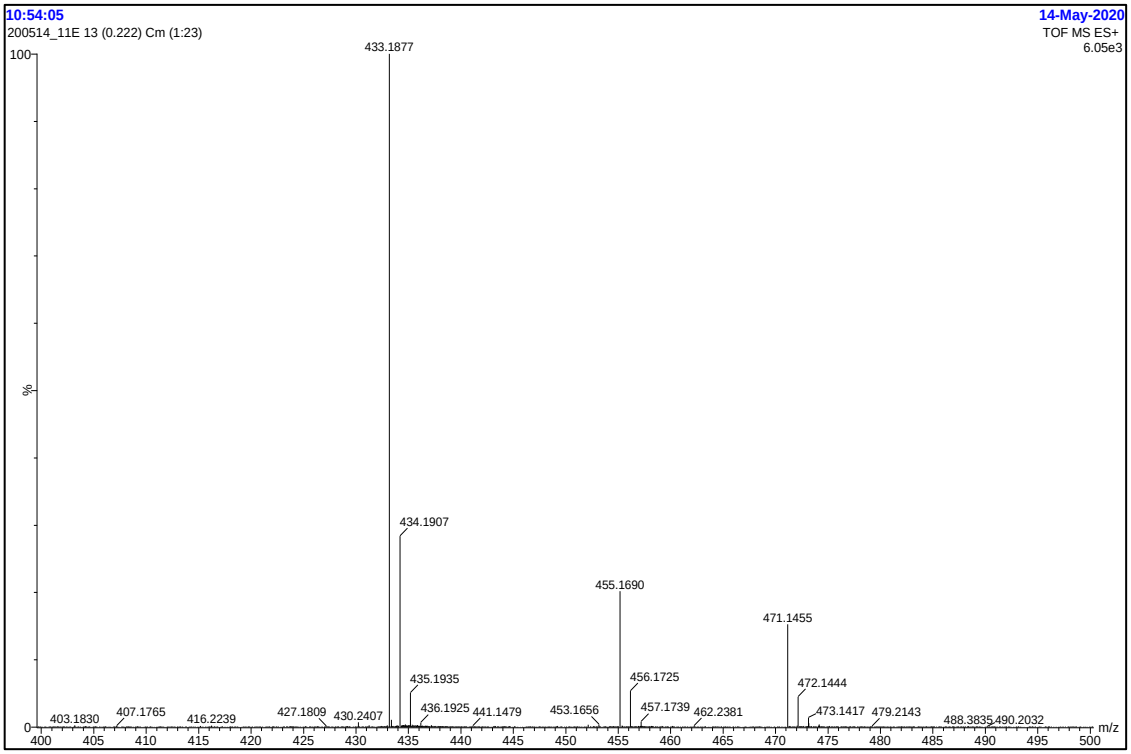

compound **15a**

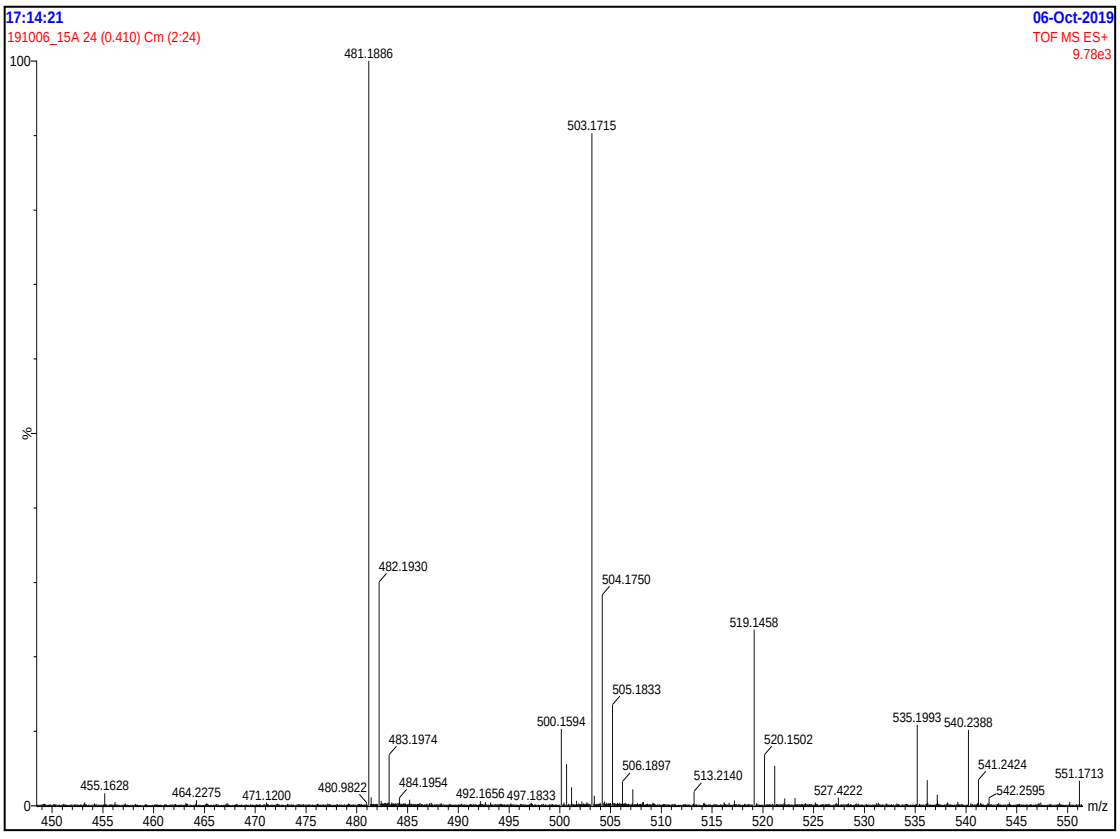

compound **15b**

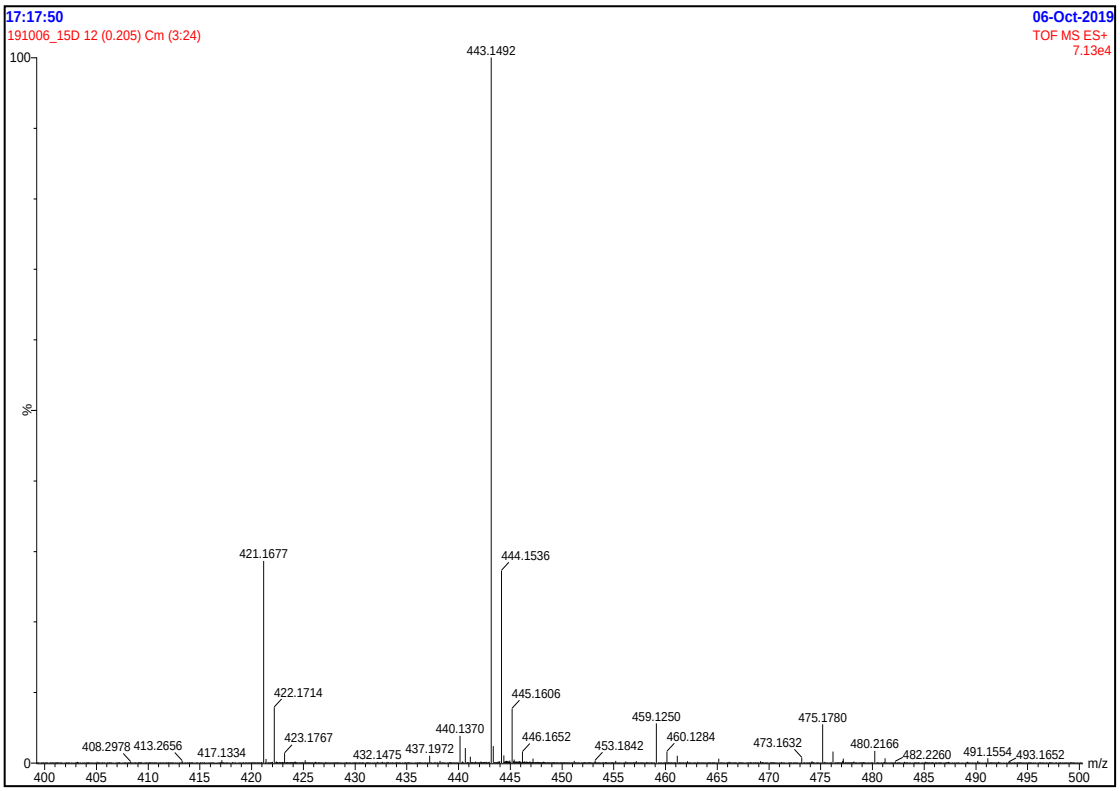

compound **15c**

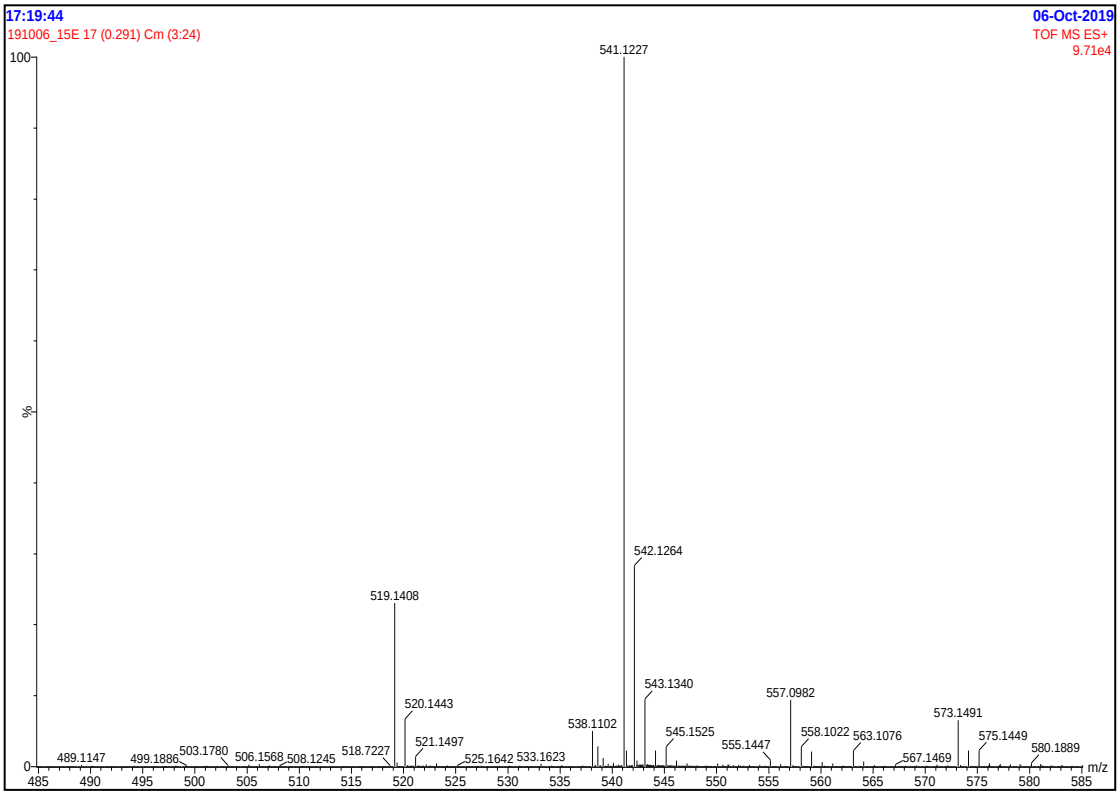

compound **15d**

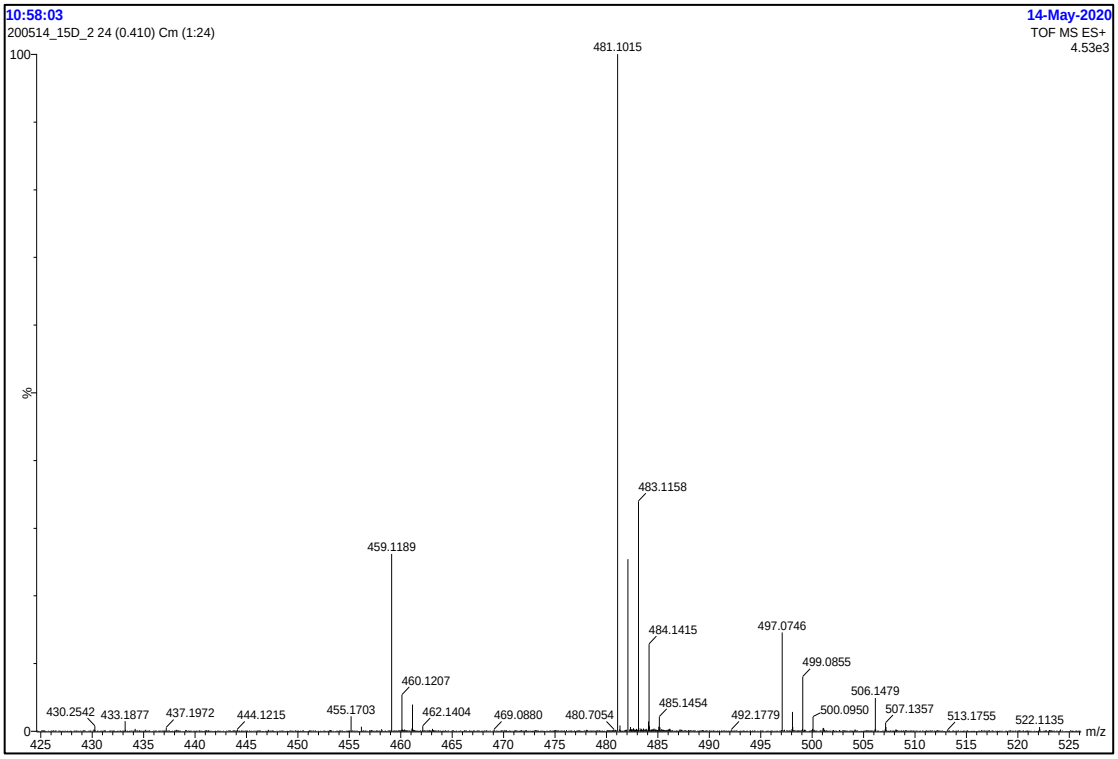

compound **15e**

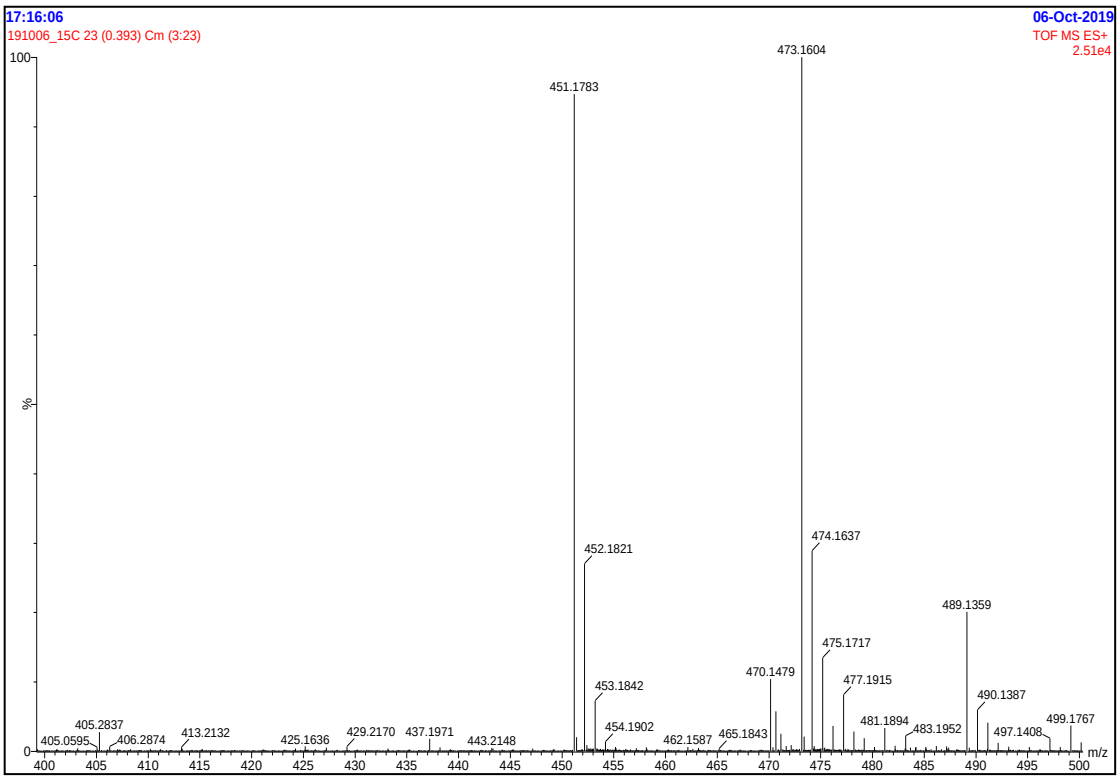

compound **19a**

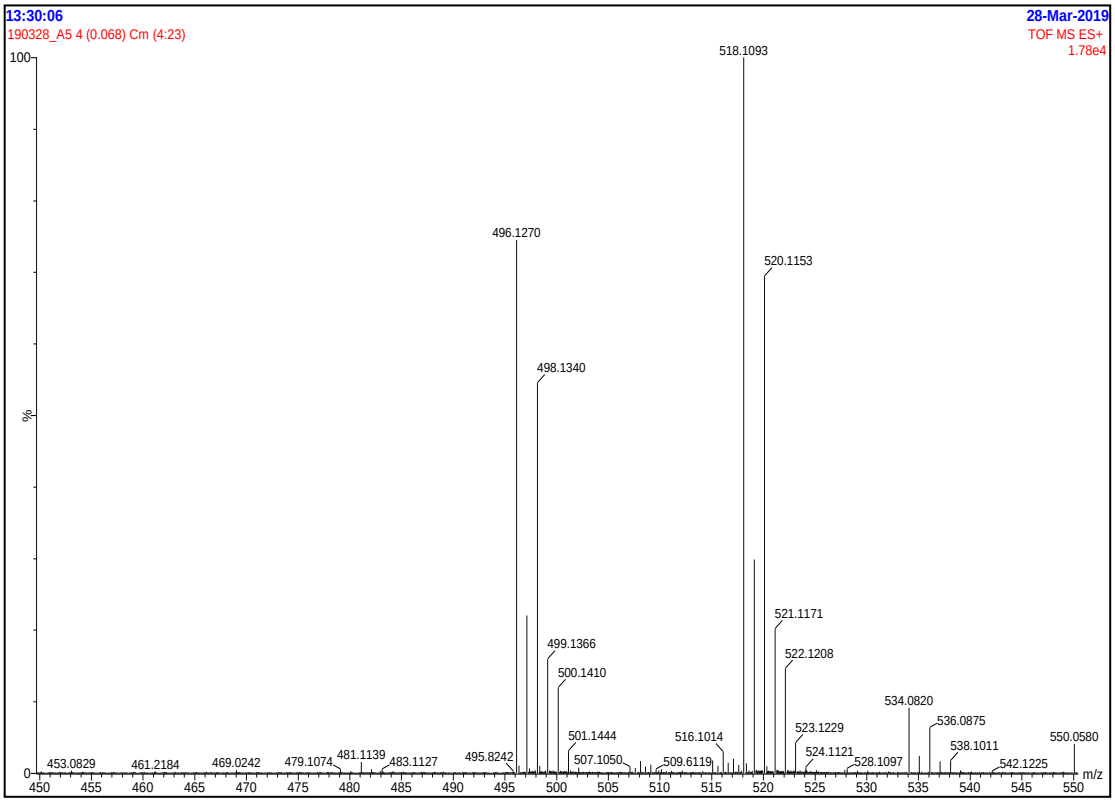

compound **19b**

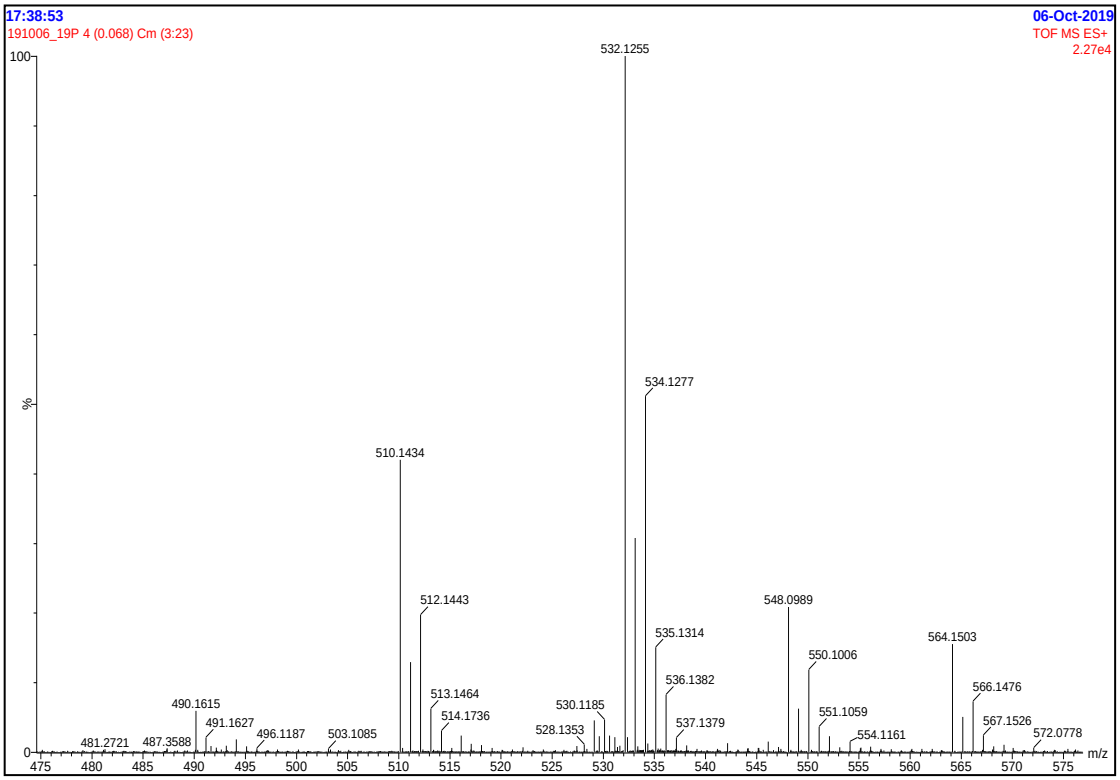

compound **19c**

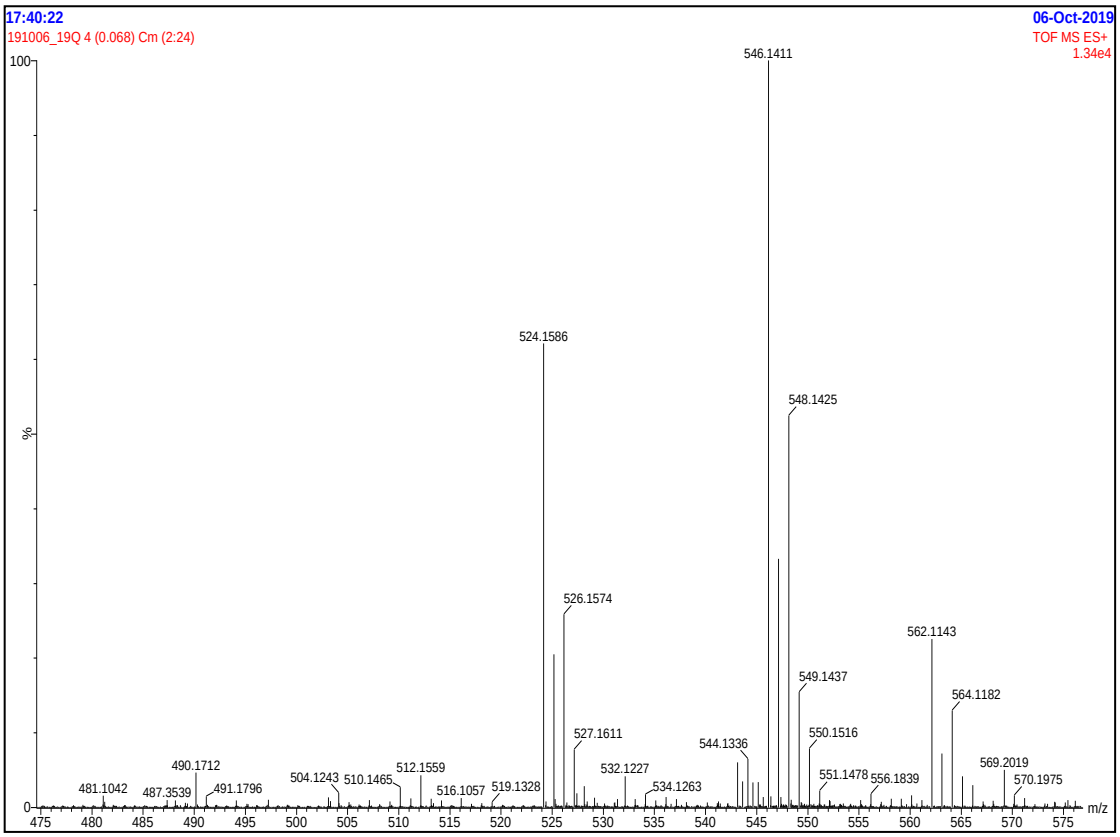

compound **19d**

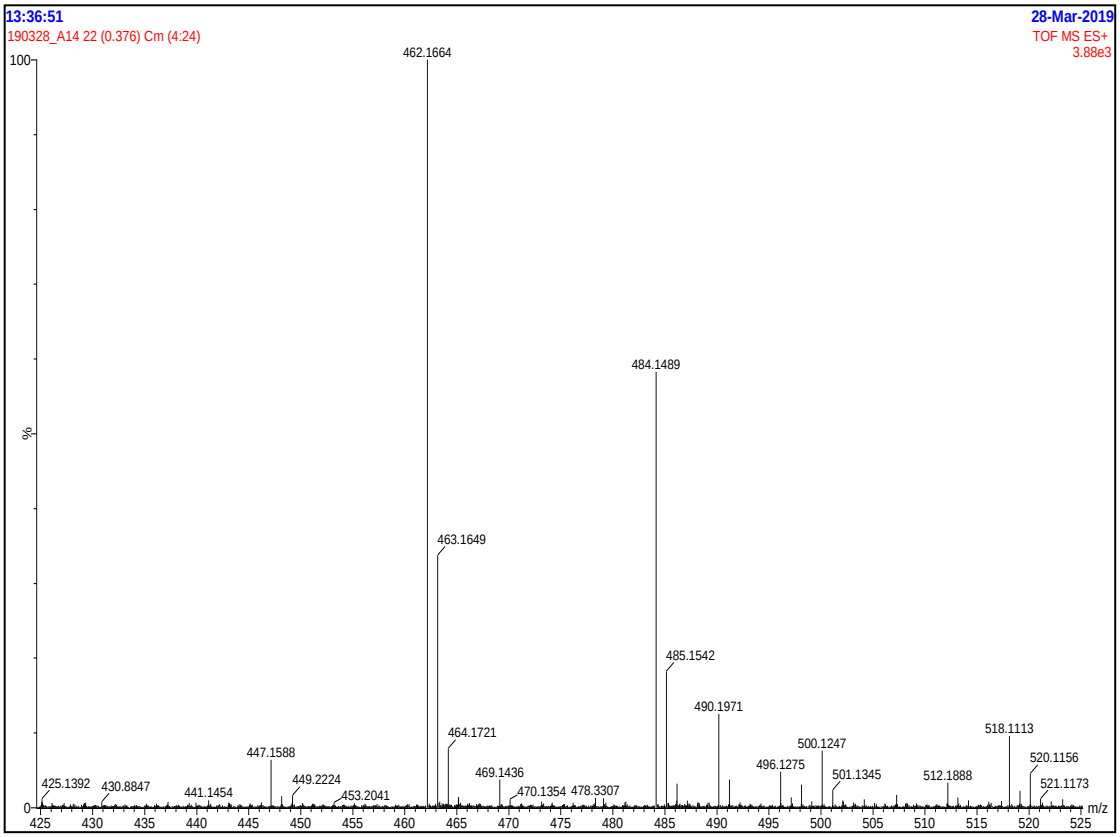

compound **19e**

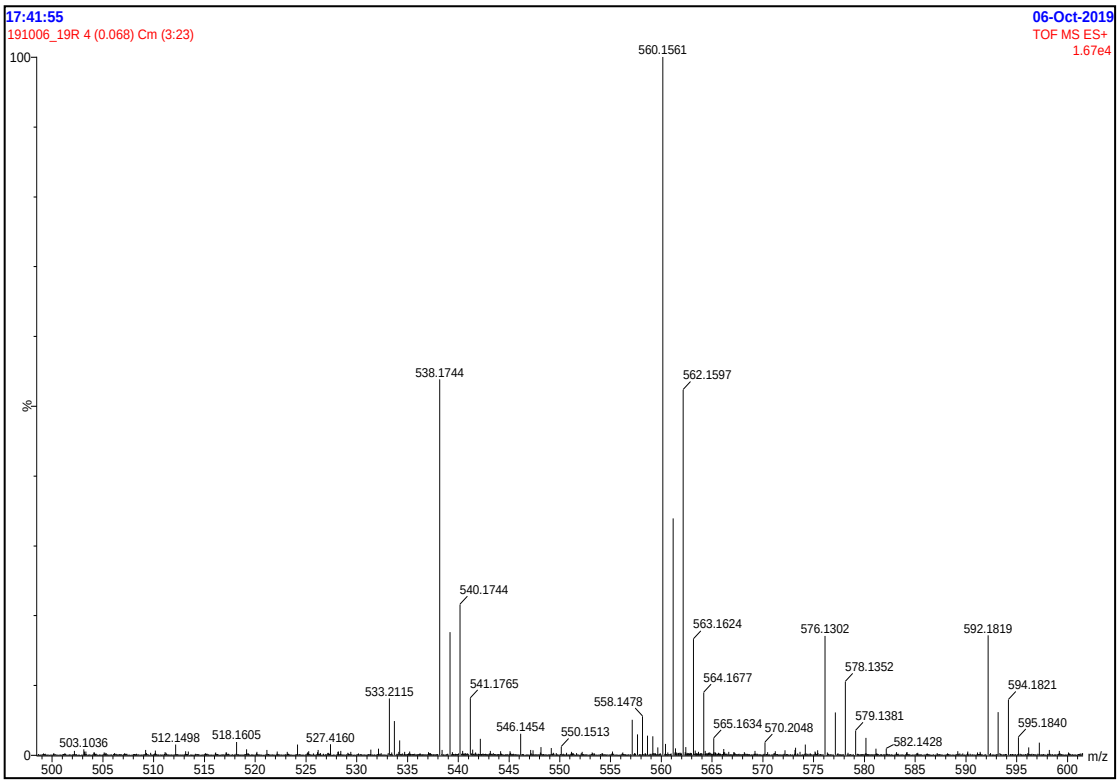

compound **19f**

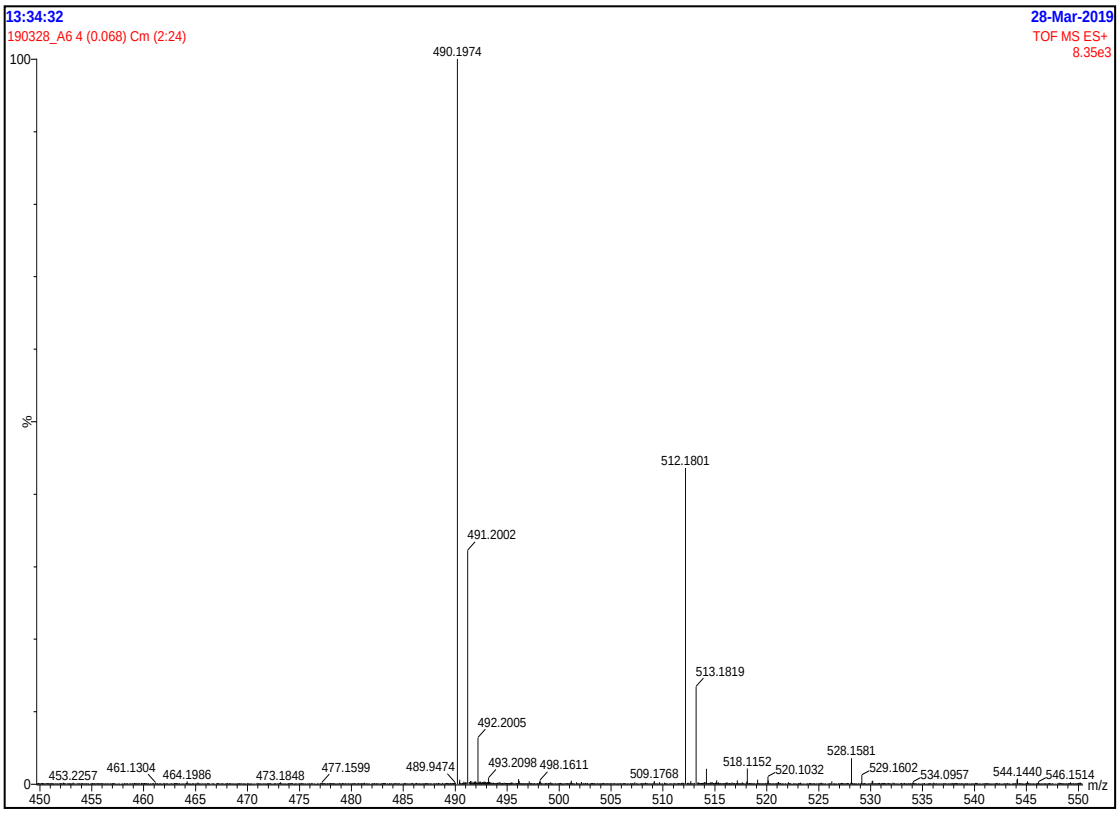

compound **19g**

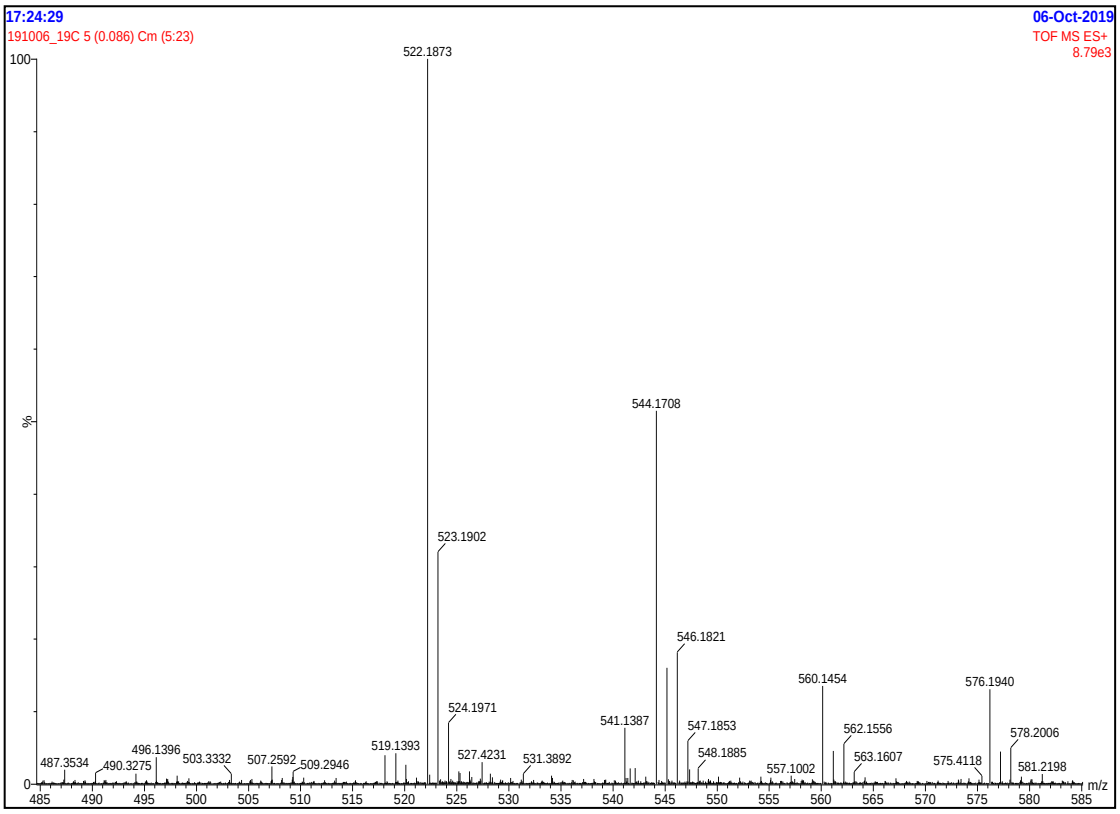

compound **19j**

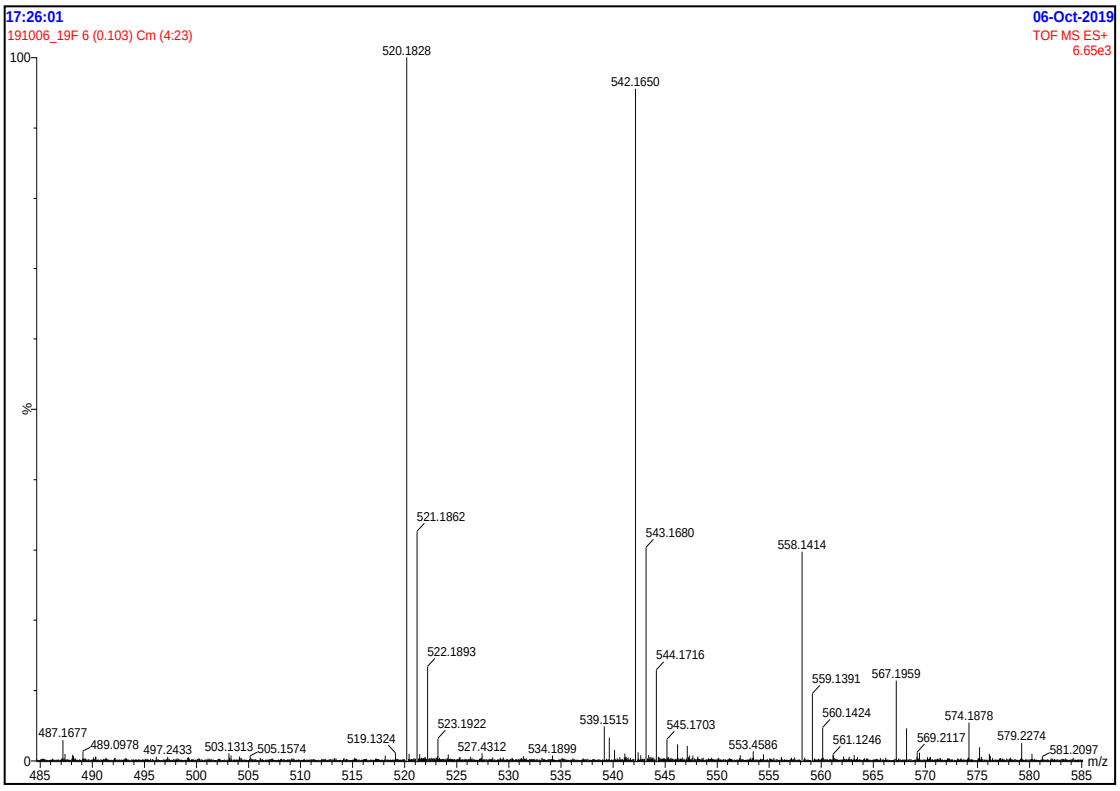

compound **19k**

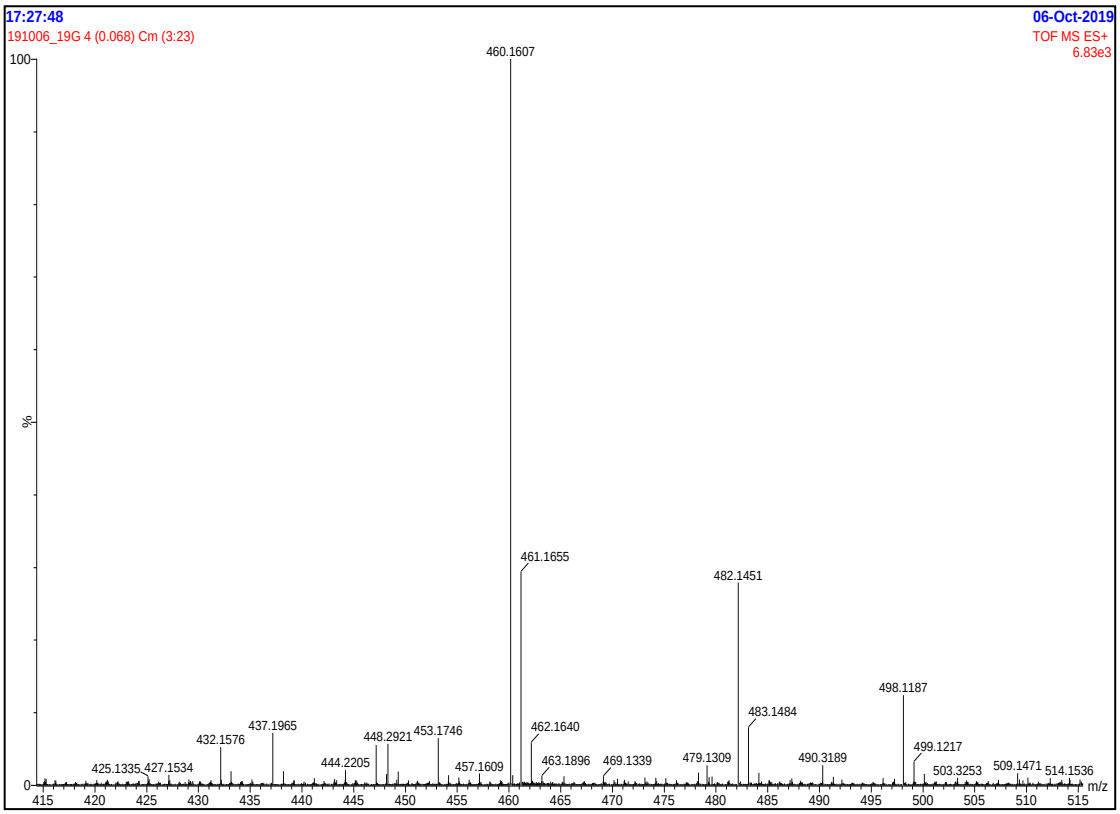

compound **19l**

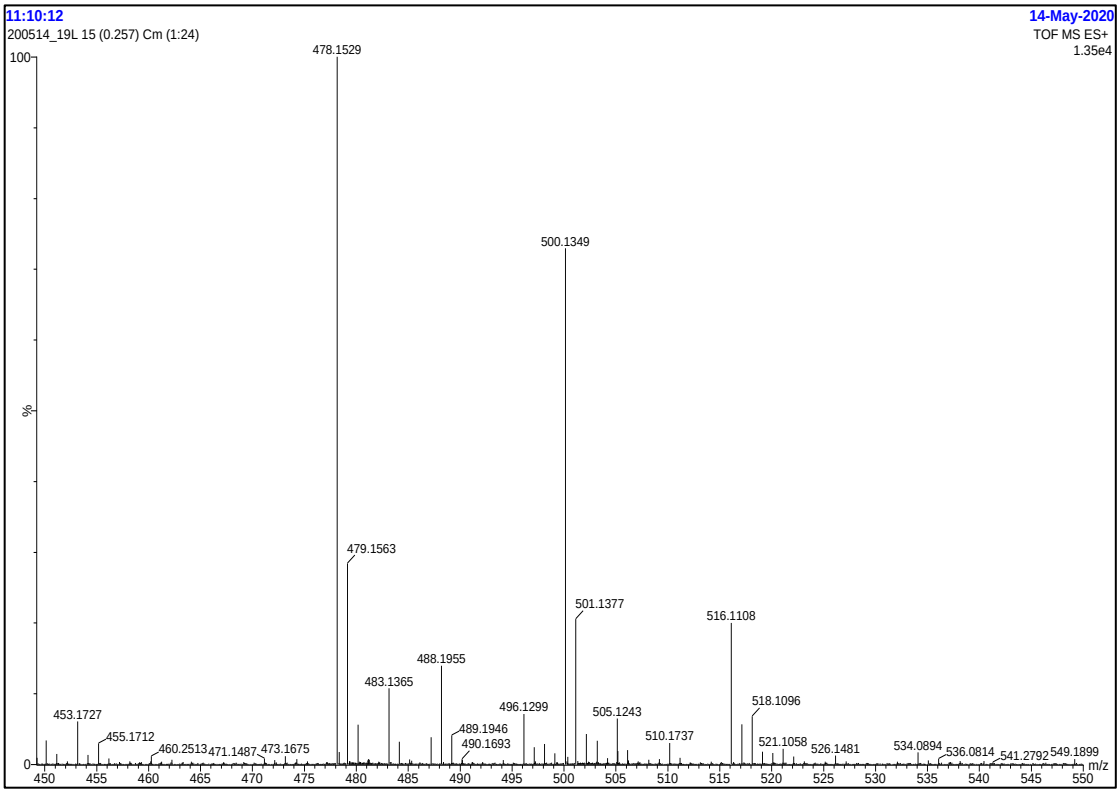

compound **19m**

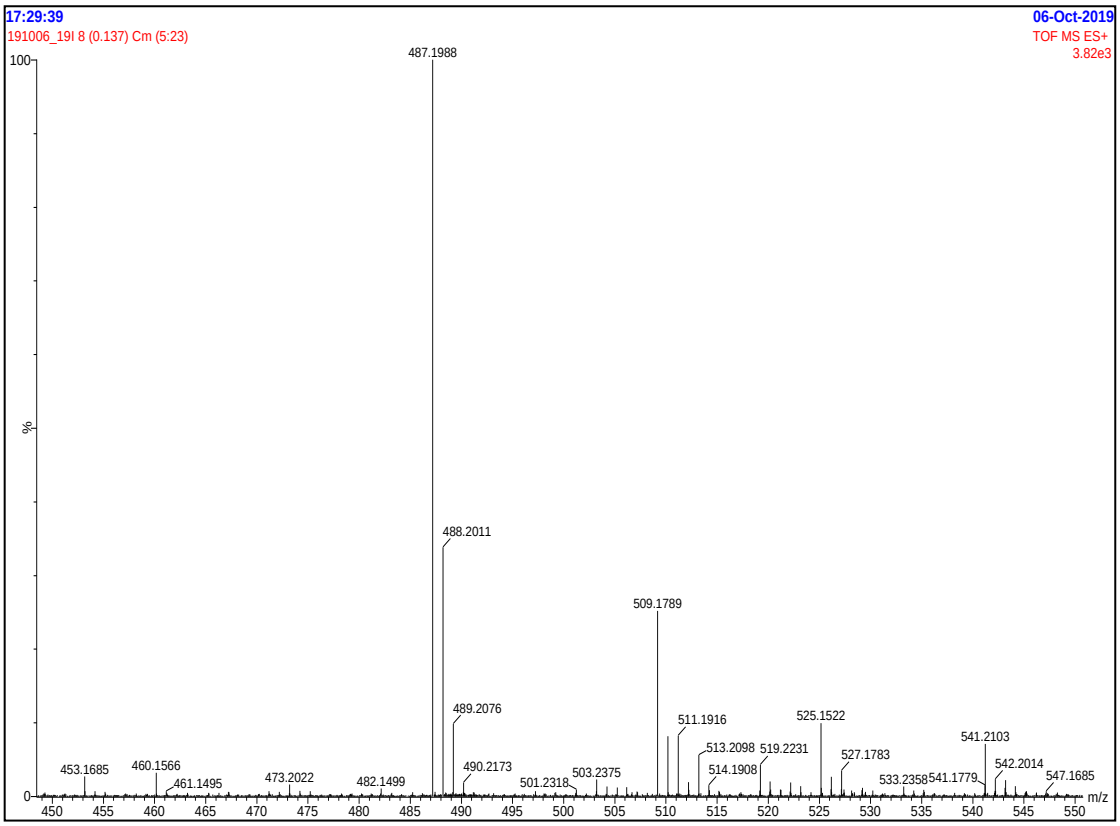

compound **19n**

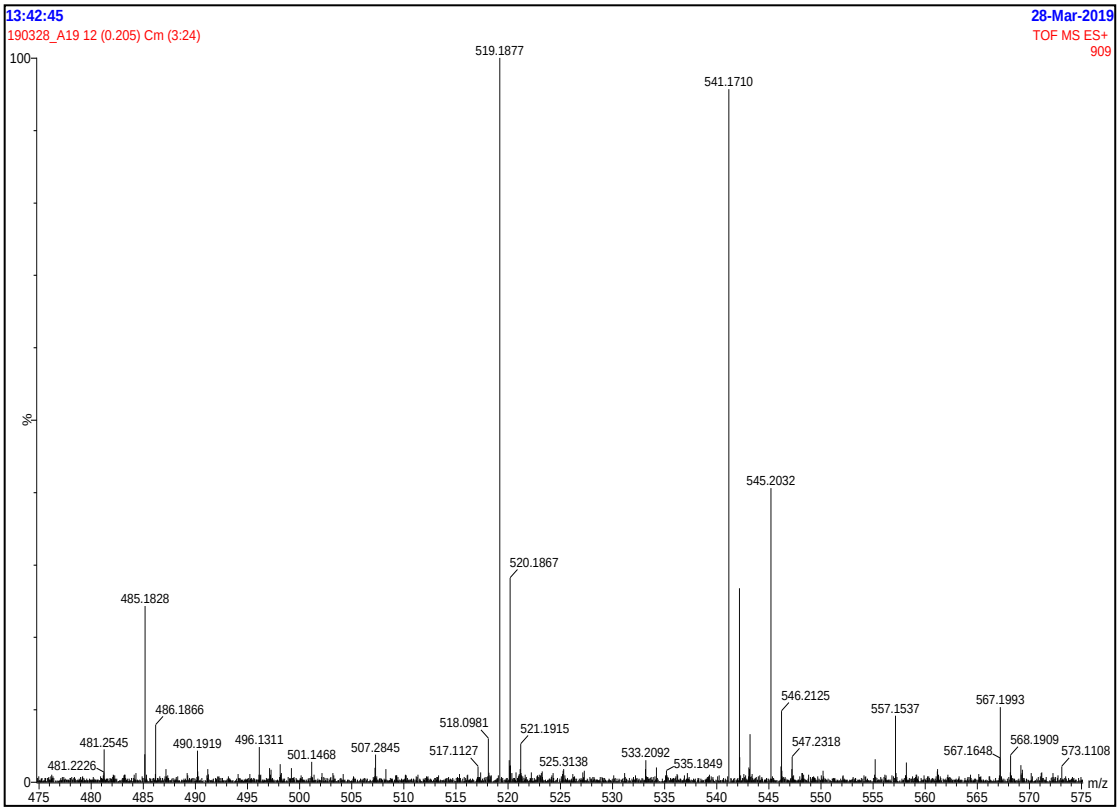

compound **19o**

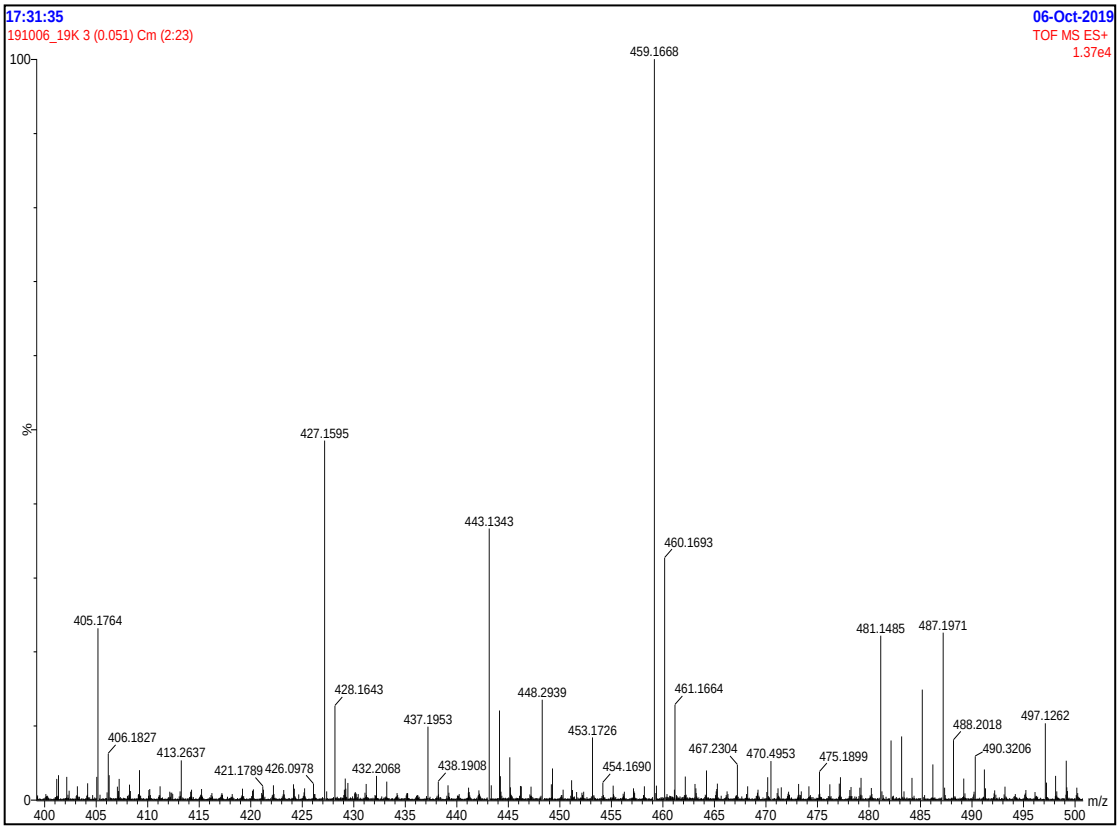

compound **19p**

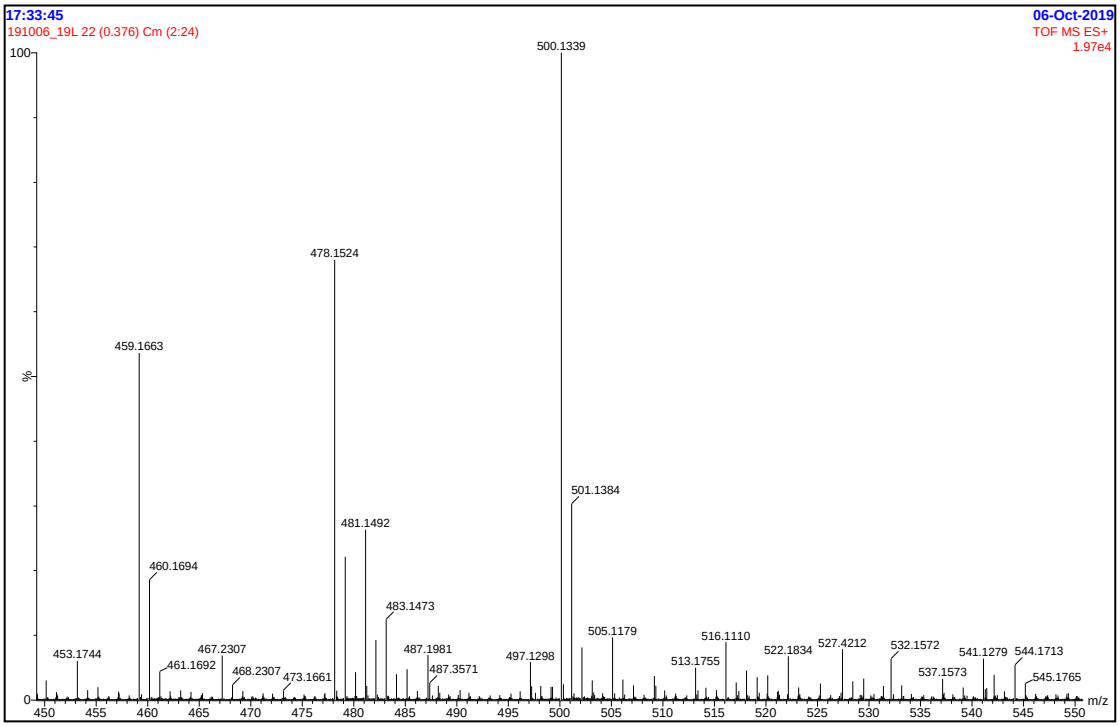

compound **19q**

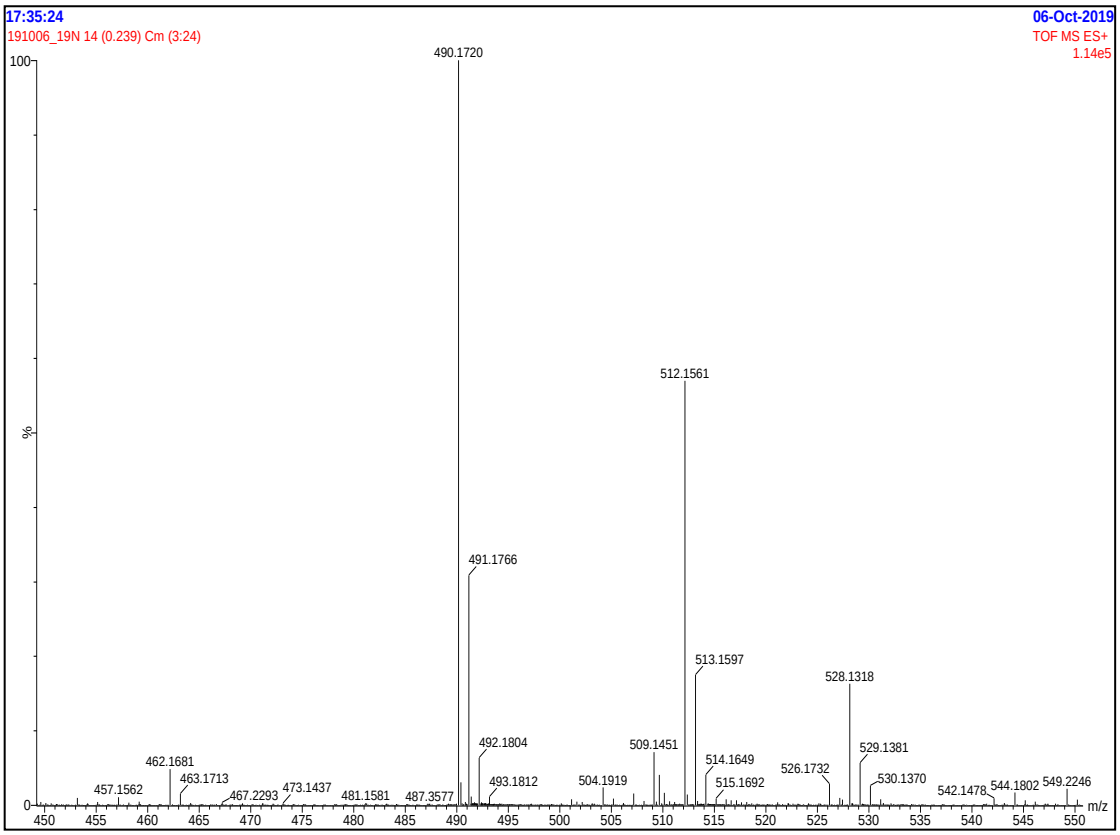

compound **19r**

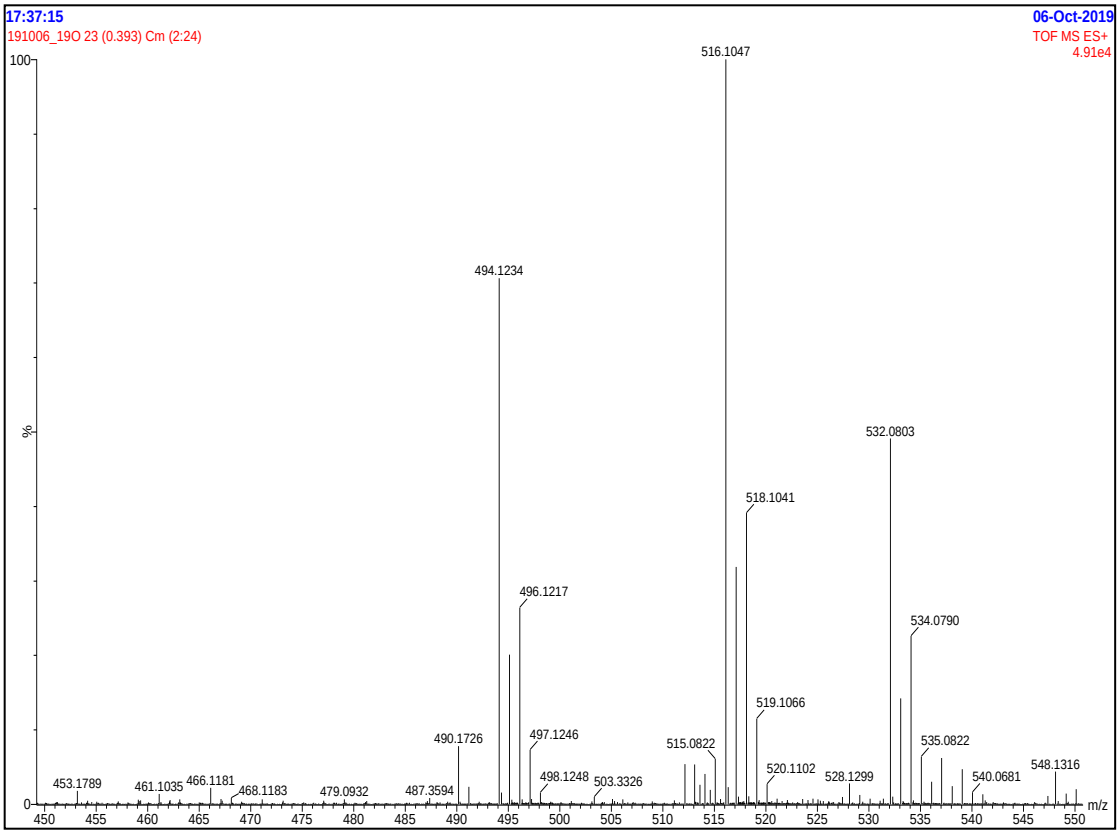

compound **19t**